Electromagnetic Induction in the Earth and Oceans

by

David McAllister McKirdy

Presented for the degree of Doctor of Philosophy in the Faculty of Science of the University of Edinburgh 1980.

DECLARATION

This is to certify that the work presented in this Thesis has been my own, unless a citation is given to the contrary, and that the Thesis has been composed by myself.

C O N T E N T S

LIST OF DIAGRAMS

LIST OF TABLES

ACKNOWLEDGEMENTS

I wish to thank my supervisor Dr. Bruce Hobbs for sugesting this topic of research and for his assistance and advice over the past three years.

I am grateful to the Department of Geophysics for providing me with the facilities to pursue my research, especially when office accommodation was scarce after my alloted time was over, and I an indebted to my friends and colleagues in the department for making my time with them a pleasant one.

I wish to acknowledge my debt to Mr. Graham Dawes, who wrote many of the computer programs which I merely adapted for my own purposes. Dr. David Summers was very helpful by drawing several relevant papers to my attention and Dr. Sheila Kirkwood very kindly permitted me to use her computer process. My gratitude is extended to Dr. Rosemary Hutton, Dr. Alan Jones and Mr. Ebong Mbipom for allowing me to accompany them on field work, which not only let me see a different side of geomagnetism, but also provided me with enjoyable summer holidays.

My thanks are due to the Natural Environment Research Council who paid my fees and studentship (No. GT4/76/GS/38) and the International Seismological Centre, my future employers, who allowed me a generous period in which to write my thesis.

Abstract

The introduction contains a review of published work on the oceanic induction problem up to the end of November 1979 and concentrates on induction in the ocean by magneto variations, although a brief account is also given of dynamo processes. The aim of the research was to model the effects of mutual induction between oceanic electric currents and a finitely conducting mantle, since previous authors had only considered the simpler case of a perfectly conducting mantle. A method for calculating these effects is derived in Chapter 2 by considering induction by a vertical magnetic dipole at the earth's surface leading to a generalised form of the Hobbs-Price mutual induction kernel.

A simple uniform earth and a more realistic seven-layered model represent the mantle while considering induction in a hemispherical ocean, in Chapters 3 and 4 respectively, where details of the calculation of the electromagnetic responses are given. Alterations and improvements were made to an existing computer program so that Banks' profile could be used to model induction in a thin sheet in the shape of the oceans and contour plots of results obtained with Banks' model and with the perfect conductor are compared in Chapter 5.

Using a spherical harmonic representation of the Sq inducing field, a qualitative comparison is made between the equivalent current systems of the modelled results with those computed from observatory measurements at different instants of Universal Time. The use of Banks' profile did not give a better comparison with the observations than the perfectly conducting mantle. The application of spherical harmonic analysis to the complete solutions showed that

the electromagnetic responses to each of the principal Sq harmonics were greater with the finitely conducting mantle than with the perfect conductor, while both were greater than the observed responses. When the analysis was restricted to using only the values at the sites of geomagnetic observatories the coefficients of the vertical magnetic field were found to be different from before, while the ratios of internal to external parts were found to be smaller. These discrepancies are due to aliasing by harmonics absent from the analysis and they suggest that the determination of the responses based on spherical harmonic analysis of observatory measurements must be suspect, which will influence any global geoelectric profile determined from these ratios.

CHAPTER 1

INTRODUCTION

1.1) The idea that temporal variations of the geomagnetic field could induce electrical currents in the earth was born in 1889, when Schuster put forward a theory of terrestrial diurnal magnetic variations. His separation of the field into parts with sources internal and external to the earth was consistent with the theory that the internal part was due to electrical currents induced by the external part. Further analysis of the daily variation resulted in Chapman (1919) proposing that the electrical conductivity structure of the earth could be represented by an insulating layer 250 km. thick with an underlying uniform sphere of conductivity 0.036 Sm^{-1}. The work of Chapman and Whitehead (1922) demonstrated that the thickness of a uniformly conducting sheet at the surface of the earth had considerable influence on the conductivity of the central uniform core which gave the best fit with observations. The justification for proposing such a conducting layer near the surface of the earth was that the conductivity of sea water (4 Sm^{-1}) was known to be higher than that of surface rocks, which marked the beginning of interest in electromagnetic induction in the oceans.

Lahiri and Price (1939) developed the theory of induction in non-uniform radially symmetric spheres for both periodic and aperiodic inducing fields and, in order to explain analyses of the daily variation and magnetic storms, they proposed that the conductivity of the earth increased rapidly to at least 1 Sm^{-1} at depths of about 700 km and that a better comparison between observations and calculations could be obtained by including a uniformly conducting shell at the earth's surface which had a

vertically integrated conductivity equivalent to 1 km of sea water.

These pioneering studies of geomagnetic induction showed that the oceans could exert influence on the global aspects of the time-varying geomagnetic field but more recent studies have established that the oceans could also be important in more localised studies.

Interest in the effect of the oceans on geomagnetic variations must have been boosted by the work of Parkinson (1959 and 1962), who discovered high correlations between the changes in the vertical and horizontal fields recorded at geomagnetic observatories at time intervals in the range of five minutes to one hour. By plotting the directions of these changes for a large number of equal time intervals on a polar diagram, he demonstrated that the fluctuations tended to lie in a preferred plane inclined to the horizontal. These results could be presented in an alternative way by means of the 'Parkinson Vector', which pointed in the direction of the greatest upward slope of the preferred plane, and its length was defined as the ratio of the vertical to horizontal variations in the direction of the vector.

It was observed that at coastal stations the vector was often oriented towards the nearest region of deep water and that the magnitude was much greater than that obtained at stations inland. This effect was initially demonstrated for Australian observatories but was later observed to occur world wide, particularly in regions where a straight coastline was near deep water. It was suggested that this effect could be explained by eddy currents induced in the sea, thereby modifying the field near the coastline, but analogue studies with a model of the

earth and its oceans, or terrella, were unable to produce large vertical fields near the coasts, from which Parkinson inferred that the coast effect might have been due to conductivity contrasts between the continental and oceanic mantle (Parkinson, 1964).

Schmucker in his array study in the south-west of the U.S.A. (Schmucker, 1964 and 1970) detected what can be described as a classic coast effect, where the amplitude of the Z variations was considerably enhanced near the coast compared with stations inland. This effect was observed in both geomagnetic bays and the daily variation and was demonstrated by the fact that the length of the Parkinson arrows increased near the coast. This phenomenon was interpreted by assuming that the induced currents flowed in the ocean on the seaward side, while the currents on the landward side were presumed to be flowing at depth in the upper mantle. The distance inland, over which it took the enhancement of Z to disappear, was used to find the depth to the conducting mantle. Coast effects of this type have been observed world wide; in South Australia for example (White and Polatajko, 1978).

Another type of induction anomaly that has been detected is the so-called island effect. A simple explanation of this phenomenon is that an island which rises from the ocean floor causes currents in the ocean to diverge and pass round it on either side on account of the contrast in conductivity between rocks and sea water. This means that it is possible to detect considerable variations in the vertical magnetic field due to the fact that the currents are flowing in opposite senses on the opposite sides of the island and can cause a reversal of the direction of the vertical field across the island. This has been

observed in Oahu, Hawaii (Mason, 1963) and Miyake-jima, Japan (Honkura, 1972). Techniques have been developed to remove the island effect from observations so that the conductivity profile of the crust and upper mantle could be determined (Klein and Larsen, 1978).

The island effect can be more complicated when the island is close to the continental shelf, where the deep oceans and shallow coastal seas can influence the direction of the Parkinson arrow at different periods. An array study in the British Isles (Edwards, Law and White, 1971) demonstrated that the induction vectors on the east coast of Ireland pointed towards the Atlantic at a period of 144 minutes but were directed towards the Irish Sea at a period of 40 minutes. Work carried out in Sutherland, Caithness and the Orkney Islands (Robinson, 1977) demonstrated that the directions of the induction vectors were dictated by the local coastline in the period range of 5-30 minutes, while the effect of the Atlantic continental shelf dominated at periods in the range 30 minutes - 3 hours.

Interesting results have been obtained from the analysis of magnetic data recorded on icebergs (Zhigalov, 1960), when correlations were obtained between the ratio of vertical to horizontal geomagnetic variations and the bathymetry. The deep oceans can be thought of as being uniform over large horizontal scales, except near mid-oceanic ridges, and an iceberg is unlikely to perturb the circulation of currents in the ocean in the same manner as an island rising from the sea floor. Electromagnetic theory shows that the presence of a large uniform highly conducting body, i.e. an ocean, causes a reduction in the amplitude of the vertical magnetic variations compared with the horizontal variations, and

the vertical variations are completely cancelled out in the limit of infinite frequency or conductivity. It was expected that the reduction would increase as the depth of the ocean increased as was demonstrated experimentally.

1.2) Analogue models have been used in electromagnetic induction studies to examine situations for which mathematical models are either inaccurate or totally lacking and some insight into the oceanic induction problem has been gained through this approach. The terrella experiments of Parkinson have been mentioned breifly in the previous section and they were performed on a model in which the oceans were simulated by a thin copper sheet surrounding the mantle, which was modelled by an aluminium sphere at a depth corresponding to 0.9 earth radii. The inducing field was produced by a coil, which was wound in such a way as to model the current system of a geomagnetic bay, and the fields were measured with the aid of a small search coil. In analogue modelling it is vital to ensure that the scaling factors are selected in such a way that the model is truly analagous to the geophysical situation it is meant to represent. This occurs when the following condition is obeyed:

$$\sigma\omega(1)^2 = \sigma'\omega'(1')^2 \qquad (1.1)$$

where the primed and unprimed quantities are characteristics of the model and geophysical cases respectively.

Much of the early work in this field has been reviewed by Dosso (1973), who refers to models of Iceland, by Hermance (1968), and Japan, by Roden (1964), who modelled the respective islands by cutting the appropriately shaped holes in a metal sheet. Dosso then compared his own work on modelling the coast effect, for the two dimensional situation in which there was a

vertical interface between the ocean and the land, with some of the early attempts at numerical modelling. The agreement between the two approaches was close except near to the coast where the measured fields were smaller in magnitude than the numerical calculations, which was probably due to the finite dimensions of the search coil used to measure the field.

The work of Launay (1970) was referred to in which the Z/H ratio for the Californian and Australian coast effects were modelled by two copper sheets; one represented the oceans and the other the mantle, which was located at the following depths: 450-500 km. for Australia and 180-210 km. for California. More complicated coastline models were also discussed, e.g. the case of a shelving ocean overlying a conducting step. The Californian coast effect has also been modelled by Spitta (1977), who chose to locate his conductosphere at a depth of 270 km.

More recently interest has been revived in modelling three-dimensional systems, to enable the comparison between field observations and analogue measurements to be made; examples of this work are Vancouver Island (Chan and Dosso,1978) and the British Isles (Dosso, Nienaber and Hutton, 1978).

6.3) Theoretical studies of the oceanic induction problem have been considerably simplified by two assumptions: namely the quasi-static approximation and the thin sheet approximation. The former is used virtually universally in the field of geomagnetic induction, since the periods of interest are considerably longer than the time it would take for electromagnetic radiation to travel a distance typical of the dimensions of geophysical interest. Propagation of the electromagnetic field can be assumed to be instantaneous, which is tantamount to ignoring the displa-

cement current in Maxwell's equations and means that the magnetic field obeys the diffusion equation in conductors and Laplace's equation in insulators as opposed to the wave equation, which governs high frequency electromagnetic phenomena. The thin sheet approximation is particularly applicable to the oceanic induction problem since, for the periods of interest, there is little attenuation of the electromagnetic field across 4km., which is a typical depth of the oceans, whose horizontal dimensions can be three orders of magnitude greater than their vertical dimensions. In a uniform conducting half-space, an electromagnetic field is attenuated in the following manner: the amplitude of the field variations is reduced by a factor 1/e as the field penetrates the distance of one skin-depth into the conductor, where skin-depth, (δ), is defined as:

$$\delta = (2/\mu\sigma\omega)^{1/2} \qquad (1.2),$$

where σ is the conductivity of the half-space, ω is the frequency of the inducing field and μ is the permeability of the medium.

Inserting the appropriate values shows that the skin-depth in sea water is about 80 km. for periods of 24 hours and 15 km. at one hour, which implies that the thin sheet approximation should be valid for the daily variation and its harmonics since the amplitude of the electromagnetic field is practically constant throughout the depth of the ocean.

The fact that the conductivity of sea water is generally at least two orders of magnitude higher than that of surface rocks means that, in the low frequency limit, it should be possible to treat the rocks as insulators so that any induced electrical currents are constrained to flow in the ocean and that the theory of Price (1949) for induction in infinitesimally thin sheets is

applicable.

Price derived the following equation for the problem of induction in a thin sheet:

$$\underline{\nabla}.\rho\underline{\nabla}\psi = -\mu\left(\frac{\partial Z^e}{\partial t} + \frac{\partial Z^i}{\partial t}\right) \qquad (1.3)$$

where $1/\rho$ is the vertically integrated conductivity defined as:

$$1/\rho = \int_o^h \sigma(z)\, dz \qquad (1.4)$$ (h being the depth of the ocean). ψ is the current streamline function which defines the current density in the following manner:

$$\underline{j} = -\hat{\underline{n}} \times \underline{\nabla}\psi \quad (1.5),$$

where $\hat{\underline{n}}$ is the outward unit normal. Z^e and Z^i are the external and internal vertical components of the magnetic field intensity (effectively the inducing and induced vertical fields).

Ashour (1950) developed an integral equation method for solving the problem of induction in uniform circular discs and surfaces of revolution by an axially-symmetric inducing field, which enabled him to make numerical estimates of the time constants, which would govern the decay of currents in the ocean. If currents were permitted to decay in a circular ocean, of radius 5000 km. and depth 4km., their amplitude would be reduced by a factor 1/e in 5.2 hours, if the conductivity of sea water was taken as 4 Sm^{-1}.

The problem of calculating the initial current induced in a perfectly conducting hemispherical thin shell by the instantaneous switching off of a uniform magnetic field, directed parallel to the plane of the equatorial rim of the shell, was examined by Rikitake and Yokoyama (1955). Their approach involved making a spherical harmonic expansion of the current function and solving for the coefficients, subject to the constraints that the total vertical field vanished at the surface of the shell and

that the current function was zero outwith the shell. To simplify the calculation, only twelve coefficients were used in the analysis, which was an insufficient number since currents were predicted to flow outside the shell and it seemed that the convergence of the spherical harmonic series was slow. The solution did partially agree with theory in that the total vertical field was close to zero at the surface of the shell, but it was unlikely that the truncated expansion was accurate in the vicinity of the discontinuity in conductivity at the rim of the shell.

Rikitake (1961) examined a similar problem, in which there was a concentric perfectly conducting sphere located below the hemispherical shell, where the ratio of the radii of the two conductors was 0.94. Although the method of analysis used by Rikitake in both of these examples was later to be proved wrong by Hobbs (1972), it was quite clear that the inclusion of the perfectly conducting sphere considerably reduced the current function and the induced vertical field. This implied that it was essential to consider electromagnetic coupling between the ocean and the mantle in attempts to model the effect of the oceans on geomagnetic variations.

Roden (1964) developed a numerical scheme for calculating the magnetic field induced in a thin uniform strip, which overlay a perfectly conducting half-space and predicted that very large fields would be observed close to the edges of the conducting strip. Although the method of accounting for the effects of the underlying half-space, which simulated the mantle, was later shown to be inaccurate, his prediction of the enhancement of the magnetic fields near the edge of the sheet was shown to be

correct by the work of Parker (1968), who devised an analytic scheme for solving the problem of induction in a thin uniform strip. Parker came to the conclusion that, in a finitely conducting strip, the current density was finite everywhere but that the vertical magnetic field had a logarithmic singularity at the edges of the strip.

Another analytic solution had been obtained by Ashour(1964, 1965), who used the technique of coordinate inversion and the solution of dual integral equations to solve the problem attempted by Rikitake and Yokoyama (1955). He demonstrated that the current density became infinite at the edge of the shell and that the vertical field became infinite on the non conducting side of the coastline. The solution of a similar problem, in which the inducing field was directed along the symmetry axis of the shell, was also presented, and the vertical field was again singular on the landward side of the rim.

Approximate solutions for induction in a uniform finitely conducting hemisphere were derived by Doss and Ashour (1971), who found that the induced vertical field was enhanced at the coastline on both sides of the coast, although it underwent a reversal on crossing the coast. The region over which enhancement occurred on the landward side was smaller than that found with the perfectly conducting shell and the horizontal field was enhanced on the seaward side. Further papers by Ashour (1971(b), 1971(c)) dealt with the cases of induction in thin discs and hemispheres, in which the conductivity decreased towards the edge. It was discovered that enhancement of the magnetic field near the edge was more pronounced at high frequencies and when the decrease in conductivity was confined to a region close to

the edge, corresponding to the continental shelf being near to the coastline. A method of calculating the field perturbations by an island had been presented, also by Ashour (1971(a)), by modelling the island as a circular or elliptical area of small, or vanishing, conductivity in a plane uniformly conducting infinite sheet. The magnetic fields were expressed in terms of contour integrals around the edge of the island but since the integrand contained the electrical potential, which was assumed to be known, this work could not be regarded as a solution of an induction problem, but rather of a current channeling problem.

The analytic methods of Ashour were only capable of dealing with highly symmetric conductors and it was clear that any attempt to model the real oceans would have to resort to numerical methods on account of the highly assymetric distribution of the oceans over the surface of the earth. In fact suitable numerical methods were becoming available at that time.

A paper by Hobbs (1971) described two algorithms for calculating the effects of induction in thin spherical shells, of varying conductivity, overlying a perfectly conducting concentric sphere, which were applicable to either high or low frequency inducing fields. Only the low frequency method is described here, since it forms the basis of the work presented in the following chapters.

This algorithm provides the means for solving Price's equation (1.3) for calculating the current streamline function induced in a thin sheet when only the primary external field is known. Equation (1.3) cannot be solved as it stands because the internal magnetic field, Z^i, is itself a function of the current streamline function ψ. If the primary inducing field arises from

ionospheric currents, the external inducing field Z^e is taken to be the sum of the primary vertical field, Z^p, and the vertical field, Z^c, due to currents that would be induced in the inner perfectly conducting core in the absence of any thin sheet at the surface.

$$Z^e = Z^p + Z^c \qquad (1.6)$$

If the radii of the inner and outer conductors are b and a respectively, and if the primary currents are described by a single spherical harmonic of unit amplitude and of degree n, then

$$Z^e = (1 - (b/a)^{2n+1}) Z^p \qquad (1.7)$$

The first step of the iterative method is to find an approximation, denoted by ψ_o, to the current function by solving equation (1.3) but neglecting the term in Z^i. The current fuction ψ_o will itself produce a vertical magnetic field, Z^s, which can induce further currents in the shell (the self induction effect) and will also induce currents in the central core, the vertical field of which, Z^m, would in turn induce more currents in the surface shell (the mutual induction effect). A first approximation to the internal field could be found by taking the sum of the vertical fields due to self and mutual induction:

$$Z_1^i = Z^s + Z^m \qquad (1.8)$$

The vertical fields due to self and mutual induction were calculated with the aid of surface integral formulae derived by Hobbs and Price (1970), the numerical calculation of which was based on the method of basic integrals of Price and Wilkins (1963).

By taking Z_1^i as a first approximation to the internal field, a correction term for the current function, ψ_1, could be found by solving equation (1.3) but this time the term in Z^e is to be

neglected. Repetition of this procedure resulted in the generation of further correction terms, ψ_2, ψ_3, etc., and the complete solution to equation (3.1), ψ, could be found iteratively, where:

$$\psi = \psi_0 + \psi_1 + \psi_2 + \ldots . \qquad (1.9)$$

and $$Z^i = Z_1^i + Z_2^i + Z_3^i + \ldots . (1.10)$$

For harmonic inducing fields, with frequency ω, the calculations were performed by removing the time dependence from equation (1.3) and soving for $\phi = \psi/\omega$, where $\omega^{n+1}\phi_n = \psi_n$. Equation (1.9) could then be transformed into the form:

$$\psi = \omega (\phi_0 + \omega \phi_1 + \omega^2 \phi_2 + \ldots .) \qquad (1.11)$$

Analysis of induction in a uniform spherical shell, for which an analytic solution could be found, demonstrated that equation (1.11) would only be convergent for periods greater than 15 - 20 hours, depending on the degree of the inducing field.

Application of the above method to the model of a hemispherical ocean demonstrated the enhancement of the vertical field on either side of the coast.

Bullard and Parker (1971) reformulated equation (1.3) as an integro-differential equation in ψ and solved the problem for the case of induction in the real oceans by the diurnal harmonic of Sq but, as has already been shown, Prices's iterative method could not be used at higher frequencies. However their maps of the current function did show how the coastlines distorted the current vortices from the shape that would have been expected, had the oceans been uniformly distributed over the surface of the earth.

Parkinson (1975) devised an algorithm, which was effectively a hybrid of the high and low frequency algorithms of Price, to solve the high frequency problem of induction in the real oceans

by substorms, however his solutions were unsatisfactory on two accounts. Firstly the calculations were performed on a coarse grid and it was not possible to state if the iterative method of solution had converged. Secondly the values of the current function on the continents were obtained by an averaging process, which had no physical basis, and resulted in artificially high current densities around the coastlines.

Hobbs and Brignall (1976) overcame the problems of divergence at high frequencies by making a Möbius transformation of the complex frequency plane and using analytic continuation to find a convergent series by transforming equation (1.11). An optimal Möbius transformation was found which also resulted in the improved convergence of the solutions to low frequency problems in addition to obtaining convergence at high frequencies. Application of this method to the model of a hemispherical ocean, by using the diurnal variation and its first seven harmonics, showed that the real part of the coast effect increased at higher frequencies, while the enhancement of the imaginary part decreased. The methods of Price and analytic continuation were used to predict the influence of the oceans on Sq by Hobbs and Dawes (1979) at frequencies of 1, 2, and 3 c.p.d., but the attempt to compare the calculated internal part with that obtained from observatory data was not particularly successful.

Almost contemporary with the work of Hobbs et al., several papers were published by Kendall and his co-workers, who adopted different approaches for solving the oceanic induction problem. An integral equation involving the current density and the vector magnetic potential was derived and solutions obtained for

axi-symmetric problems, e.g. induction in spherical caps (Hutson, Kendall and Malin,1972). The convergence of the iterative method of solving the integral equation was improved by using a technique of functional analysis, known as shifting the spectrum, (Hutson, Kendall and Malin, 1973) and a research note showing how shifting the spectrum of a linear operator and analytic continuation of a series could be related by a mathematical transformation was published by Kendall (1978).

An alternative approach to tackling the oceanic induction problem was developed in terms of calculating the scalar magnetic potential in three regions: above the ocean, in the neighbourhood of the land and between the ocean and the underlying conductosphere (Hewson-Browne and Kendall, 1978(a)). Analytic solutions involving Legendre series were found for the induction problem in a perfectly conducting hemispherical shell above a concentric perfectly conducting sphere and compared with the results obtained by an approximate numerical method, which showed that the two methods were in agreement except near the edge of the shell. A suitable edge correction, using the method of matched asymptotic expansions, was found (Hewson-Browne and Kendall, 1978(b)) and later applied to finitely conducting shells (Hewson-Browne, 1978). An edge correction for plane sheets has also been derived by Quinney (1979). Preliminary solutions, without the use of the edge correction, have been calculated for modelling the effect of the oceans on Sq, and although the effect of treating Antarctica and Australia as separate land masses altered the flow paterns, little improvement in the comparison with observatory observations was obtained (Beamish et al., 1978, I & II).

It should be stated that the oceanic induction problem has

received attention from Soviet scientists, but unfortunately not all of this work has been translated. Berdichevskiy and Zhdanov (1974) developed a formalism for isolating the field perturbations due to conductivity anomalies deep in the earth, provided that the normal conductivity profile and surface conductivity distribution (i.e. oceanic thin sheet) were known. Fainberg's review (1978) contained further details of the Soviet contribution to this field, which included his own approach where, although the method was not completely rigorous, he suggested that account should be taken of the earth's sedimentary cover in the conductance of the thin shell at the surface.

6.4) The techniques based on the work of Price described above are only capable of dealing with induction by the vertical component of the time-varying magnetic field in a thin sheet which is electrically isolated from any other conductors. Models have been studied in which these assumptions have not been made but, as yet, only in the case of plane geometry.

Weidelt (1971) provided an analytic solution of induction in two adjacent half-sheets of different conductances, which were insulated from an underlying perfectly conducting half-space, for the E-polarisation case. In this situation the primary uniform horizontal magnetic field is perpendicular to the junction between the two sheets and induces a horizontal electric field parallel to the strike, and the currents which it drives only give rise to the orthogonal horizontal and vertical induced magnetic fields. If a non-uniform inducing field had been used, Price's equation could still not have been used, since it contains terms involving the gradient of the integrated conductivity which is not defined at the boundary between the two sheets in the model described

above. However a suitable boundary condition was found in terms of the magnetic vector potential and its first vertical derivative. The solutions demonstrated that there was a logarithmic singularity in the vertical magnetic field at the junction, while the horizontal magnetic field remained finite although it was discontinuous there.

A model in which an oceanic strip and a perfectly conducting mantle were connected by a crust of small, but non-zero, conductivity was examined by Brewitt-Taylor (1975), who demonstrated that electric currents could be made to flow along the ocean, down through the crust, back along the mantle and return upwards into the ocean through the crust, for the case of H-polarisation. In this situation the inducing magnetic field is parallel to the strike, with the result that no induced magnetic field can be detected outside the conductor, provided the conductivity structure is strictly two-dimensional. The numerical solution of a related three-dimensional problem demonstrated that it was possible for the induced horizontal field normal to the coast and the vertical field to be large, while the induced horizontal field parallel to the coast was small, which was compatible with the concept of the Parkinson vector.

A more rigorous account of self induction effects was taken in a later paper (Brewitt-Taylor, 1976), where the horizontal magnetic field below the sea floor was calculated and the effect of return currents in the mantle was shown to be important provided that the width of the ocean was greater than two skin-depths in the crust.

Bailey (1977) used the Wiener-Hopf technique for solving mixed boundary value problems to find the effects of H-polarisa-

tion in a thin perfectly conducting half-sheet placed on a conducting half-space. Since the model was two-dimensional, no induced magnetic field could be detected above the surface. Solutions were presented for the magnetic field below the sheet, for the induced electric fields as well as the amplitude and phase of the magnetotelluric response function. Diagrams of the induced currents demonstrated how they flowed vertically from the thin sheet into the substratum.

Nicoll and Weaver (1977) obtained the solution for H-polarisation in a similar model, which now included a perfectly conducting mantle below a poorly conducting crust, also with the aid of the Wiener-Hopf technique.

The Pyrenean induction anomaly was modelled by a conductor between the Atlantic Ocean and the Mediterranean Sea, all of which were confined to a thin sheet at the surface of a two-layered half-space, by Vasseur and Weidelt (1977), who solved the problem of induction by solving an integral equation, involving Green's functions, over the region of anomalous conductivity in the thin sheet.

The E-polarisation counterpart of the problem solved by Bailey was published by Fischer, Schnegg and Usadel (1978) by numerically solving an integral equation, in the derivation of which the terms involving the displacement current had not been discarded, so that the method would also be applicable to modelling inductive prospecting.

An integral equation was derived, and solved numerically, by Green and Weaver (1978) for dealing with a thin sheet of variable conductivity in electrical contact with a conducting half-space. This method did not require the surface conductivity to be

separated into normal and anomalous parts, as was required by the approach of Vasseur and Weidelt, and both E- and H-polarisation problems could be tackled. The E-polarisation case was shown to be equivalent to the quasi static form of the method of Fischer et al. A further application of the Wiener-Hopf method enabled Dawson and Weaver (1979) to obtain an analytic solution for H-polarisation induction in a more generalised form of the model used by Weidelt (1971), where the two thin sheets were now connected to a conducting half-space. This analytic solution could serve as a useful check on numerical schemes such as that of Green and Weaver.

1.5) The work cited in the previous sections has been concerned with the electric currents that have been induced in an ocean, or oceanic model, by a time-varying magnetic field. This however is not the only mechanism by which electrical currents can be made to flow in the oceans, since studies have shown that it is possible to detect magnetic fields which arise from the movement of sea water through the main part of the geomagnetic field. Although motionally induced currents are not considered in the following chapters, they do merit at least a brief mention in any review of induction in the oceans. An electric field, defined by $\underline{E} = \underline{v} \times \underline{B}$, is generated by the motion of the conducting seawater, with velocity $\underline{v}$, across the main field of the earth, $\underline{B}$, which is a dynamo process, as opposed to a magnetovariational process. Geomagnetic variations are not really important for this kind of study since even a magnetic storm, with a typical amplitude of a few hundred nanoteslas, is comparatively insignificant compared with the steady main field, which is of the order of 45,000 nT in strength. There are two main categories: tidal

effects and wave effects.

Faraday, the discoverer of electromagnetic induction, predicted that sea tides could give rise to a motionally induced electromotive force which would be detectable across the width of the English Channel. This was in fact achieved by Wollaston in the middle of the nineteenth century and more recently by Cherry and Stovold (1946), who detected correlations between the tides and voltage measurements on cross-channel electric cables. The observed potential difference turned out to be smaller than that calculated by Barber and Longuet-Higgins (1948), who explained the discrepancy by postulating that return currents would flow in the sea floor and stated that the magnetic field of these poloidal currents would not be detectable ashore.

A theoretical study of large scale ocean flow by Sanford (1971) showed that the effects of mutual induction between the motionally induced currents and the mantle became important when the skin depth in the mantle was much smaller than the horizontal scale of the flow patern, which was in accordance with the Larsen's (1968) conclusion that it was necessary to know the spatial variability of the tides before they could be used as a technique for geomagnetic depth sounding.

Further work with submarine cables was done by Richards (1977), who detected the Sq harmonics with frequencies of 1, 2, 3 and 4 c.p.d. in addition to three tidal dynamo harmonics with frequencies .928, 1.896 and 1.932 c.p.d. in his signals. The assumption that any night time contribution to the lunar daily geomagnetic variation must have had an oceanic, rather than ionospheric, origin has formed the basis of a technique for separating this geomagnetic variation into parts with oceanic,

essentially tidal, and ionospheric sources (Malin, 1977).

The initial work on the magnetic field produced by waves was mainly concerned with wind driven surface waves, but larger scale and deeper phenomena have also been studied. Fraser (1965) studied the effect of waves with a magnetometer mounted on the sea floor at a depth of 120 feet. By using the shallow water approximation, the Biot-Savart Law and the power spectrum of the waves, it was possible to obtain a close correlation between the observed and calculated magnetic spectra in the frequency range .05-.15 Hz. In the work of Weaver (1965) the magnetic fields were calculated with the use of an assumed velocity potential, which was more direct than the approach of Fraser. It was demonstrated that wave amplitude and wavelength were important variables in the analysis and that the effects of wind generated waves and swell could be comparable.

The effects of longer period (1-30 minutes) internal waves were found to be less significant than surface waves by Beal and Weaver (1970), while Larsen (1971) restated the dependence on frequency and wavenumber in addition to self induction in the ocean and mutual induction in the mantle in his study of long and intermediate period water waves.

While operating a magnetometer on the sea floor, Cox et al. (1978) detected a signal which was not correlated with the fields measured at a nearby land site, but which seemed to be correlated with the surface waves with periods twice that of the anomalous signal. They proposed that the mechanism for this was due to non-linear interactions between surface waves, travelling in opposite directions, resulting in motion across geomagnetic field lines. Such a process has also been suggested to be responsible

for the generation of microseisms.

Semerskiy et al. (1978) have examined the possibility of detecting the wave generated magnetic field with a magnetometer towed by a ship, which involved taking the velocity of the magnetometer into account.

Chapter Two

The Method for Dealing with a Finitely Conducting Mantle.

2.1) All of the work, refered to in the introduction, on the solution of the oceanic induction problem in spherical geometry has been done by using a perfectly conducting shell to model the highly conducting regions of the mantle. (Rikitake,Ashour,Bullard & Parker,Hobbs,Kendall et al.) The reason for this choice of conductosphere is because it is easy to deal with, mathematically. However, since much effort has been used to make models more realistic, by using a surface conductivity distribution resembling the real oceans, it seems reasonable that an attempt should be made to use a conductosphere which is more representative of the earth's conductivity.

The perfectly conducting shell is easy to deal with because of the special electromagnetic boundary conditions, which have to be satisfied at its surface: the tangential electric field and the normal magnetic field must vanish. Consequently any magnetic field induced in a perfect conductor must be exactly 180^{o} out of phase with the inducing field, whereas with a finite conductor the boundary conditions only demand continuity of the above mentioned fields across an interface and there is a quadrature, or out-of-phase, component of the induced magnetic field. The response of a perfect conductor can be assigned a purely real value, which is known analytically, while that of a finite conductor is complex and has to be calculated numerically, except for a few special cases, for each frequency used for general conductivity distributions.

Analysis of results shows that the internal contribution due to induction in the conductosphere alone is greater than the

oceanic part, which emphasises the need to use a realistic inner conductor , especially when a comparison between modelling and observations is to be made. As an example, the ratio of internal to external parts, defined at the surface of the earth (r=a), for a perfect conductor of radius b and an inducing field of degree n has the value $n/(n+1)\ (b/a)^{2n+1}$. For a second order harmonic and if (b/a)=0.9, this ratio has the value of 0.393. If a thin surface sheet with integrated conductivity of 16,000 S (corresponding to an ocean 4 km deep) is added to the model then the ratio of internal to external parts can still be found analytically (Hobbs, 1971, eqn.18) and has the following value: $(.511, 14.9^{o})$ in terms of amplitude and phase and (.494,.131) in terms of real and imaginary parts.

Bullard and Parker actually suggested a method for dealing with a finitely conducting mantle (Bullard & Parker, p718) but they excused themselves for not using it by stating that it was mathematically rather involved. However their suggested method is the approach the author has elected to pursue and the following text should demonstrate the simplicity of the method.

2.2) The Hobbs-Price surface integrals were originally derived by taking an implicit spherical harmonic expansion of the current streamline function and using potential theory and well known series of Legendre polynomials. The author however found it instructive to think in terms of a system equivalent to a current streamline function, namely a surface distribution of radially oriented magnetic dipoles (Stratton, 1941, 237-8). The approach used was to find the vertical magnetic field at the surface of the conductosphere, as a function of colatitude, due to a magnetic dipole at the surface of the earth and to perform

spherical harmonic analysis to find the source harmonics in this inducing field. The justification for this is that the theory for induction in a radially symmetric earth by an inducing field, which can be represented by a series of spherical harmonic terms, is well known (Rikitake, 1966,p128-9).

It is instructive to demonstrate that a current streamline function $\psi(\theta,\phi)$ and a surface distribution of vertical magnetic dipoles, with surface density $m(\theta,\phi)$, give rise to the same magnetic field when the functions m and ψ are identical.

Initially consider the scalar magnetic potential at a point $P(r,\theta,\phi)$ due to an elemental area dS of a dipole distribution of density m at the point $Q(r',\theta',\phi')$ (see Fig. 2.1) so that the potential at P is

$$d\Omega = \frac{\mu_0 m}{4\pi}(r',\theta',\phi')dS\cos\chi/R^2 \quad \text{and} \quad \underline{B} = -\underline{\nabla}\Omega \qquad (2.1).$$

Where $\cos\chi = (r^2 - r'^2 - R^2)/2r'R$, $R^2 = r^2 + r'^2 - 2rr'\cos\Theta$

and $\cos\Theta = \cos\theta\cos\theta' + \sin\theta\sin\theta'\cos(\phi-\phi')$. (2.2)

Therefore $d\Omega = (\mu_0 m/4\pi)\,(r\cos\Theta - r')/(r^2 + r'^2 - 2rr'\cos\Theta)^{3/2}$ (2.3)

Accordingly the potential at the point $P(r,\theta,\phi)$ due to a surface distribution of radial dipoles of moment density $m(\theta',\phi')$/unit area over the spherical shell r=a is given by:

$$\Omega_p = (\mu_0 a^2/4\pi)\int_0^{2\pi}\int_0^{\pi} \frac{(r\cos\Theta - a)\sin\theta'}{(r^2 + a^2 - 2ra\cos\Theta)^{3/2}}\, m\,(\theta',\phi')\, d\theta' d\phi' \qquad (2.4)$$

It is instructive to consider the case of a uniform dipole density distribution to demonstrate the relation between a dipole distribution and an equivalent current function. In this case let $m(\theta',\phi') = m_0$ (a constant) and by spherical symmetry Ω is independent of θ and ϕ. Without loss of generality take P on the axis $\theta=0$, so that $\Theta = \theta'$. Therefore by eqn. (2.4)

$$\Omega(r,\theta,\phi) = (\mu_0 a^2\, 2\, m\, /4\,)\int_0^{\pi} \frac{(r\cos\theta' - a)\sin\theta'}{(r^2 + a^2 - 2ra\cos\theta')^{3/2}}\, d\theta' \qquad (2.5)$$

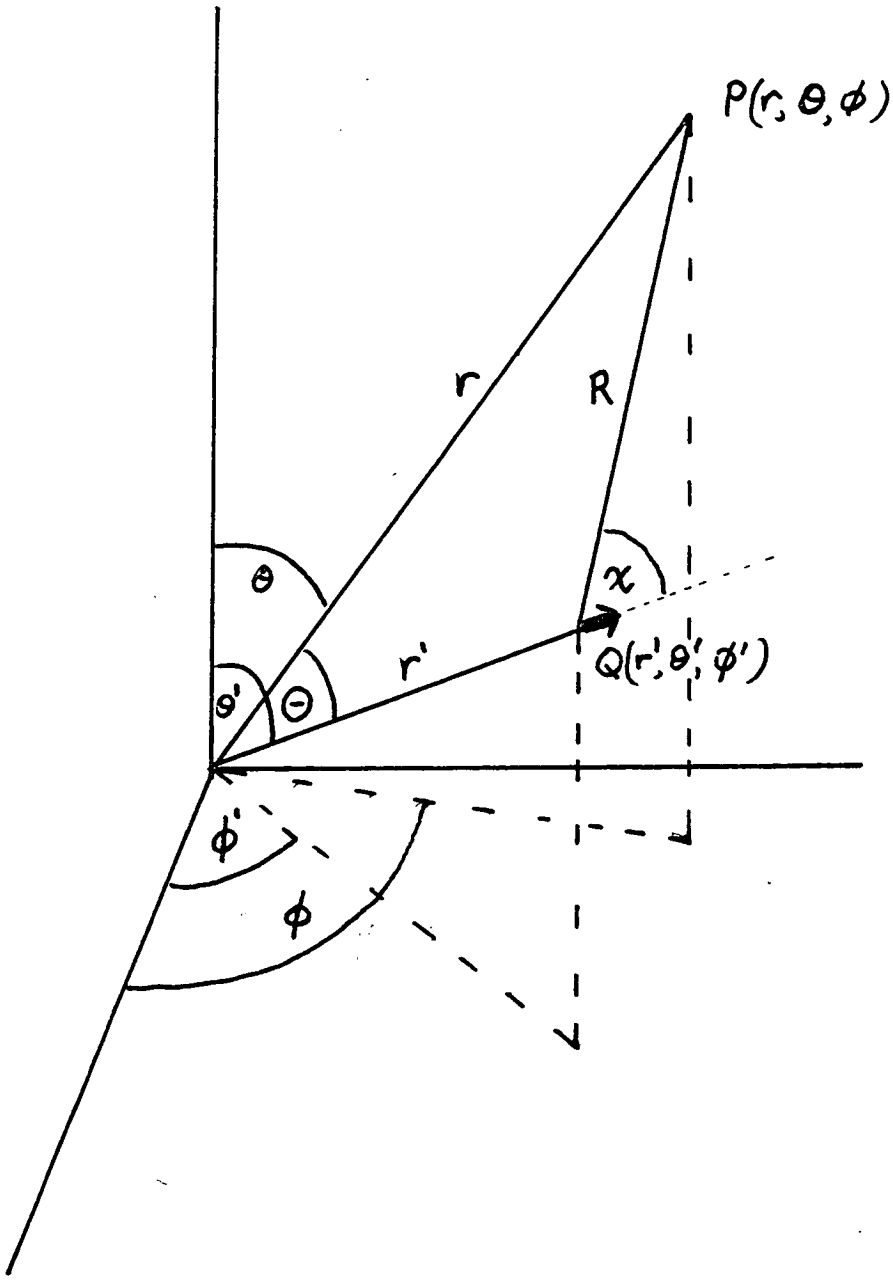
P(r, θ, φ)
r
R
θ
χ
r'
Q(r', θ', φ')
θ'
Θ
φ'
φ

substituting $u = (r^2 + a^2 - 2ar\cos\theta')^{1/2}$ yields:

$$\Omega(r,\theta,\phi) = (\mu_0 m_0/4r)\int_{r-a}^{|r-a|} 1 - ((r^2 - a^2)/u^2)\,du = (\mu_0 m_0/4r)\begin{cases} 0 & ,r>a \\ -4r & ,r<a \end{cases}$$

The introduction of the Heaviside unit step function defined as $H(x) = \begin{cases} 1 & x>0 \\ 0 & x<0 \end{cases}$ leads to the following expression for the potential: $\Omega(r,\theta,\phi) = -\mu_0 m_0 H(a-r)$ (2.6)

This special case demonstrates that the magnitude of the discontinuity in the potential across the dipole layer at any point is given by the product of the permeability constant and the density of the distribution at that point, which is also the case if one is considering the potential due to a current function, where $\psi(\theta',\phi') = 1/\mu_0\,(\Omega_+ - \Omega_-)$ (Price, 1949, eqn 8).

It is of greater interest to examine the magnetic fields of the dipole distribution rather than the potential, since the field is a directly measureable quantity. Only the vertical field (Z) will be considered here, where $Z = -\frac{\partial\Omega}{\partial r}$.

Accordingly the vertical field at the point P can be found by performing differentiation under the integral sign in eqn. (2.4), but care must be taken if the point P should lie on the surface r=a when the kernel of the surface integral tends to a limit of order $1/\Theta^2$ as $\Theta \to 0$. In this case the resulting integral would not be uniformly convergent when $\theta' = \theta$ and $\phi' = \phi$ and the differentiation under the integral sign would be an invalid operation.

Convergence can be secured with the aid of the example of the uniform dipole distribution, where (2.4) can be rewritten as:

$$-m(\theta,\phi)\mu_0 H(a-r) = (\mu_0 a^2/4\pi)\int_0^{2\pi}\int_0^{\pi} m(\theta,\phi)\; f(r,\theta,\phi,a,\theta',\phi')\,d\theta'\,d\phi' \quad (2.7)$$

where m_0 has been replaced by $m(\theta,\phi)$, the dipole density at the point P and f is the integrand (excluding the factor $m(\theta',\phi')$)

in eqn. (2.4). Subtracting this result from the general form of eqn. (2.4) yields $\Omega(r,\theta,\phi)+\mu_0 m(\theta,\phi)H(a-r) =$

$$(\mu_0 a^2/4\pi)\int_0^{2\pi}\int_0^{\pi}\{m(\theta',\phi') - m(\theta,\phi)\}\, f(r,\theta,\phi,a,\theta',\phi')\, d\theta' d\phi' \qquad (2.8)$$

Differentiation under the integral sign is now permitted because the difference term removes the singularity at $\theta'=\theta$ and $\phi'=\phi$. Strictly speaking care is needed in dealing with the derivative of the Heaviside function at r=a otherwise a term involving the Dirac delta function arises but this can be prevented if the vertical field at r=a is redefined as $Z_{r=a} = \lim_{r\to a} -\frac{\partial\Omega}{\partial r}$. On this basis $Z(r=a) =$

$$-(\mu_0 a^2/4\pi)\int_0^{2\pi}\int_0^{\pi}\{m(\theta',\phi') - m(\theta,\phi)\}\lim_{r\to a}\frac{\partial}{\partial r} f(r,\theta,\phi,a,\theta',\phi')\, d\theta' d\phi'$$

$$= -(\mu_0 a^2/4\pi)\int_0^{2\pi}\int_0^{\pi}\{m(\theta',\phi') - m(\theta,\phi)\}\,\frac{(1+\sin^2\Theta/2)\,\sin\theta'}{8a^3\sin^3\Theta/2}\, d\theta' d\phi'$$

$$= -(\mu_0 a^2/4\pi)\int_0^{2\pi}\int_0^{\pi} m(\theta',\phi')\,\frac{(1+\sin^2\Theta/2)\,\sin\theta'}{8a^3\sin^3\Theta/2} d\theta' d\phi' + (\mu_0/4\pi a)m(\theta,\phi) \qquad (2.9)$$

This final expression is equivalent to the self induction surface integral (Hobbs & Price, 1970, eqn. 66) as can be seen by substituting ψ for $m(\theta',\phi')$ and ψ_A for $m(\theta,\phi)$ provided allowance is made for the use of S.I. units and an outward vertical field in this presentation. It is straightforward to demonstrate that the limit of the derivative is the same when $r \to a$ from both outside and inside the shell as is required by the continuity of the vertical field across a dipole sheet, or equivalent current sheet.

The vertical field can be found at any point not on the dipole shell by differentiating (2.4) directly since the problem with uniform convergence does not arise when $r \neq a$. In particular the vertical field at a point on a shell of radius b ($b \neq a$) can be given by:

$$Z(b,\theta,\phi) = (\mu_0/4\pi)\int_0^{2\pi}\int_0^{\pi} \frac{(-3ab-ab\cos^2\theta+2(a^2+b^2)\cos\theta)\,m(\theta',\phi')\,dS'}{(a^2+b^2-2ab\cos\theta)^{5/2}} \qquad (2.9a)$$

$$= \int_0^{2\pi}\int_0^{\pi} Z_c(\theta,b)\; m(\theta',\phi')dS'$$

It now becomes possible to derive the kernel of the mutual induction integral, by using the results of the method of images, which is easily applied to problems of perfect conductivity. The currents induced in a perfectly conducting shell (radius=b), by a magnetic dipole of strength m (at r=a), give rise to the same magnetic field as an image dipole, of strength $-(b/a)^3$, at a radius of b^2/a (Bonnevier, Boström & Rostoker, 1970).

The mutual induction integral gives the induced vertical field at a surface (r=a) and can be found from eqn. (2.9a) by substituting a for b, since it is the field at the surface which is of interest, and b^2/a for a, since the sources are now situated at this depth. It is also necessary to multiply by a factor of $-(b/a)^3$, the comparative strength of the image dipoles. In this case

$$R=(a^2+b^2-2ab\cos\theta)^{1/2} \longrightarrow (b^4/a^2+a^2-2b^2\cos\theta)^{1/2}$$

$$-3ab-ab\cos^2\theta+2(a^2+b^2)\cos\theta \longrightarrow -3b^2-b^2\cos^2\theta+2(b^4/a^2+a^2)\cos\theta \text{ and}$$

$$Z_c(\theta,b) \longrightarrow Z_m(\theta,a) = -(b^3/\mu_0/4\pi)\;\frac{(-3a^2b^2+2(a^4+b^4)\cos\theta-a^2b^2\cos^2\theta)}{(a^4+b^4-2a^2b^2\cos\theta)^{5/2}} \qquad (2.10)$$

This is just $-(\mu_0/4\pi)$ times the kernel in the expression for $\left.\frac{\partial\Omega^*}{\partial r}\right|_A$ in the original paper (Hobbs & Price, 1970, eqn.91).

It is easy to find the mutual induction kernel in the case of a perfect conductor, because there is only a single image dipole, but the situation is not so simple in the case of a finitely conducting mantle. There is in fact a theory of complex images for the case of induction in a plane earth (Weaver, 1971 & Thomson & Weaver, 1975) but this involves making certain

approximations and no attempt was made to apply the theory in spherical geometry and an alternative approach was used.

Using the properties of the magnetic dipole provides a simple method of deriving the surface integral kernels for finding the vertical field due to self and mutual induction and the scalar magnetic potential but the method is not so suitable for finding some other kernels. Examples of the latter kind are the equivalent current system integral kernel (Hobbs and Dawes, 1979, eqn. 28) and the kernel for finding the current function giving rise to a known vertical field (Hobbs & Price, eqn.63), which is used in the high frequency iterative method.

Henceforth the angular argument in the kernel $Z_c(\Theta,b)$ is defined as the angle subtended at the centre of the earth by radii passing through the source and observation points, which also applies to all other kernels used. Since this is the only angle to appear in the expression for Z_c, it is possible to rewrite it as the infinite sum of Legendre polynomials:
$Z_c(\Theta,b) = \sum_{n=1}^{\infty} a_n P_n(\cos\Theta)$ (2.11). The coefficients a_n can be found by using the orthogonal properties of Legendre polynomials:
$\int_0^{\pi} P_n(\cos\Theta)\, P_m(\cos\Theta)\, \sin\Theta\, d\Theta = 2/(2n+1)\,\delta_{nm}$ (2.12)
where δ is the Kronecker delta symbol.

Once the coefficients have been found, the response can be determined for each harmonic, and the induced vertical field can be expressed as an infinite Legendre series. There are no problems with convergence in the case when $b < a$.

This approach is similar to that used by Ducruix, Courtillot and Le Mouel (1977), who drew comparisons between results obtained from modelling induction due to the equatorial electrojet, in both plane and spherical geometries. The electrojet, in

the spherical case, was modelled by a line current at a height of 100 km. above the equator, passing half-way round the earth, and with return currents following the meridian over the North Pole at the same height. This system of line currents, enclosing a quarter of a spherical shell, is of course equivalent to a uniform distribution of radial magnetic dipoles (or a magnetic double layer, in the authors' terminology) over the same quarter spherical surface.

The inducing magnetic potential at a point is then defined in terms of the solid angle subtended by the current loop at that point, which can be expressed as an infinite series of spherical harmonics.

The disadvantage of this approach is that by concentrating on the structure of the complete source, which is implicitly done in using the solid angle relation, it is necessary to consider all spherical harmonics, zonal, tesseral and sectoral, in the series, which involves finding $(n+1)^2-1$ coefficients for an nth. order analysis, although the symmetry of this electrojet model would actually reduce this number. It is necessary to calculate the effects of mutual induction after each iteration in the Price scheme for solving the thin sheet induction problem. If the approach of Ducruix et al. had been used, it would have been necessary to find the spherical harmonic coefficients of the solid angle subtended by a non-uniform source, the current streamline function, after each iteration, which would have involved considerable computation. Alternatively by concentrating on the field of a single dipole, it is only necessary to use zonal harmonics in the spherical harmonic analysis, because of the axial symmetry, therefore after

synthesising the mutual induction kernel, the basic integrals only need to be calculated once and, having been stored, can be used during every iteration.

An alternative approach to the problem of solving the problem of induction in a finitely conducting spherical earth by an arbitrary inducing field has been used by Mareschal and Kisabeth (1977) to model the mid-latitude effect of substorms. This method involved expressing the induced field as an infinite series involving the inducing field and its derivatives, but the authors stated that the method was not suitable for high-latitude studies and that the truncation of the series after only two terms was valid only for high frequency inducing fields. With these reservations in mind, it did not seem that this approach was suitable for solving a global problem associated with the diurnal geomagnetic variation and its harmonics.

2.3) Calculation of the Legendre Coefficients.

1) Semi-analytic Method.

The Legendre coefficients a_n can be found by integration:

$$a_n = \frac{2n+1}{n} \int_0^{\pi} Z_c(\theta,b)\, P_n(\cos\theta)\, \sin\theta\, d\theta \quad (2.13)$$

Since $Z_c(\theta,b)$ is a rather involved algebraic function of $\cos\theta$, which does not seem to have any obvious relation to the generating function for Legendre polynomials, the first attempt to calculate the coefficients involved solving the integral of the product of $Z_c(\theta,b)$ with a single power of $\cos\theta$, rather than with a Legendre polynomial, which is a finite sum of powers of $\cos\theta$.

These integrals could be solved in three parts since the numerator of $Z_c(\theta,b)$ involves three different powers of $\cos\theta$ (namely 0,1,2). Taking the integral of the mth power of $\cos\theta$

divided by the denominator of Z_c defines the following integrals:

$$I_m = \int_0^{\pi} \frac{\cos^m\theta \sin\theta \, d\theta}{(a^2 + b^2 - 2ab\cos\theta)^{5/2}} \quad (2.14)$$

Redefining $a^2+b^2=c$ and $2ab=d$ yields:

$$I_m = \int_0^{\pi} \frac{\cos^m\theta \sin\theta \, d\theta}{(c - d\cos\theta)^{5/2}}$$

and changing the variable to $t=c-d\cos\theta$ gives:

$$I_m = \frac{1}{d^{m+1}} \int_{c-d}^{c+d} \frac{(c-t)^m}{t^{5/2}} \, dt = \frac{1}{d^{m+1}} \int_{c-d}^{c+d} \sum_{n=0}^{m} \binom{m}{n} (-1)^n t^{n-5/2} c^{m-n} dt$$

$$= \frac{1}{d^{m+1}} \sum_{n=0}^{m} \binom{m}{n} (-1)^n \left[\frac{t^{n-3/2}}{n-3/2} \right]_{c-d}^{c+d} c^{m-n}. \text{ The following back substitutions are now made:}$$

$c\pm d=(a\pm b)^2$, $d=2ab$, $c=a^2+b^2$, then

$$I_m = \frac{1}{(2ab)^{m+1}} \sum_{n=0}^{m} \binom{m}{n} (-1)^n \frac{(a+b)^{2n-3} - (a-b)^{2n-3}}{n-3/2} (a^2+b^2)^{m-n} \quad (2.15)$$

Adding together the three terms from the numerator of Z_c yields:

$$\int_0^{\pi} Z_c(\theta,b) \cos^m\theta \sin\theta \, d\theta = (-3abI_m + 2(a^2+b^2)I_{m+1} - abI_{m+2}) = b_m \quad (2.16)$$

$$\text{and } \int_0^{\pi} Z_c(\theta,b) P_n(\cos\theta) \sin\theta \, d\theta = \sum_{k=0}^{n} g_k b_k \quad (2.17)$$

$$\text{where } P_n(\cos\theta) = \sum_{k=0}^{n} g_k \cos^k\theta \quad (2.18)$$

Only the alternate coefficients g_k have non-zero values, depending on the parity of the polynomial and they can be calculated recursively from the expanded form of the Legendre polynomial:

$$P_n(z) = \frac{(2n)!}{2^n(n!)^2} \left(z^n - \frac{n(n-1)}{2(2n-1)} z^{n-2} + \frac{n(n-1)(n-2)(n-3)}{2 \cdot 4 \cdot (2n-1)(2n-3)} z^{n-4} + \ldots\right) \quad (2.19)$$

(Gradshteyn & Ryzhik, 1965), where $g_n = \frac{(2n)!}{2^n(n!)^2}$ (2.20)

and $g_{n-k-2} = -\frac{(n-k)(n-k-1)}{(k+2)(2n-k-1)} g_{n-k}$ (2.21)

These calculations were performed by computer but the attempt to resynthesise $Z_c(\theta,b)$ up to order 20 for the case

b/a=0.875 was not very successful, which was probably due to careless programming when calculating the expressions given in eqn. (2.15). This could have been overcome by using double precision and taking care to avoid subtracting similarly sized quantities, but it was decided to resort to other methods.

11) Full Numerical Method.

It is possible to generate Legendre polynomials by using one of the many recurrence relations e.g.

$$(n+1)P_{n+1}(\cos\theta) - (2n+1)\cos\theta P_n(\cos\theta) + nP_{n-1}(\cos\theta) = 0 \quad (2.22)$$

or $$P_{n+1}(\cos\theta) = ((2n+1)\cos\theta\, P_n(\cos\theta) - nP_{n-1}(\cos\theta))/(n+1) \quad (2.23)$$

Although the right hand side involves a subtraction, which is often the source of numerical instability, analysis shows that this recurrence relation is numerically stable (N.P.L., Modern Computing Methods,p.149), which makes it easy to calculate the Legendre coefficients numerically.

A step length of $\pi/1024$ was used in calculating the first fifty Legendre coefficients using Simpson's rule, which was a sufficiently fine partition, since there was excellent agreement between the original function and the sum of the first fifty terms for the case b/a =0.875.

It should be stressed that it was essential to calculate the integrals in the angular domain, e.g. as $\int_0^{\pi} Z_c(\theta,b)\, P_n(\cos\theta)\, \sin\theta d\theta$, rather than, having made a change of variable to $t=\cos\theta$, as $\int_{-1}^{+1} Z_c(t,b) P_n(t)\, dt$, since the $\sin\theta$ term is necessary to remove the sharp peak that occurs in $Z_c(\theta,b)$ at small angles, which would otherwise make it more difficult to obtain an accurate value of the integral numerically.

Although the numerical method gave excellent results, it would have been necessary to rerun the program each time a

different size of conductosphere was used; it was therefore still desirable to find an analytic expression.

111) Full Analytic Method.

This method makes use of the addition theorem of spherical harmonics (Hochstadt, 1971, p149). If (θ, λ) and (θ', λ') are the coordinates of two points on the surface of a sphere and the radii passing through them subtend an angle Θ at the centre then:

$$\cos\Theta = \cos\theta\cos\theta' + \sin\theta\sin\theta'\cos(\lambda-\lambda') \quad (2.24)$$

and $$P_n(\cos\Theta) = P_n(\cos\theta)P_n(\cos\theta') + 2\sum_{m=1}^{n}\frac{(n-m)!}{(n+m)!} P_n^m(\cos\theta)P_n^m(\cos\theta')\cos m(\lambda-\lambda') \quad (2.25)$$

It is also helpful to use some of the analytic results from Hobbs and Price (1970), derived for the case of a current function represented by a single surface harmonic, of degree n, $P_n^m(\cos\theta)\cos m\lambda$, at the surface r=a. The currents induced in a perfectly conducting shell, at radius b, give rise to a magnetic field, which at the surface $r=a$ has a vertical component given by :

$$Z = -\mu_0\frac{n(n+1)}{(2n+1)a}(b/a)^{2n+1} P_n^m(\cos\theta)\cos m\lambda \quad (2.26)$$

(Hobbs & Price 1970, eqn. (1) & (18), the factor 4π, which appears in the original paper, is replaced by μ_0 when S.I. units are used).

Because of the boundary conditions which apply to perfect conductors, the induced field must be equal and opposite to the inducing field at the radius r=b, while its value is reduced by an upward continuation factor of $(b/a)^{n+2}$ at the surface r=a.

Therefore if the inducing field at r=b ,due to a unit radial dipole at r=a, is given by:

$$Z_c(b,\theta) = \sum a_n P_n(\cos\theta) \quad (2.26a),$$

then the induced field at the surface of the earth will have the

value $-\sum(b/a)^{n+2} a_n P_n(\cos\theta)$, which is equivalent to the mutual induction kernel $K_m(\theta)$. The vertical field at the surface due to mutual induction is given by integrating the product of the mutual induction kernel with the current streamline function (or equivalently, the magnetic dipole distribution) over the surface of the earth.

$$\iint K_m(\theta)\,\psi\,dS = Z_m \quad (2.27)$$

If the current function is given by one harmonic, $P_n^m(\cos\theta')\cos m\lambda'$, then:

$$-Z_m = \mu_0 \frac{n(n+1)}{(2n+1)a} (b/a)^{2n+1} P_n^m(\cos\theta')\cos m\lambda' \quad (2.28)$$

Substituting the series for $K_m(\theta)$ into equation (2.27) yields:

$$-\iint \sum_f a_f (b/a)^{f+2} P_f(\cos\theta) P_n^m(\cos\theta')\cos m\lambda'\, dS = Z_m \quad (2.29)$$

By using the addition theorem (eqn. 2.25), expanding $\cos m(\lambda - \lambda') = \cos m\lambda \cos m\lambda' + \sin m\lambda \sin m\lambda'$ and using the orthogonality of spherical harmonics, it is possible to reduce the left hand side of eqn. 2.29 to:

$$-a_n (b/a)^{n+2} \frac{2(n-m)!}{(n+m)!} P_n^m(\cos\theta) \cos m\lambda \int_0^{\pi} \left[P_n^m(\cos\theta')\right]^2 a^2 \sin\theta' d\theta' \times \int_0^{2\pi} \cos^2 m\lambda'\, d\lambda'$$

Hence $-4\pi a^2 a_n (b/a)^{n+2} \frac{1}{2n+1} P_n^m(\cos\theta)\cos m\lambda = Z_m(\theta,\lambda) \quad (2.30)$

Substituting for Z_m and solving for a_n yields:

$$a_n = \mu_0 \frac{n(n+1)}{4\pi a^3} (b/a)^{n-1} \quad (2.31)$$

This defines the Legendre coefficients of the vertical inducing field at the surface of the conductosphere and the numerically determined values were in excellent agreement with the analytically derived values.

2.4) Calculating the Mutual Induction Kernel.

Allowing for the upward continuation factor of $(b/a)^{n+2}$ and using the values obtained for a_n, the mutual induction kernel for

the perfect conductor can be written as:

$$K_m(\theta) = \frac{\mu_0}{4\pi a^3}\sum n(n+1)(b/a)^{2n+1} P_n(\cos\theta) \quad (2.32).$$

This can be shown to reduce to eqn.2.10 by using the methods of Hobbs & Price (1970).

Equation (2.32) incorporates the response of the conductosphere , which, for a perfect conductor, is given by $n/(n+1)$. If the response of a general conductor is denoted by: i_n/e_n , then the mutual induction kernel can be written as:

$$K_m(\theta) = \frac{\mu_0}{4\pi a^3}\sum (n+1)^2 (b/a)^{2n+1} \, i_n/e_n \, P_n(\cos\theta) \quad (2.33)$$

The only problem remaining is to calculate the response, i_n/e_n, for a finite conductivity distribution.

It was not strictly essential to calculate the Legendre coefficients of equation (2.26a) since it would have been possible to derive the mutual induction kernel for a finite conductor from the series form of the kernel for the perfect conductor by substituting i_n/e_n for $n/(n+1)$. However the calculations presented here outline the actual approach used by the author and show an interesting link between the approaches of Hobbs and Price and Ducruix et al. to solving induction problems with inducing fields for which a suitable current streamline function can be found as a source. The calculations of Legendre coefficients might also be of use if a Green's function approach were to be used to solve the oceanic induction problem. It would also be required to find the source terms in the expansion of the field of a horizontal electric dipole in the more general problem in which the oceans were in contact with the mantle.

CHAPTER THREE

THE UNIFORM FINITELY CONDUCTING SPHERE

3.1) Why a uniform sphere ?

Although the ultimate aim was to solve the oceanic induction problem with a general conductosphere, albeit with the constraint that the conductivity distribution was a function of radius only, the first finitely conducting model for the mantle that the author chose to examine was the uniform sphere. The main justification for this was that this is one of the few models for which analytic solutions of the induction problem exist (Hobbs,1975).

The solution for the field involves modified spherical Bessel functions of the first kind, usually denoted by $I_{n+\frac{1}{2}}(z)$, where n denotes the order of the inducing field. It was more convenient to use a response function, i.e. the ratio of internal to external parts, rather than the magnetic fields themselves and this ratio can be found by applying the standard electromagnetic boundary conditions at the surface of the sphere. If the relative permeability of the sphere is taken as unity (as is usually the case in global induction studies), the ratio of internal to external parts, defined at the surface of the conductosphere (r=b) is given by:

$$i_n/e_n = \frac{n}{n+1}\left[1 - \frac{(2n+1)\, I_{n+\frac{1}{2}}(kb)}{kb \quad I_{n-\frac{1}{2}}(kb)}\right] \qquad (3.1)$$

where $k^2 = i\mu_0\omega\sigma$ (3.2),

μ_0 is the permeability of free space, σ is the conductivity of the sphere and ω is the frequency of the inducing field.

Since it was the author's intention to compare the results obtained with finitely and perfectly conducting mantles, the

radius b was taken to be 0.875 earth radii, a radius used by Ashour (1971c), and the value of the finite conductivity was chosen as 1 Sm^{-1}. This value is approximately the appropriate conductivity at .875 earth radii in some global conductivity estimates (Banks 1972).

3.1) Equation 3.1 shows that the ratio of internal to external parts involves the ratio of two Bessel functions, for which Rikitake gave the first three terms of a series expansion. It was possible that three terms might not have given sufficient accuracy for high orders, so it was necessary to calculate the Bessel functions themselves.

It is convenient to make the following definition :

$$f_n(z) = \sqrt{\frac{\pi}{2z}} I_{n+\frac{1}{2}}(z).$$

The modified spherical Bessel functions obey the following recurrence relation (Abramowitz & Stegun, 1965):

$$f_{n-1}(z) - f_{n+1}(z) = (2n+1)\, z^{-1} f_n(z) \quad (3.3)$$

It would therefore be possible in theory to generate all the higher order Bessel functions for any argument given that:

$$f_0(z) = \frac{\sinh z}{z} \quad (3.4)$$

and $$f_1(z) = -\frac{\sinh z}{z^2} + \frac{\cosh z}{z} \quad (3.5)$$

The recurrence relation is numerically unstable for forward recursion, since any round-off error can be considered as contamination by modified spherical Bessel functions of the third kind, $K_{n+\frac{1}{2}}(z)$, which increase rapidly with increasing order and obey a recurrence relation similar to (3.3)

It can be seen from tables that, for real arguments, the functions f_n decrease monotonically as the order n increases. This makes it possible to calculate the functions by assuming that $f_{100}=0$, expressing the recurrence relation as a tri-diagonal

matrix and solving the system of equations for f_1 up to f_{99} subject to the boundary values f_0 and f_{100}.

The 99x99 matrix has leading diagonal elements given by $(2n+1)/z$, while the elements on the upper and lower diagonals are given by +1 and -1 respectively. The elements of the right hand side are all zero except for $f_0(z)$ in the first row. The solution of a tri-diagonal system of equations can be solved simply and accurately by computer and a trial run using real arguments was successful in reproducing a table of modified spherical Bessel functions (Abramowitz & Stegun, 1965, p473) up to order n=50, thereby ensuring the accuracy and stability of this method of calculation.

The ratios of internal to external parts, calculated for three periods (24, 12, 8 hours), are presented in Figure 3.1) along with the frequency independent response of a perfect conductor. The imaginary parts decrease and the real parts increase as the frequency increases, as expected, because an increase in frequency can be thought of as being equivalent to an increase in conductivity. These two quantities appear as the product $\sigma\omega$ in the induction equations.

3.3) Calculation of the Mutual Induction Kernel.

Once the response of the conductosphere has been found, the mutual induction kernel can be calculated from eqn. (2.33):

$$K_m(\theta) = \frac{\mu_0}{4\pi a^3}\sum_n (n+1)^2 (b/a)^{2n+1} (i_n/e_n) P_n(\cos\theta)$$

In this case the term i_n/e_n involves the ratio of two Bessel functions and the series bears a resemblance to a series, involving the ratio of two Hankel functions, for a radio frequency problem (Sommerfeld,p282), for which there is a complicated analytic method, due to Watson (1918), for finding

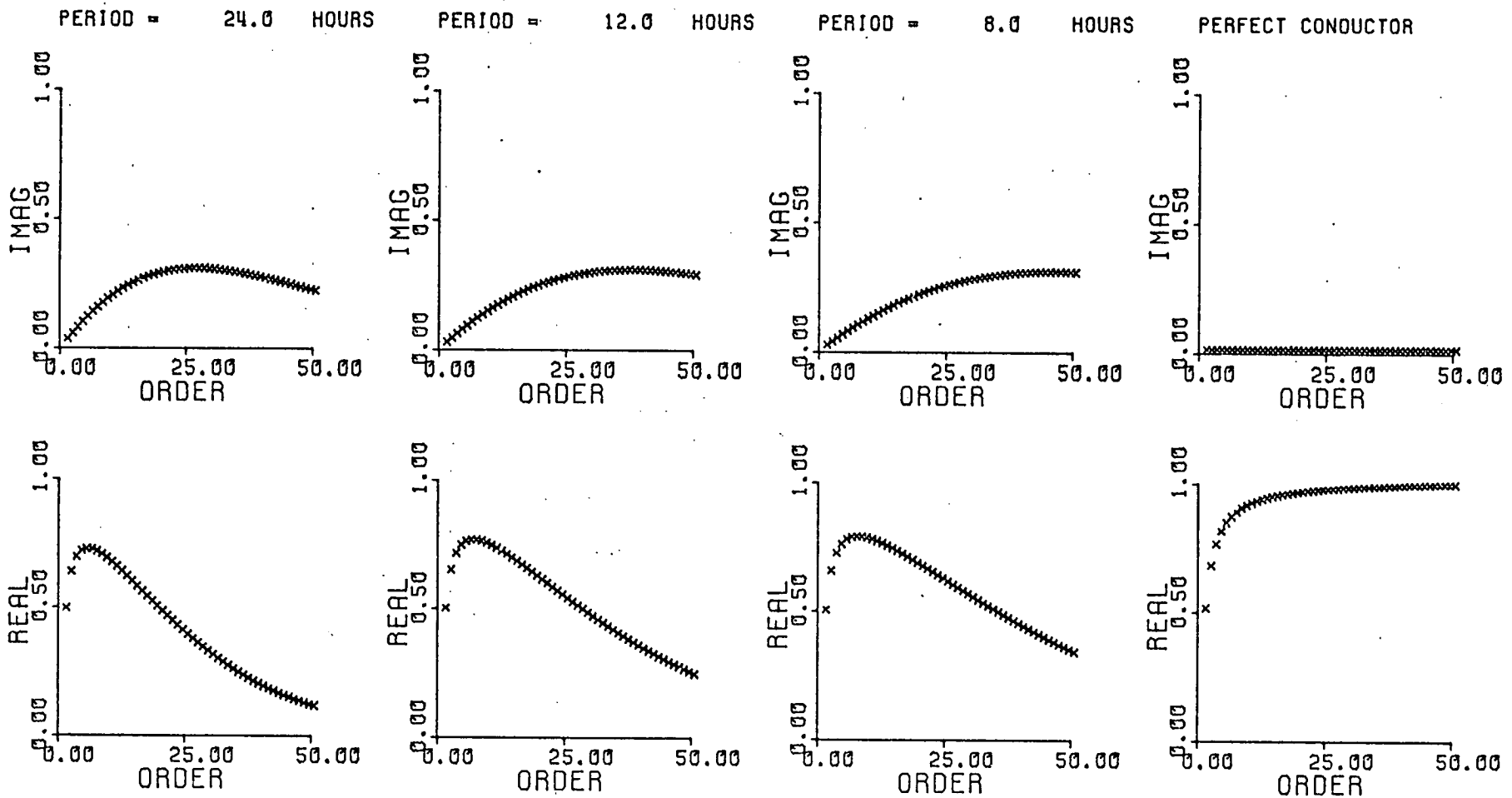
PERIOD = 24.0 HOURS
PERIOD = 12.0 HOURS
PERIOD = 8.0 HOURS
PERFECT CONDUCTOR
IMAG
REAL
1.00
0.50
0.00
0.00
25.00
50.00
ORDER
RESPONSES LINEAR SCALE

the limit. Since the radius of the conductosphere has been taken here to be .875 earth radii, the terms $(b/a)^{2n+1}$ ensure the rapid convergence of the series for $K_m(\theta)$.

The kernels, calculated from 50 terms, for 24, 12, and 8 hourly variations are shown in Figure 3.2), together with the kernel for the perfect conductor with the same radius. Again the graph for the perfectly conducting case can be seen to act as the limit of the finitely conducting cases as the frequency of the inducing field increases.

3.4) Numerical Integration of the Mutual Induction Kernel.

The method of calculating $Z_m(\theta) = \int K_m(\theta)\psi \, dS$ involves assuming that ψ is fairly constant over a $5^\circ x 5^\circ$ tesseral element and numerically evaluating the integral of $K_m(\theta)$ over each tesseral element, which is the method of basic integrals (Price & Wilkins,1963). Originally the basic integrals were evaluated by Gaussian integration over the tesseral element and taking successively finer partitions until a certain accuracy was obtained (Hobbs,1971). This was a simple procedure in the case of the mutual induction kernel for the perfect conductor, because the kernel was defined as an explicit function of the angle θ (eqn. 2.10) but in the case of the finite conductor it was necessary to calculate the values of the kernel at $1/8^\circ$ intervals so that the values at the Gaussian integration points could be found by cubic interpolation. The basic integrals for the poles could be calculated analytically in the perfectly conducting case but it was easier to use interpolation followed by Romberg integration with the sum of the series for the finitely conducting conductosphere.

It was possible to check the calculation of the basic

Figure 3.2

Mutual Induction Kernels of the Uniform Conductosphere with a Conductivity of 1 Sm^{-1} and Radius 0.875 Earth Radii at Periods of 24, 12 and 8 hours for Comparison with a Perfect Conductor of the same size.

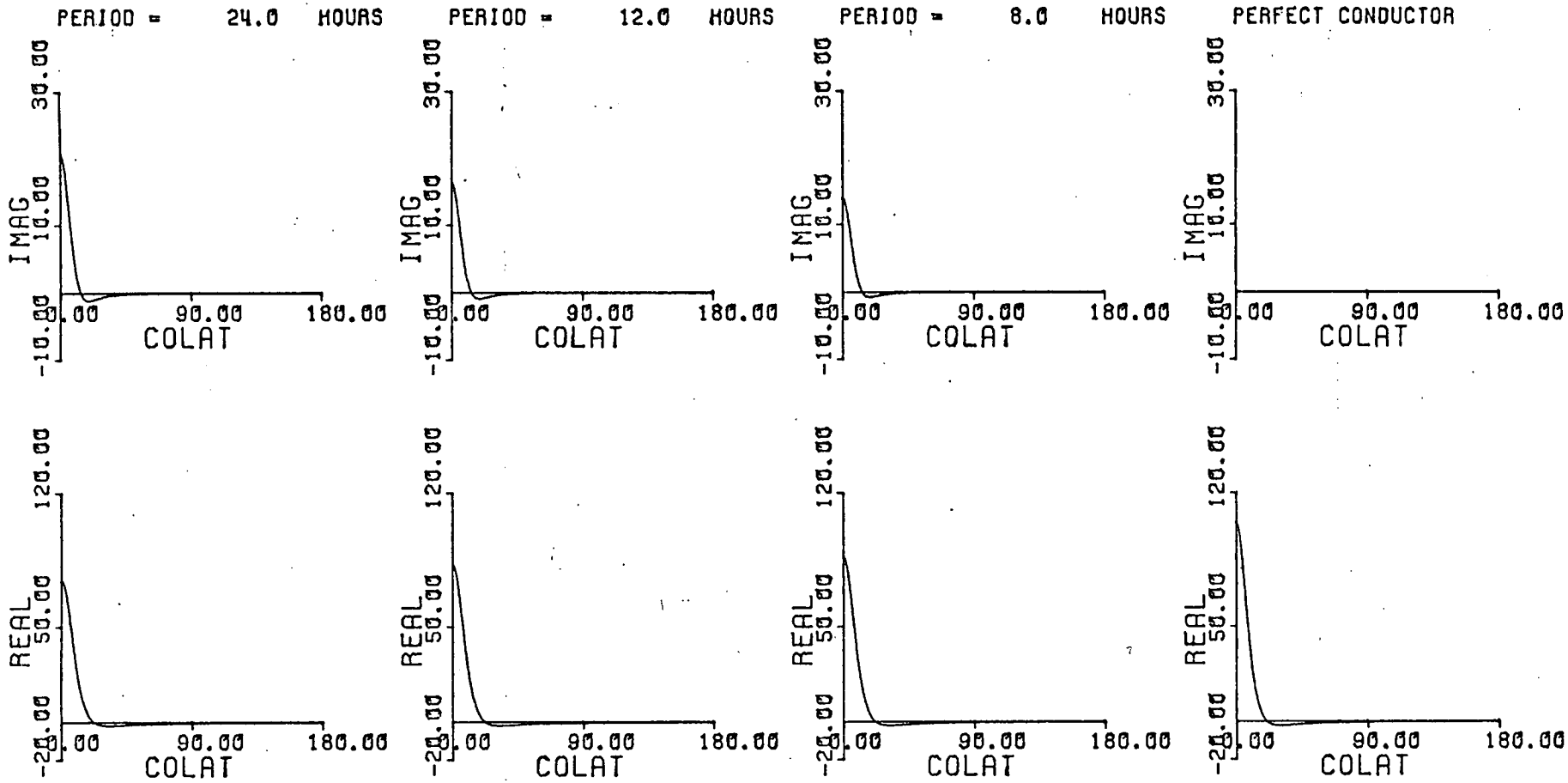

MUTUAL INDUCTION KERNELS

integrals by calculating the vertical field due to mutual induction by a current streamline function consisting of a single spherical harmonic. Obviously the induced field should only be represented by the same harmonic and it can be shown that the ratio of the induced vertical field to the current streamline function is given by:

$$Z/\psi = \frac{\mu_o (n+1)^2}{q(2n+1)} (b/a)^{2n+1} i_n/e_n \quad (3.6)$$

The fact that the calculated and predicted values always agreed to within 0.5%, demonstrated that the mutual induction kernel for this particular conductosphere is a suitable function to have its basic integrals calculated in this way on a 5° grid.

3.5) Discussion of Results.

It was decided to adapt an existing program for solving the induction problem in a thin hemispherical shell, in which the conductance decreased towards the edge, with an underlying perfectly conducting mantle for use with the uniform finitely conducting mantle. This generally involved altering some of the subroutines to deal with complex numbers, as opposed to real numbers, which arose as a result of the complex response of the finitely conducting mantle. The configuration of the hemispherical shell and the conductosphere is shown in Figure (3.3a) and the colatitudinal variation of the conductance of the shell is shown in Figure (3.3b).

The real and imaginary parts of the current function, total vertical field, external and internal vertical fields are presented in Figures (3.4a-3.4l) for three inducing fields at periods of 24 and 12 hours, for models with either a perfectly or finitely conducting mantle. The main difference between the solutions obtained with the different mantles is that there is a

Figure 3.3a

Configuration of the Conductosphere and the Thin Hermispherical Shell.

Figure 3.3b

Conductance of the Thin Hemispherical Shell.

HEMISPHERICAL SHELL AND CONDUCTOSPHERE

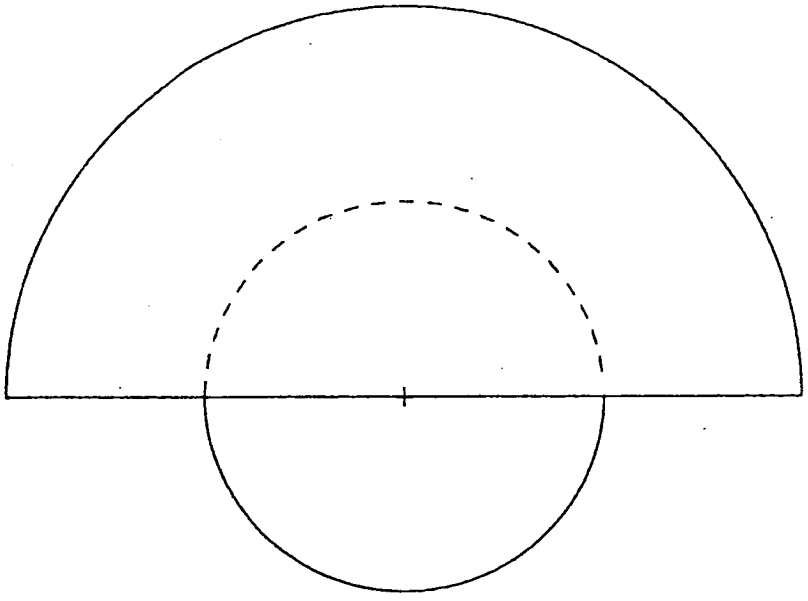

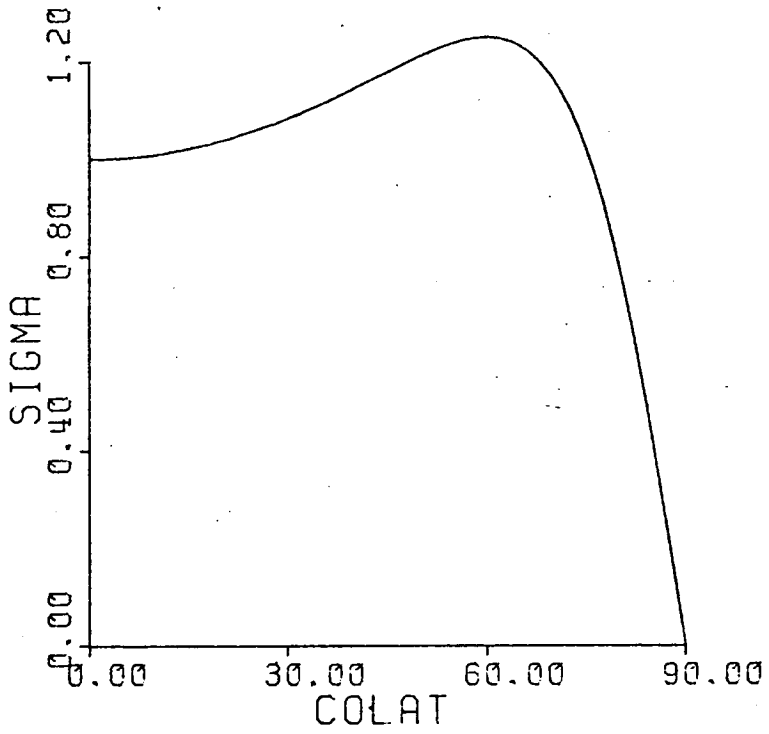

CONDUCTANCE DISTRIBUTION OF SHELL
(IN UNITS OF 16.000 S)

Figures 3.4a to 3.4l.

Solutions of the current function, total, external and internal magnetic fields obtained in the cases of a Hemispherical Ocean overlying Finitely and Perfectly Conducting Mantles, for different inducing fields at periods of 24 and 12 hours.

P_2^1 T=24 SIGMA=1S/M

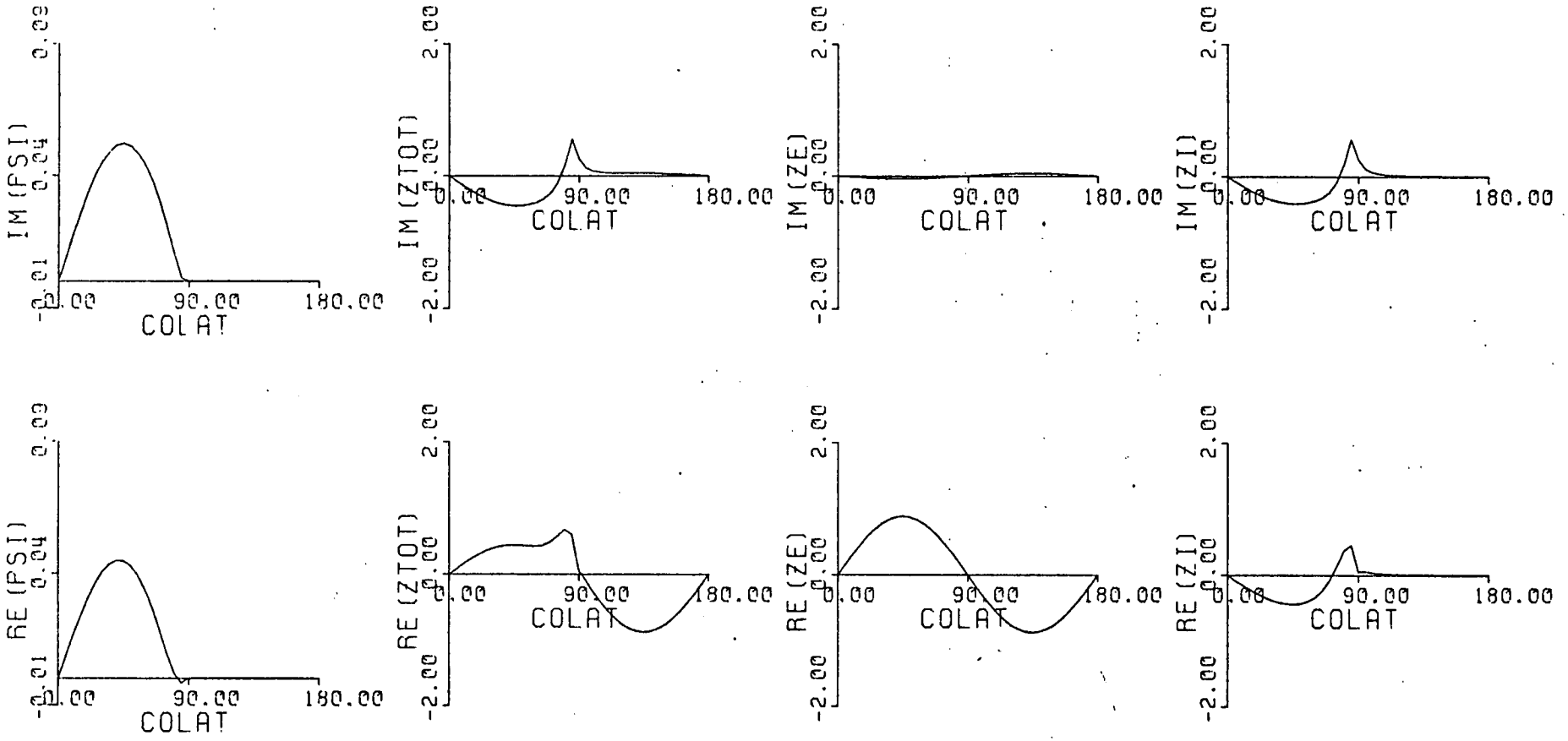

P_2^1 T=24 SIGMA=∞

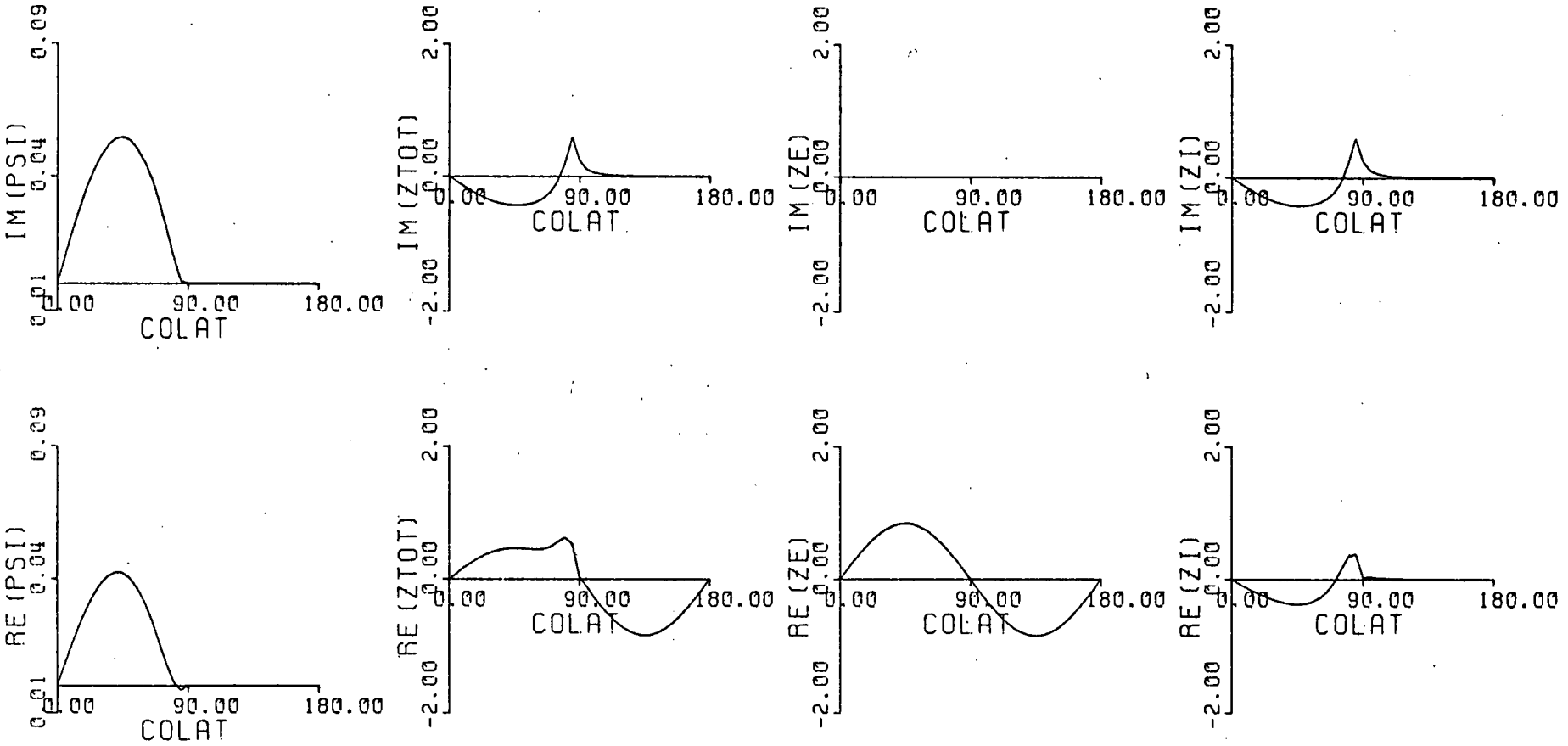

P_2^1 T=12 SIGMA=1S/M

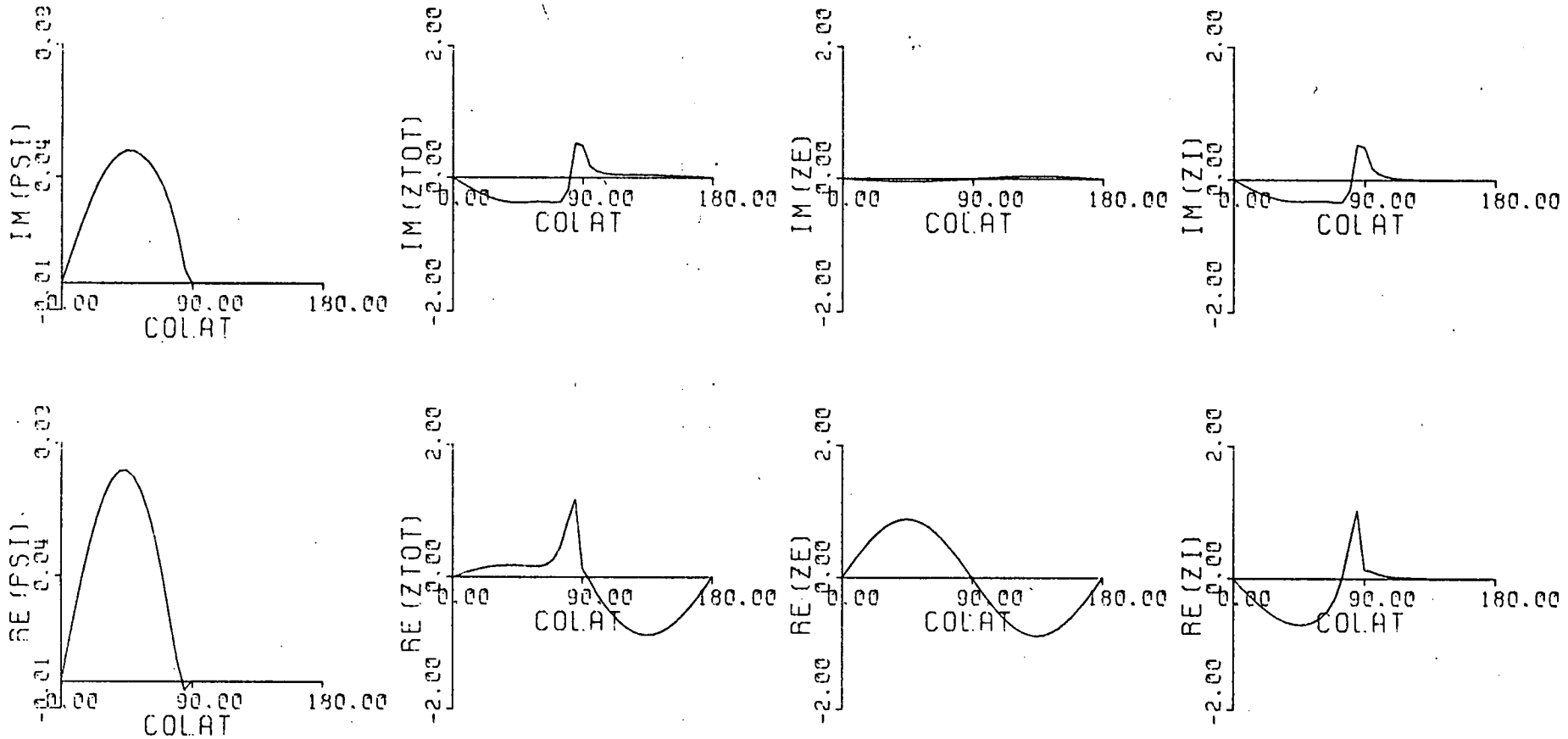

P_2^1 T = 12 SIGMA = 8

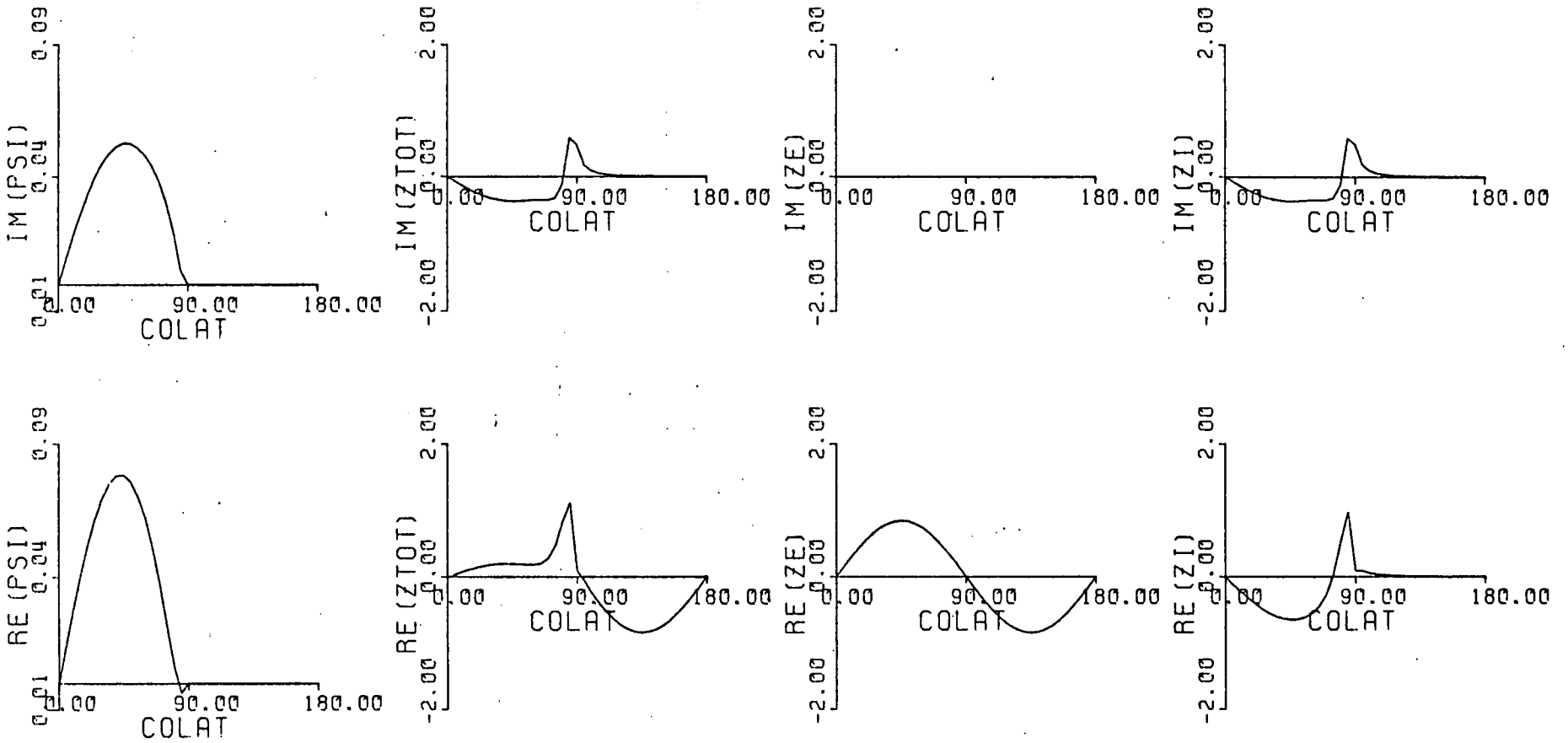

P 2 3

T = 24

SIGMA = 1 S/M

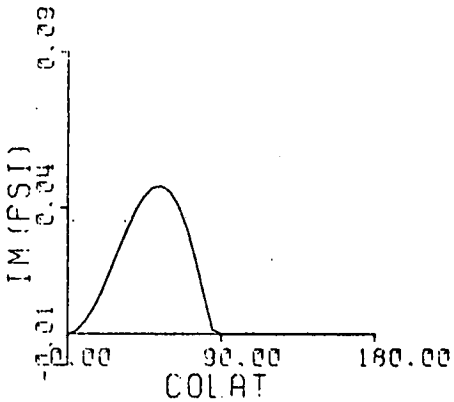

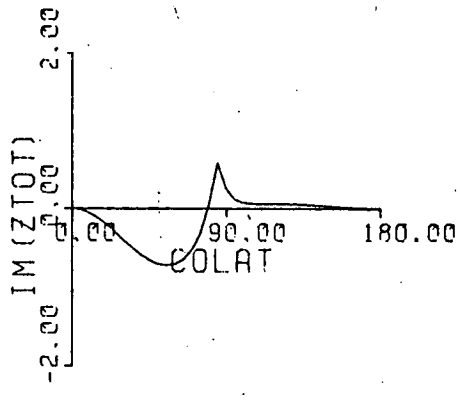

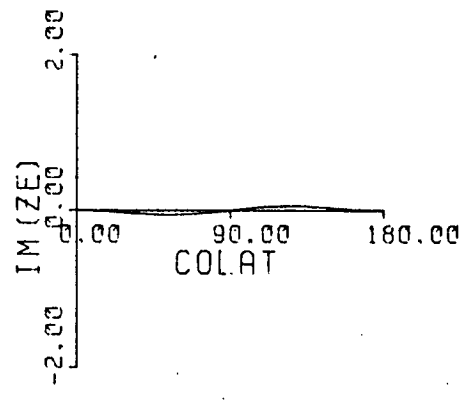

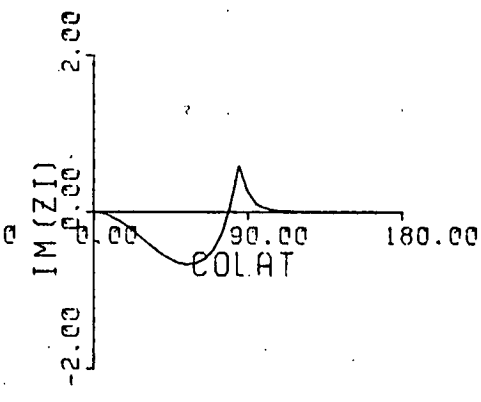

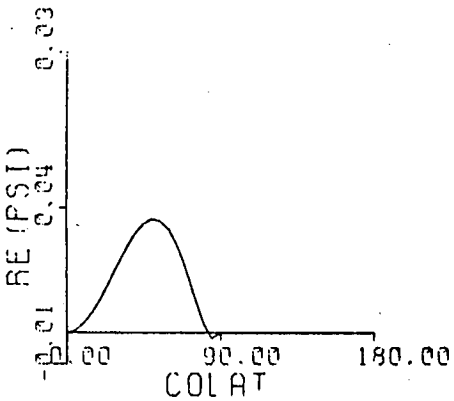

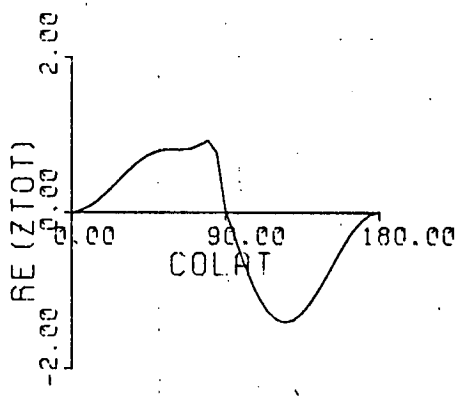

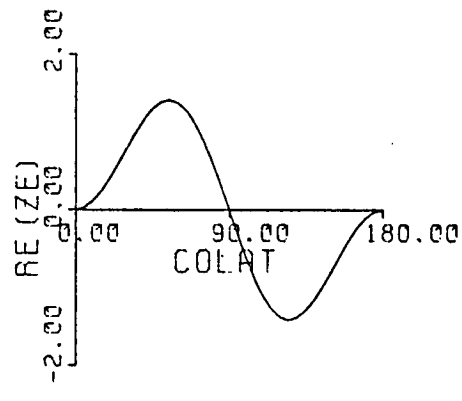

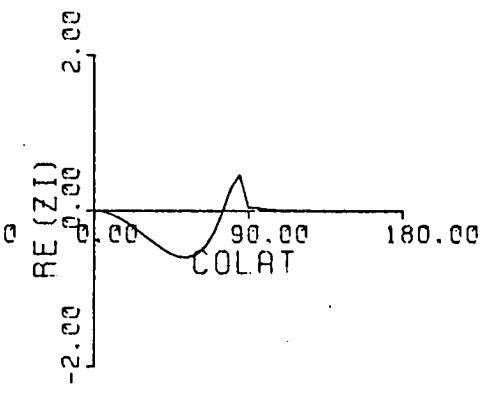

P_3^2 T = 24 SIGMA = 8

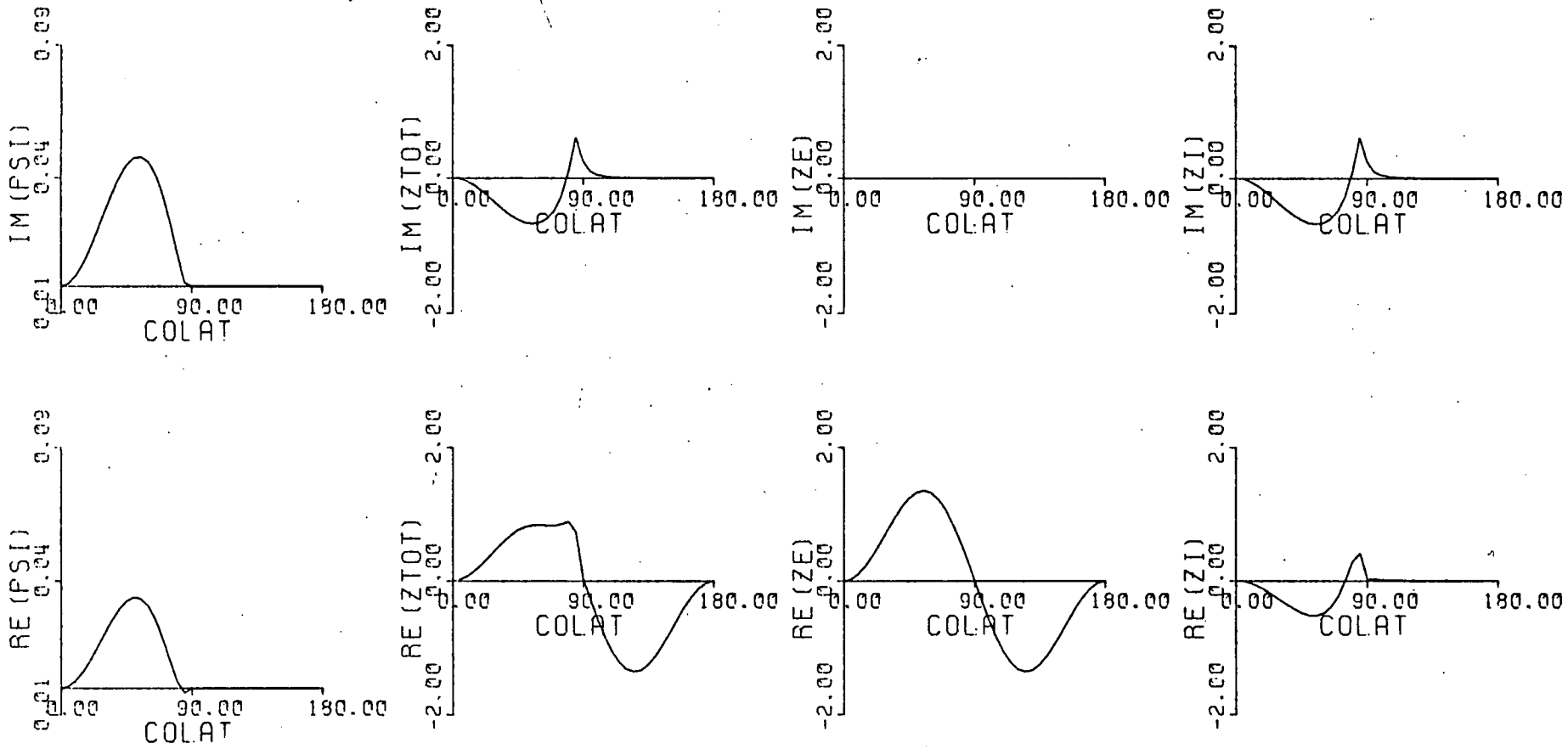

P_3^2 T = 12 SIGMA = 1 S/M

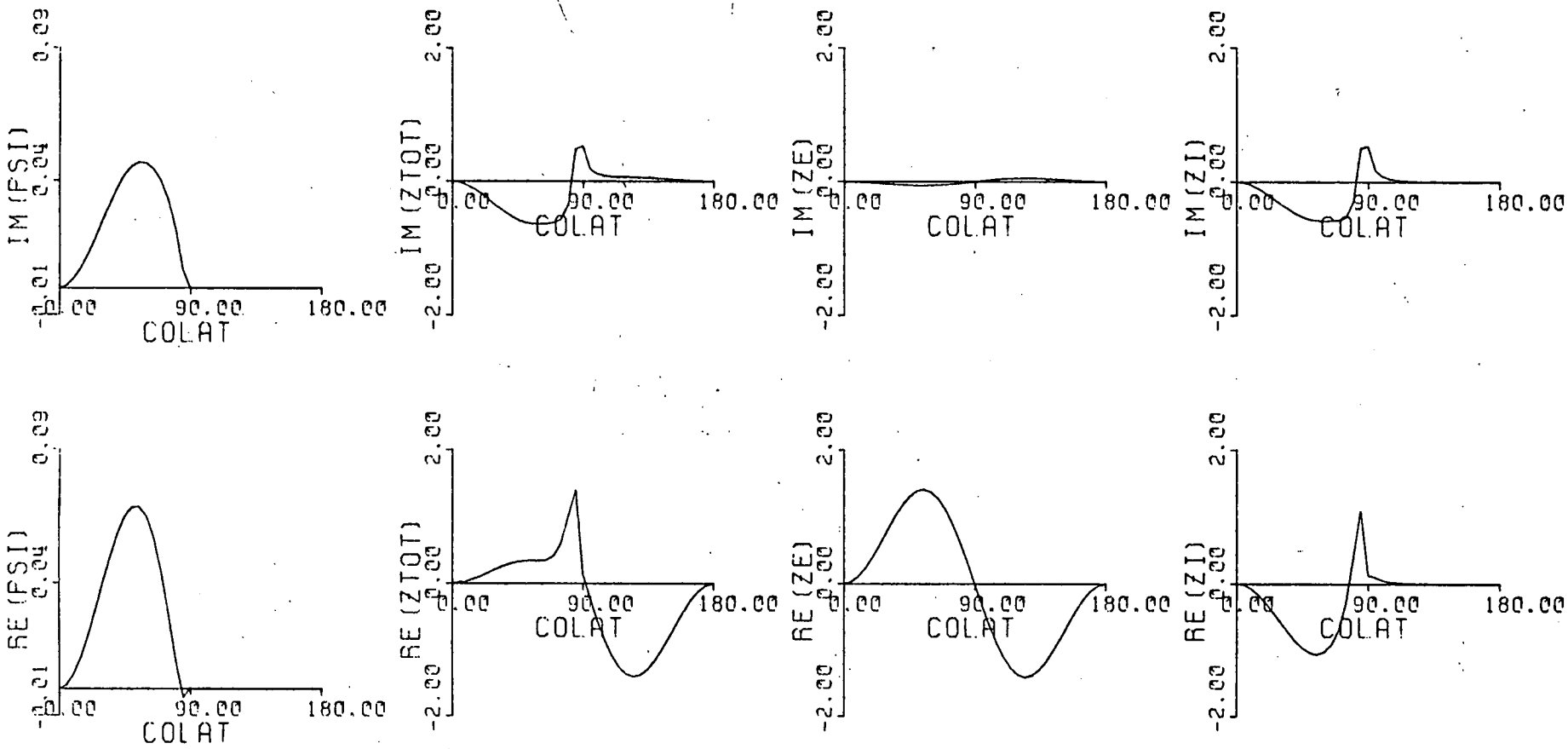

P_3^2 T = 12 SIGMA = ∞

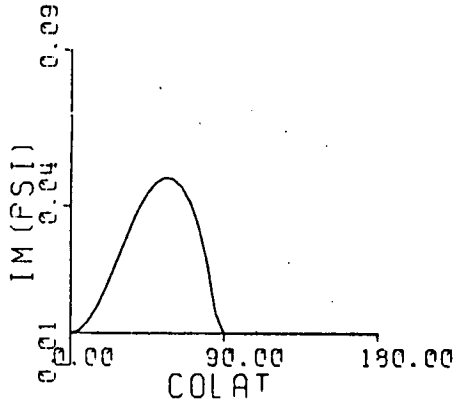

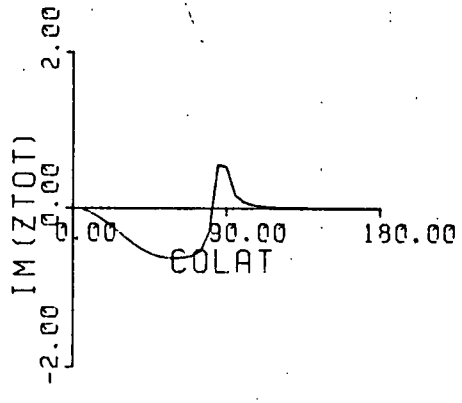

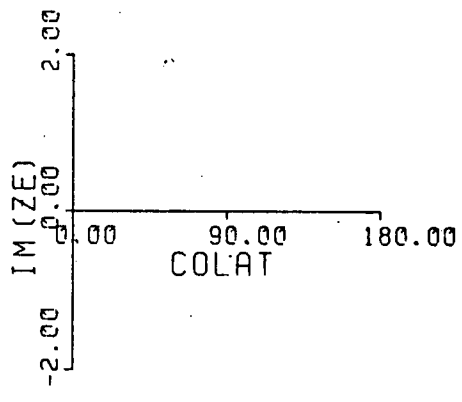

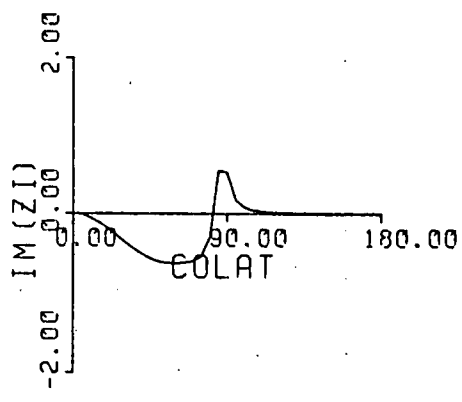

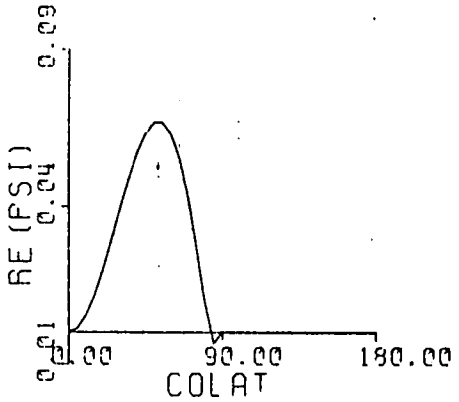

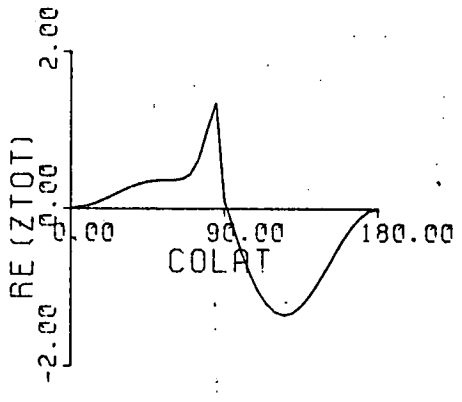

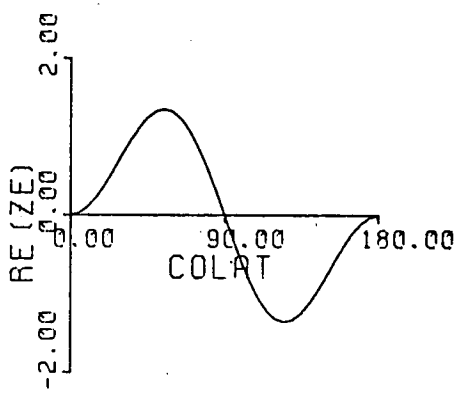

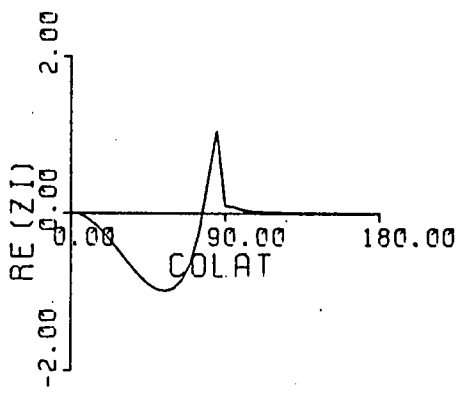

P $_4^3$ T=24 SIGMA=1S/M

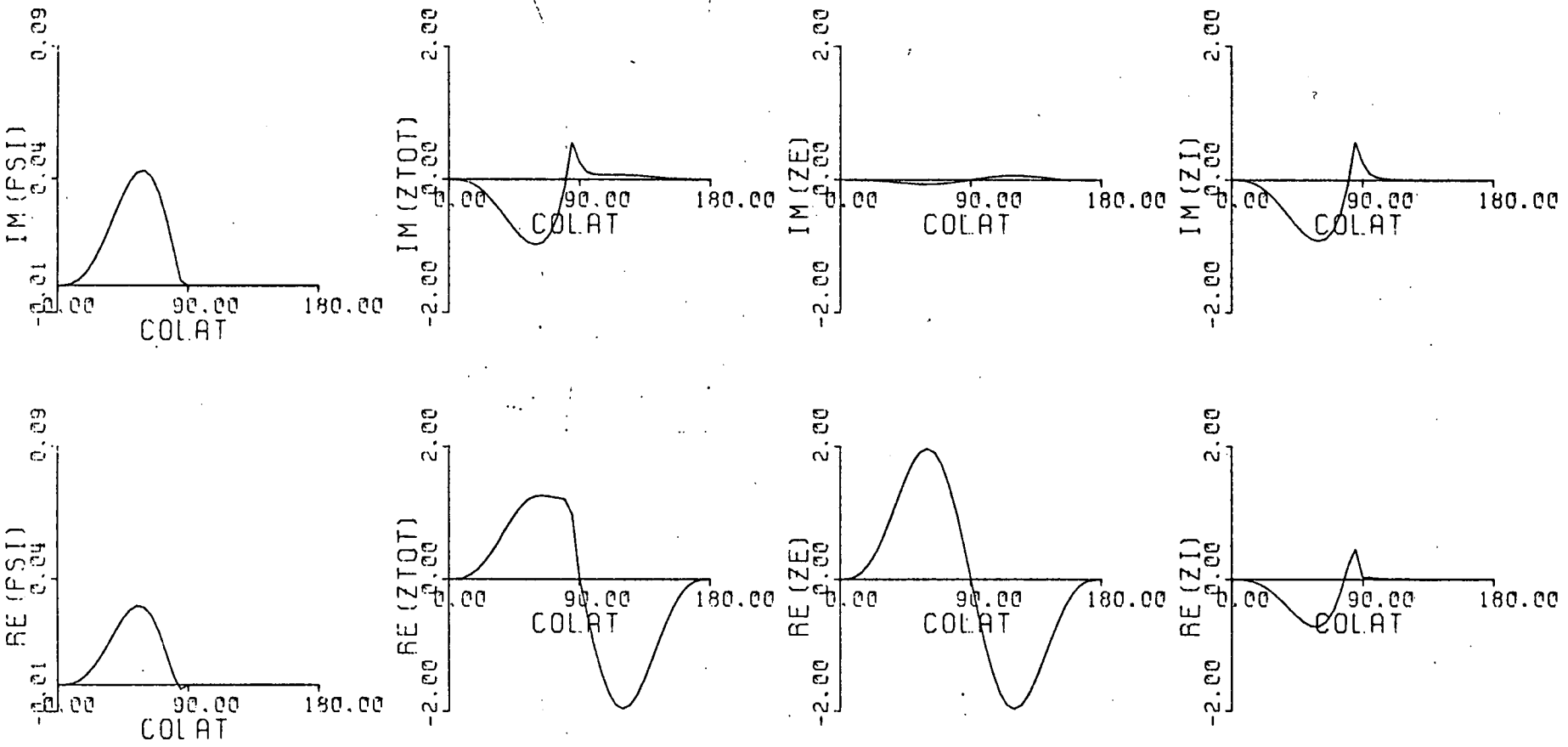

P 3/4 T=24 SIGMA=∞

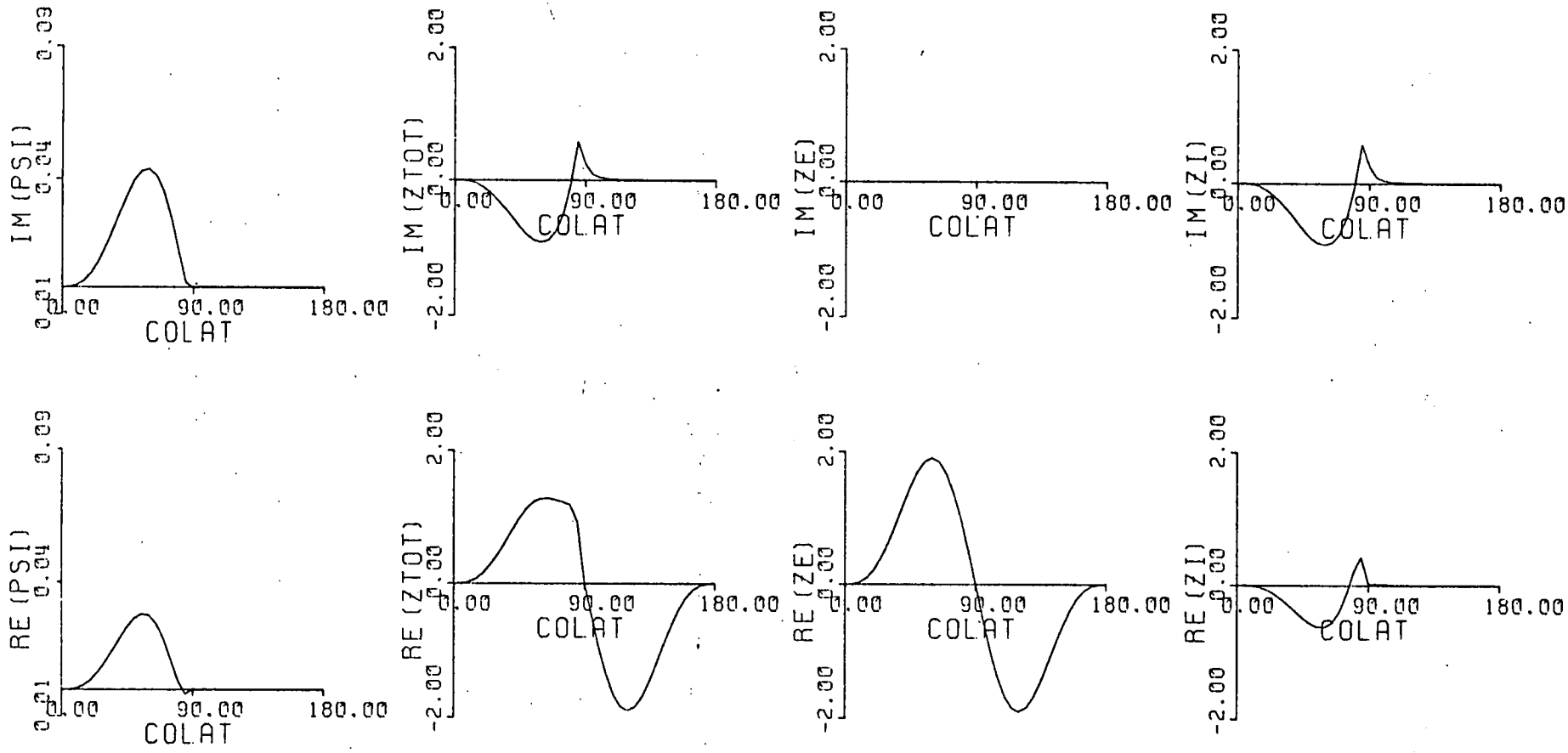

P 3 4

T = 12

SIGMA = 1 S/M

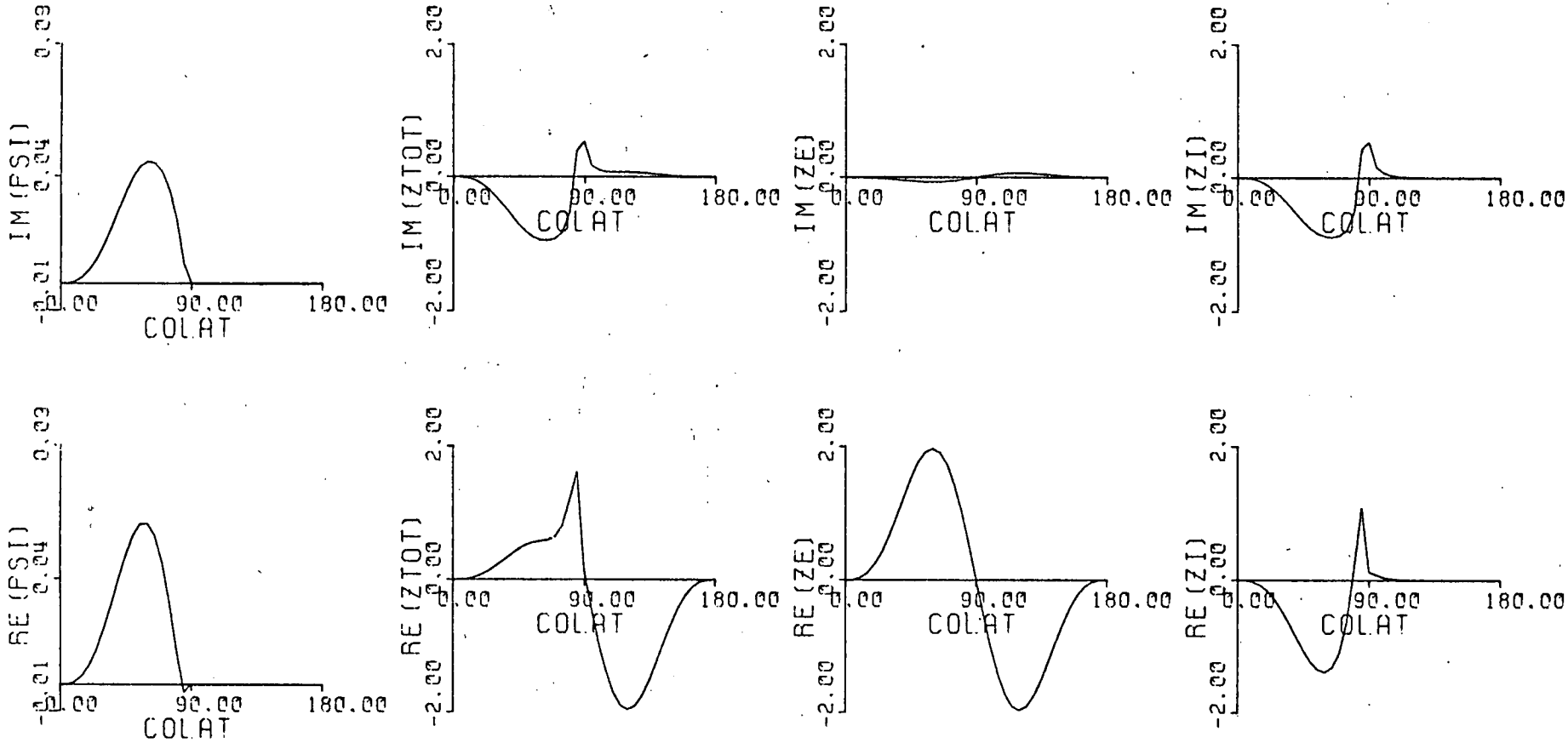

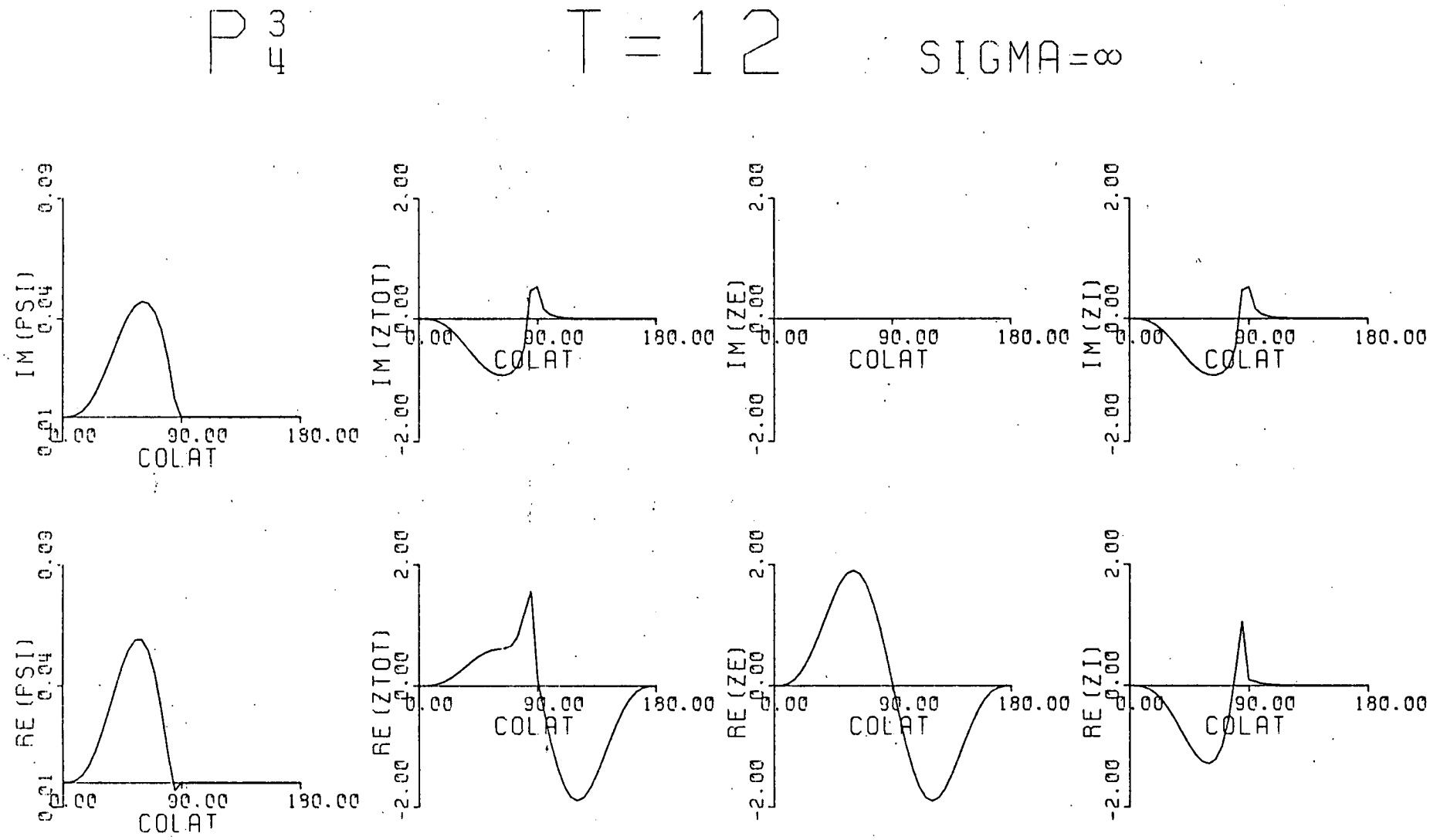
P 3 4
T = 12
SIGMA = ∞
IM (PSI)
0.03
0.01
0.00
90.00
180.00
COLAT
IM (ZTOT)
2.00
-2.00
IM (ZE)
IM (ZI)
RE (PSI)
RE (ZTOT)
RE (ZE)
RE (ZI)

small quadrature component of the external vertical field in the finitely conducting case which arises from the complex response of this mantle to the primary inducing field. The other differences between the two models are not very distinct because a conductivity of 1 Sm^{-1} is very close to perfect conductivity at the frequencies under consideration, but the imaginary part of the current function is smaller, while the real part is larger, in the finitely conducting case. These differences can be seen to decrease at the higher frequency, although this effect is more noticable in the real part. The calculations were performed on a 5^{o} grid in both cases.

The accuracy of the solutions was poorer near the edge of the hemisphere when an inducing field with a period of 12 hours was used. This was overcome by the use of an improvement scheme whereby the residual, obtained after substituting the current function and the internal vertical field into the original differential equation, was used as an inducing field to calculate correction terms for the current function in the vicinity of the edge of the hemispherical shell. The corrections were added to the current function directly, without using analytic continuation, which was the method originally used for calculating the solutions of low frequency problems, and the process could be repeated if necessary. Although the changes to the current function were small, it was possible to obtain a significant improvement in the accuracy near the edge but it was not entirely clear why adding the corrections in a manner only suitable at low frequencies could improve the solution of a high frequency problem.

It is possible that because the corrections were confined to

a small region near the coast, they could be represented by harmonics of high degree. The equation (Hobbs, 1971, eqn. 20) defining the limiting frequency, below which it is possible to use the low frequency summation, can be used to show that the maximum usable frequency is greater for high order inducing fields, like those arising from the correction terms, than for the low order inducing fields, e.g. the primary inducing field.

CHAPTER 4

BANKS' CONDUCTIVITY MODEL

4.1) Details of the Model:

After examining the results obtained by using the finite conductor (with σ =1 S/m) it was decided to use a conductivity distribution proposed by Banks (1972) to represent the earth. This model was the outcome of the analysis of the estimates of the earth's response to a P_1^0 inducing field in the frequency range 0.01 - 1 c.p.d., from all sources in the literature available at that time. It is possible, in theory, to calculate the conductivity distribution of a radially symmetric earth, provided the response is known over all frequencies, subject to certain restrictions (Bailey,1970).

Geomagnetic variations with this spatial structure and frequency band are generally associated with the ring current and the longer period variations are known to penetrate deeper into the earth than the harmonics of Sq, which are studied in this work, although Banks claimed that his model also fitted Sq observations. It is therefore quite probable that some of the deeper structure in this model has no effect on the daily variation and its harmonics, with the result that it is the upper layers which are particularly of interest. Banks' model was chosen in preference to that of Parker (1971) basically for the reason that the former had lower conductivities near the surface of the earth and was expected to produce a more convergent mutual induction kernel. It should be stressed that the assumption of a radially symmetric earth is least realistic close to the surface because of the difference in the thicknesses of oceanic and continental crust.

The model is basically a seven layer model (see Figure 4.1) with the main feature being an increase in conductivity to 2 Sm^{-1} at a depth of 500 - 600 km., which accounts for the fact that values around 0.9 earth radii have been chosen for the radius of the perfect conductor, in earlier attempts to model the highly conducting mantle.

Banks, however, did not include a conducting surface sheet, to model the oceans, as had been done by earlier workers in this field (Chapman & Whitehead, Lahiri & Price, et al.), so it was decided to see what effect would arise from the inclusion of an oceanic sheet.

4.2) Calculation of the Response:

Banks only gave the response, i_n/e_n, for the three principal Sq harmonics, which meant the author had to generate the ratios of internal to external parts up to order $n=200$ in order to calculate the mutual induction kernels. The published ratios however served as a check on the method of calculation used.

Since Banks' model is a layered model, it was possible to calculate the response analytically, because, in any layer, the solution to the radial part of the induction equations could be given by a linear combination of two spherical Bessel functions. The functions $K_{n+\frac{1}{2}}(z)$ would then be present, except at the innermost layer where they would have a singularity at the centre of the earth, and the coefficients of the Bessel functions could be found by satisfying the boundary conditions at the interfaces between layers. Banks described a matrix method for calculating the response of a layered spherical earth in an earlier paper (Banks,1969), which was based on a method originally derived for calculating the dispersion of seismic

Figure 4.1

Banks' Conducting Model

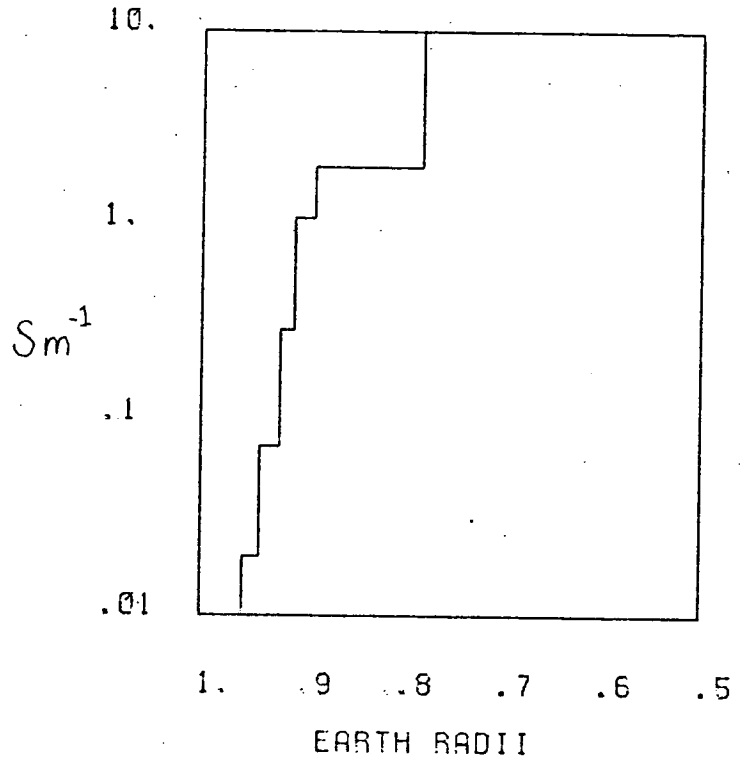

LAYER	INNER RADIUS	CONDUCTIVITY
1	0.957	0.010
2	0.940	0.020
3	0.920	0.074
4	0.907	0.293
5	0.887	1.100
6	0.780	2.000
7	0.500	10.000

surface waves, but it was suspected that this method would be troublesome to use at high orders. In this method the boundary conditions at each boundary are expressed in matrix form, the elements of which are defined in terms of Bessel functions, and because of the numerical instability of the recurrence relations for some of these functions, a considerable amount of computation, using the method described in chapter 3, would have been necessary before this method of calculating the response could be used. It should be stated that the modulus of the arguments of the Bessel functions used in global induction studies can quite often be relatively large (sometimes of the order of 100) and it would probably have been acceptable to have used certain asymptotic expansions (Watson, 1922, chapter 7), but since it was hoped to model general conductivity distributions ultimately, it was decided to resort to numerical methods.

It is undesirable to solve the radial induction equation numerically, since the sharp attenuation of the magnetic field with depth makes it necessary to use a very short step size, but by expressing the ratio of internal to external parts as a function of the solution of the radial differential equation, and performing the appropriate substitutions, it is possible to derive a differential equation for calculating the response directly. This has been done by Eckhardt (1963) and results in the following first order, non-linear, ordinary differential equation:

$$\frac{dS_n}{dr} = -k^2 \frac{r(n+1)}{(2n+1)n}\left[S_n - \frac{n}{n+1}\right]^2 - \frac{(2n+1)}{r} S_n \qquad (4.1)$$

where $S_n = i_n / e_n$, $k^2 = -i\mu_0\omega\sigma$, n is the order of the inducing field and r is the distance from the centre of the earth. It is

interesting to note that the conductivity only appears in the first term on the right hand side of eqn. (4.1), while the second term introduces the appropriate upward and downward continuation factors for dealing with currents at depth, even if the structure contains any insulating layers. A similar equation for calculating the impedance of a plane earth, with layers of continuously varying conductivity, has been given by Abramovici & Chlamtac (1978).

Eckhardt discussed the solution space of the equation in the original paper, but it is sufficient to state here that there are two possible initial conditions which can be used, when solving the equation numerically. It is possible to initialise the value of S_n to $n/(n+1)$, corresponding to a perfect conductor, or zero, corresponding to a perfect insulator, at any depth, below which one would expect the electromagnetic field to have penetrated, which is less restrictive than the initial condition used in the propagator matrix method (Banks, 1969). The quartic Runge-Kutta method (Stark, 1970, p. 265) was chosen as a suitable way of finding the numerical solution, since analysis shows that Runge-Kutta methods are generally stable provided the step increment is below a critical value. By using both possible initial conditions (i.e. $S_n = n/(n+1)$, and $S_n = 0$), it was possible to check the accuracy of the numerical scheme by comparing the values obtained for S_n at the surface of the conducting sphere. The step length was decreased until both solutions coincided and any further reduction provided no further change in the solution, although the perfectly conducting initial condition generally led to a stable solution more quickly. Another check on the accuracy was made by solving the

equation for the uniform sphere used in Chapter 3 and the excellent agreement between the numerical and analytic solutions gave assurance of the accuracy of the numerical solution. The responses for the principal Sq harmonics, P_2^1, P_3^2 and P_4^3, with periods of 24, 12 and 8 hours respectively, were the same as those given by Banks for his model, even although the conductivities and layer thicknesses for this work had only been read from the graph in the original paper (Banks 1972, Figure 10). It is hardly surprising that it was necessary to use a smaller step length when the response was being calculated at higher frequencies.

The ratios of internal to external parts, defined at the surface of the conductosphere, for Banks' conductivity structure are shown in Figure (4.2) for periods of 24, 12 and 8 hours and are compared with the response of a perfect conductor. The behaviour of the lower order responses is best shown by plotting them on a linear scale, while the higher order responses are better displayed on a logarithmic scale where the imaginary parts are greater than the real parts. At high orders both the real and imaginary parts increase as the frequency increases, which differs from the uniformly conducting case where the imaginary part decreased at shorter periods. This is because the conductivity increases with depth in Banks' model and since the electromagnetic field cannot penetrate as deeply at shorter periods, a smaller average conductivity is being 'sampled' giving rise to a larger imaginary part of the response at high orders. The imaginary parts do decrease with increasing frequency at low orders.

With the aim of ensuring the convergence of the mutual

Figure 4.2a

Responses of Banks' Conductivity Distribution in comparison with a perfect conductor on a Linear Scale.

Figure 4.2b (overleaf)

Responses of Banks' conductivity distribution in comparison with a perfect conductor on a Logarithmic Scale.

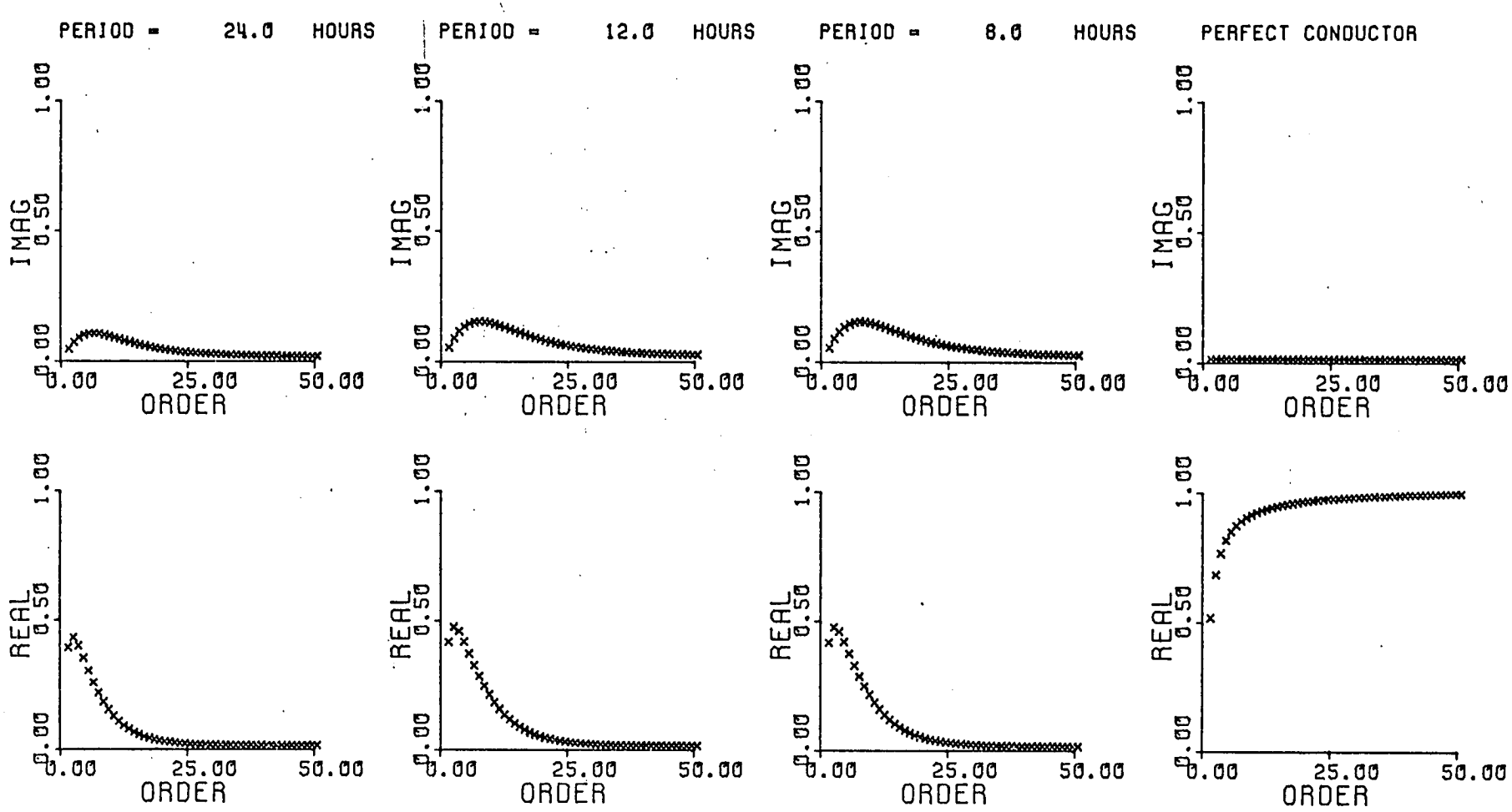

RESPONSES LINEAR SCALE

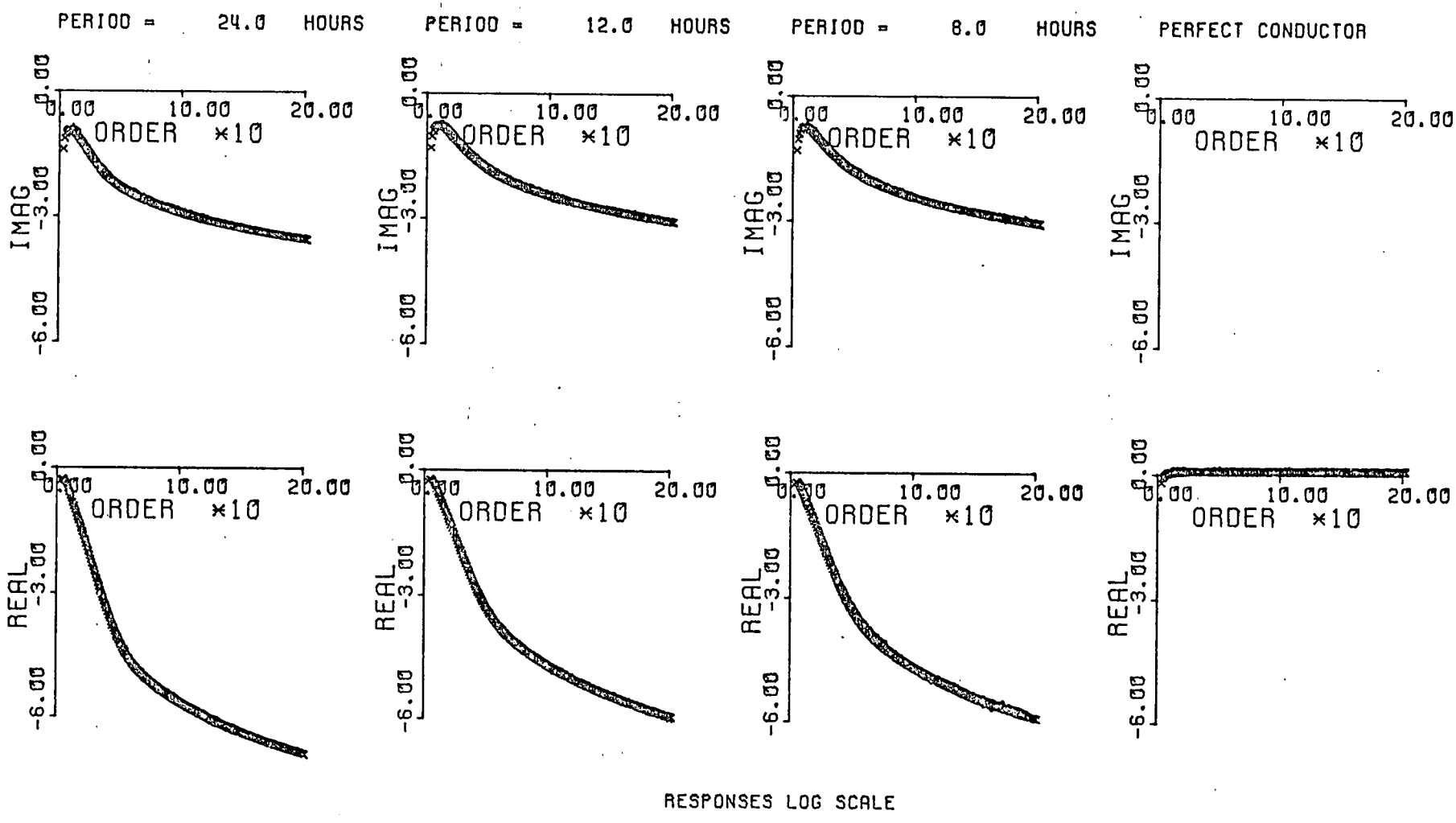

RESPONSES LOG SCALE

induction kernel, the author elected to scale down the Banks' conductivity model so that the radius of the conductosphere was .99 earth radii. This step ensured that the higher order terms in eqn. (2.33) were damped out by the factor $(b/a)^{2n+1}$, although the effect on the low order terms was small. This step was equivalent to assigning an insulating layer to the top 1% (or 64 km.) of the earth and if this step had not been, taken, it would have been necessary to postulate a thin insulating sheet beneath the ocean, since this approach to the oceanic induction problem cannot cope with the flow of electric current between the mantle and the oceans.

4.3) Calculation of the Kernels.

Having calculated the responses, the mutual induction kernel was calculated, for a period of 24 hours, as for the uniform sphere but it was necessary to use a higher number of terms in the expansion because the convergence was slower on account of the larger radius of the conductosphere (.99 earth radii, as opposed to .875). It is strictly not sufficient to assume that convergence has occured once the individual terms have reached a small value, but for the 24 hour variation it was found that the in-phase part of the kernel had reached a limiting value after 200 terms, but the quadrature part had still not converged. This was because the imaginary part of the ratio of internal to external parts exceeds the real part at high orders.

It was simplest to check for convergence by examining the value of $K_m(\theta)$ when $\theta=0^\circ$, since for zero angular separation, $P_n(\cos\theta)=1$. This fact ensures that the set of partial sums approaches the limit monotonically as the successive terms are

added, whereas it approaches the limit in an oscillatory manner when $\theta=180^{\circ}$, because $P_n(-1)=(-1)^n$. Because the amplitude of the mutual induction kernels is large at small angles and small at the antipodal point, the effect of truncating the series is to produce a large absolute error, but small percentage error, near $\theta=0^{\circ}$ and vice versa near $\theta=180^{\circ}$. This effect could easily be demonstrated by truncating the series for a perfect conductor, for which the limit is known analytically.

It was possible to check the convergence of the series when $\theta=0^{\circ}$ and $\theta=180^{\circ}$ by using techniques to accelerate the convergence. This was done in the case of $\theta=180^{\circ}$ by using the Euler transformation (N.P.L., 1965, p124), in which an alternating series can be converted into a more rapidly convergent series involving successive finite differences of the original series. The Euler transformation could not be used directly in the case of $\theta=0^{\circ}$, since the terms were all of the same sign, but it is possible to convert a series of positive terms into an alternating series by applying Van Wyngaarden's transformation (N.P.L., p126), and having done this, Euler's transformation was used.

The technique of using a combination of the two transformations was checked by comparing the analytic value of $K_m(0)$ for a perfect conductor of radius b, given by $2(b/(1-b^2))^3$ taking the earth's radius as unity, with the answer obtained by the double transformation of the first 200 terms of the original series. This was done for the case of b=.99 earth radii, which gave good agreement between the two answers, despite the fact that this kernel had a very sharp spike at $\theta=0^{\circ}$. Since the response of a finite conductor is smaller than that of a perfect conductor

with the same radius, the kernels of the finite conductor were better behaved and this type of analysis showed that even the direct sum of the first 200 terms of the imaginary part was not very different from that obtained by the double transformation.

The basic integrals were therefore calculated in the same manner as for the uniform sphere and the accuracy of the numerical integration was checked by calculating the induced field due to induction by a current function consisting of a single harmonic. Although the real part of the induced field contained only the same harmonic (with the predicted amplitude), the values of the imaginary part were accurate near the equator and at mid-latitudes, but were progressively inaccurate towards the poles. This was the case at a period of 24 hours; higher periods were even less accurate in both real and imaginary parts. Several tests were done to try to rectify this.

Initially it was suspected that the inaccuracy might have arisen from the fact that the values of the kernel, for use in the Gaussian integration scheme were obtained by interpolating a truncated series, but the same fault was observed while making the same test on a perfect conductor of radius .97 earth radii, whose mutual induction kernel is known in closed form. Next it was suspected that the calculation of the basic integrals, for points near the pole, was suspect. The reason for this was that the Gaussian integration procedure was continued until the difference between successive values was less than a specified amount and since the area of a tesseral element is proportional to the sine of its colatitude, it seemed possible that if the absolute values of some of the basic integrals were smaller than the specified accuracy in the program, then the correct value

would never be obtained. However using smaller accuracies and using the sine of the colatitude as a weight factor had no effect on the test.

As a further check on the evaluation of the basic integrals for small angular separations, it was decided to calculate the induced vertical field for a single harmonic in the following way:

$Z_A = \int K_m(\theta)\ (\psi - \psi_A)\ dS$. This was permissible because the current function is only uniquely determined to within an arbitrary constant and the effect of subtracting ψ_A, where A is the point at which the field is to be calculated, is to place less emphasis on the basic integrals at nearby points, at which the kernel is large. This method gave the same inaccurate result as the original form of the test:

$Z_A = \int K_m(\theta)\,\psi\, dS$.

The author was therefore forced to the conclusion that kernels with such sharp peaks near $\theta = 0^\circ$ were just not suitable functions to have their basic integrals calculated on a 5° x5° grid. It was undesirable to switch to using a smaller grid, since it was hoped to apply this method of dealing with finite conductivity to a program for modelling the effect of the real oceans on a 5°x5°grid. It seemed possible that this problem could be overcome by subtracting a known analytic function from the kernel for Banks' conductivity model, so as to reduce the spike. The basic integrals of the residual could then be calculated in the normal fashion and the analytic function (say the mutual induction kernel of a perfect conductor of suitable radius) could be treated by using the methods of Hobbs (1971) for treating the singularity in the self induction kernel. This

would have involved a considerable amount of work but after considering the type of problem to which the method was intended to be applied, it was considered unnecessary to attempt it.

Both the program for the oceanic induction problem and the test of the accuracy of the basic integrals were designed for calculations on a $5^{\circ}x5^{\circ}$ grid, on which terms of order greater than about 35 have little meaning. Consider the test for calculating the field induced by an arbitrary current function, with a well defined longitudinal variation (say $\cos\lambda$), on a $5^{\circ}x5^{\circ}$ grid, which comprises 37 different colatitudes and 72 separate longitudes over the whole globe. Neglecting the poles, where the induced field must vanish, leaves 35 points at which the current function and the induced field are to be specified and these 35 values can be uniquely defined by a series of 35 harmonics, P_1' to P_{35}'. It did not make sense to consider any harmonics of order higher than 35 on a $5^{\circ}x5^{\circ}$ grid and it seemed better to take only 35 terms in the expansion for the mutual induction kernel, rather than take more while striving for better convergence. This was done for all three periods considered and the accuracy test for the low order harmonics was passed, although some of the polar values were 1 - 2% high.

It seemed that including high order terms in a sharply peaked kernel added numerical 'noise' to the result of the surface integration, which was akin to the problem of aliasing in data analysis.

4.4) Discussion of Results.

Results obtained by using Banks' conductivity profile are compared with those calculated with the perfectly conducting mantle (of radius .875 earth radii) using the same hemispherical

Figure 4.3

Mutual Induction Kernels for Banks' Model at periods of 24, 12 and 8 hours in comparison with that of a perfect conductor of Radius 0.9 Earth Radii.

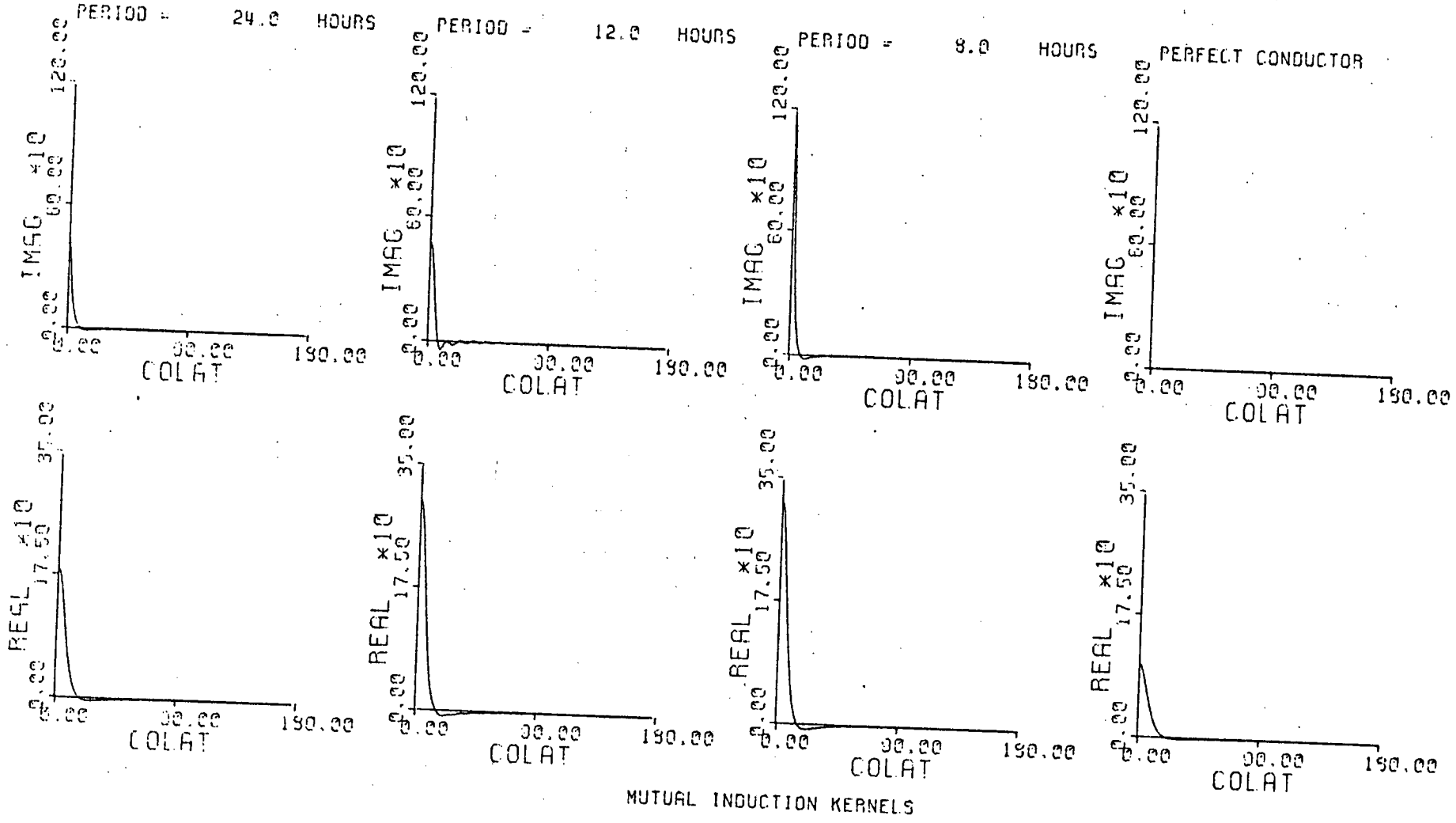

MUTUAL INDUCTION KERNELS

ocean as described in Chapter 3. There are now two factors which influence the comparison between the two sets of solutions: the difference in conductivity and the difference in the radii of the conductospheres. The effect of the increased radius seems to be the dominant effect since there is a greater reduction of the primary field by the finitely conducting mantle, as can be seen in the graphs of the external field. This causes a decrease in both the real and imaginary parts of the current function and a corresponding decrease in the coast effect (as can be seen in the graphs of the total field). The differences between the two models are now more apparent at higher frequencies, which is the reverse of the situation when the uniformly conducting mantle was used.

Figure 4.4a - 4.4l

Solutions of the Current Function, Total, External and Internal Vertical Magnetic Fields obtained in the cases of a Hemispherical Ocean overlying Banks' Model and a perfect conductor at periods of 24 and 12 hours.

P_2^1 T=24 SIGMA=BANKS 72

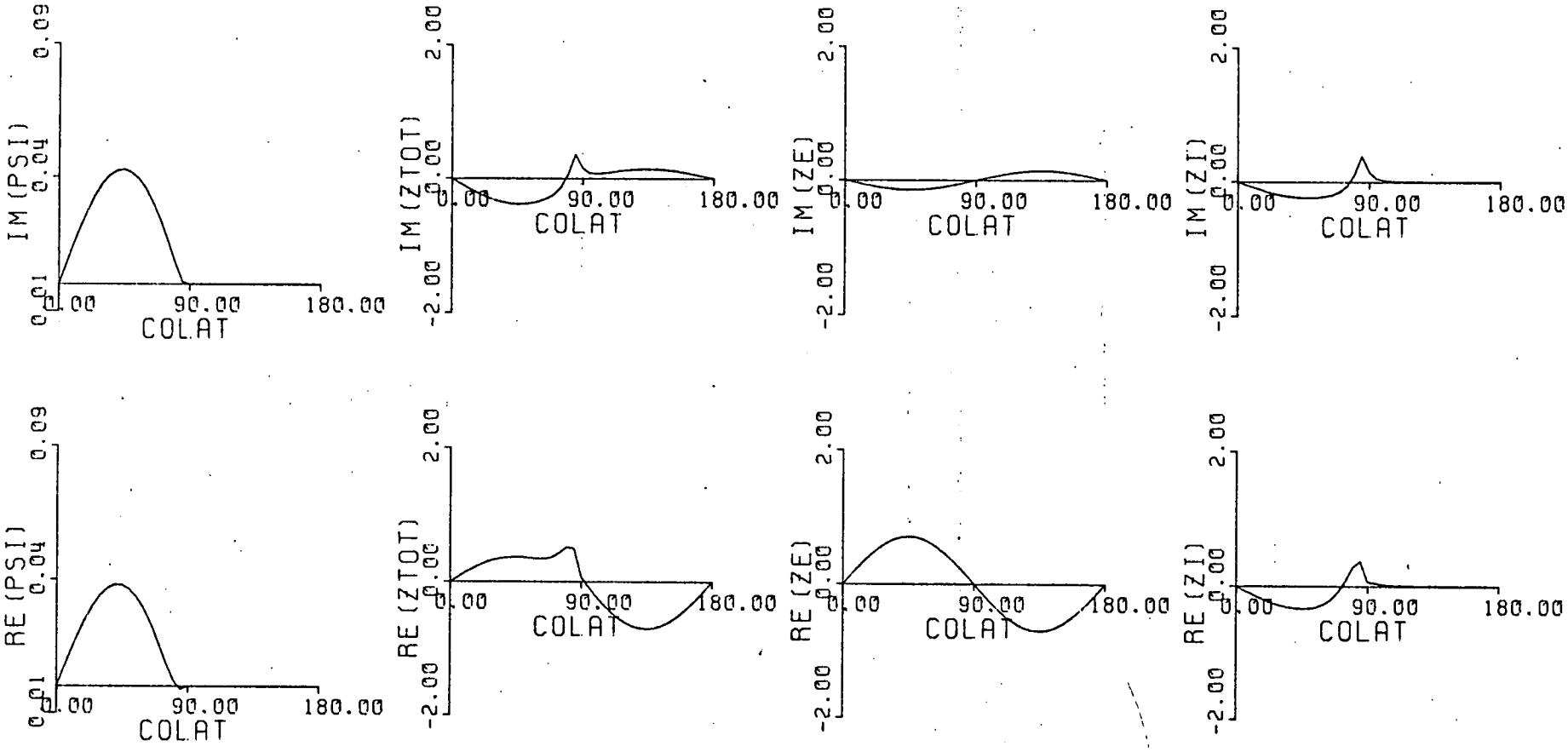

P_2^1 T=24 SIGMA=∞

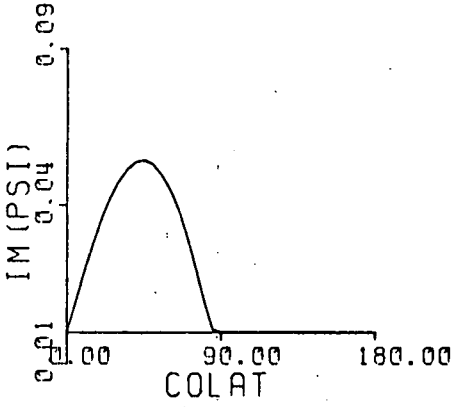

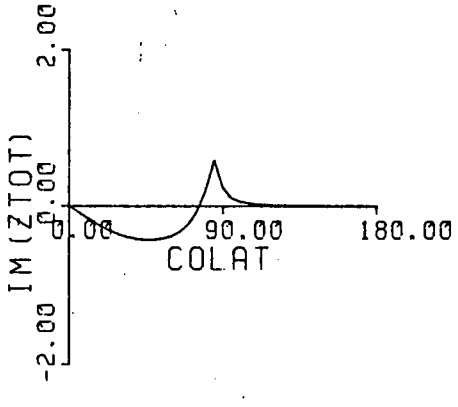

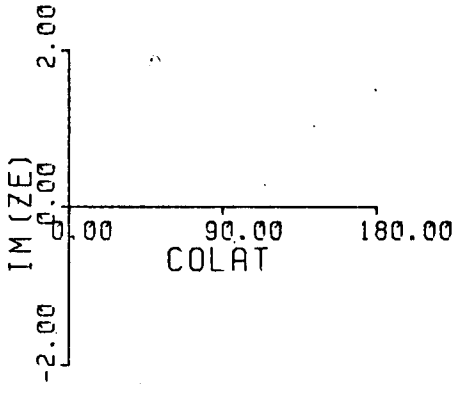

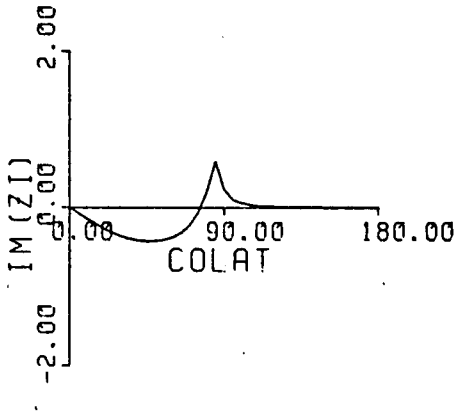

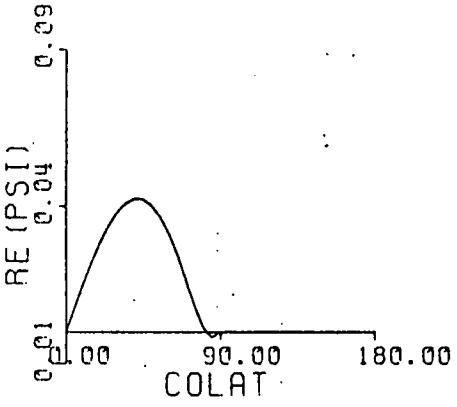

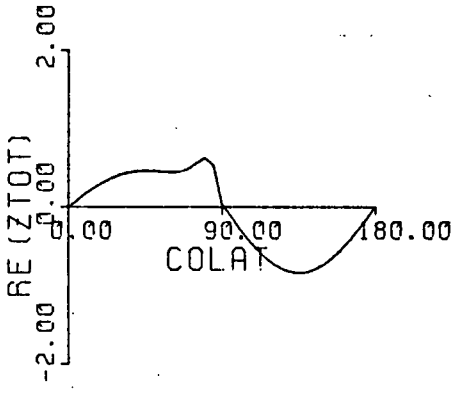

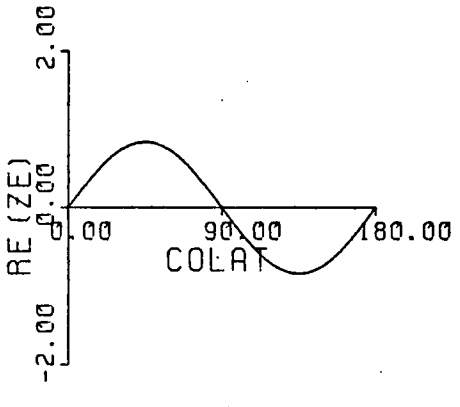

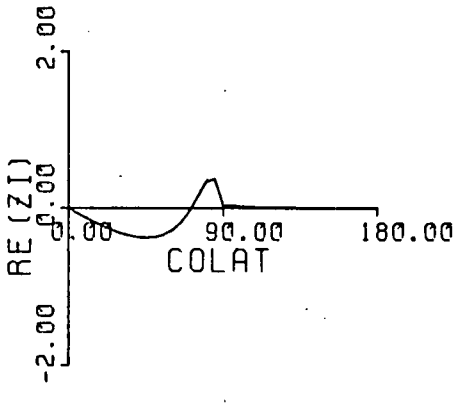

P_2^1 T=12 SIGMA=BANKS 72

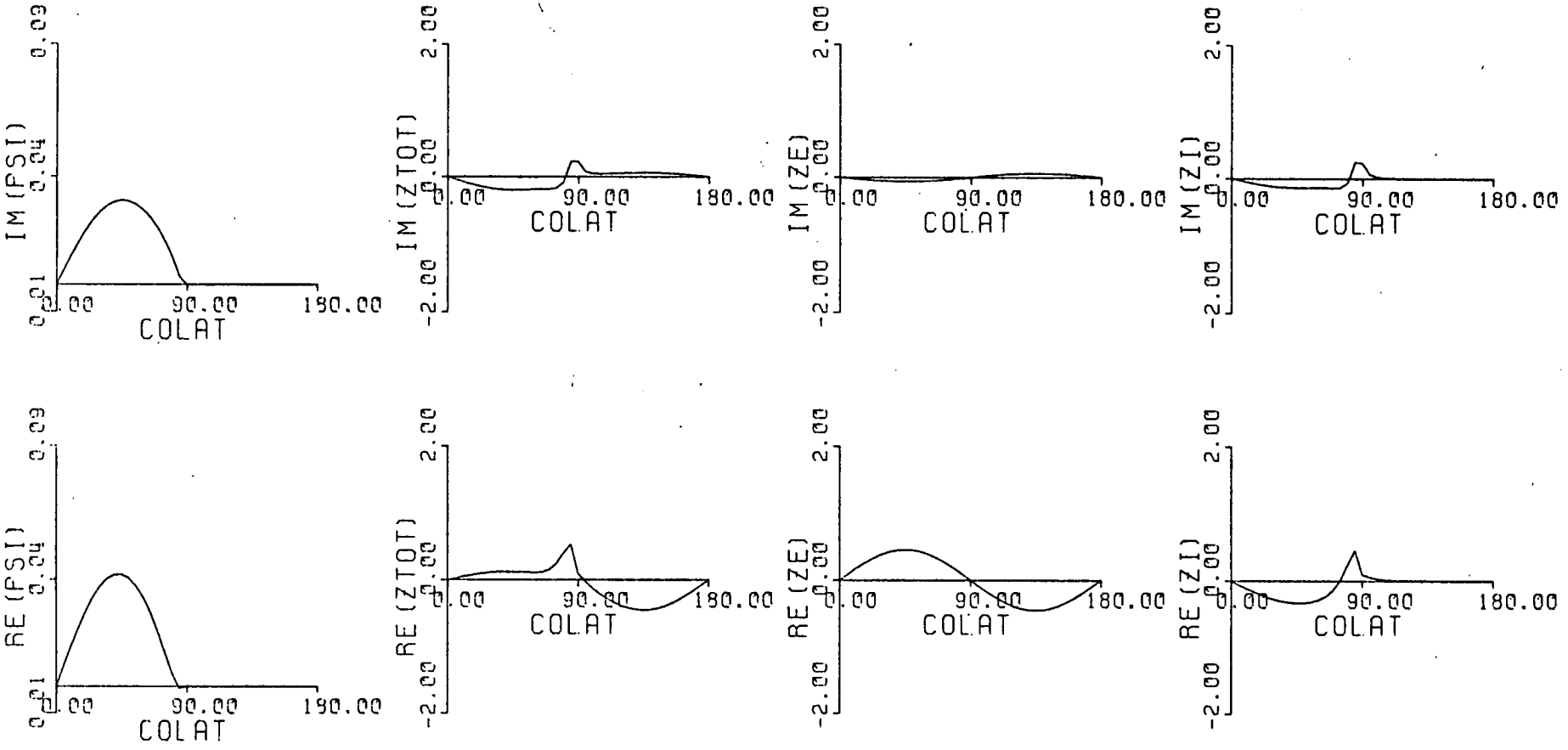

P_2^1 T=12 SIGMA=8

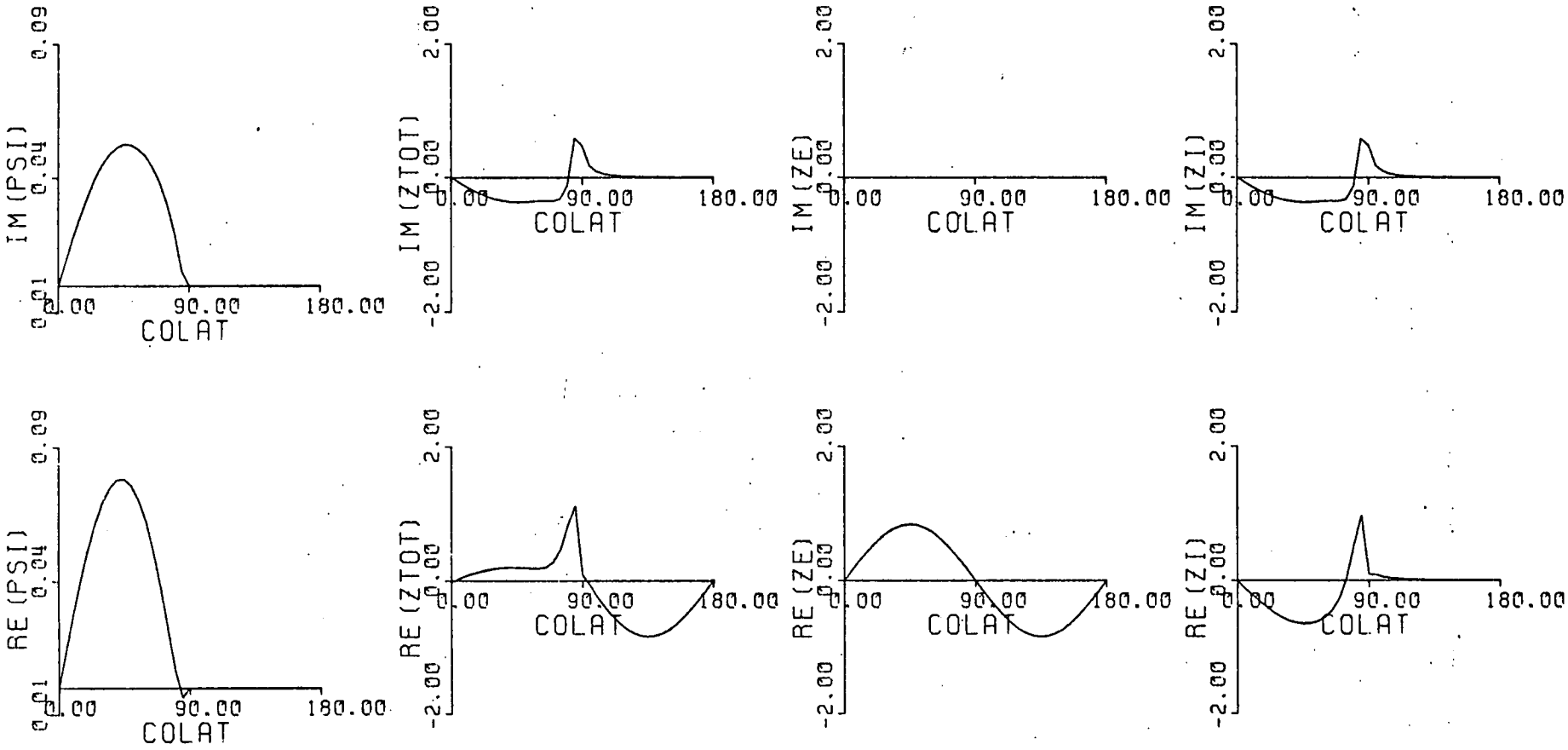

P_3^2 T=24 SIGMA=BANKS 72

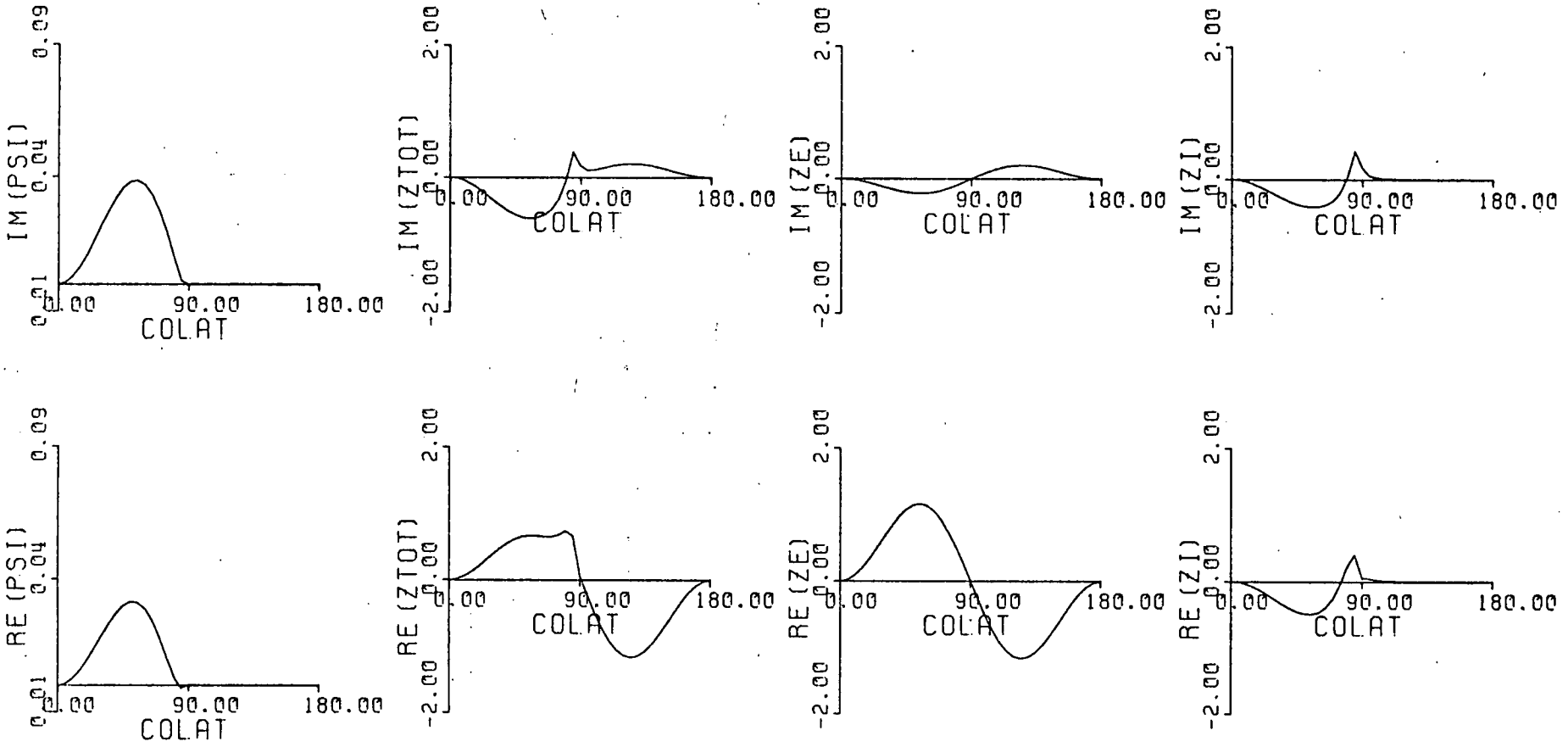

P_3^2 T = 24 SIGMA = 8

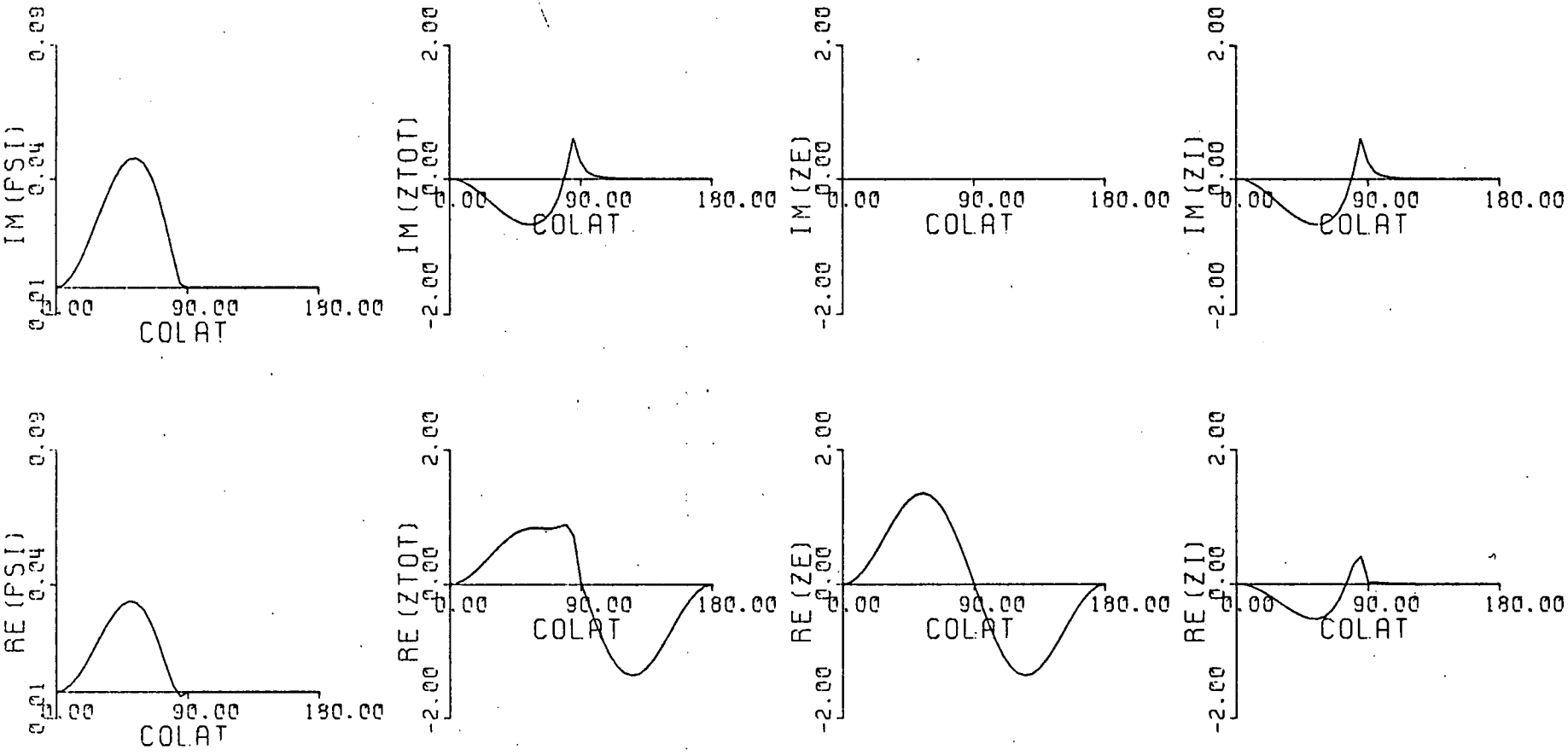

P_3^2 T = 12 SIGMA=BANKS 72

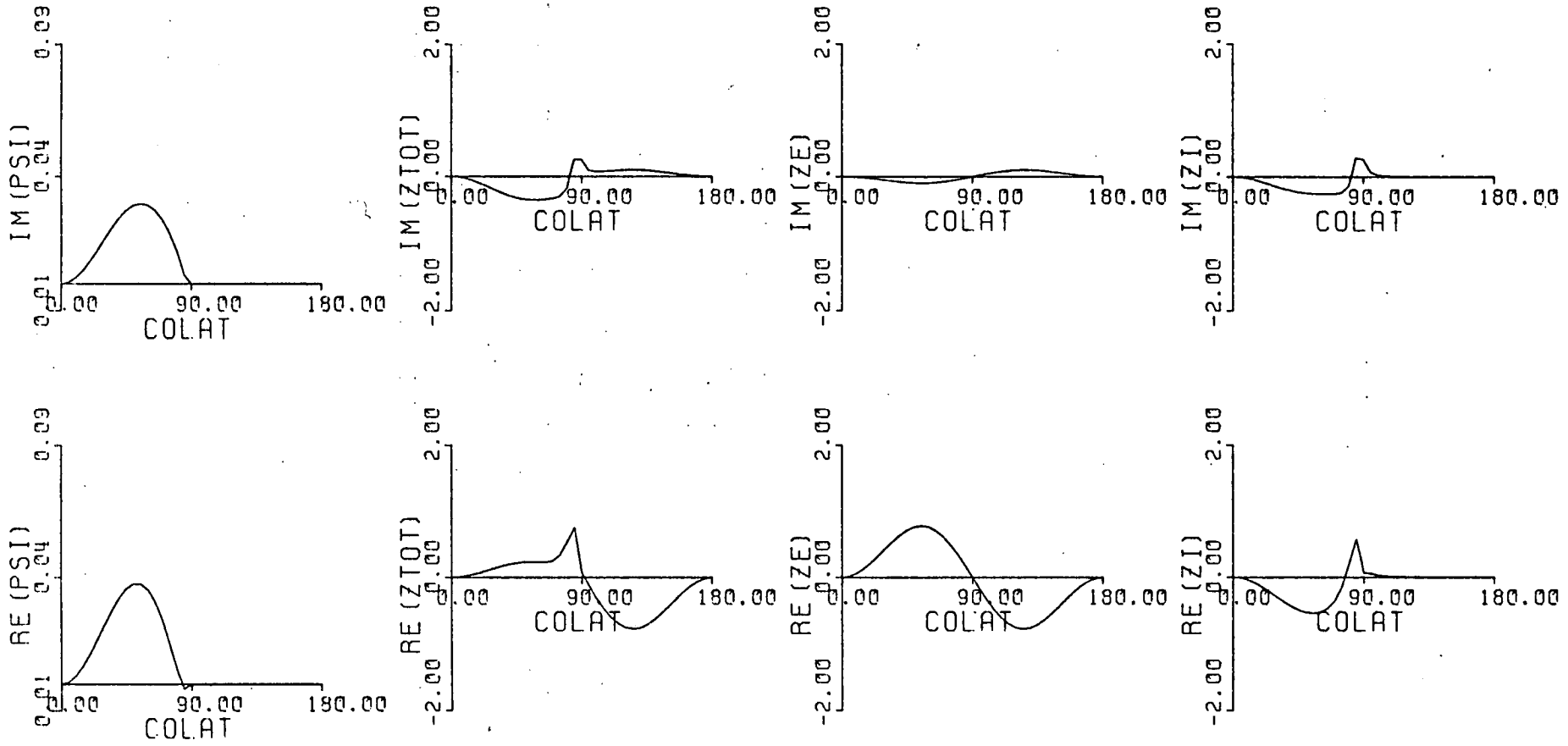

P_3^2 T=12 SIGMA=∞

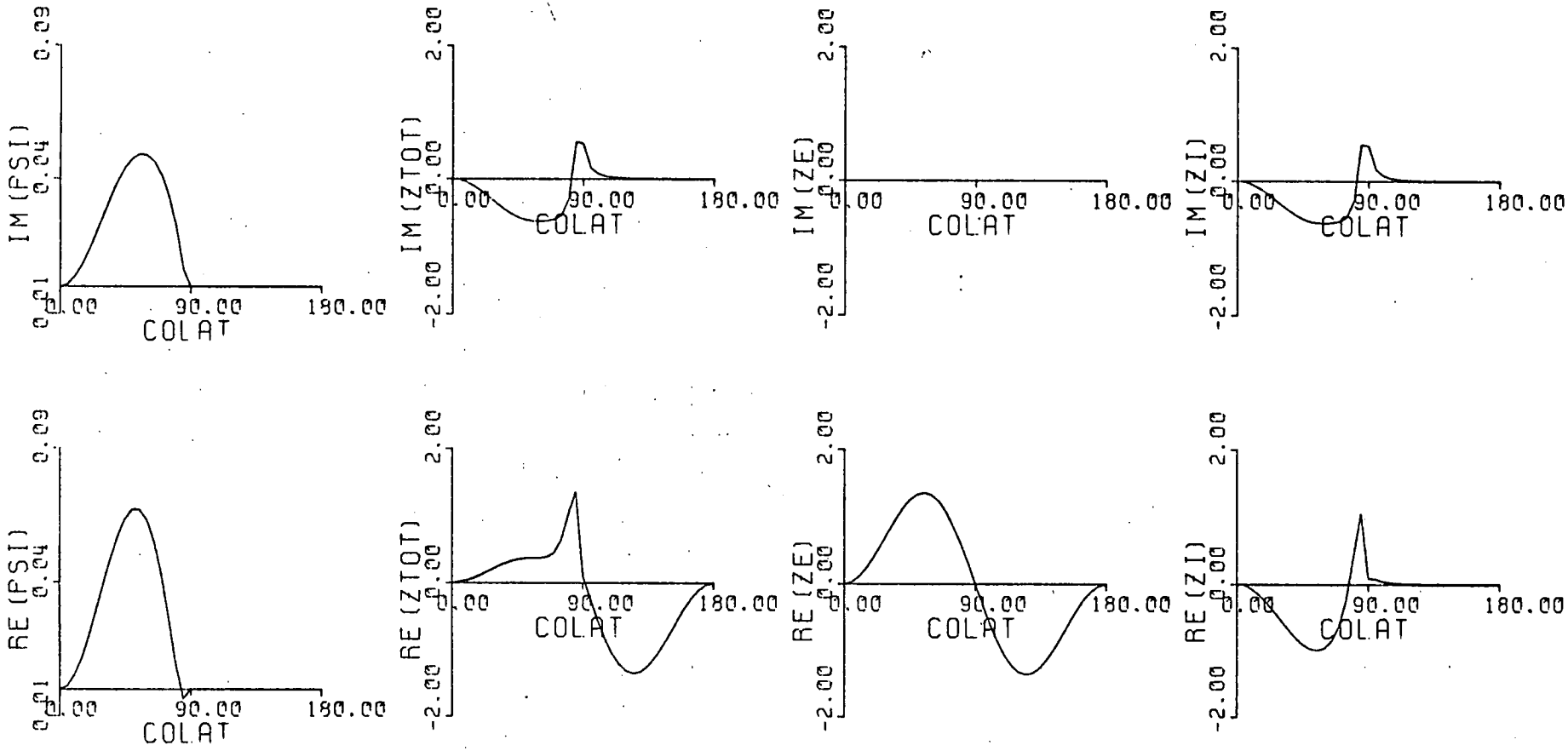

P 3
4

T=24

SIGMA=BANKS 72

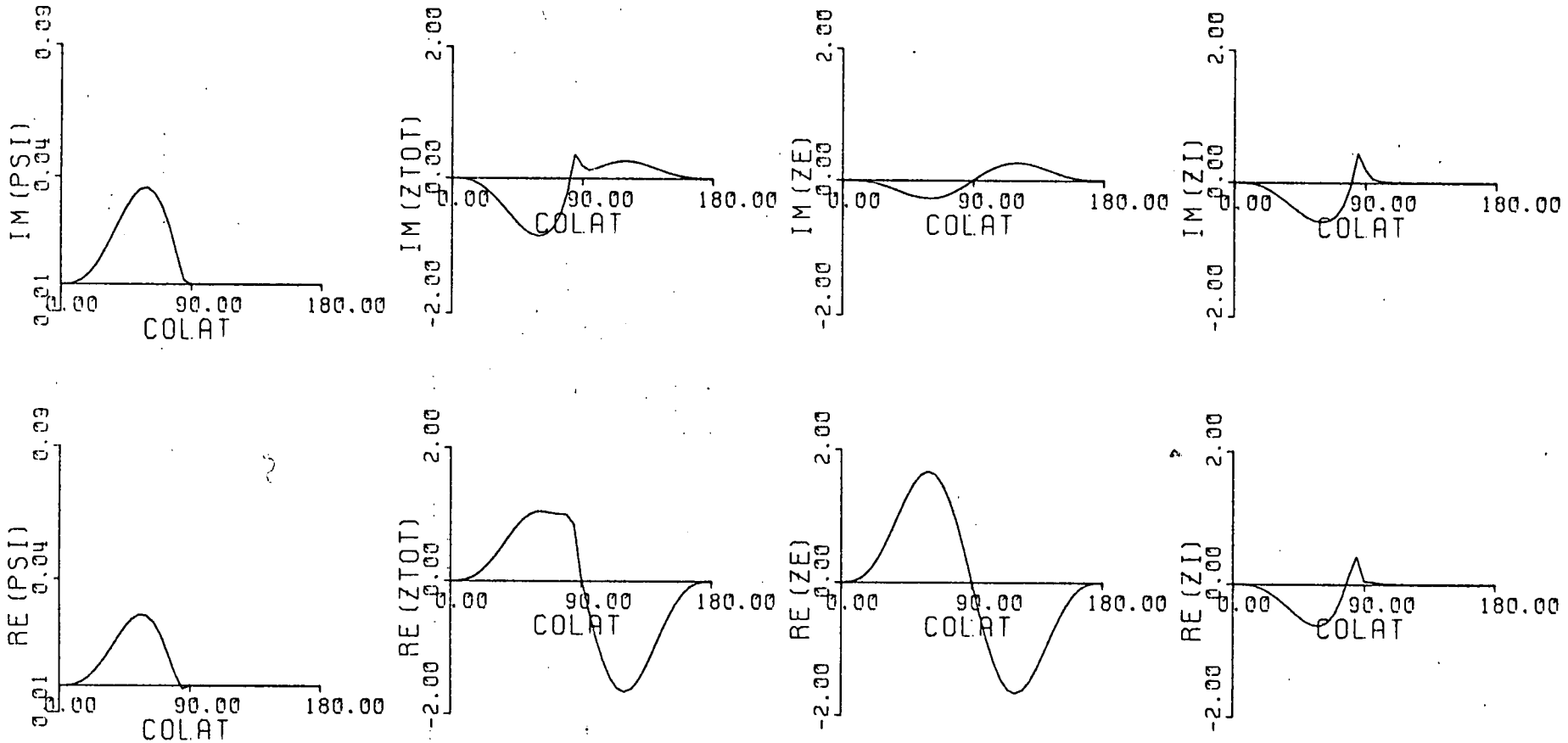

P_4^3 T=24 SIGMA=∞

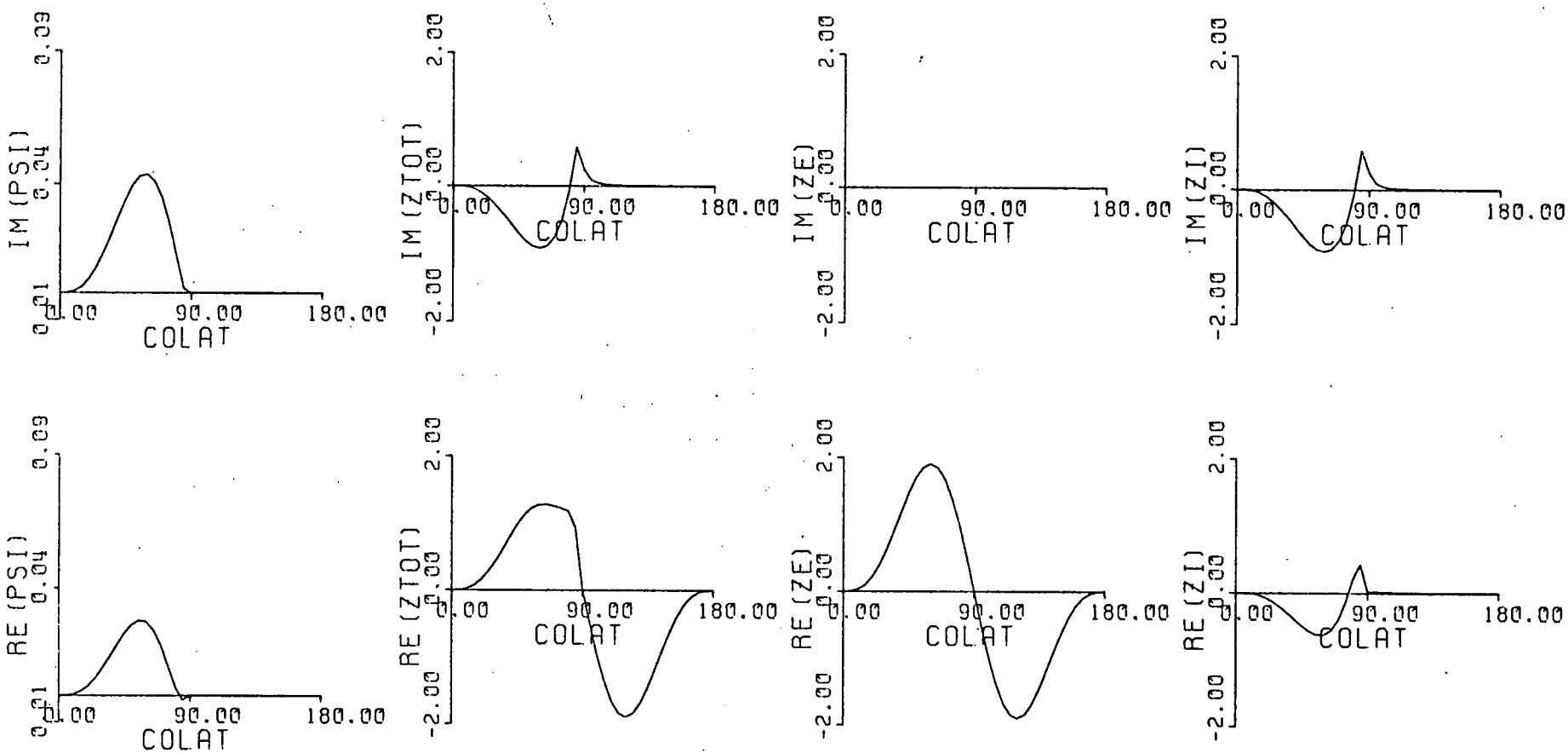

P 3 4

T = 12

SIGMA=BANKS 72

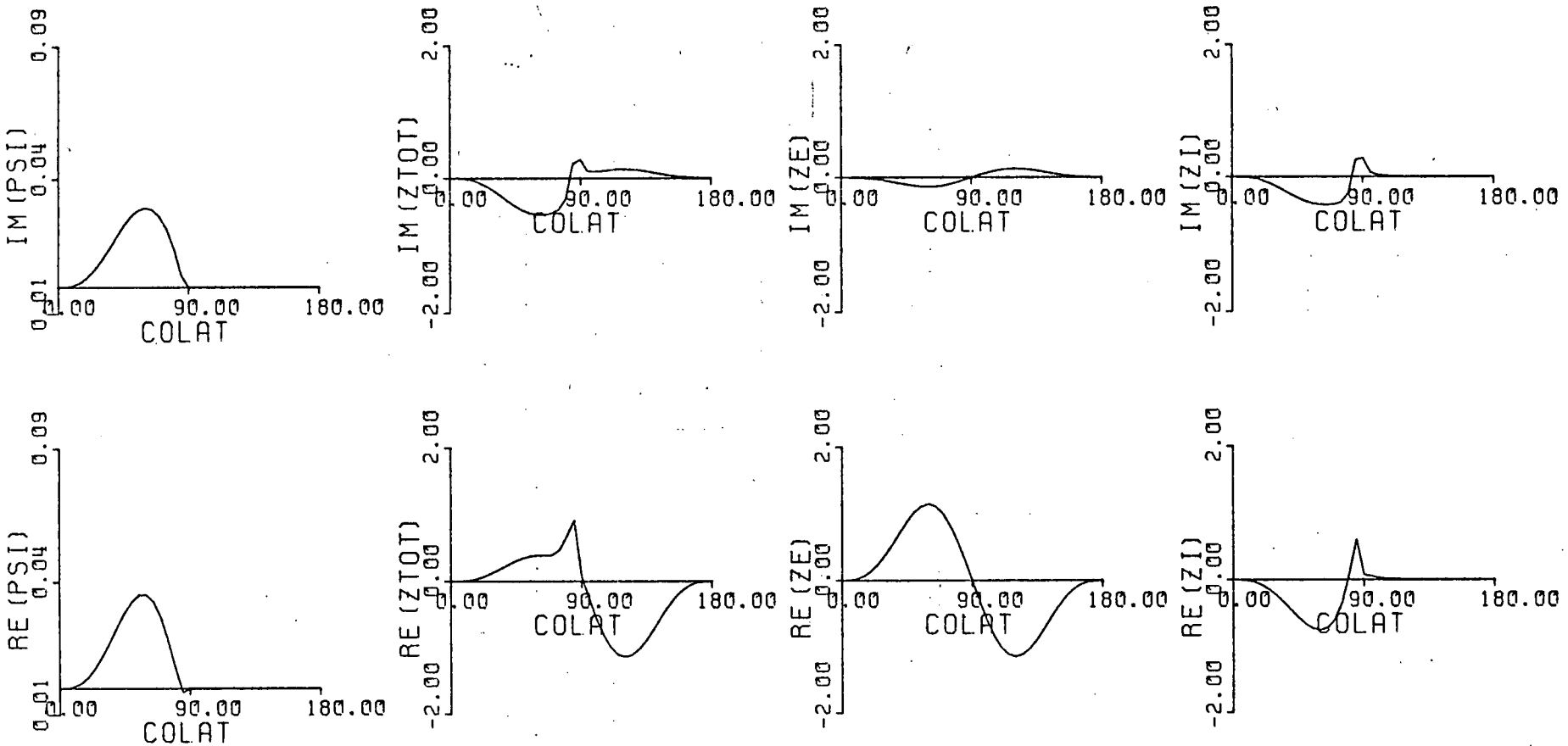

P 3 4

T = 1 2

SIGMA = ∞

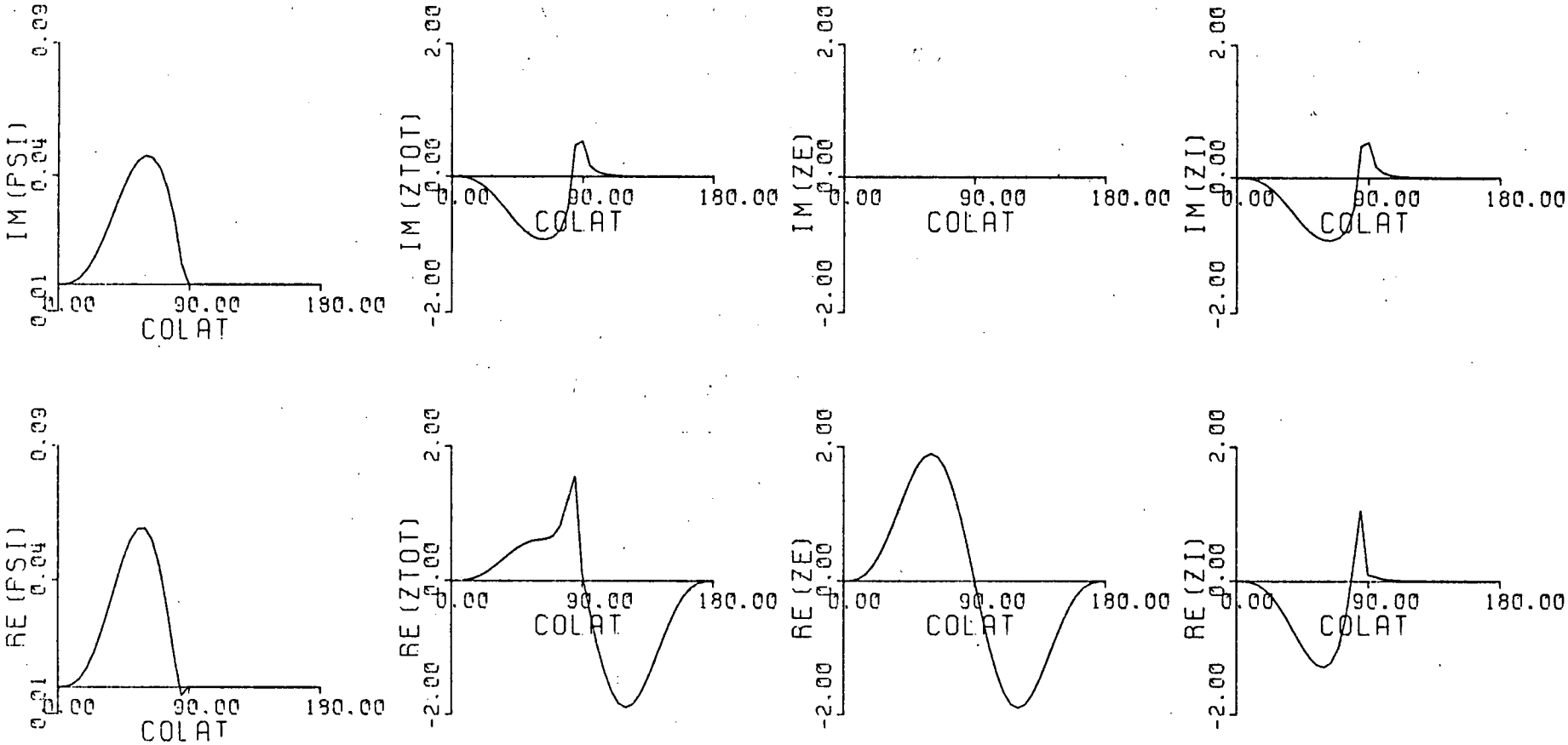

CHAPTER 5

5.1) Modelling with the Real Oceans and Banks' Conductivity.

It was decided to make alterations to an existing computer program for solving the oceanic induction problem, with a thin surface integrated conductivity resembling the distribution of the deep oceans over the globe, so that the perfectly conducting mantle could be replaced by Banks' conductivity distribution. The results of using the original program to model the influence of the oceans on Sq have been presented in a paper by Hobbs and Dawes (1979) and, as with the hemispherical modelling program, it was necessary to make changes to deal with a complex equation, at each stage of the Price iterative scheme, instead of a real equation. However further changes were essential because, having switched to solving for real and imaginary parts, the program now took approximately twice as long to run, so it was desirable to make the program more efficient. It had been possible to run the program for induction in a hemispherical shell on the relatively slow I.C.L. 4-75 machine, since the axi-symmetry of the model reduced the amount of necessary computation, but it was essential to switch to the faster I.C.L. 2980 computer to deal with the basically two-dimensional problem of induction in the real oceans. In the hemispherical case it was only required to find the current function on a meridian, since the symmetry ensured that the longitudinal dependence of the solution was the same as that of the inducing field, and this was done by taking a finite difference approximation of the differential equation on a 5^{o} grid. This involved reducing the problem to a tri-diagonal matrix equation, which could be solved exactly and directly. The known longitudinal dependence also

ensured that all the vertical fields, calculated by surface integrals, needed only to be evaluated on a single meridian.

The finite difference approximation on a $5^{o}x5^{o}$ grid for the real ocean distribution involved 1406 oceanic grid points arranged in 76 rows ,with all the points in any given row having the same colatitude, therefore it had been decided to solve the resulting matrix equation by a block iterative scheme. It also became necessary to calculate the vertical magnetic fields on all the meridians, which increased this part of the calculation 72-fold.

It was also thought that much time was being used in reading the basic integrals from sequential character files, so it was decided to rerun the programs for calculating the basic integrals to enable them to be stored on direct access files, as had been the case while solving the hemispherical problems on the 4-75.

It was also desirable to try to improve the accuracy of the solutions obtained, since some of the contour diagrams of the vertical fields showed some unexpected kinks, especially at higher frequencies (Hobbs & Dawes 1979, Figures 4 & 5). The accuracy parameter used in their paper was based on a sample of twenty mid-oceanic grid points where the accuracy was defined as the residual of the finite difference approximation divided by the inducing field, at that grid point, expressed as a percentage. It was possible to print out the accuracy parameter for the entire grid, where it could be seen that this definition of accuracy showed the solution became progressively less accurate on approaching the nodes of the inducing field, but it was quite noticable that the final solution was less accurate in

the Pacific than elsewhere. It was suspected that this was due to the fact that, in the block iterative scheme, the successive approximations of the current function were calculated over the bulk of the Pacific, Atlantic and Indian Oceans prior to finding them in the Southern Ocean, which linked the other three. Altering the order of the block iterative scheme made little difference to the accuracy parameter of the final solution, although it was reduced from 1.09% to 0.92% for a P_2^1 inducing field with a period of 24 hours, the largest inaccuracies were hardly diminished.

However, by examining the extent to which each current function satisfied the partial differential equation after each step of the Price iterative method, it could be seen that the inaccuracy of the final solution in the Pacific was due to the propagation of the inaccuracies from each iteration. This effect could have been overcome simply by increasing the number of iterations in the block iterative scheme but this would have resulted in considerably longer run times, therefore it was decided to try to accelerate the convergence of the iterations.

The program had originally been written to use successive overrelaxation (S.O.R.) to accelerate the convergence but the solution was found to be unstable after a few iterations. If ψ_i^* is the solution obtained after the ith iteration and ψ_{i+1} is the result obtained from the next application of the block iterative scheme, then the result after i+1 full iterations, ψ_{i+1}^*, is defined as:

$$\psi_{i+1}^* = \omega \psi_{i+1} + (1-\omega) \psi_i^* \qquad (5.1)$$

where ω is the acceleration parameter, or overrelaxation factor.

This procedure is usually presented in terms of matrices

(Young, 1971, p73) but it is not universally appicable, since there are restrictions on the properties of the matrix operator which contains the finite difference approximation of the partial differential equation (Young, 1971, p395 & Westlake, 1968, p82). Aitken's Δ^2 method (Westlake, 1968, p83) was used in an attempt to accelerate the convergence but it proved unsuccessful, presumably because the block iterative scheme did not have linear convergence. An attempt to program the conjugate gradient method (Szidarovsky & Yakowitz, 1978, p207), in which it was necessary to calculate the transpose of the finite difference scheme, also proved to be abortive.

The block iterative scheme used, in which maximum use was made of any new values, was similar to the Gauss-Seidel method of solving systems of linear equations (Westlake, 1968, p55), the convergence of which relies on the magnitude of the eigenvalues of the matrix being small. If the dominant eigenvalues comprise a compex-conjugate pair, then the convergence can be rather erratic although this can be overcome by using the so called back-and-forth Gauss-Seidel method (Westlake, 1968, p56). In this method the calculations of alternate iterations are made in reverse order and the iteration matrix for the double iteration has only real eigenvalues. It was decided to apply this idea to the block iterative method, in which the order of the blocks was reversed on alternate iterations, and although this did not bring about any improvement directly, it did give a stable solution when S.O.R. was used after each double iteration. It was later found that even faster convergence was obtained by using two similar iterations, as opposed to reversed iterations, between each application of S.O.R. Although an exhaustive ana-

lysis was not made, the best acceleration parameter, ω_{opt}, seemed to be given by the formula:

$\omega_{opt} = 2/(1+\sqrt{(1-\mu^2)})$, where μ was the ratio of successive norms (Westlake, p62), defined in terms of single iterations rather than double ones.

This removed most of the anomalous kinks from the graphs of the vertical magnetic field and considerably improved the accuracy parameter for the same number of iterations (forty double iterations with S.O.R. as opposed to eighty single ones). For a P_2^1 inducing field with a period of 24 hours and still using a perfect conductor to simulate the mantle, the use of the above method improved the sample accuracy parameter from 1.09% to 0.26%. The improvement brought about by using S.O.R.is shown in Figure 5.1, where the real part of the internal vertical field is plotted for a P_4^3 inducing field with a period of 8 hours. The improvement is most easily seen in the Pacific at the equator and at the Antarctic coast.

5.2) Potential Integrals.

Before presenting the results obtained, it is convenient to describe the method of calculating the induced scalar magnetic potential, which can be numerically differentiated to yield the induced horizontal magnetic fields. Surface integral formulae for calculating the potential from the current function were presented by Hobbs and Price (1970), where it was necessary to perform the calculation in two parts. The potential due to self induction could be calculated from equation (56), while the potential due to mutual induction, in a perfect conductor, was defined in equation (95). Of course, just as when calculating the induced vertical magnetic field, only the method of

Figure 5.1a

An example of the Internal Vertical Magnetic Field obtained without using S.O.R.

Figure 5.1b (overleaf)

The same solution obtained after using S.O.R.

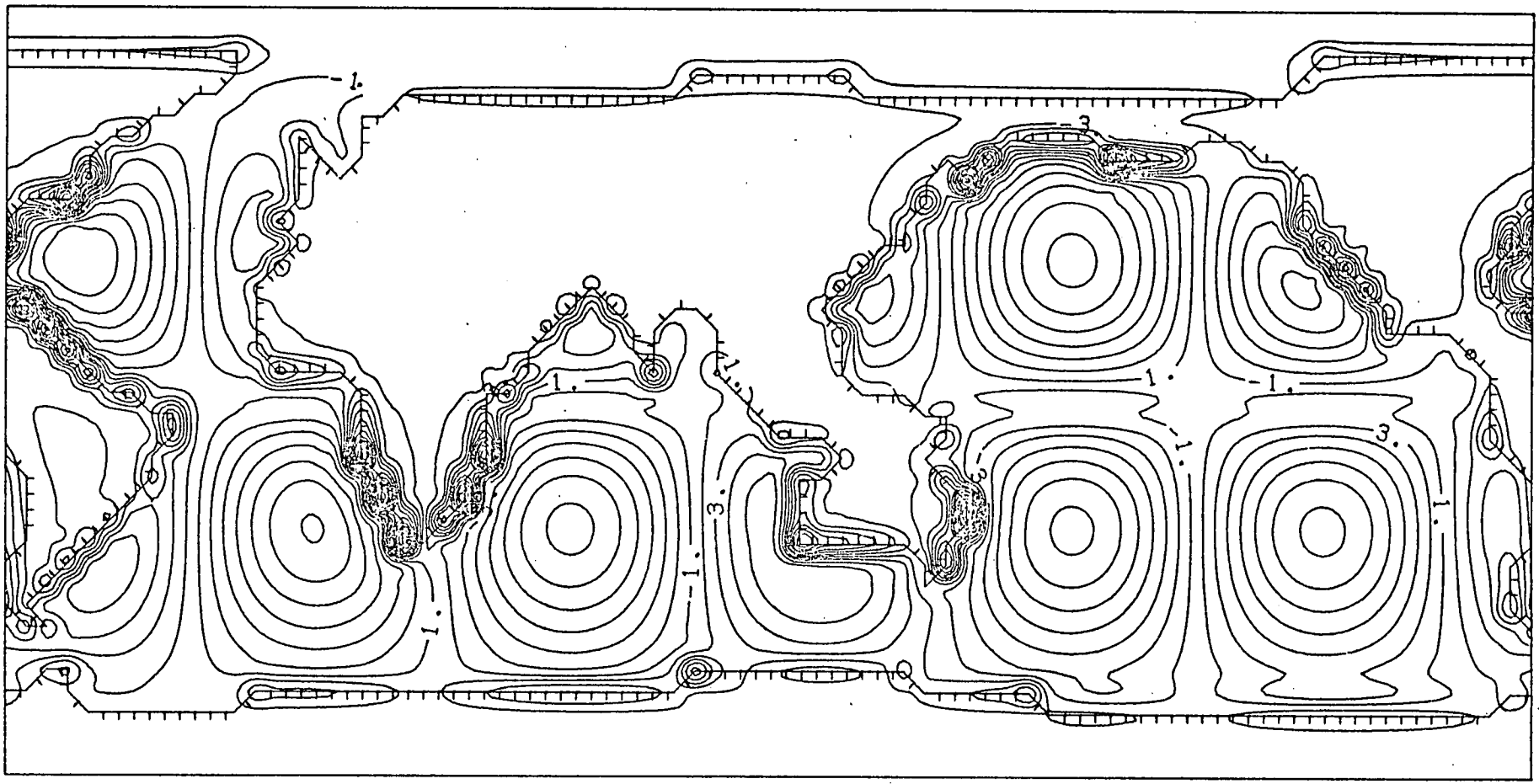

P34H08C ZR

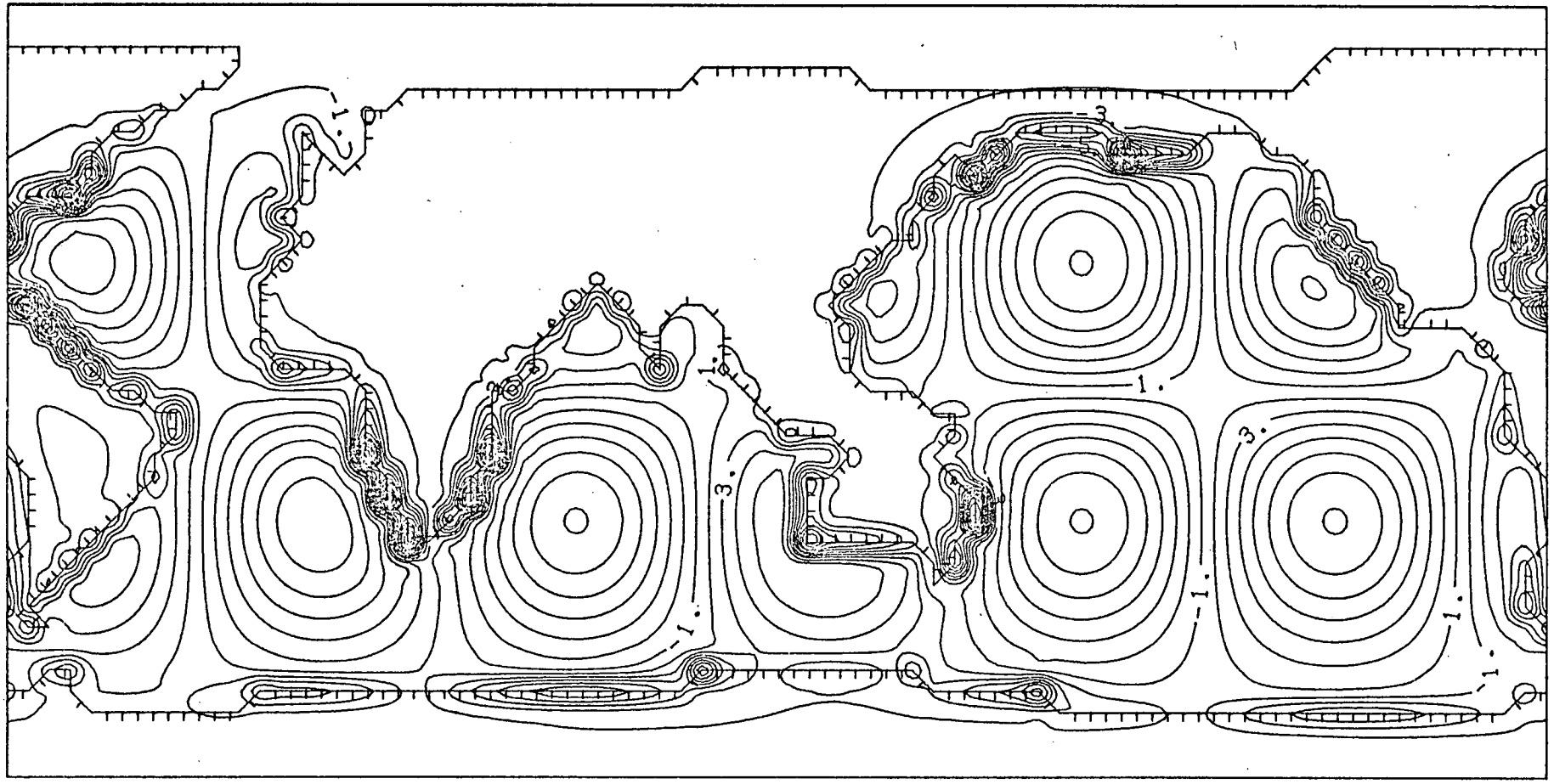

P34H08C ZR (S.O.R.)

calculating the scalar potential due to mutual induction needs to be altered when dealing with a finite conductor.

A comparison between equations (17) and (18) (Hobbs & Price,1970) shows that the coefficients in the series for the potential due to mutual induction are the same as those for the vertical magnetic field except for a factor $-a/(n+1)$. Although these equations were derived for a perfectly conducting conductosphere, this ratio of the coefficients is independent of the nature of the conductivity. Substituting the above factor into equation (2.33) yields the series form of the kernel for calculating the induced potential:

$$K_{Pot}(\theta) = -(\mu_0/4\pi a^2) \sum_n (n+1) (b/a)^{2n+1} \frac{i_n}{e_n} P_n(\cos\theta) \qquad (5.2)$$

This function is shown in Figure (5.2) for periods of 24, 12 and 8 hours together with the kernel for a perfect conductor with radius 0.9 earth radii. (the earth's radius is taken as unity and the factor $\mu_0/4\pi$ is neglected.) It can be seen that the potential kernel is much less sharply spiked than the corresponding vertical field kernel, on account of the fact that a factor $(n+1)$ appears in the coefficients as opposed to $(n+1)^2$. This ensured that the basic integrals could be calculated accurately.

5.3) Discussion of Results.

The solutions obtained with Banks' conductivity profile for the principal Sq harmonics are presented for comparison with the solutions for the model with the perfectly conducting mantle in Figures (5.3a-5.5n). The following functions are plotted: the real and imaginary parts of the current function and of the internal magnetic field (due only to self and mutual induction) (denoted by PSR, PSI, ZR and ZI respectively), the real part of the total vertical field (ZRT), and the real and imaginary parts of the internal magnetic potential (POTR

Figure 5.2

Potential Kernels for Banks' Model together with that of a perfect conductor of Radius 0.9 Earth Radii.

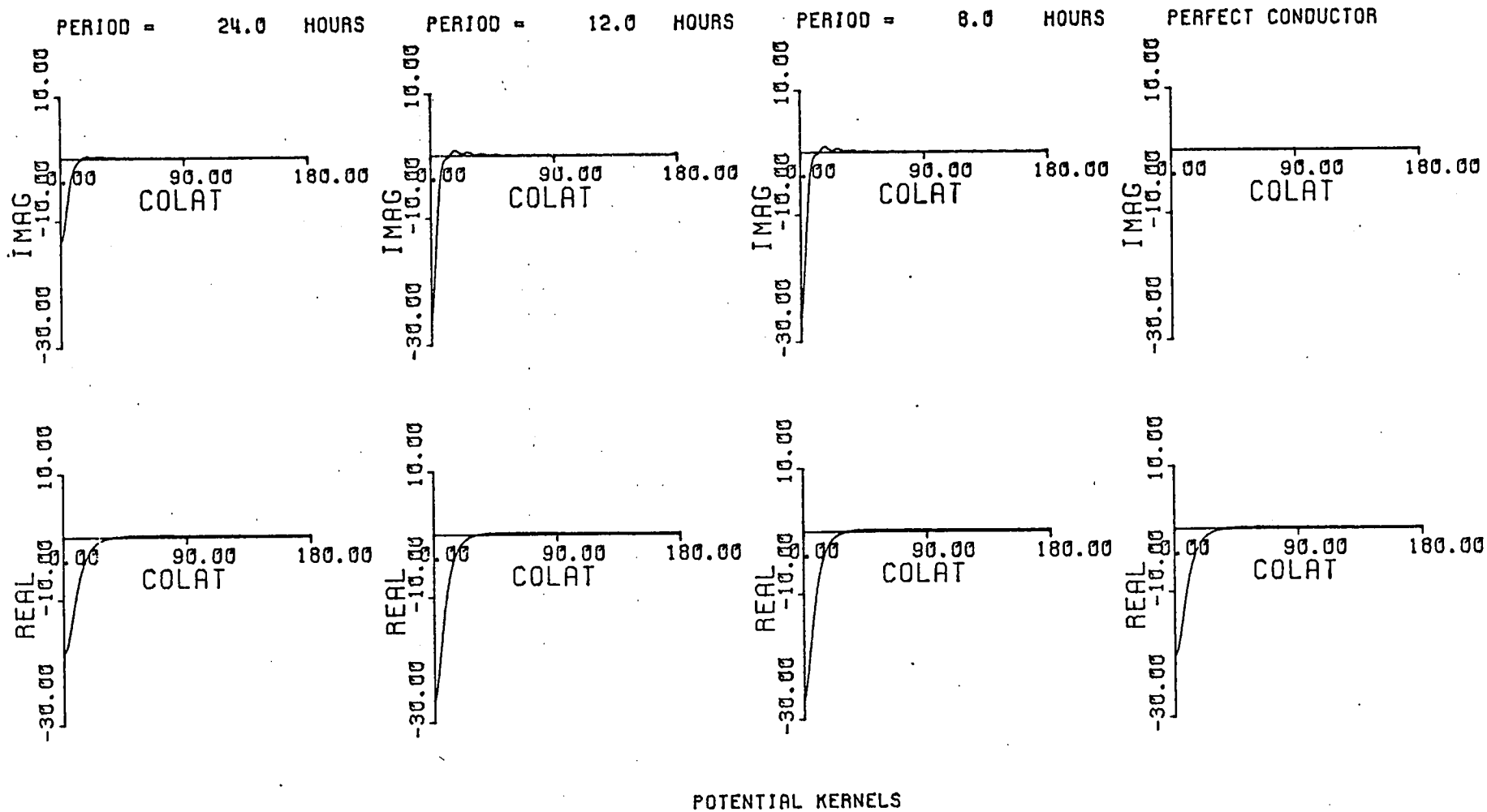

POTENTIAL KERNELS

and POTI). Each solution obtained with the perfectly conducting mantle is presented immediately after the corresponding solution in which Banks' conductivity was used. In the captions the order and degree of the harmonic are given by the two numbers following the 'P', the period in hours by the two numbers following the 'H' and the 'C' or 'S' denotes that either a sine or cosine longitudinal dependence is being considered.

Differences between the current functions and potentials for each of the two models can be seen quite easily, although they are not always so readily observed in the maps of the vertical fields at 24 and 12 hour periods. A detailed comparison of the two models is given in Chapter 6 but it is worthwhile to make a brief comment on the differences between the current functions. For the low frequency inducing field, 1 c.p.d., the strength of the imaginary part of the current function is always greater than the real part and replacing the perfectly conducting mantle by Banks' model results in an increase in the in-phase component and a decrease in the quadrature component. The real part exceeds the the imaginary part at higher frequencies and both real and imaginary parts are reduced when the finitely conducting mantle is used.

Figures 5.3a - 5.3n

Contour Plots of current functions, Internal and Total Vertical Magnetic Fields and Scalar potentials obtained using a Model of the real oceans to compare the effects of using Banks' Model and using a perfect conductor of Radius 0.9 Earth Radii. The period of the Inducing Field is 24 hours.

Contour Interval of the Current Functions is 500A

Contour Interval of the Magnetic Fields is 0.25 nT

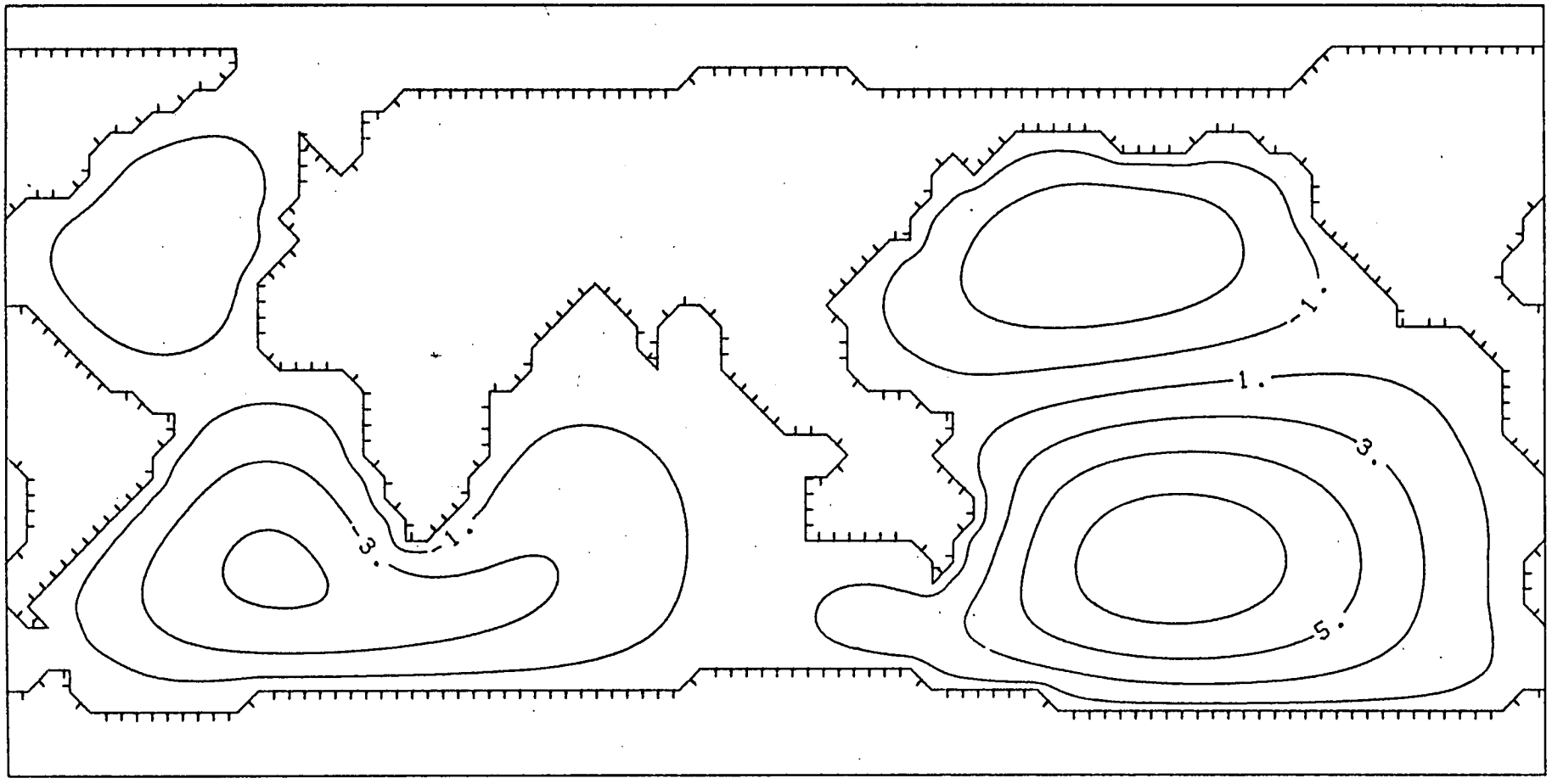

P12H24C PSR (BANKS)

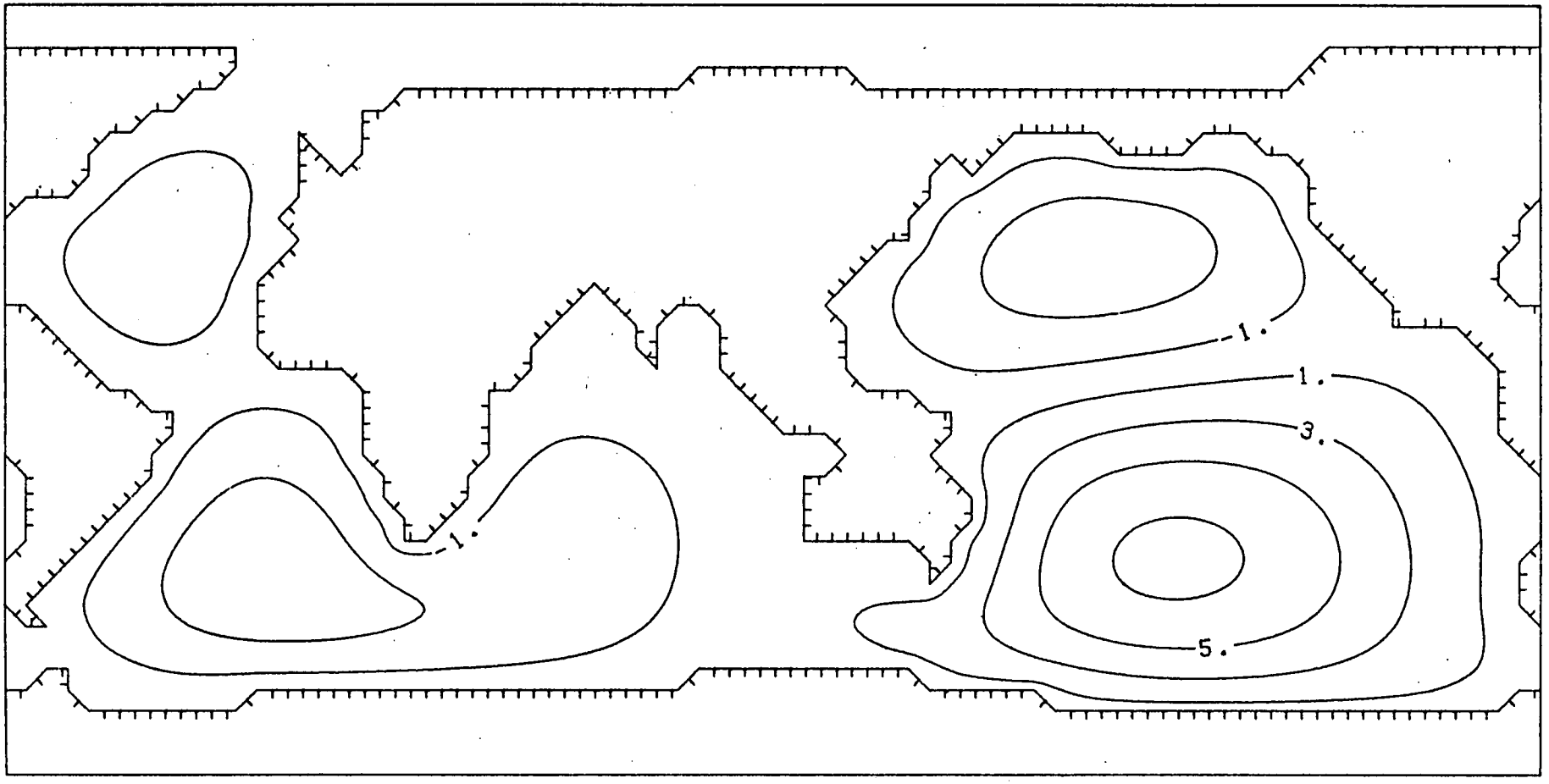

P12H24C PSR (PERFECT)

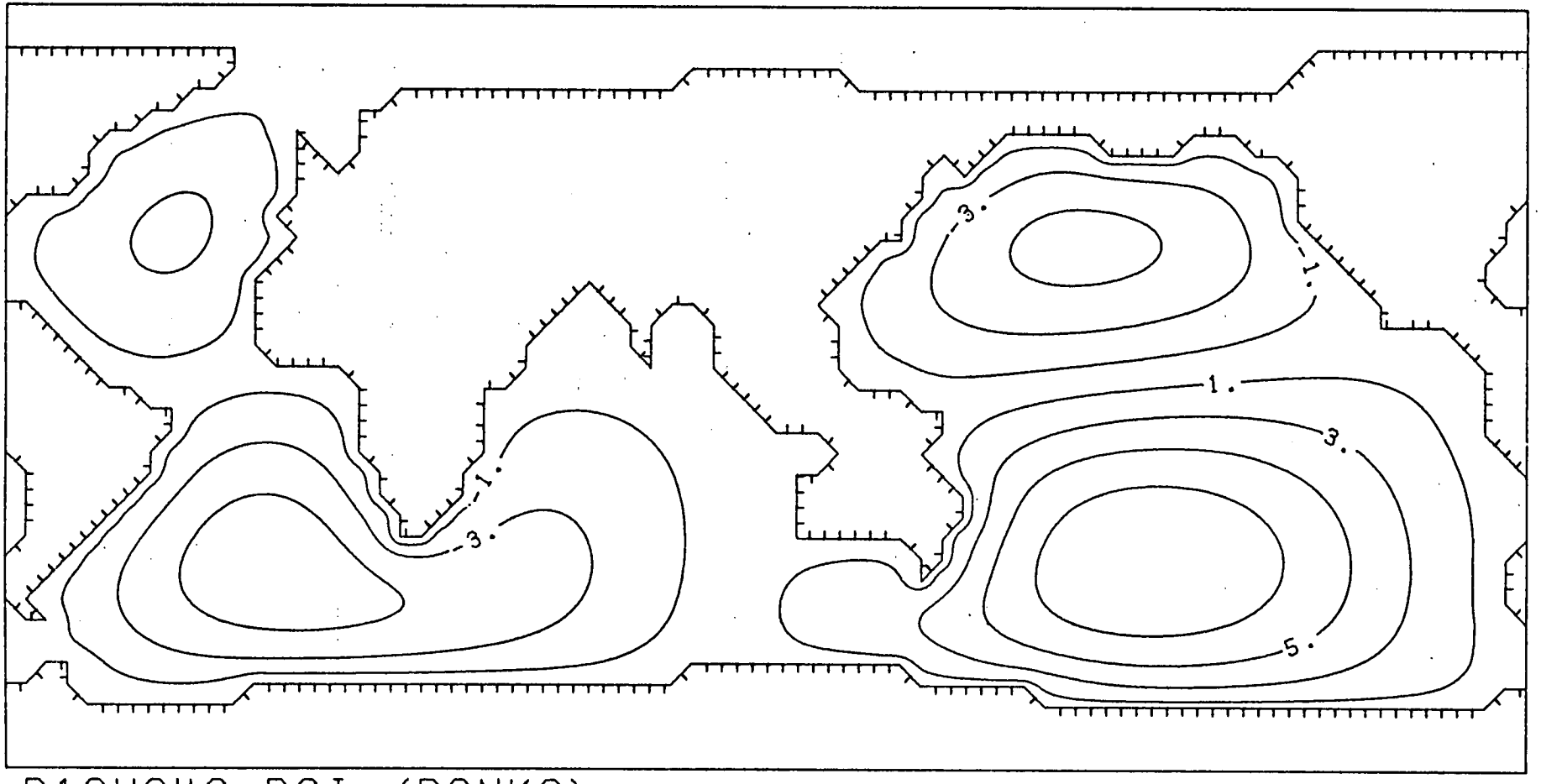

P12H24C PSI (BANKS)

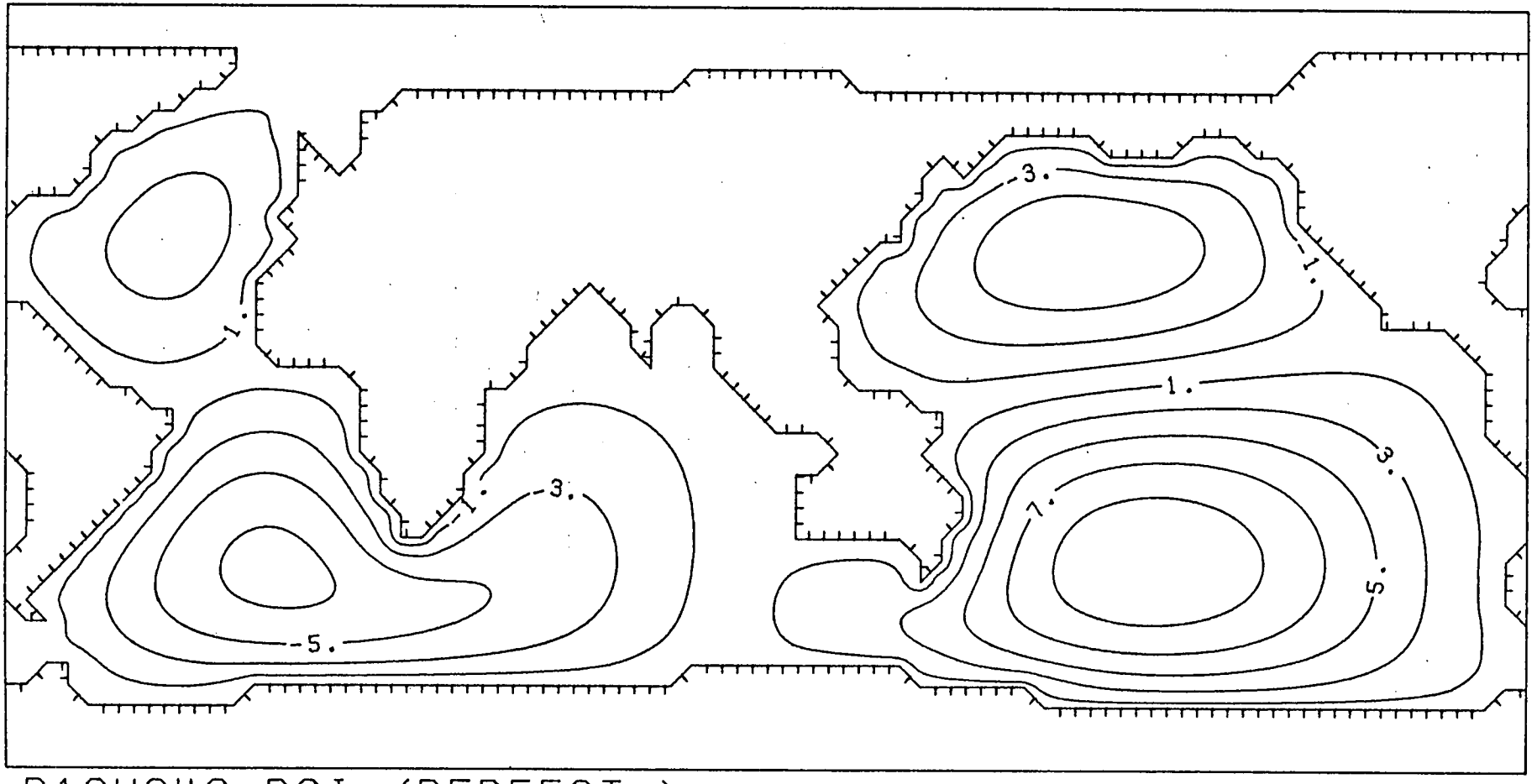

P12H24C PSI (PERFECT)

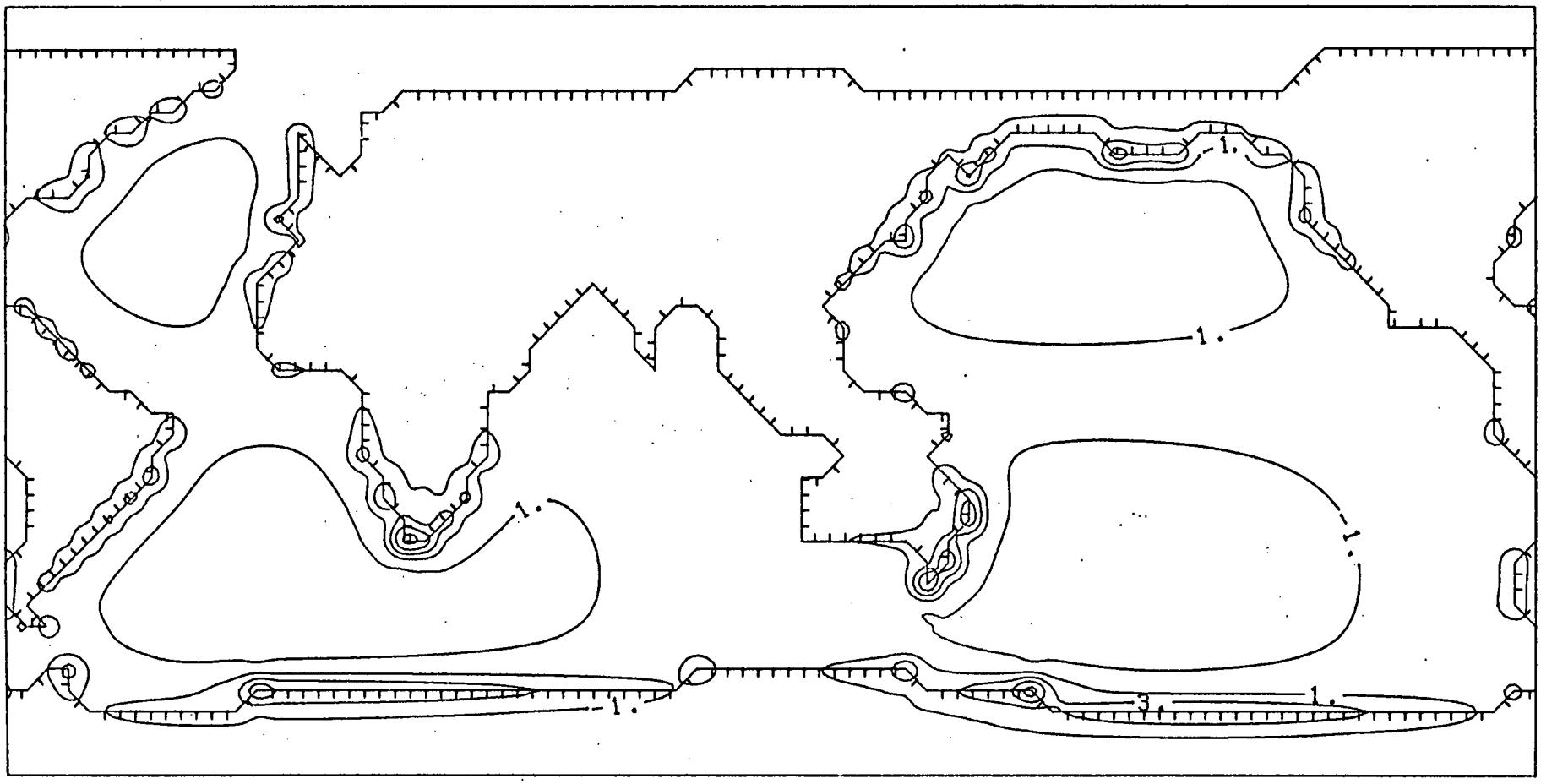

P12H24C ZR (BANKS)

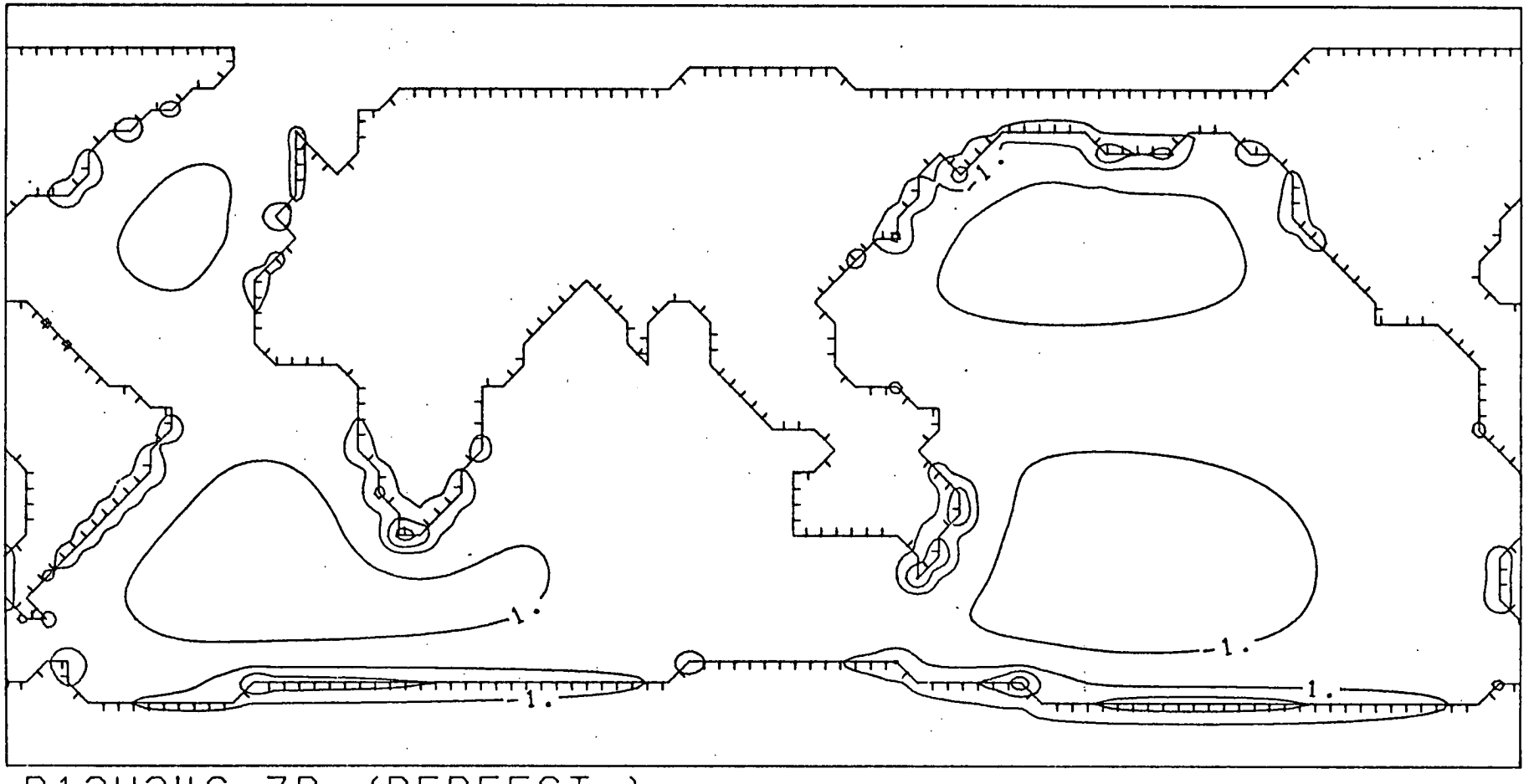

P12H24C ZR (PERFECT)

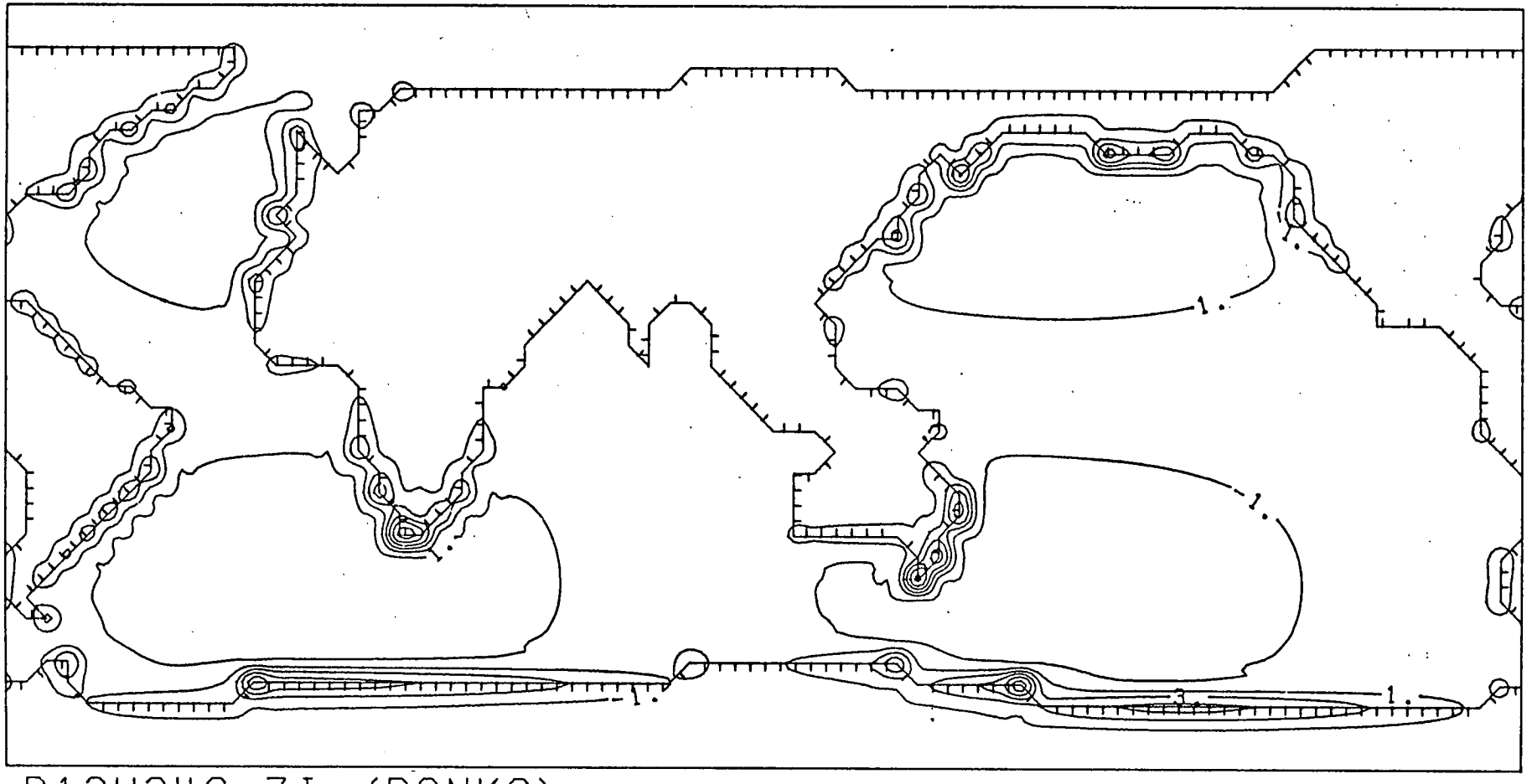

P12H24C ZI (BANKS)

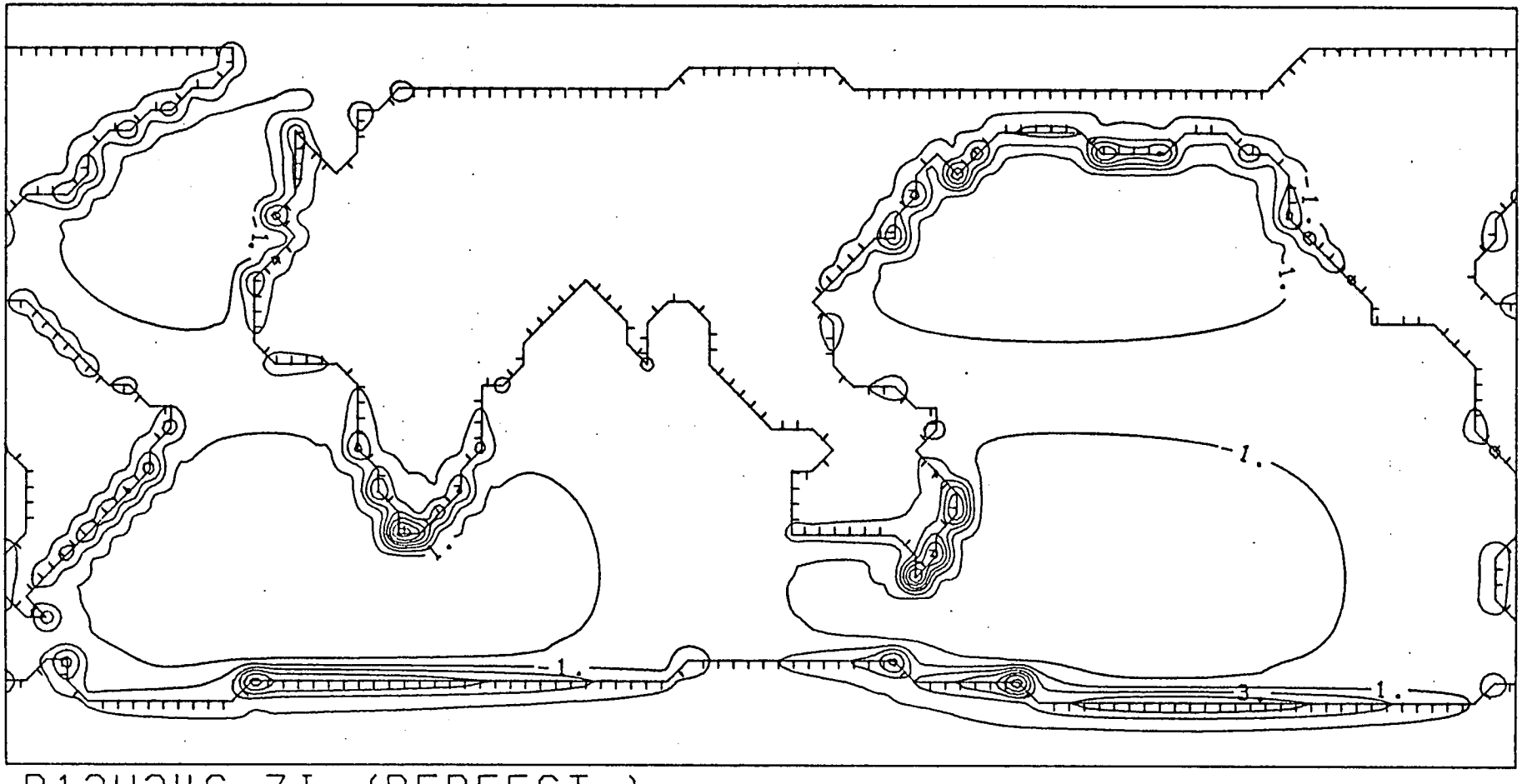

P12H24C ZI (PERFECT)

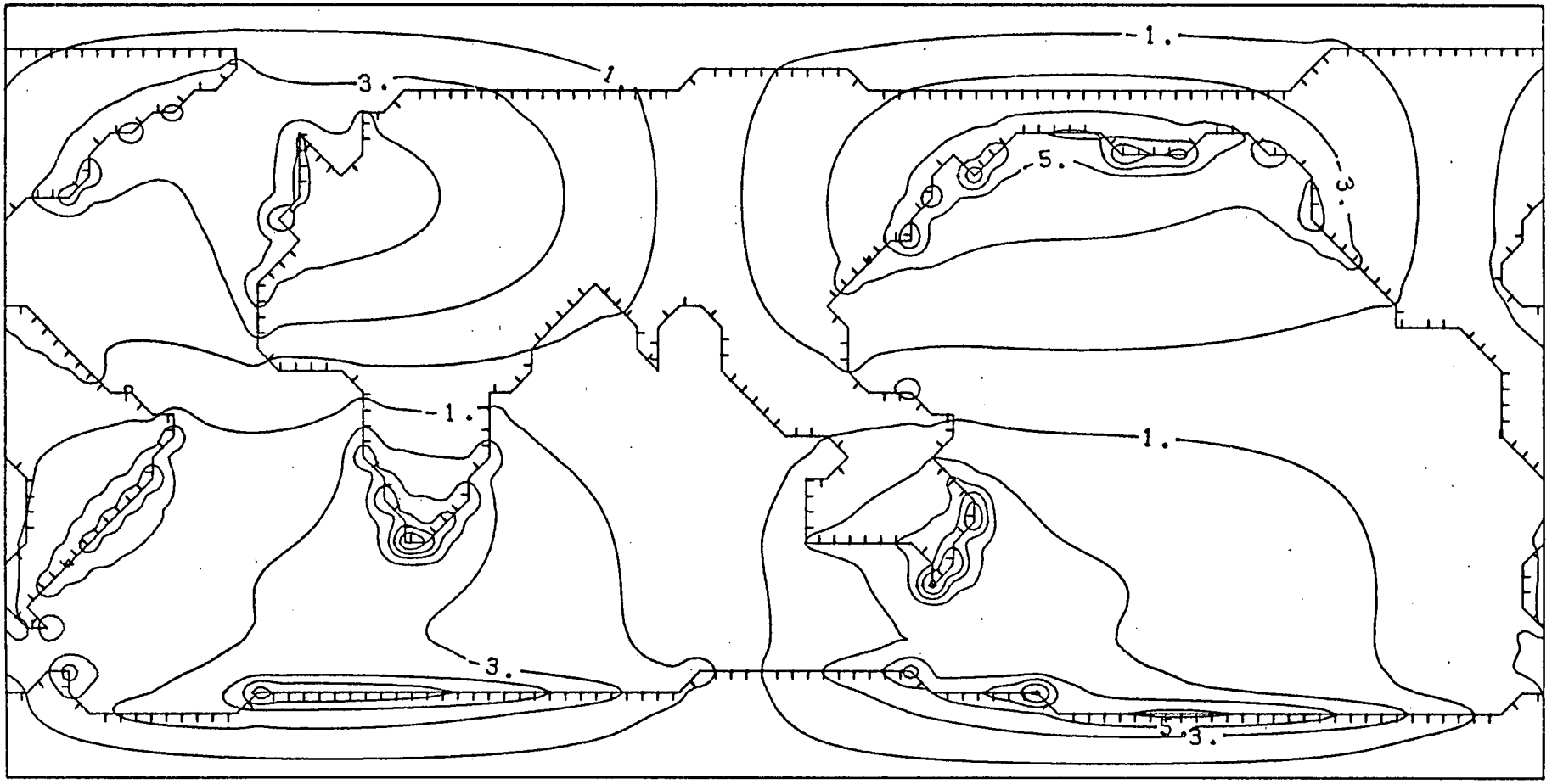

P12H24C ZRT (BANKS)

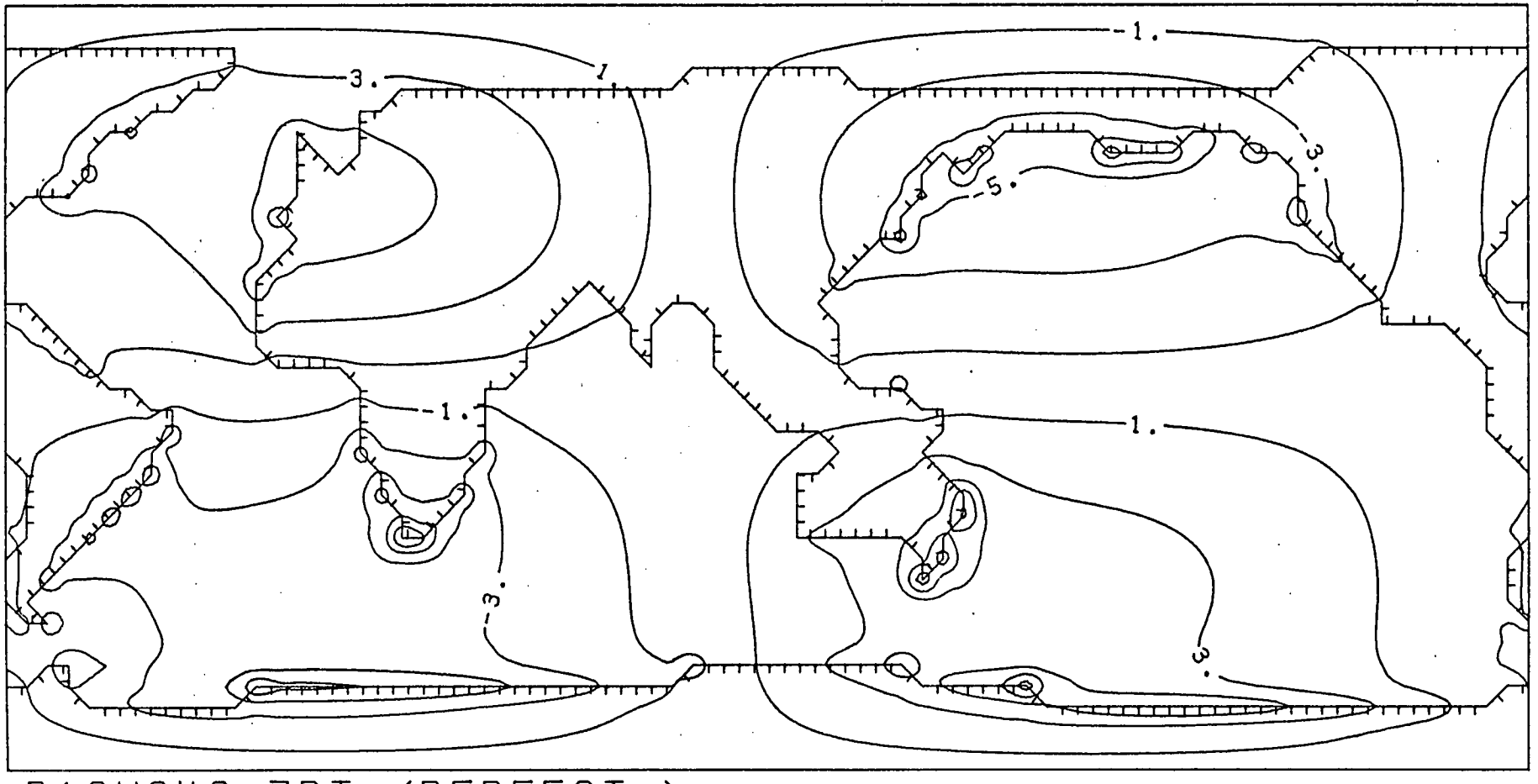

P12H24C ZRT (PERFECT)

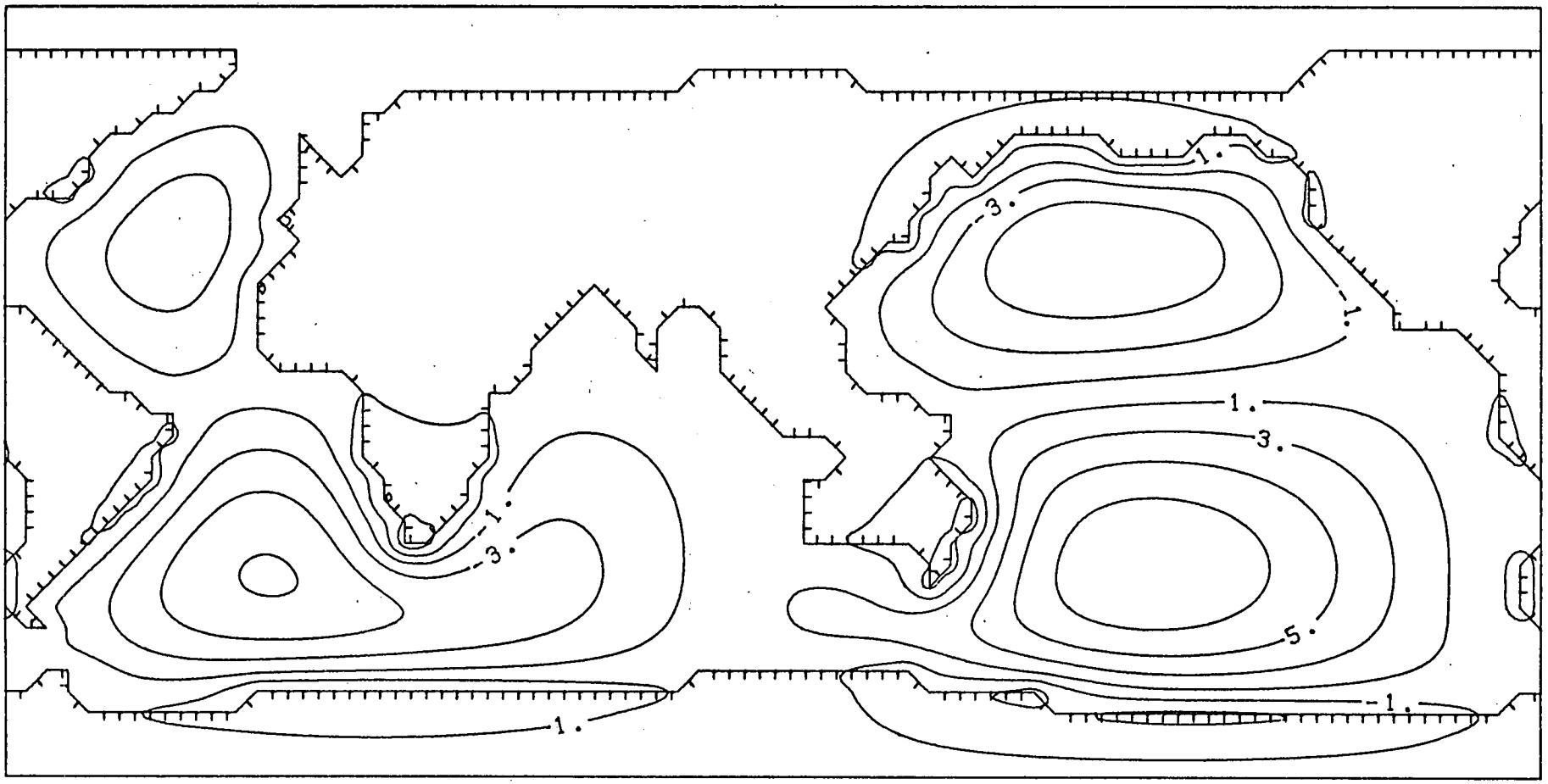

P12H24C POTR (BANKS)

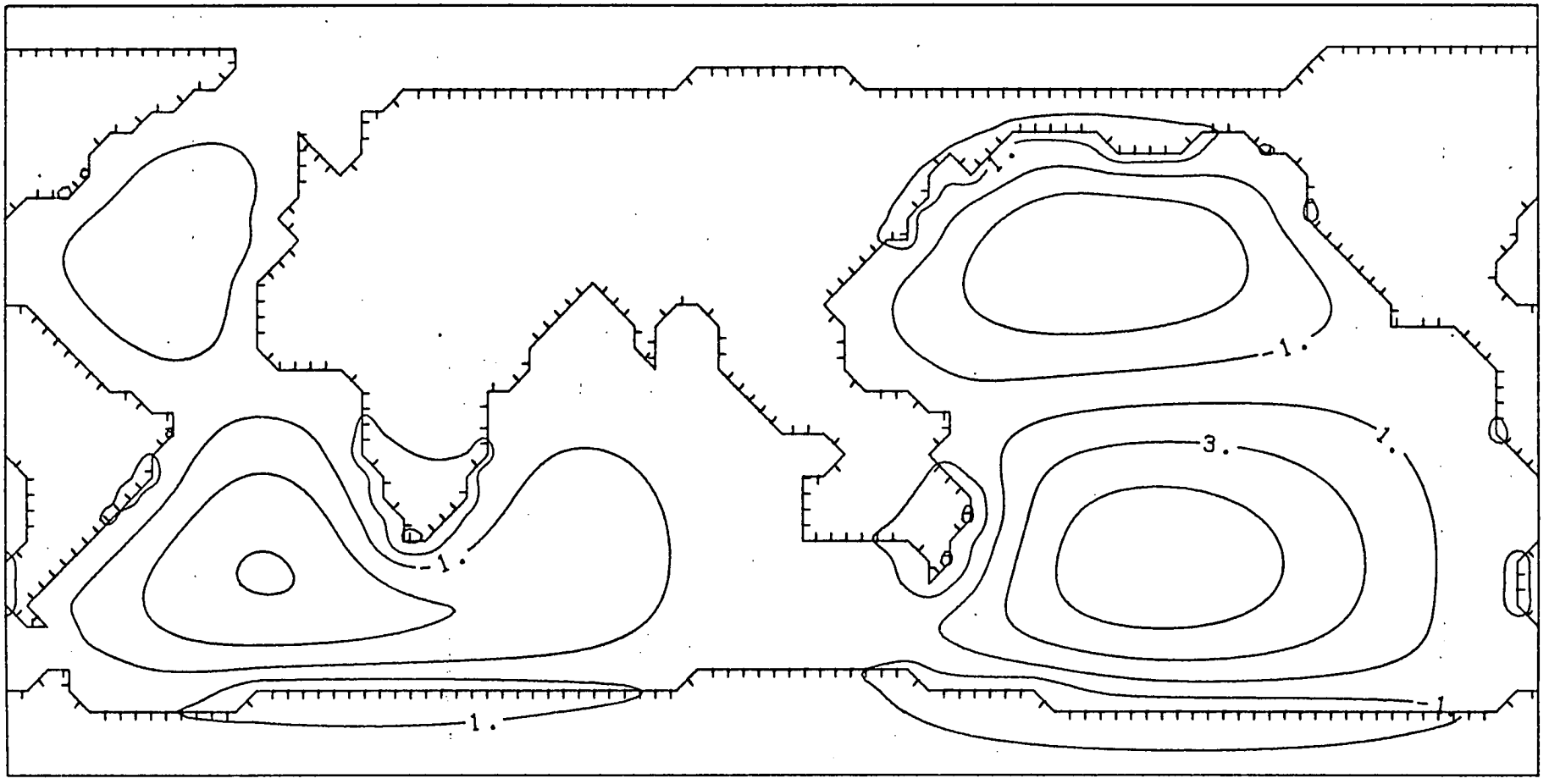

P12H24C POTR (PERFECT)

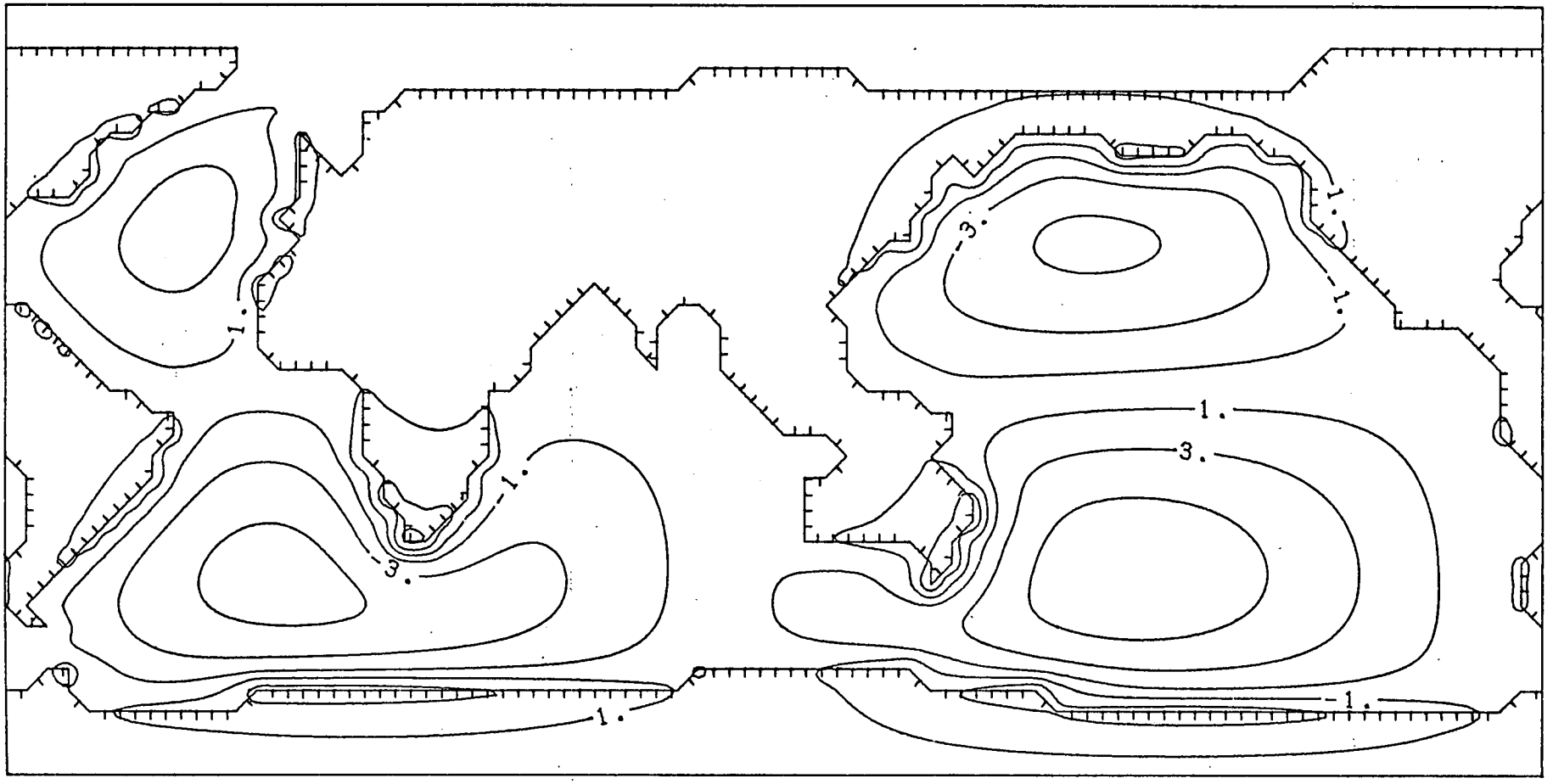

P12H24C POTI (BANKS)

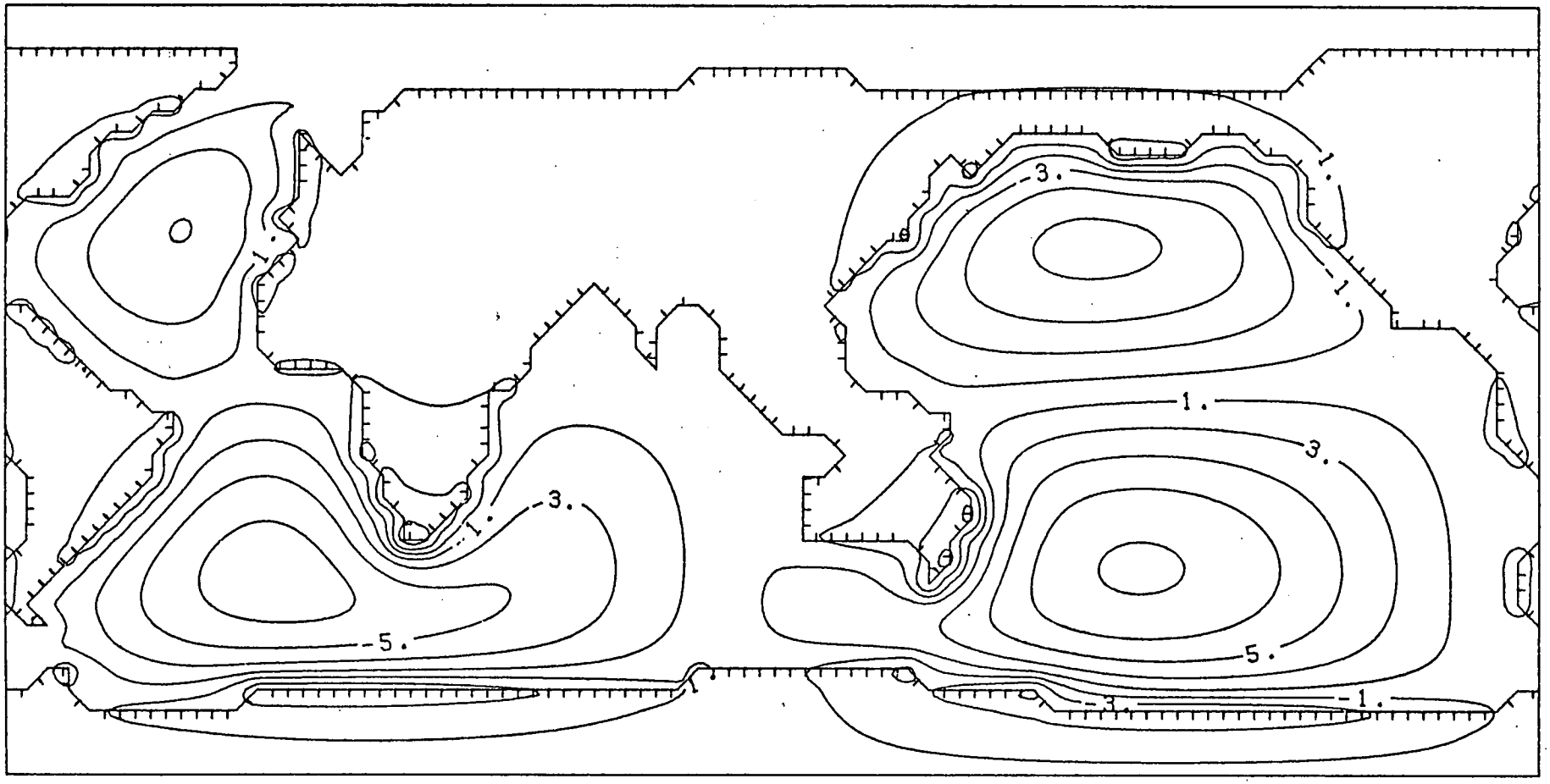

P12H24C POTI (PERFECT)

Figures 5.4a - 5.4n

As for Figures 5.3a - 5.3n but at a period of 12 hours.

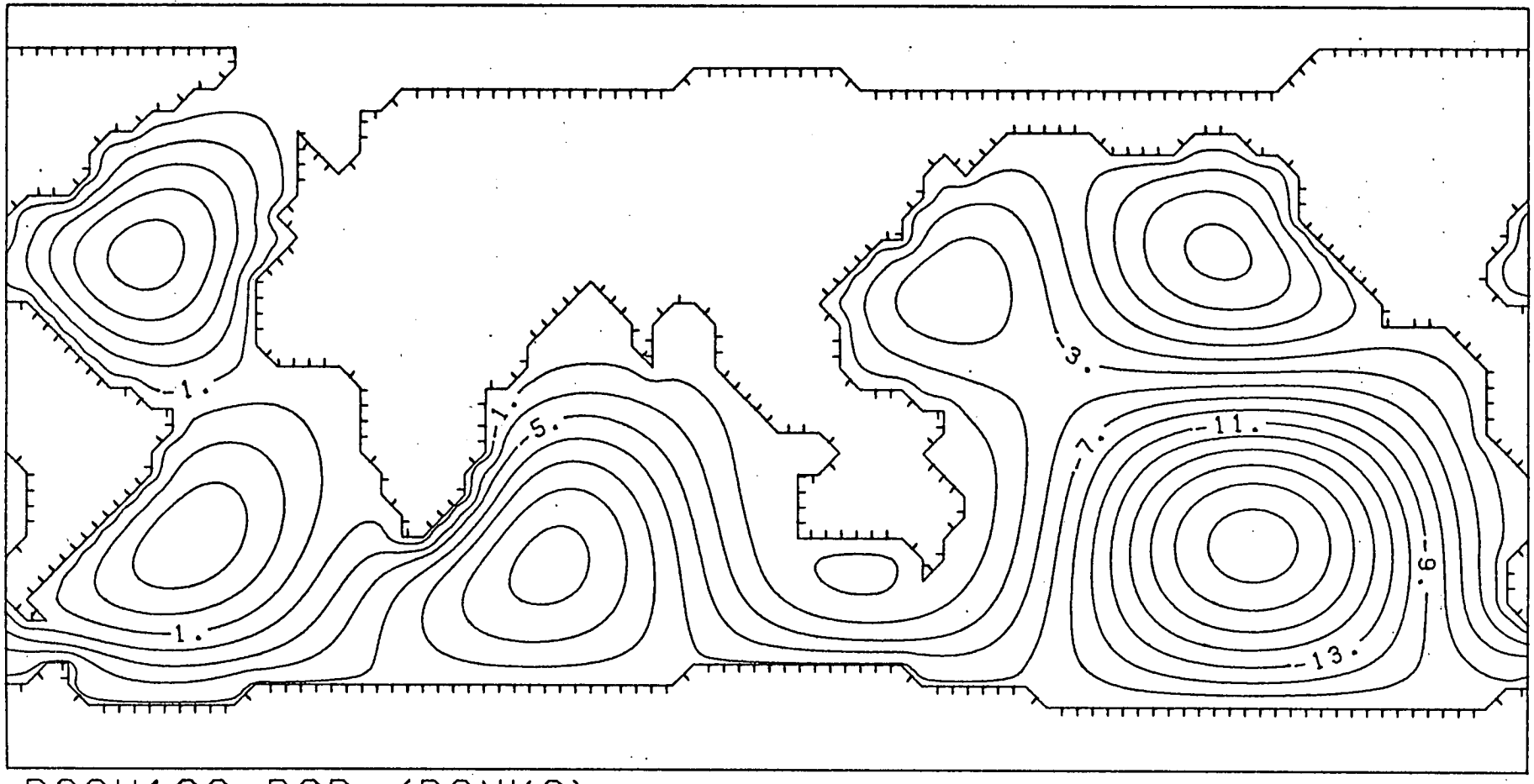

P23H12S PSR (BANKS)

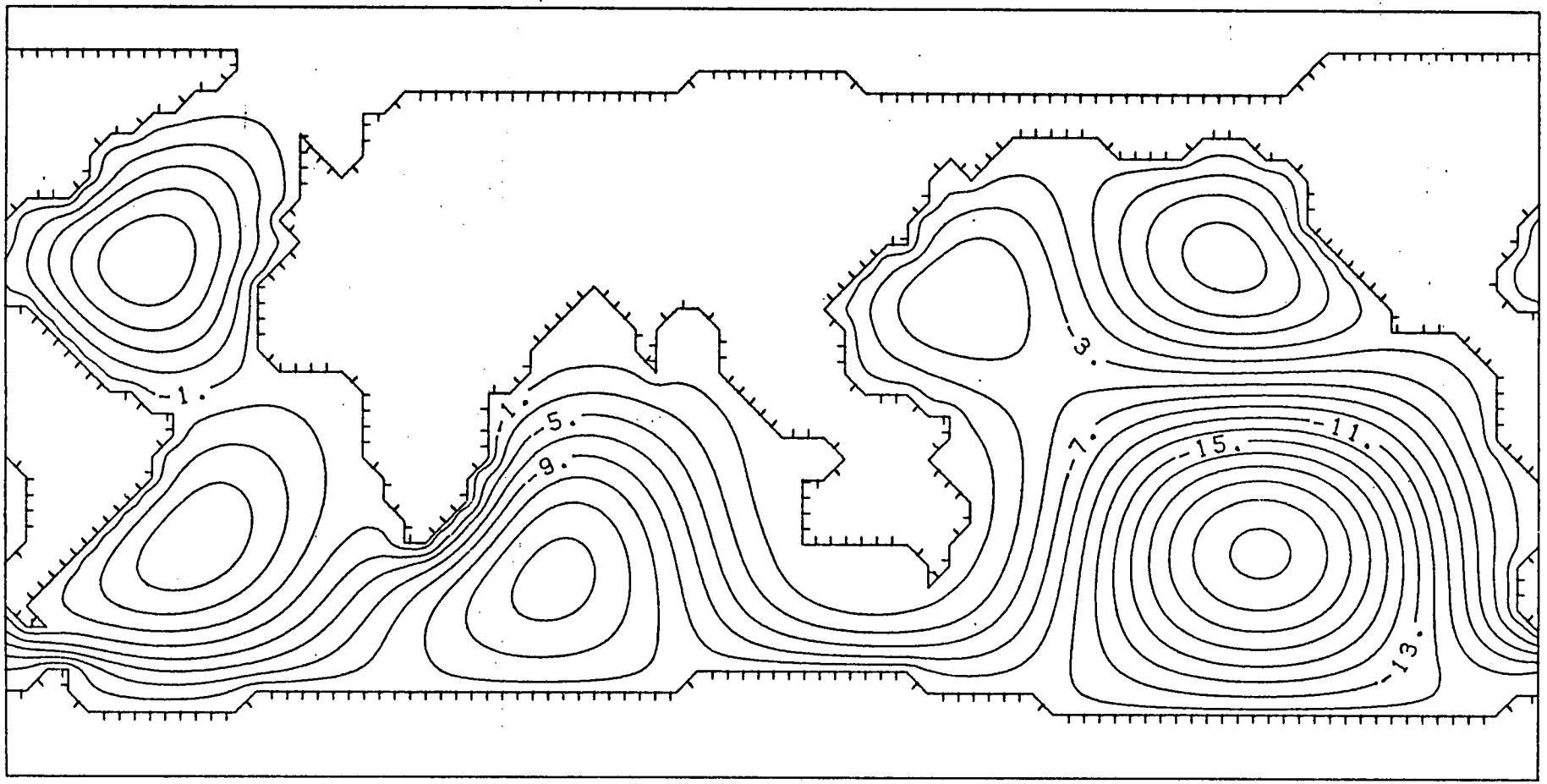

P23H12S PSR (PERFECT)

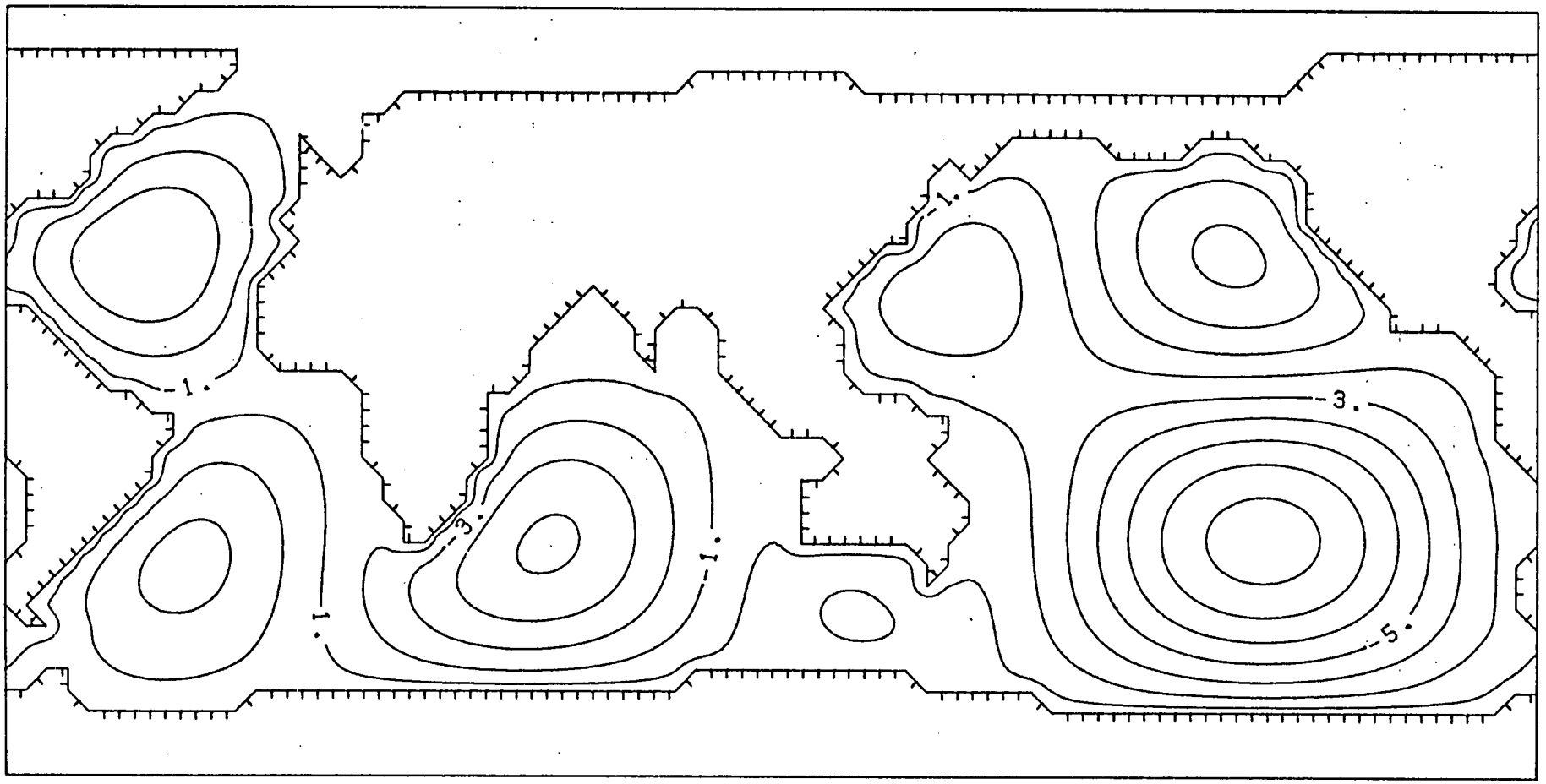

P23H12S PSI (BANKS)

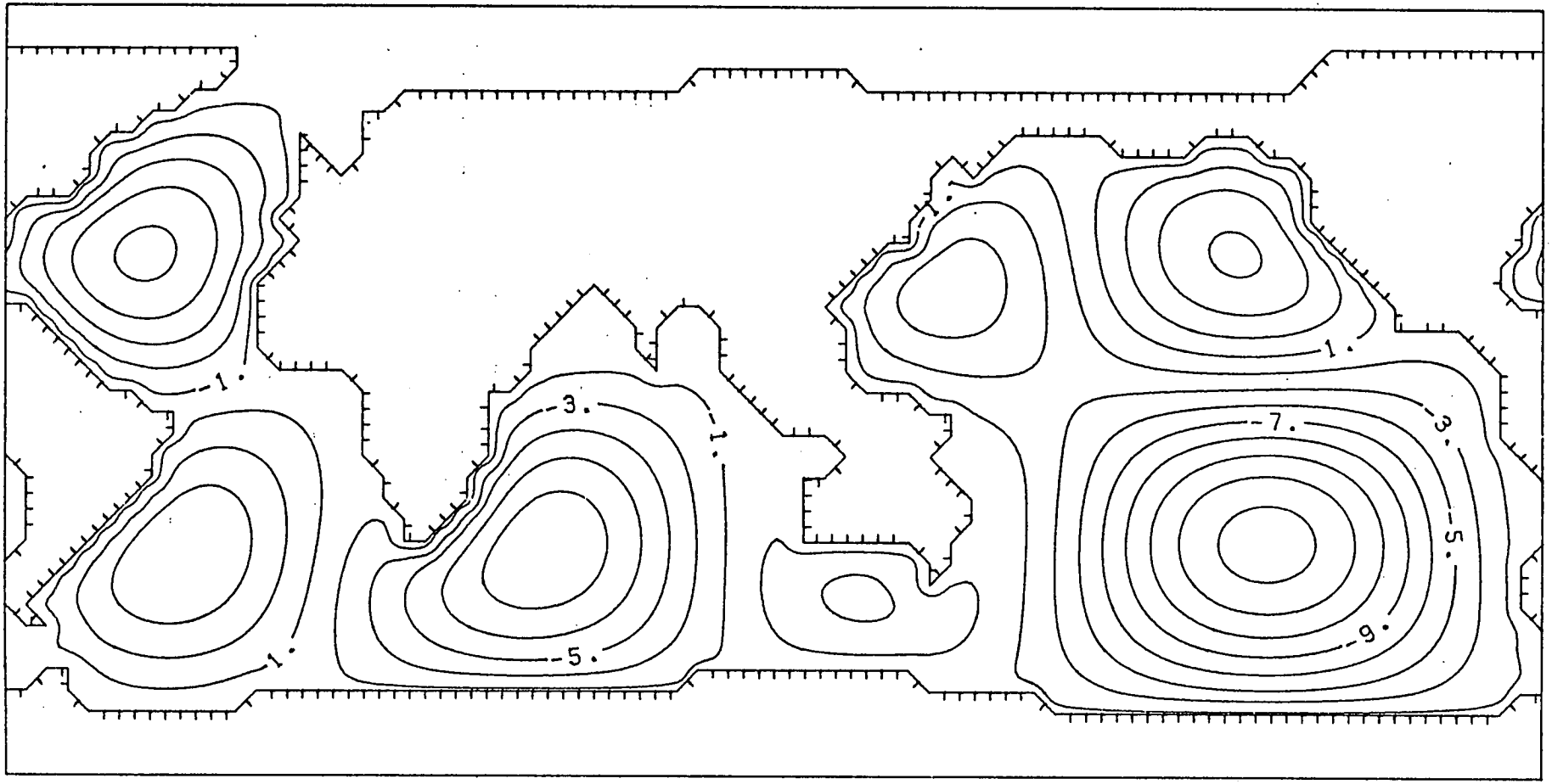

P23H12S PSI (PERFECT)

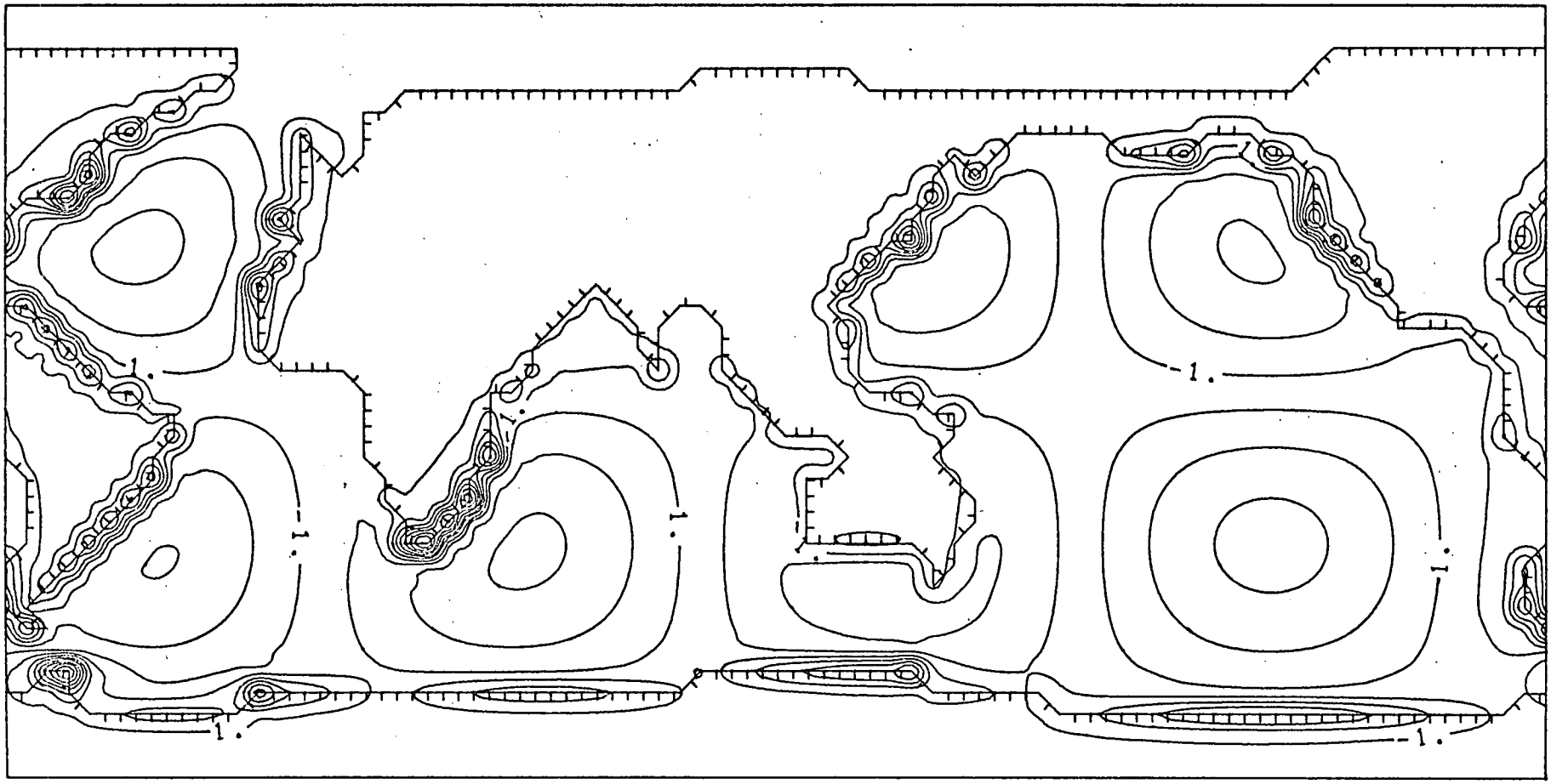

P23H12S ZR (BANKS)

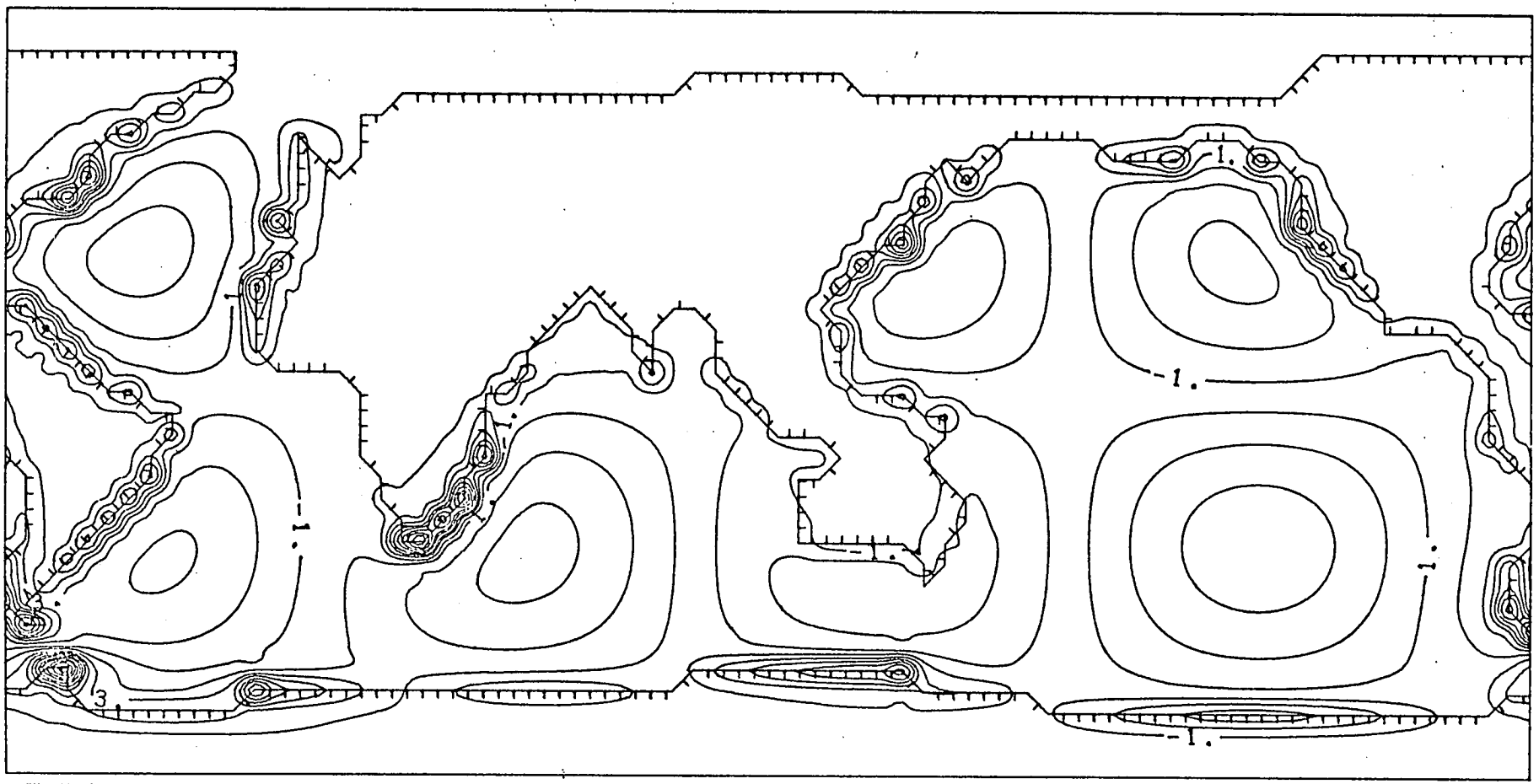

P23H12S ZR (PERFECT)

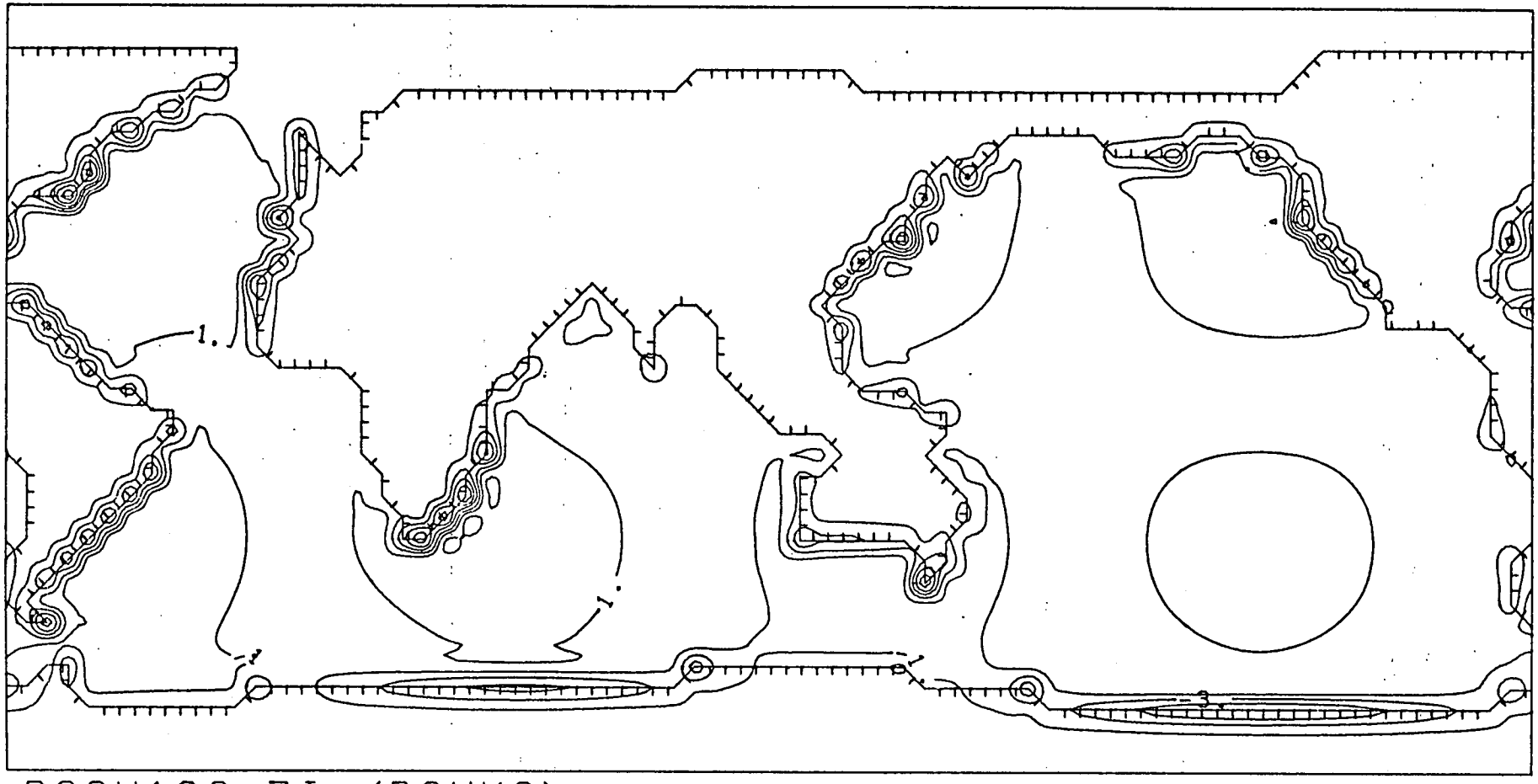

P23H12S ZI (BANKS)

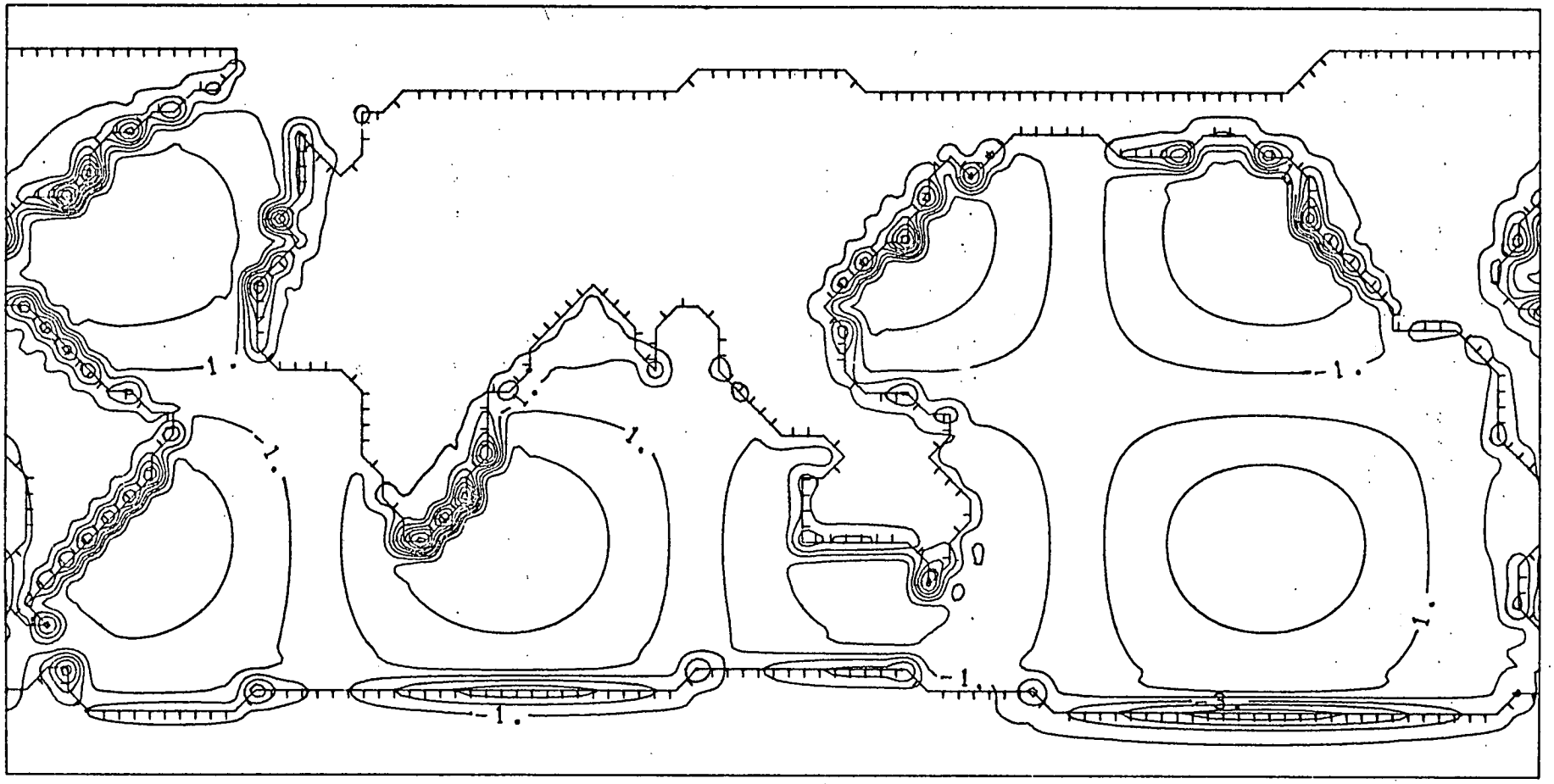

P23H12S ZI (PERFECT)

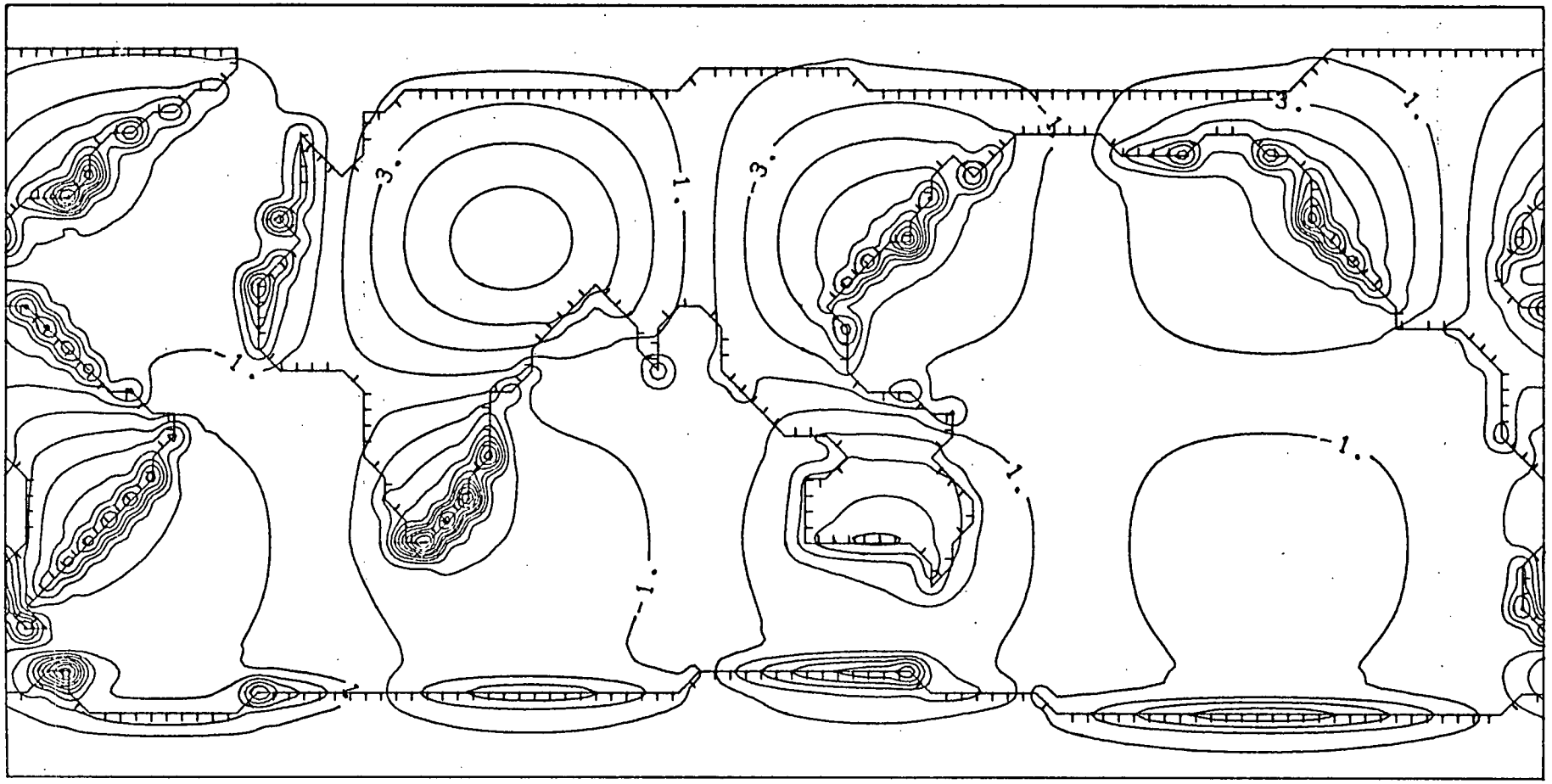

P23H12S ZRT (BANKS)

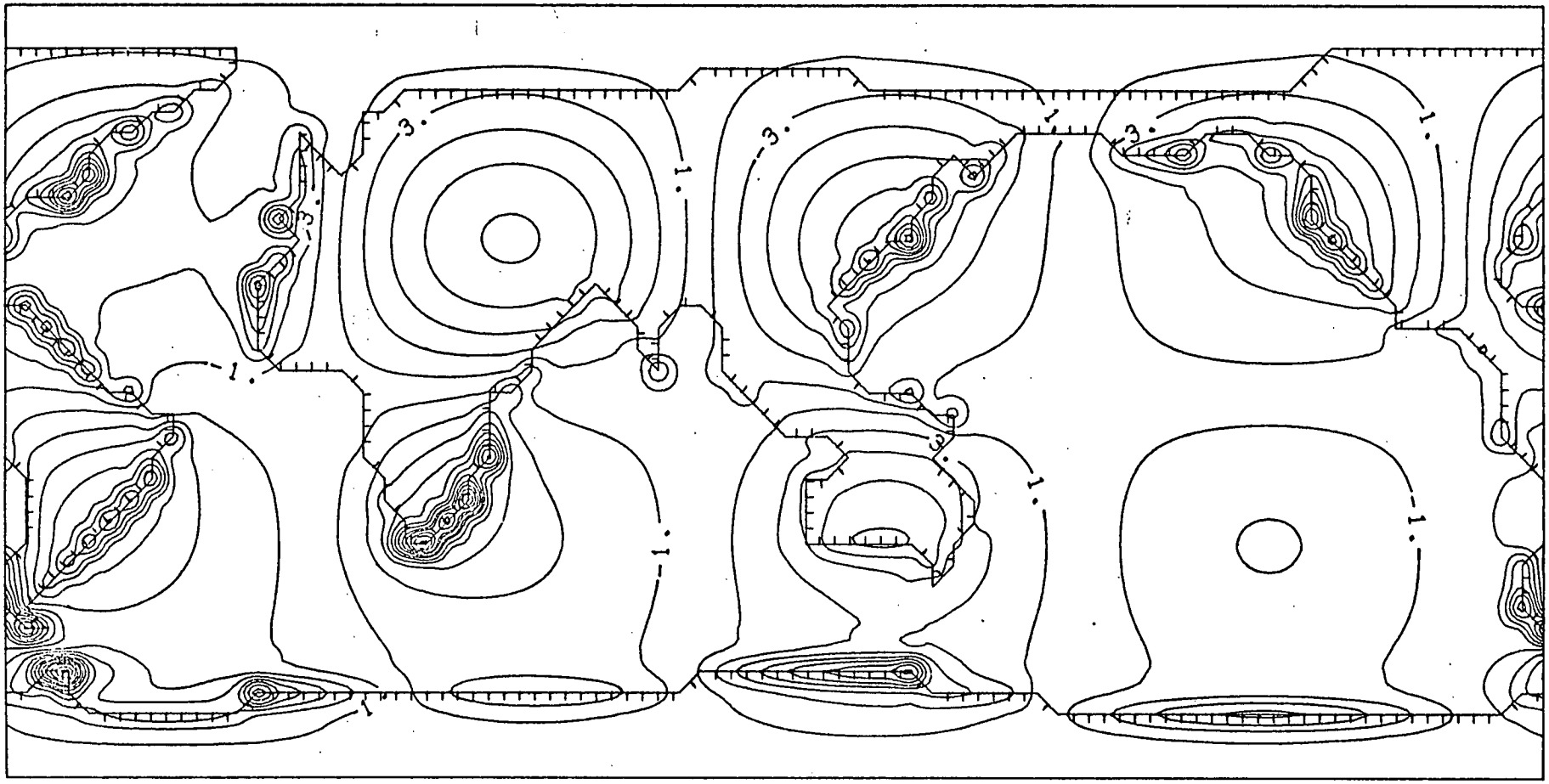
P23H12S ZRT (PERFECT)

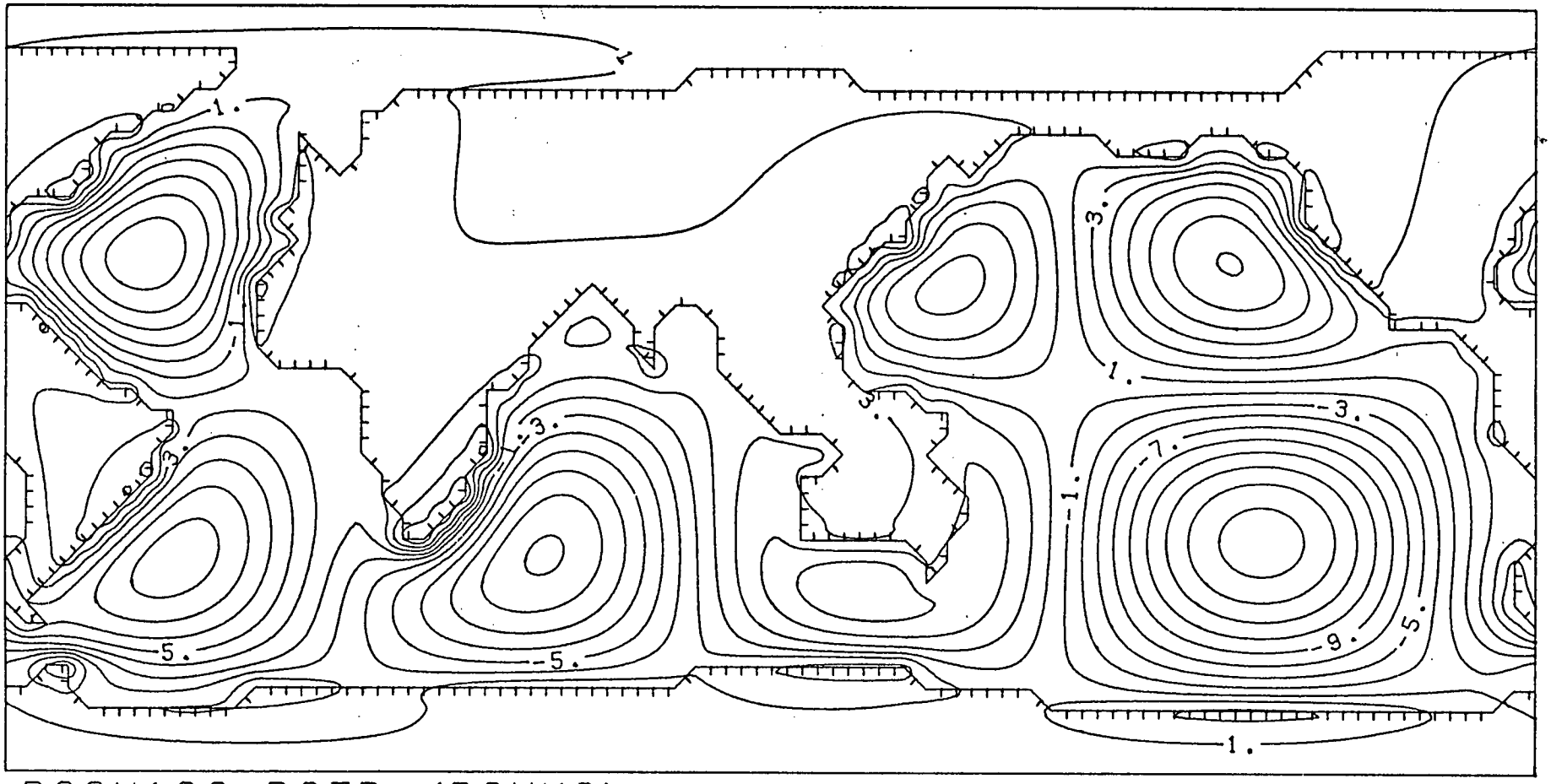

P23H12S POTR (BANKS)

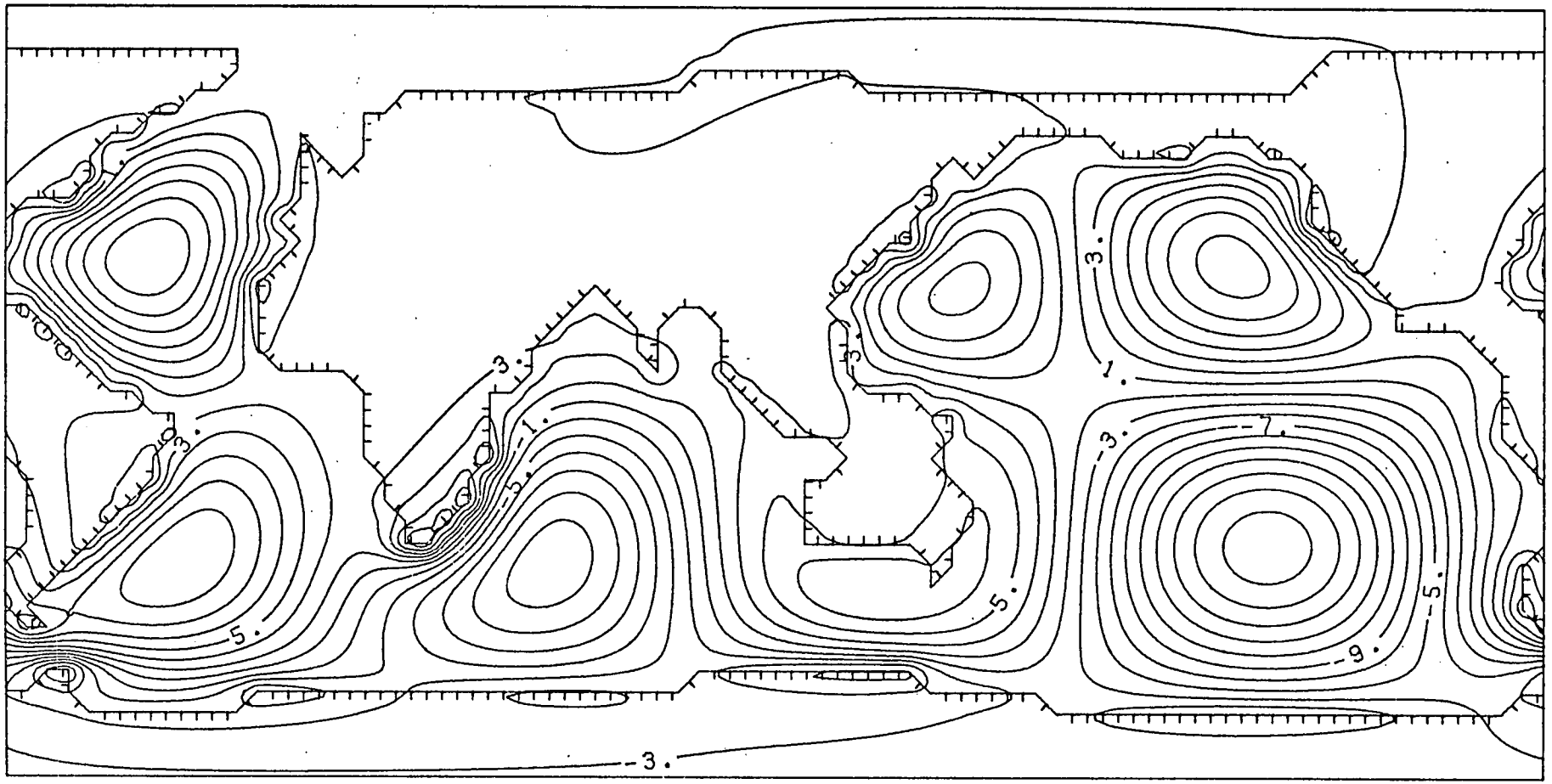

P23H12S POTR (PERFECT)

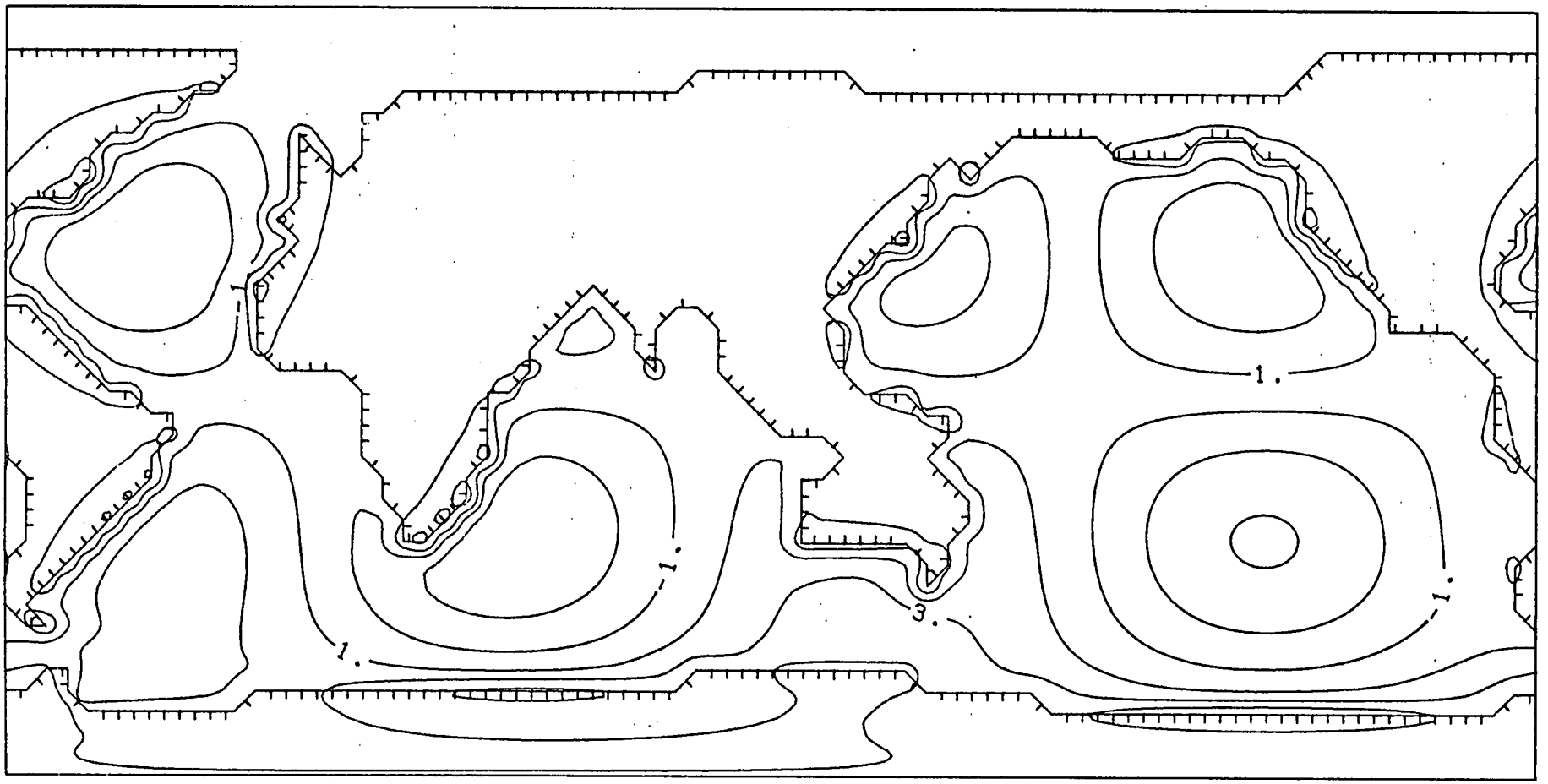

P23H12S POTI (BANKS)

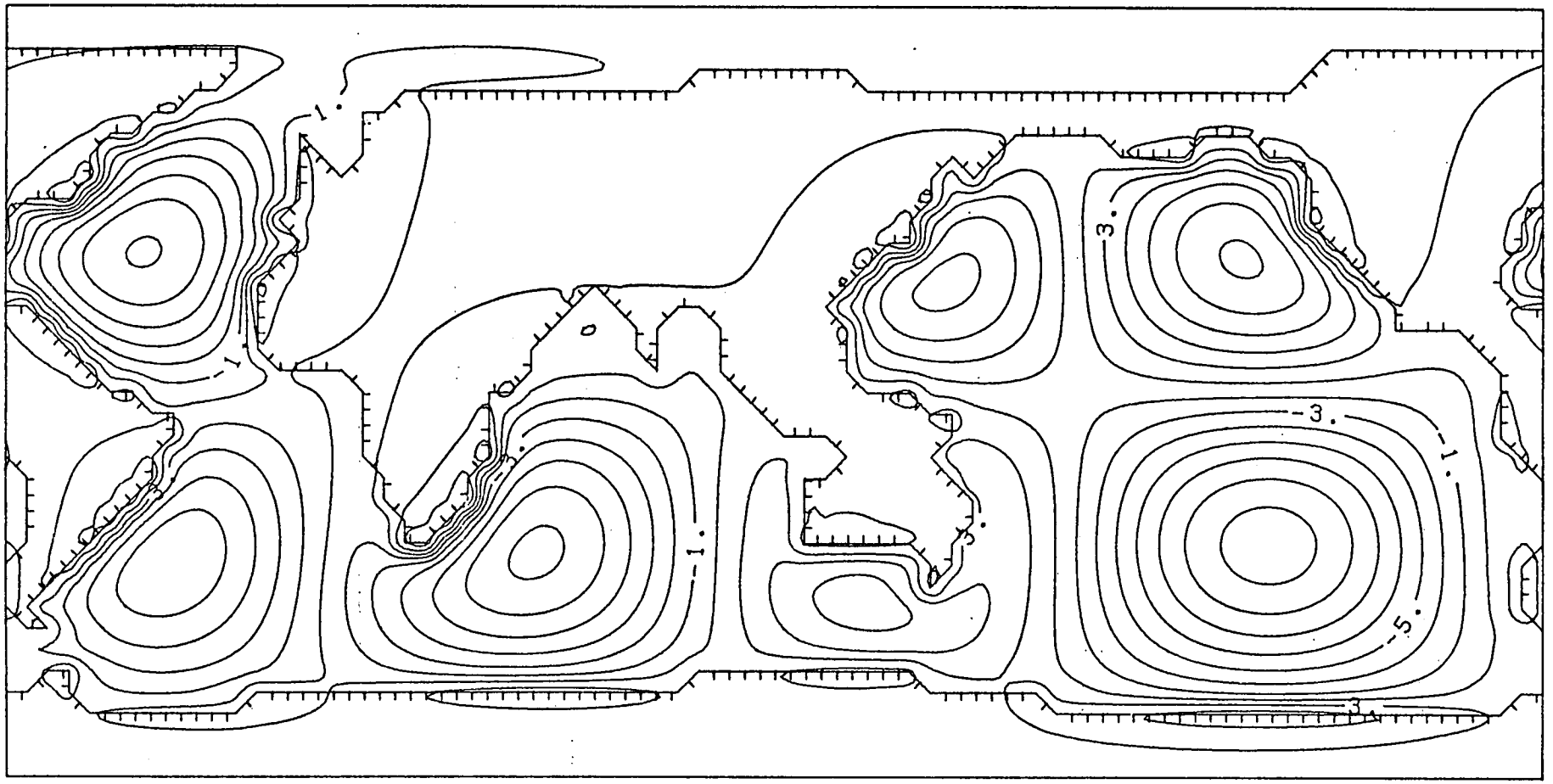

P23H12S POTI (PERFECT)

Figures 5.5a - 5.5n

As for Figures 5.3a - 5.3n but at a period of 8 hours.

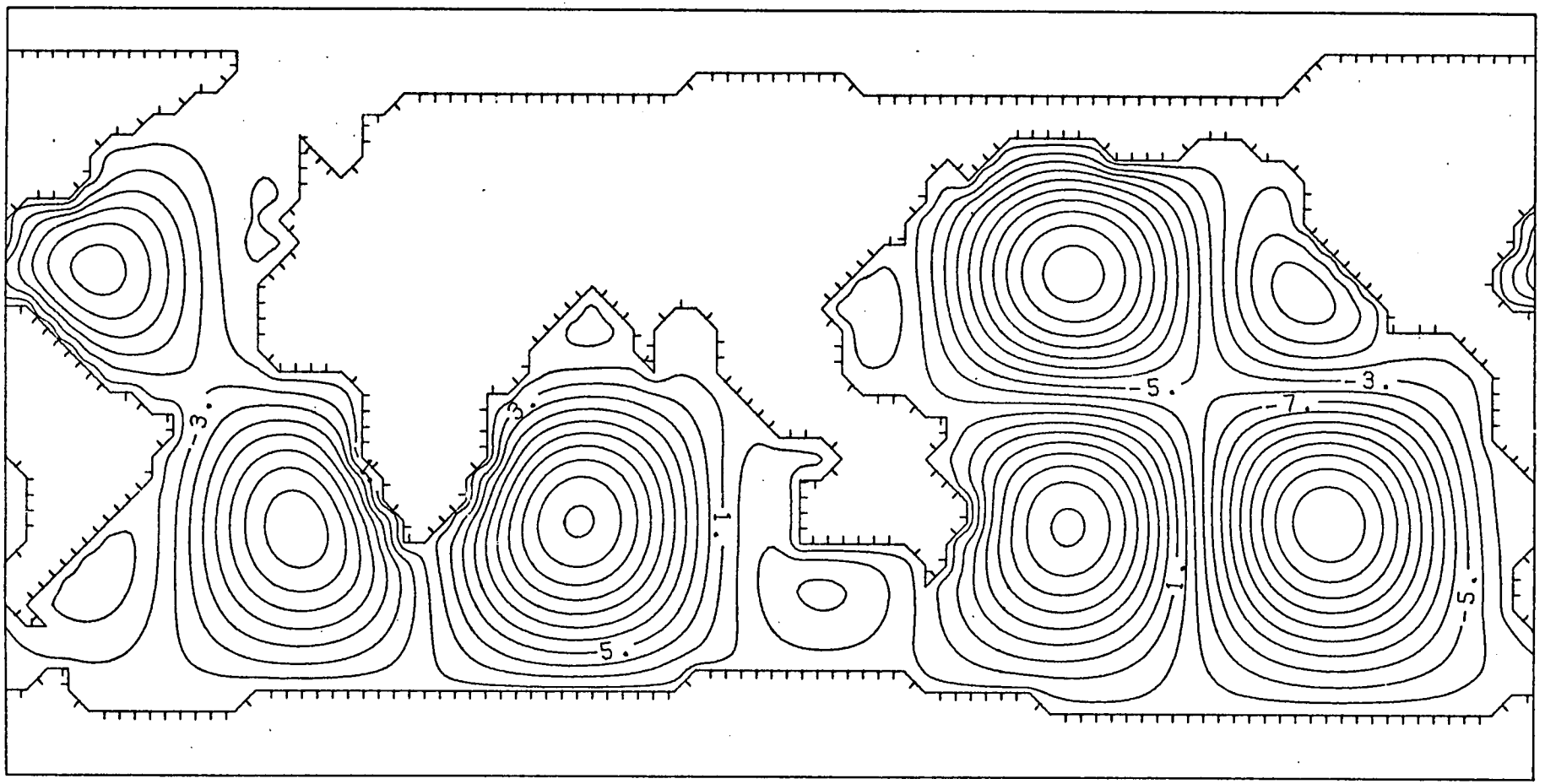

P34H08C PSR (BANKS)

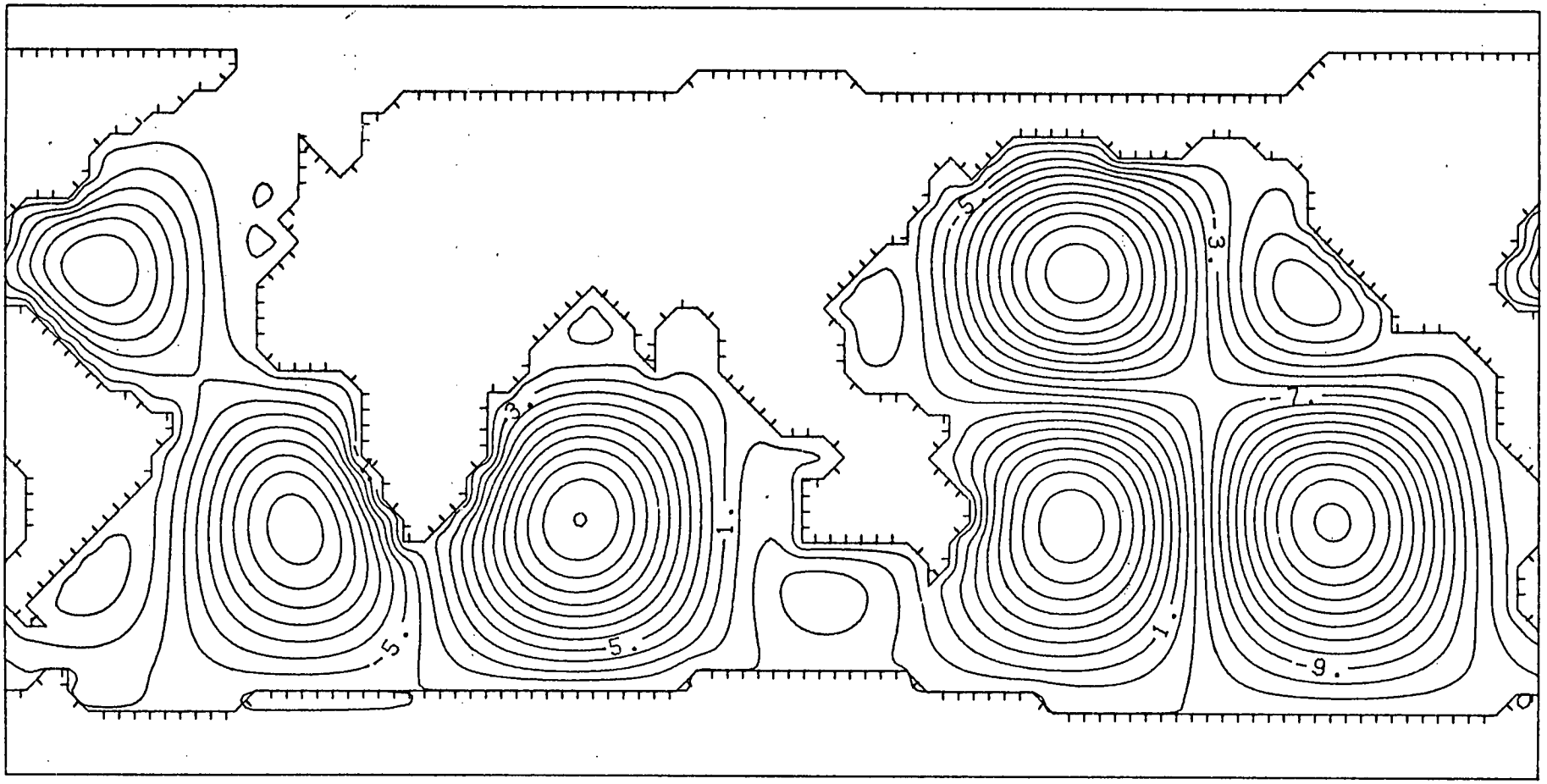

P34H08C PSR (PERFECT)

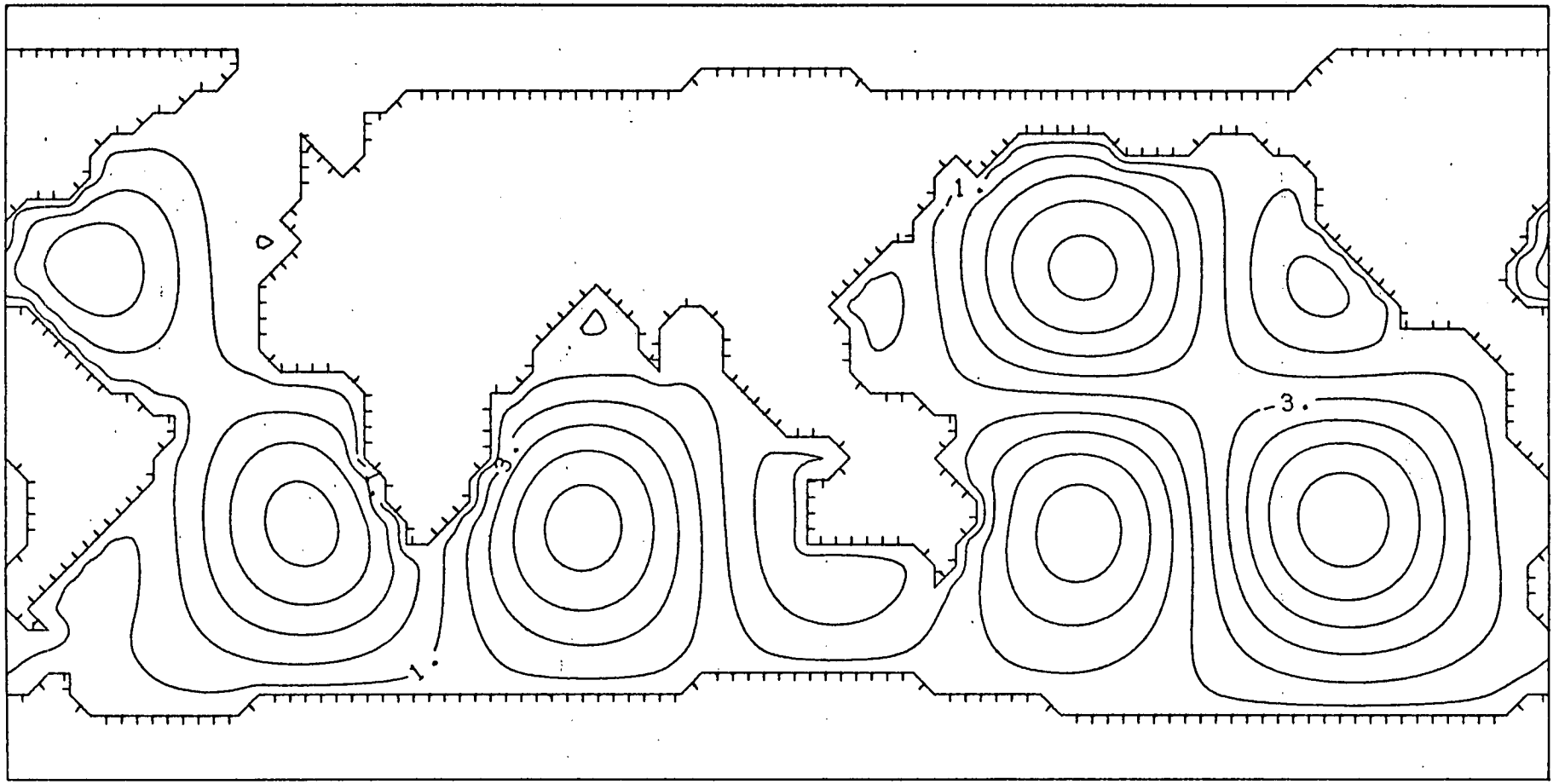

P34H08C PSI (BANKS)

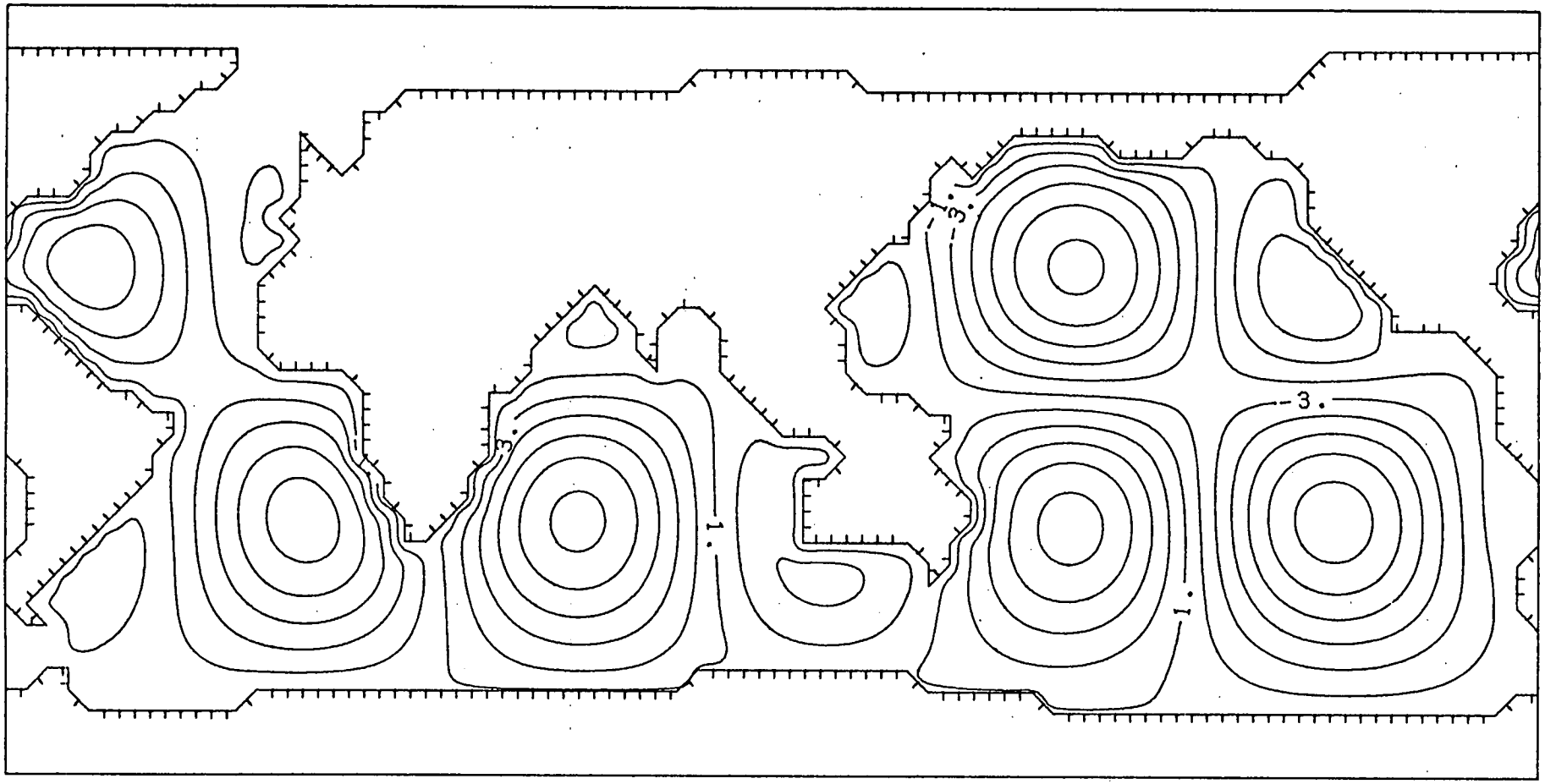

P34H08C PSI (PERFECT)

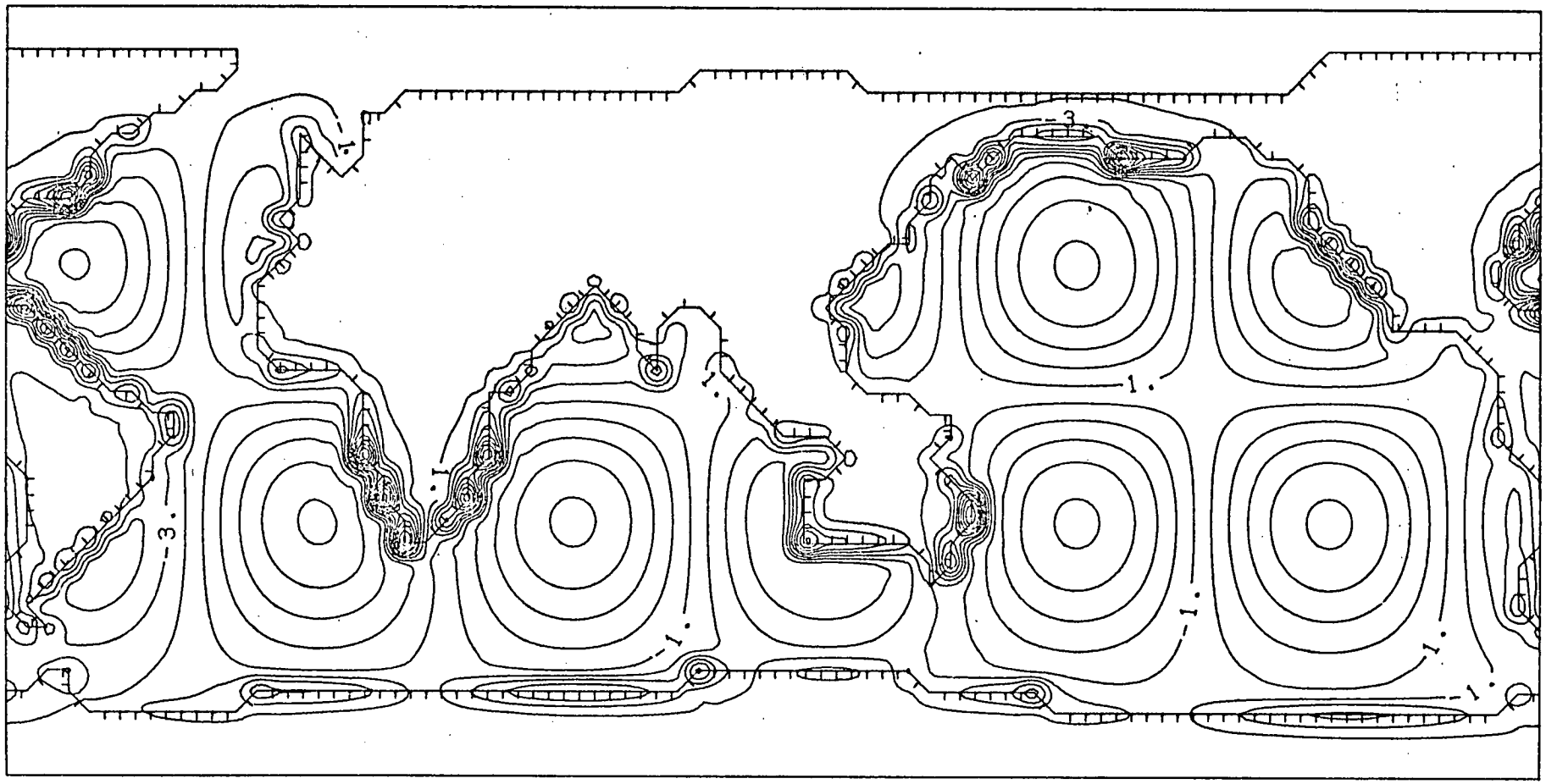

P34H08C ZR (BANKS)

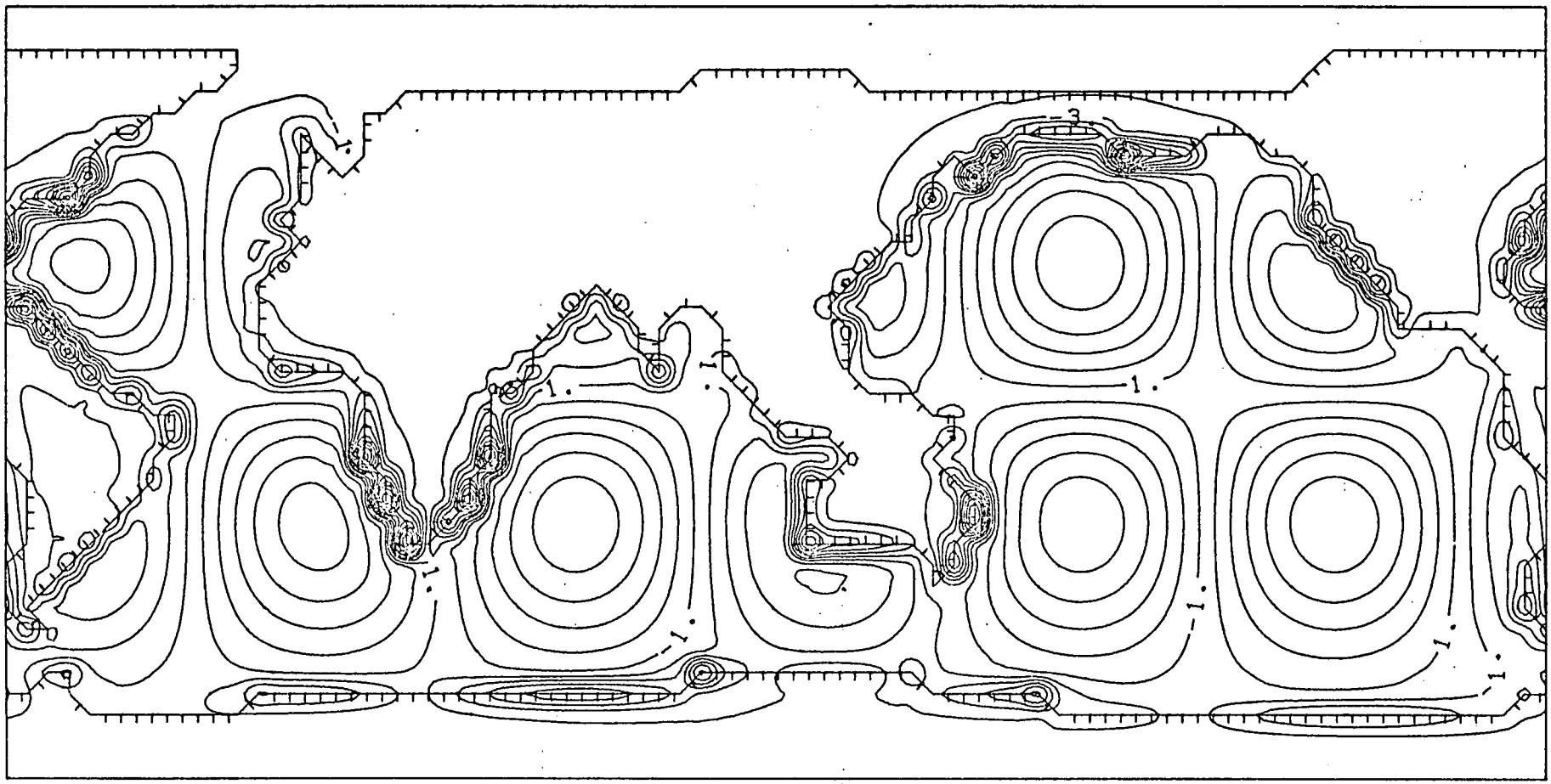

P34H08C ZR (PERFECT)

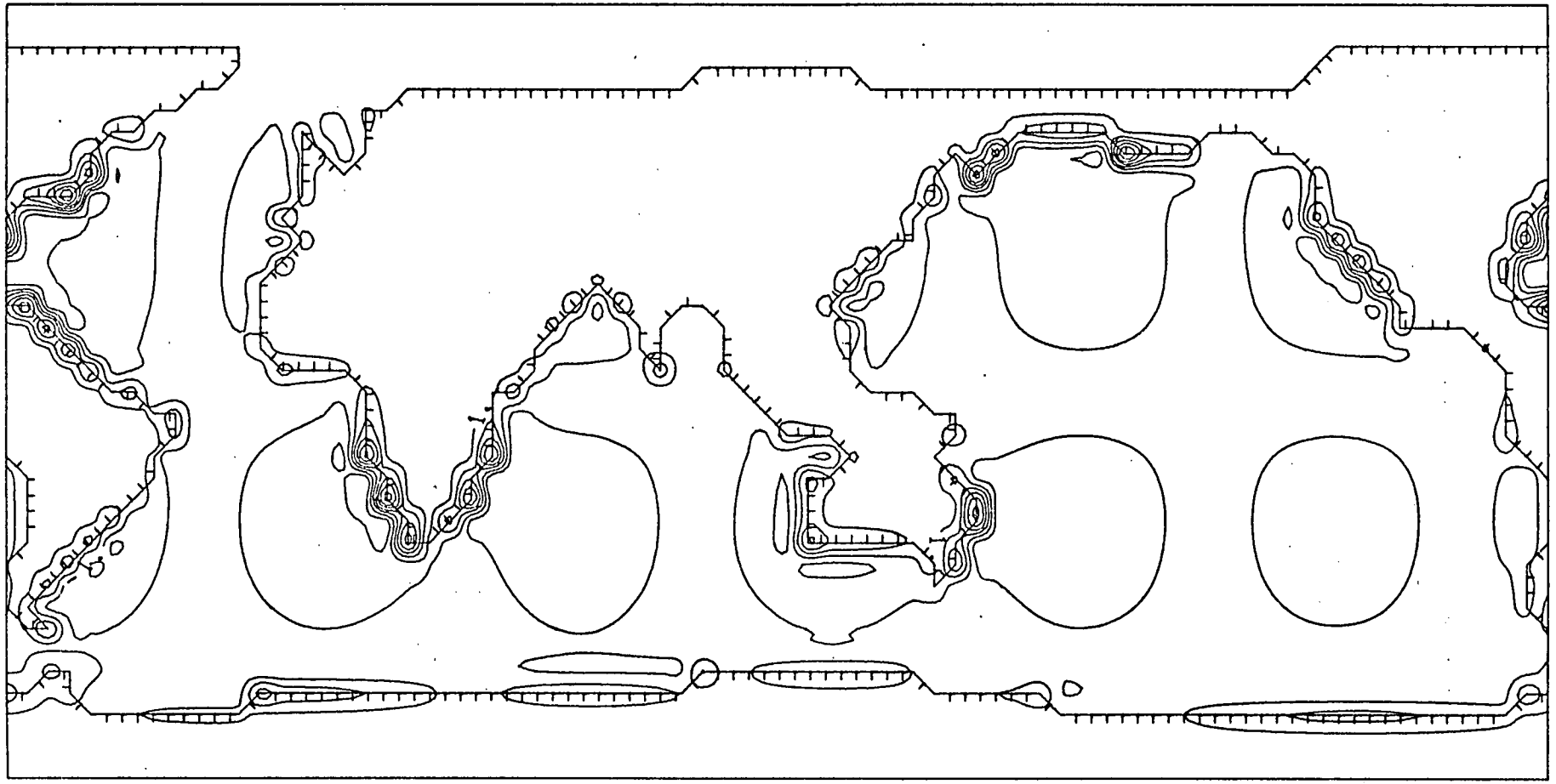

P34H08C ZI (BANKS)

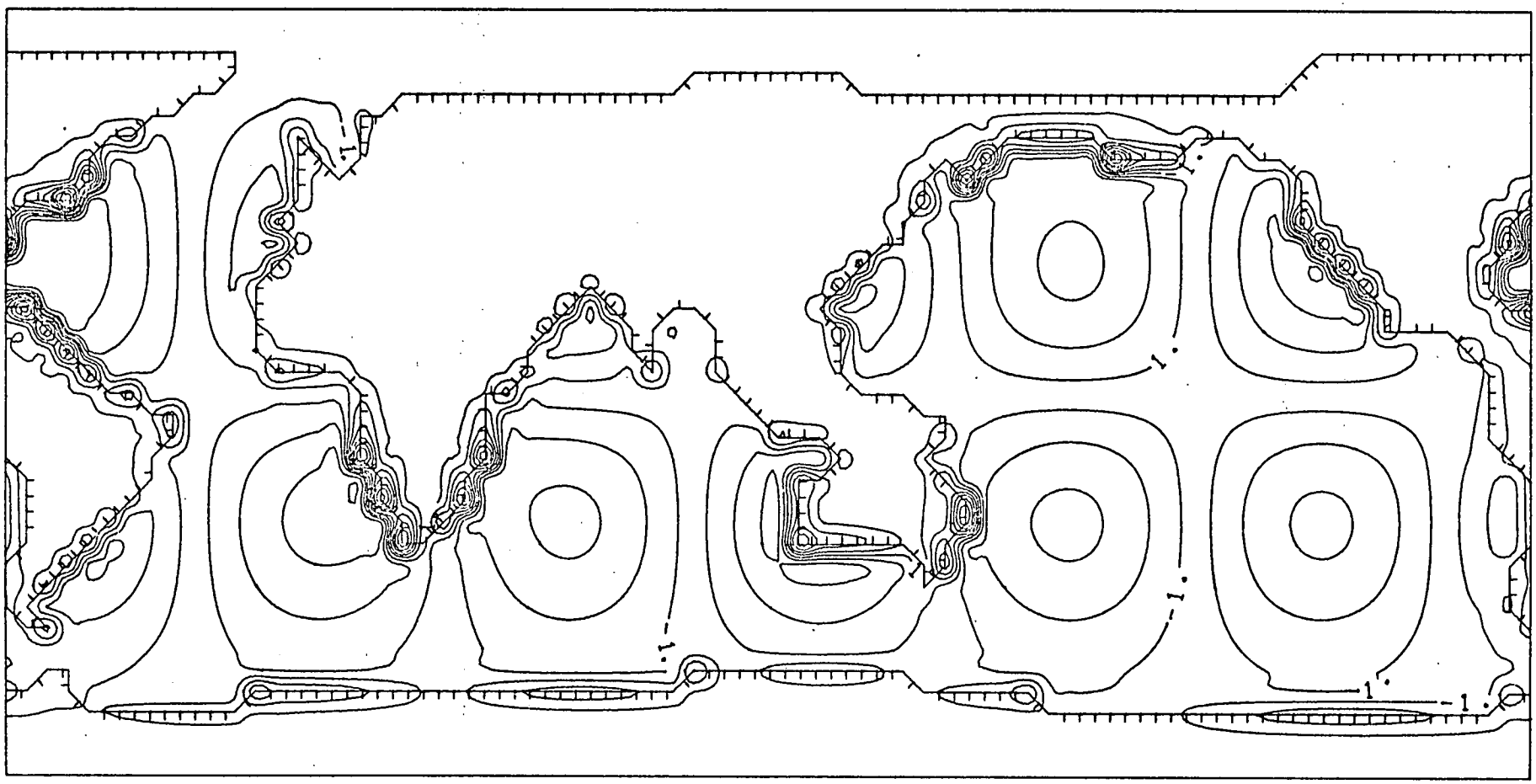

P34H08C ZI (PERFECT)

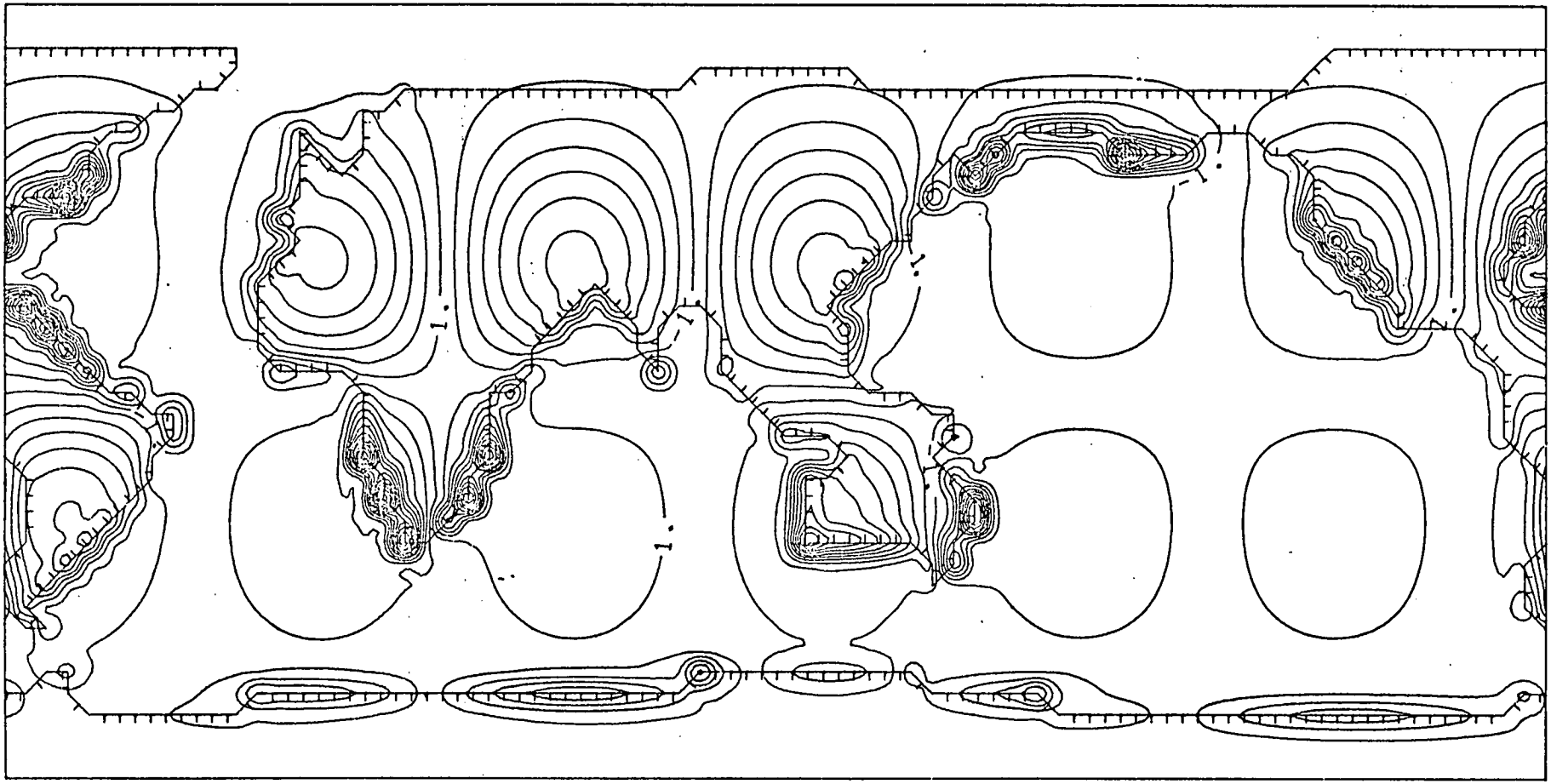

P34H08C ZRT (BANKS)

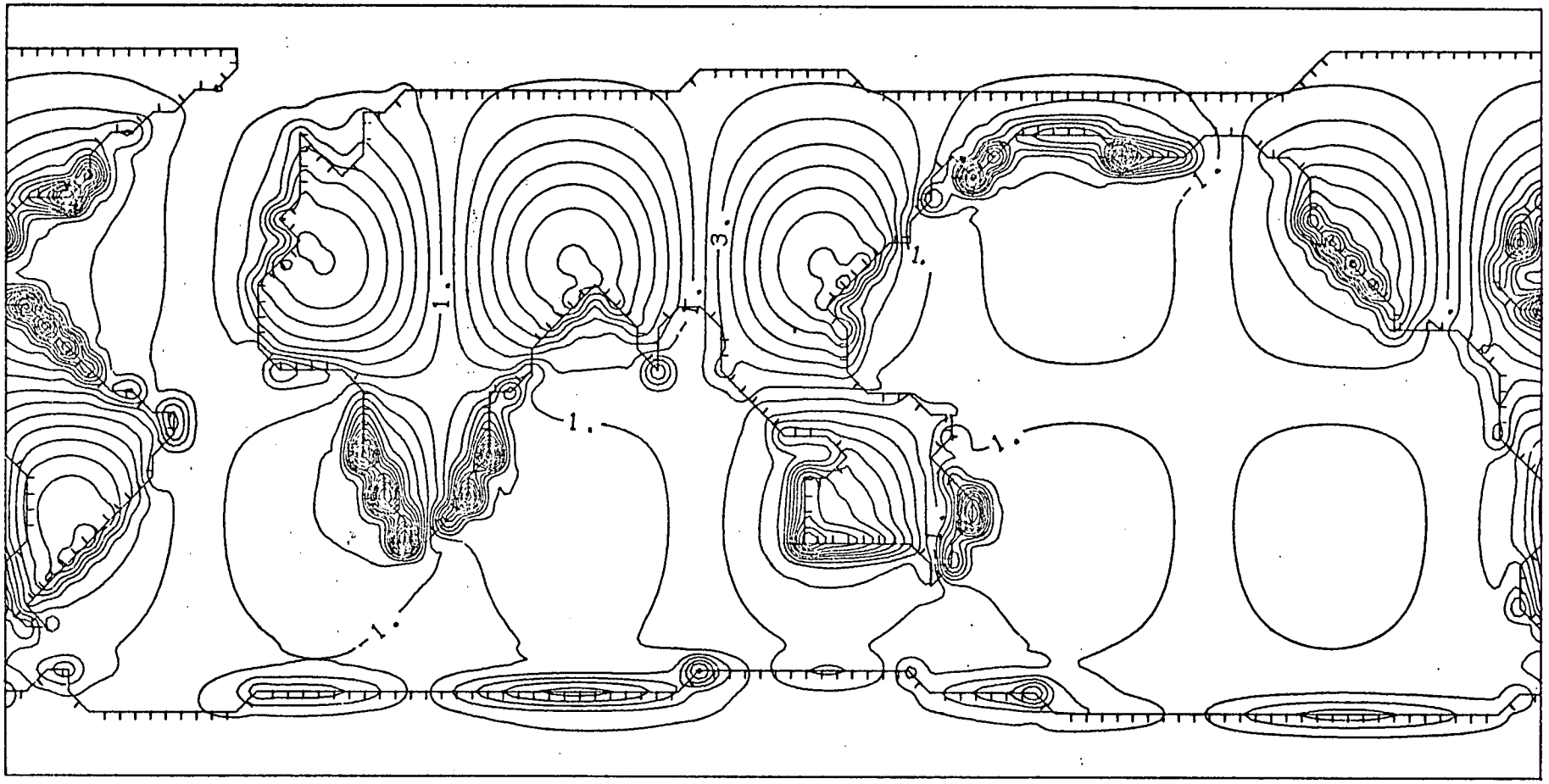

P34H08C ZRT (PERFECT)

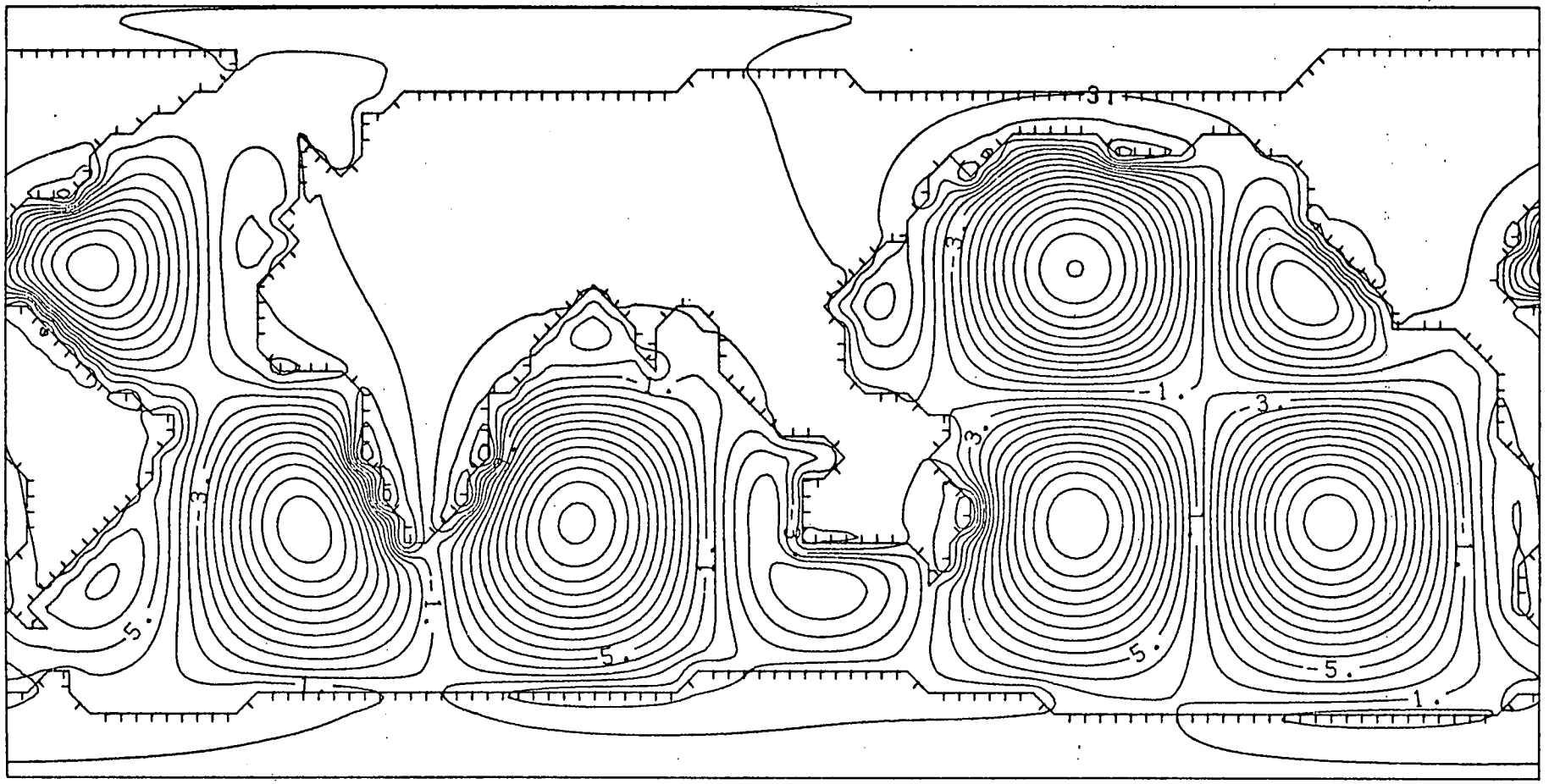

P34H08C POTR (BANKS)

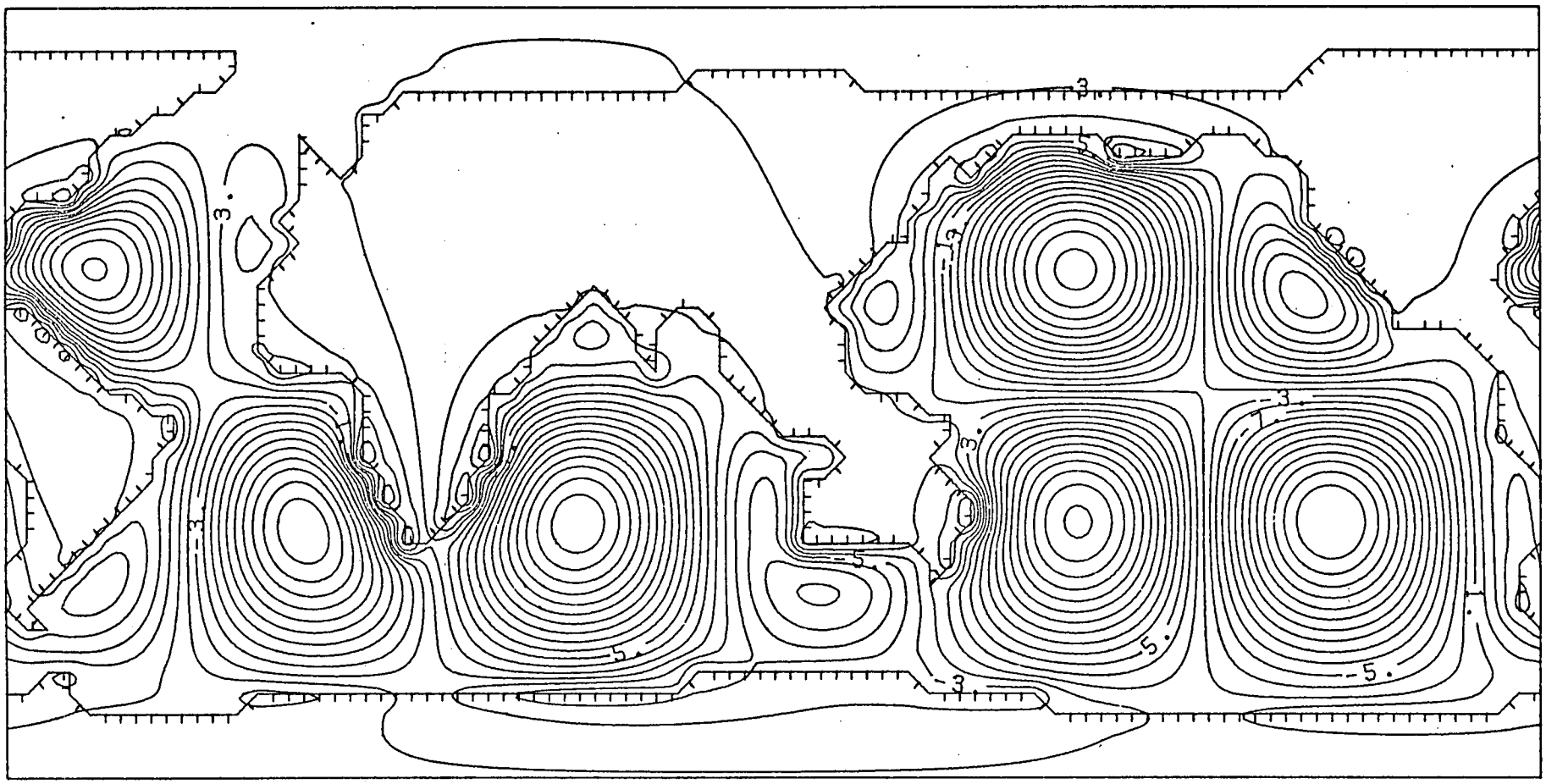

P34H08C POTR (PERFECT)

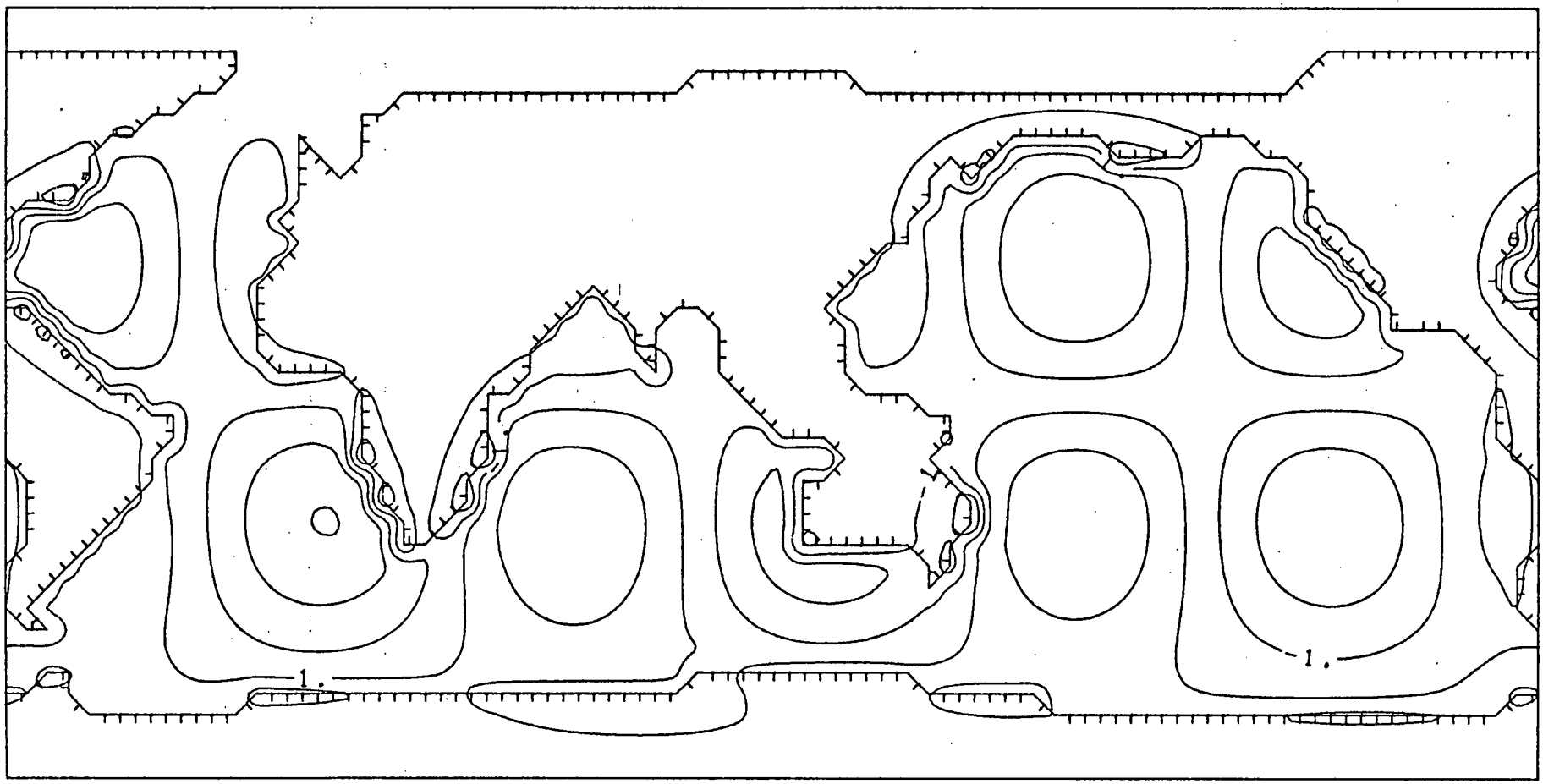

P34H08C POTI (BANKS)

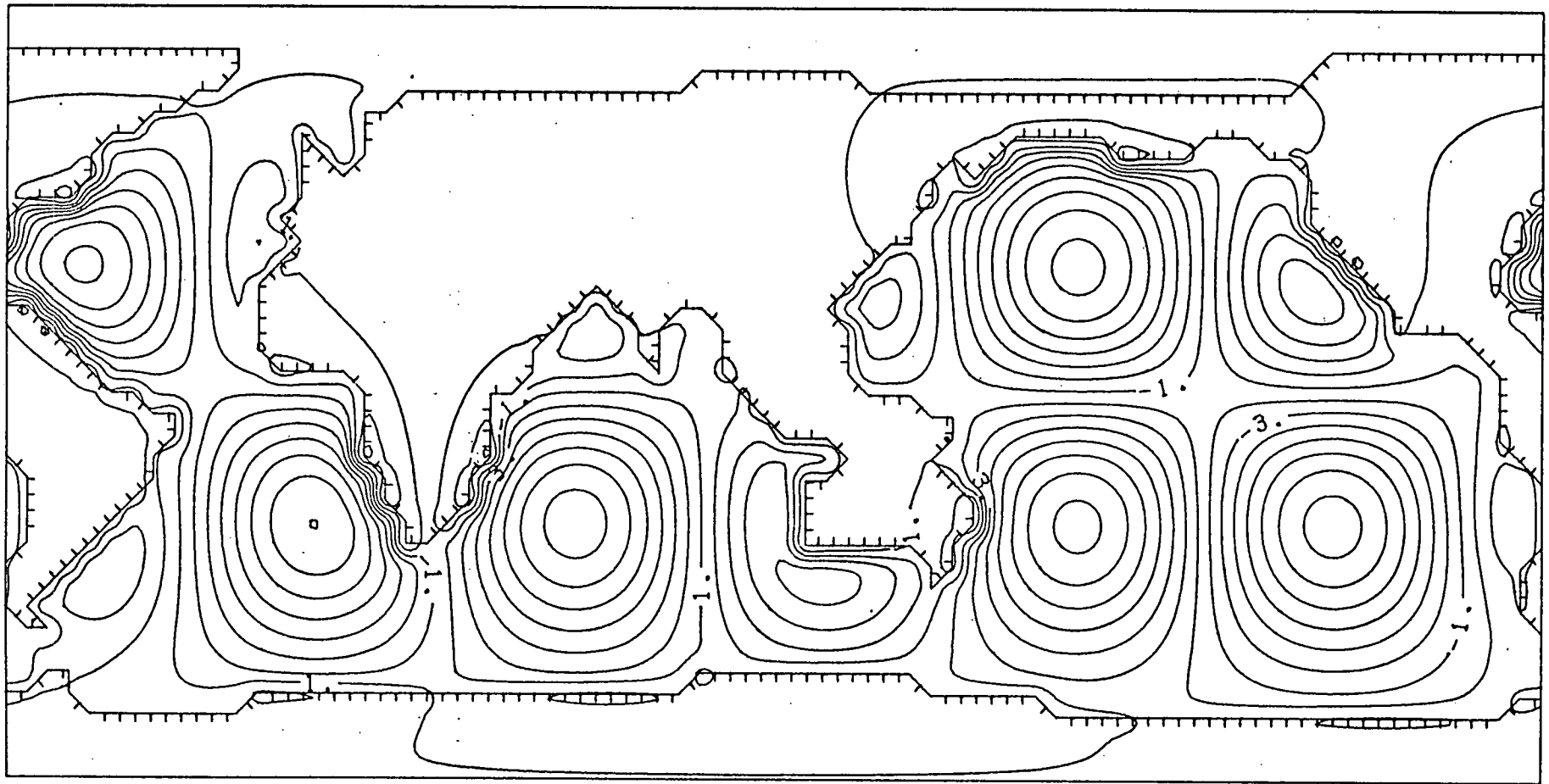

P34H08C POTI (PERFECT)

CHAPTER SIX

Modelling Sq.

6.1) Introduction.

An attempt had been made by Hobbs and Dawes (1979) to model the effect of the oceans on the Sq magnetovariational field, using an inducing field which was synthesised from the 16 major harmonics from the analysis of Sq during the International Geophysical Year (I.G.Y.) by Malin and Gupta (1977). The comparison between the internal part deduced by Malin and Gupta and the numerical model obtained by Hobbs and Dawes, who used a perfectly conducting shell at 0.9 earth radii, was far from satisfactory, therefore it was decided to discover whether any improvement could be obtained by using a finitely conducting mantle.

The method of comparison used by Hobbs and Dawes involved examining the equivalent current system which, although it has little physical significance, is a simple way of representing the internal and external current systems in a two dimensional manner. It is conventional to consider the equivalent current system to be located at the surface of the earth, even although the currents which comprise the Sq dynamo exist in the ionosphere and some of the induced currents flow at depth in the mantle. The definition of equivalent current system is simply the current streamline function at the surface of the earth which gives rise to a known magnetic field at the surface; it is usual to define separate equivalent current systems for the internal and external fields.

The work of Hobbs and Dawes demonstrated that their calculated strength of the internal equivalent current system generally ex-

ceeded that obtained by Malin and Gupta, who used spherical harmonic analysis to separate the Sq field into internal and external parts.

6.2) Calculation of the Equivalent Current System.

The equivalent current system calculated by Hobbs and Dawes to represent the induced currents consisted of three parts. Firstly there was the current streamline function, ψ(oceanic), which described the currents which had been calculated to be flowing in the oceans. Secondly there was a component which gave rise to a magnetic field equivalent to that which arose from the reduction of the primary field by the conductosphere, denoted by ψ_c. This part would in fact have been the equivalent current system for the case of induction in the conductosphere in the absence of the thin oceanic sheet and had a magnitude, proportional to the inducing field, given by:

$$\psi_c = \frac{a(2n+1)}{n(n+1)} \left(\frac{b}{a}\right)^{2n+1} \frac{Z^p}{\mu_0} \quad (6.1)$$

This was the case for a perfectly conducting mantle but it could be reduced to the following form for the more general case of a finitely conducting mantle:

$$\psi_c = \frac{a(2n+1)}{n^2} \left(\frac{i_n}{e_n}\right) \left(\frac{b}{a}\right)^{2n+1} \quad (6.2)$$

The third component represented the effect of mutual induction between the currents in the ocean and the conductosphere, denoted by ψ(mutual). For a single harmonic, of degree n, ψ(mutual) was defined as $-(b/a)^{2n+1}\psi$(oceanic) for a perfectly conducting mantle and a new surface integral formula was derived to calculate ψ(mutual) for a general oceanic current function (Hobbs & Dawes, eqn. 28).

$$\psi(\text{mutual}) = \frac{-1}{4\pi} \iint \frac{b(a^4-b^4)}{a\left(a^4+b^4-2a^2b^2\cos\theta\right)^{3/2}} \psi(\text{oceanic})\, dS \quad (6.3)$$

The kernel of this surface integral expression was obtained by using the methods of Hobbs and Price (1970) to find the limit of the following series:

$$K_{Eq}(\theta) = -(1/4\pi a^2) \sum_n (2n+1)(b/a)^{2n+1} P_n(\cos\theta). \quad (6.4)$$

This expression reduces to the following form in the case of finitely conducting mantle:

$$K_{Eq}(\theta) = -(1/4\pi a^2) \sum_n \frac{(2n+1)(n+1)(i_n/e_n)}{n} (b/a)^{2n+1} P_n(\cos\theta). \quad (6.5)$$

The equivalent current kernels for Banks' conductivity model, obtained by taking the first 35 terms of the series, are shown in the usual way along with the analytic form for the perfect conductor of radius 0.9 in Figure (6.1).

It can be seen that the values of these kernels are relatively small, when compared with the corresponding kernels for the vertical field and scalar potential due to mutual induction, which means that the basic integrals can be calculated accurately. It is quite possible that the difficulties encountered in Chapter 4 with slowly convergent mutual induction kernels could be overcome by using the equivalent current surface integral to reduce the current function by the amount required by mutual induction and by using the self induction integral to find the vertical field due to self and mutual induction in a single calculation. This could also render the surface integral for finding the potential due to mutual induction redundant, and would therefore reduce the quota required when running the programs on the I.C.L. 2980 machine. The equivalent current system kernel is much better behaved than the mutual induction vertical field kernel because the factors

Figure 6.1

Equivalent Current Kernels for Banks' Model for comparison with a perfect conductor of Radius 0.9 Earth Radii.

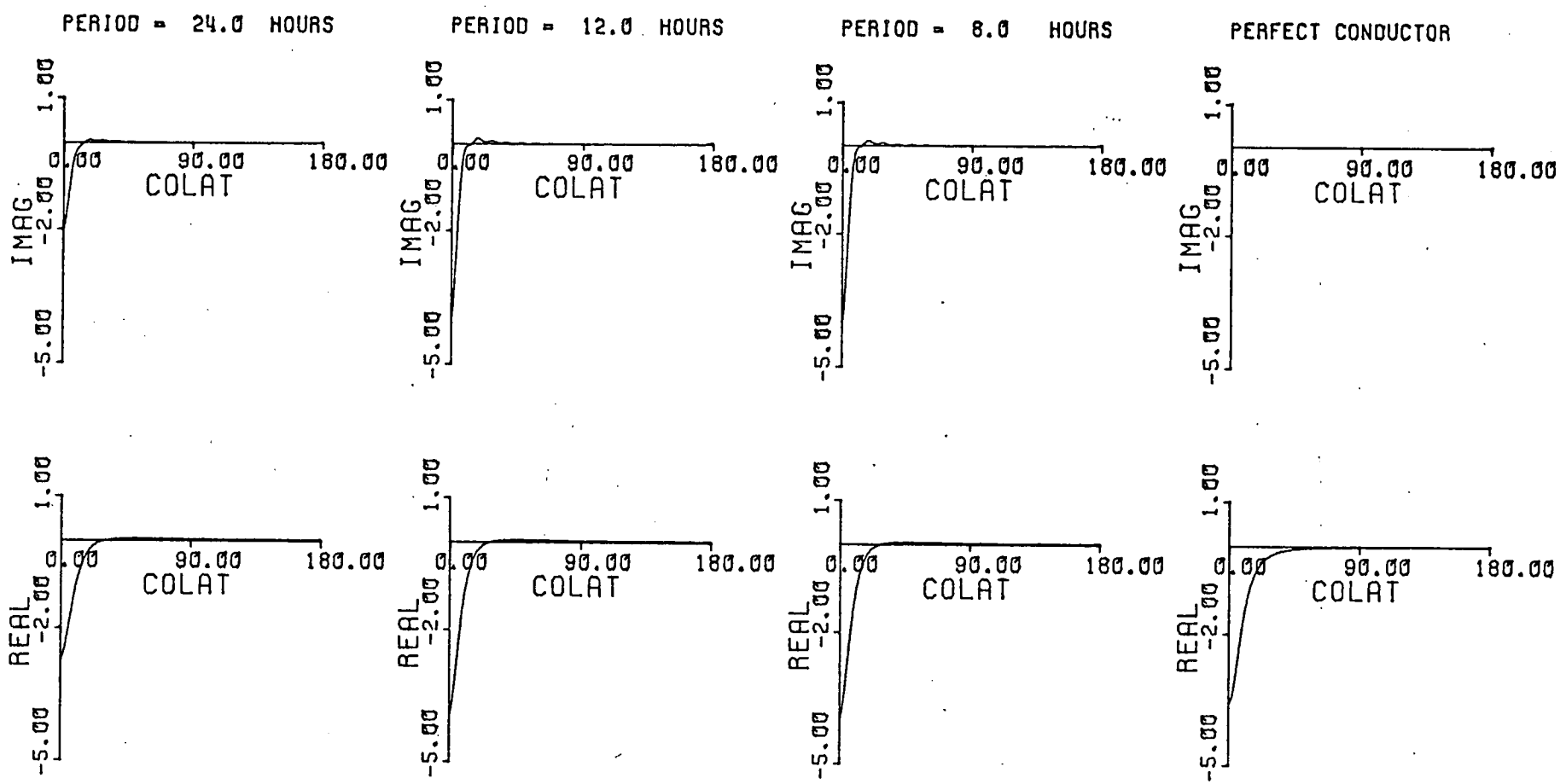

EQUIVALENT CURRENT KERNELS

involving only the order (n) in the Legendre coefficient tend to a limit of 2n as opposed to n^2 as n tends to infinity.

6.3) Equivalent Current System for Sq.

In Hobbs and Dawes (1979) the Sq inducing field was synthesised from the sixteen external coefficients, with the largest amplitudes, from the analysis of Malin and Gupta (1977), where originally 39 coefficients up to fourth order had been used. Graphs of the real and imaginary parts of the vertical magnetic field, after the effect of induction in the conductosphere alone had been considered, showed that this restriction to only 16 coeficients was not serious, although the fields for periods of 12 and 8 hours were very regular since the harmonics chosen had the same longitudinal variation in each case. The same 16 coefficients were taken in the attempt to model Sq with Banks' conductivity and are presented in Table (6.1).

The equivalent current systems are presented in Figures (6.2a-6.2r) at six different instants of Universal Time at four hourly intervals (4hU.T. to 24hU.T.) for three separate cases: modelling with Banks' conductivity, modelling with the perfect conductor and the 39 internal coefficients of Malin and Gupta.

Hobbs and Dawes demonstrated that the results of the model could give the right magnitude for the current vortices at 16h U.T. but the calculated values at 20hU.T. were too large, which also seems to be the case when modelling with Banks' conductivity. The calculated vortices appear to have the same magnitude as those of Malin and Gupta at 4, 8, 16 and 24 hours U.T. but are too strong at 12 and 20 hours U.T. It can also be seen that the strength of the vortices predicted by using Banks' model are stronger than those obtained with a perfect conductor of radius

EXTERNAL COEFFICIENTS FOR SQ HARMONICS.

Values in nanoteslas as in Hobbs and Dawes (1979).

n	m	Period	Re(cos)	Im(cos)	Re(sin)	Im(sin)
1	1	24	0.49	2.96	-4.73	0.93
2	0	24	-0.17	4.30	0.00	0.00
2	1	24	11.72	0.53	-1.29	9.72
3	0	24	1.30	-2.27	0.00	0.00
4	1	24	-2.57	0.51	-0.35	-2.33
2	2	12	1.00	-2.07	2.03	0.69
3	2	12	-5.23	-1.74	2.13	-5.09
3	3	8	-1.39	0.67	-0.61	-1.04
4	3	8	1.65	1.52	-1.68	1.60

Table 6.1

Figures 6.2a - 6.2r

Equivalent Current Systems obtained with Banks' Model and a perfect conductor for comparison with those computed by Malin and Gupta at 4,8,12,16,20 and 24 hours U.T.

Contour Interval is 20KA

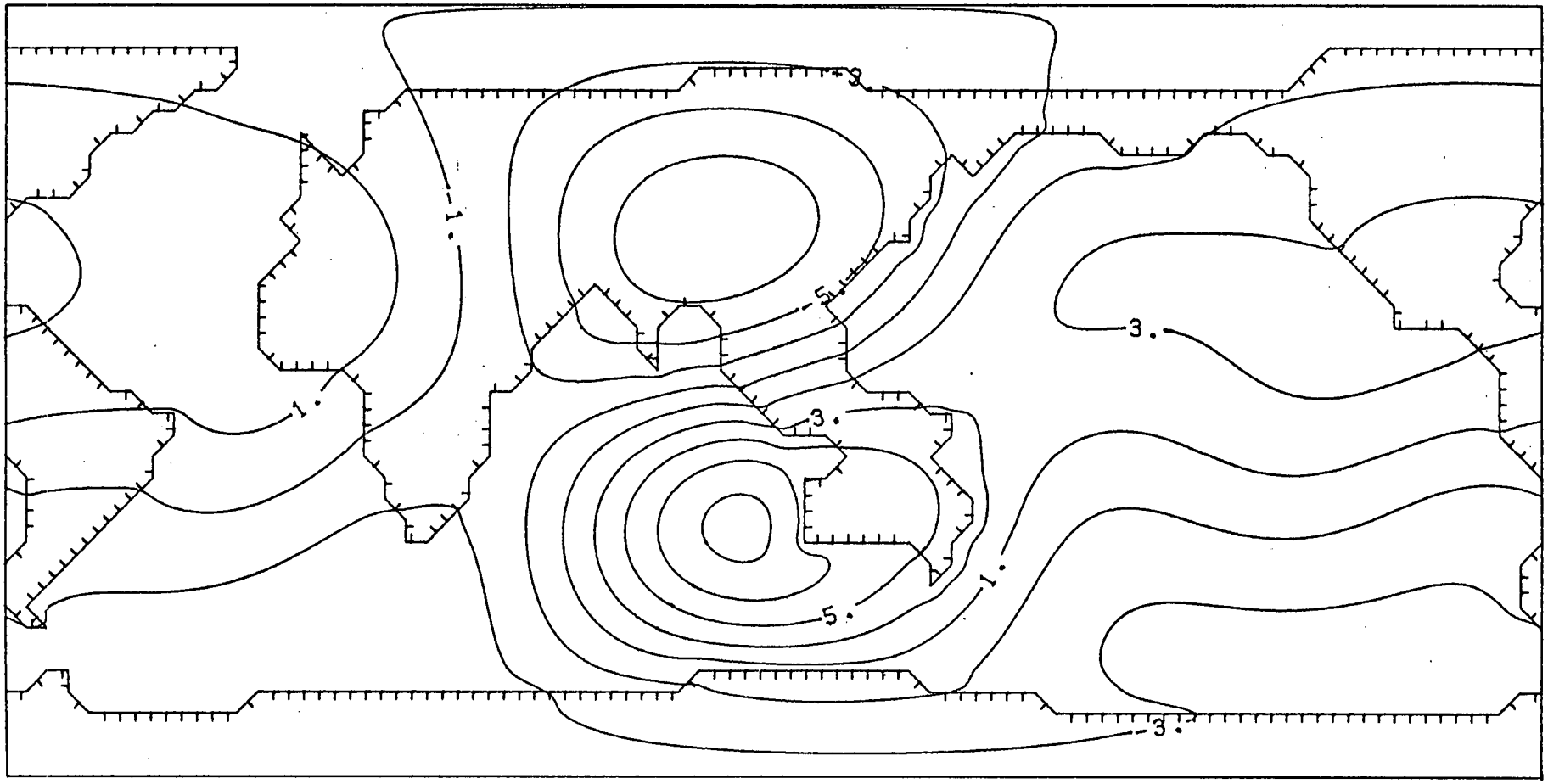

EQUIV (BANKS) U.T.=4

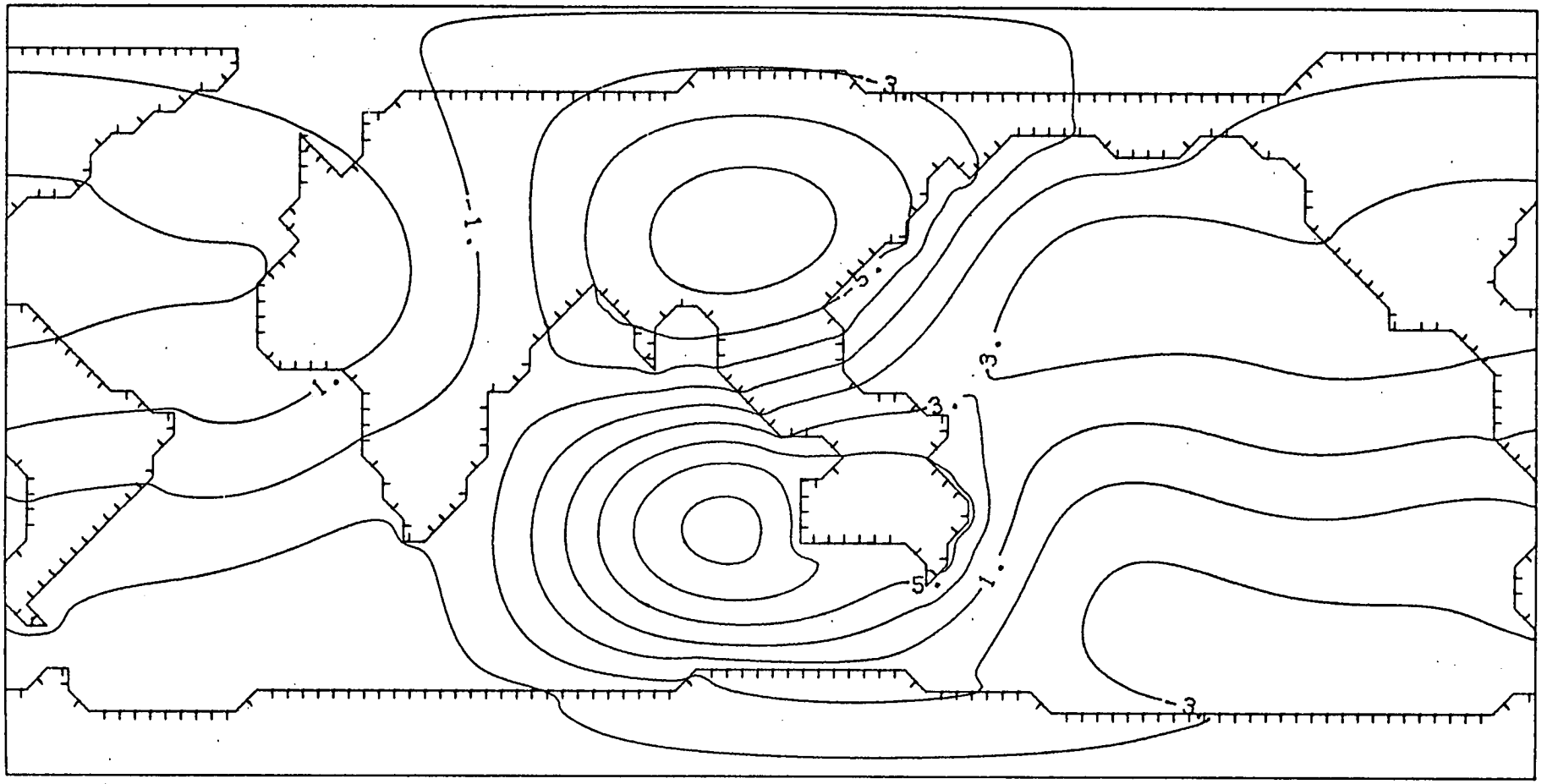

EQUIV (PERFECT) U.T.=4

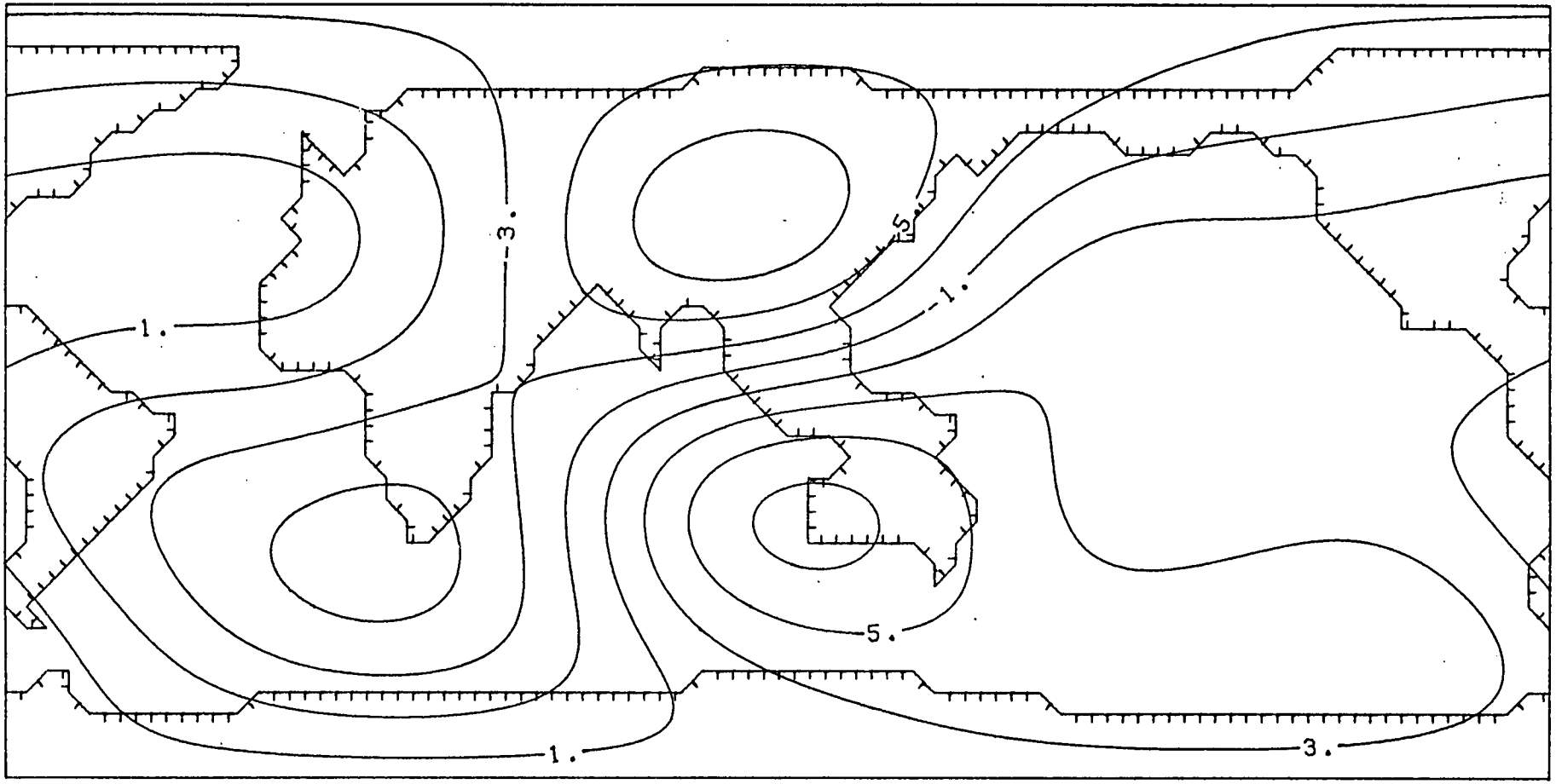

EQUIV (MALIN39) U.T.=4

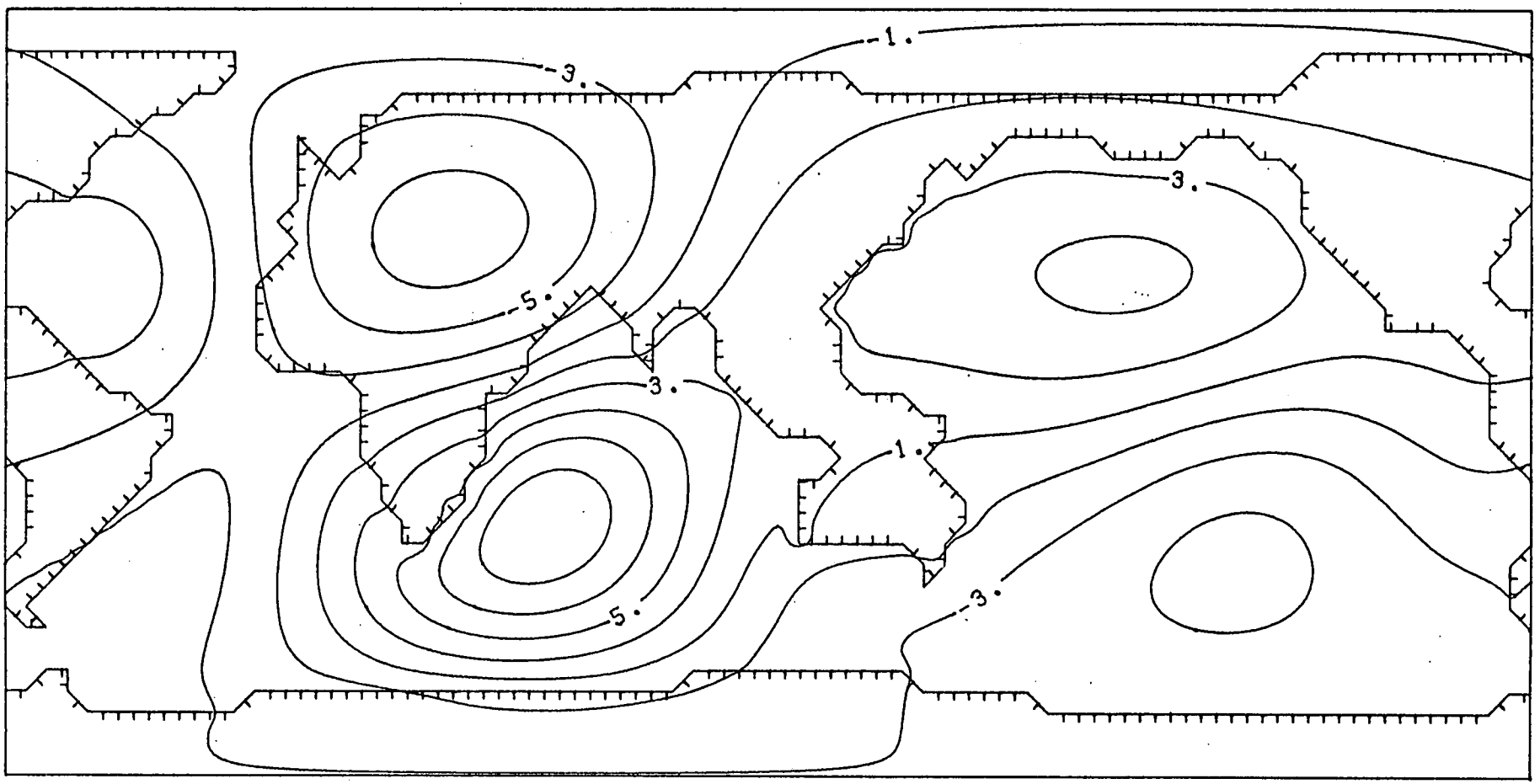

EQUIV (BANKS) U.T.=8

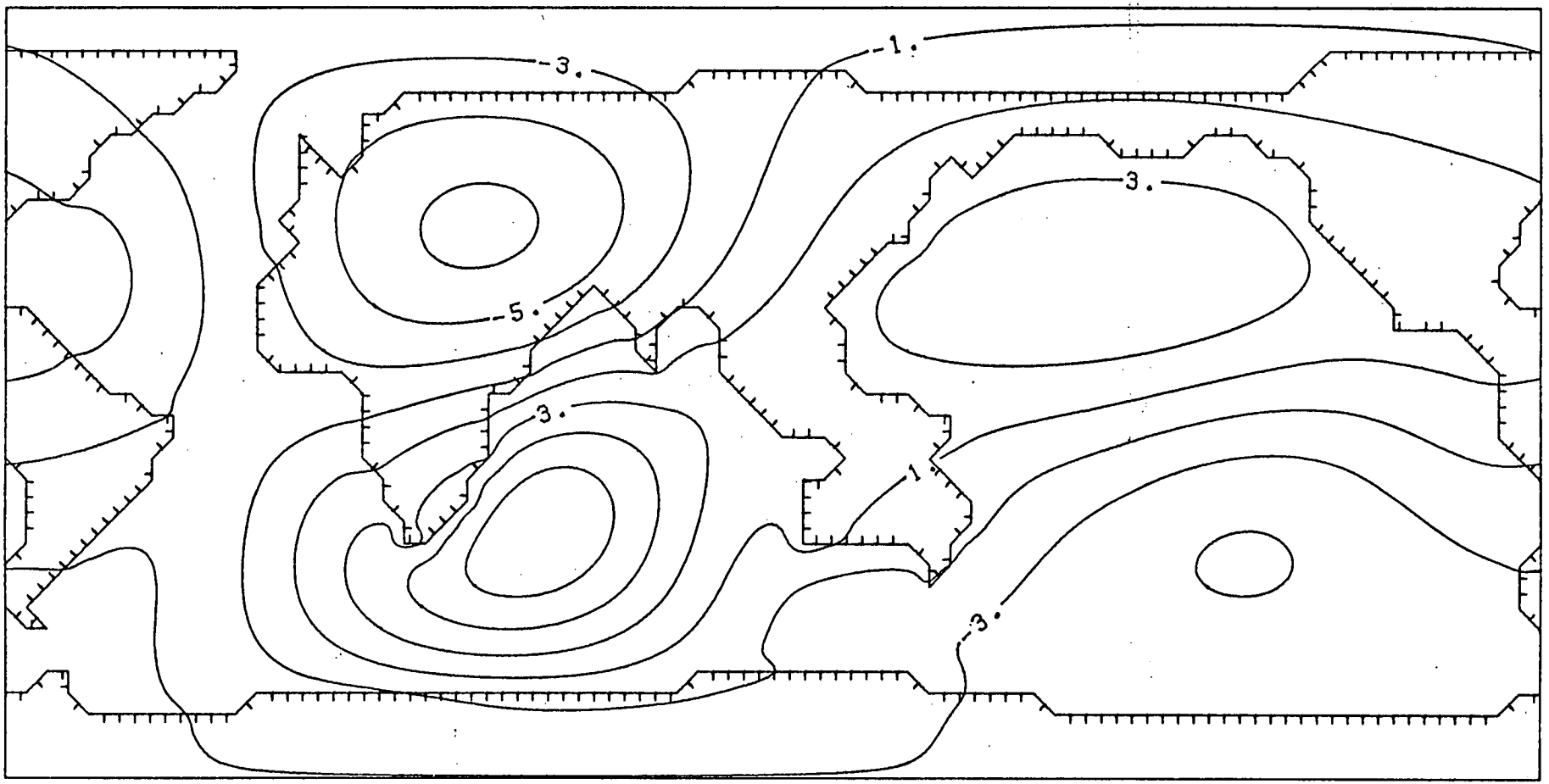

EQUIV (PERFECT) U.T.=8

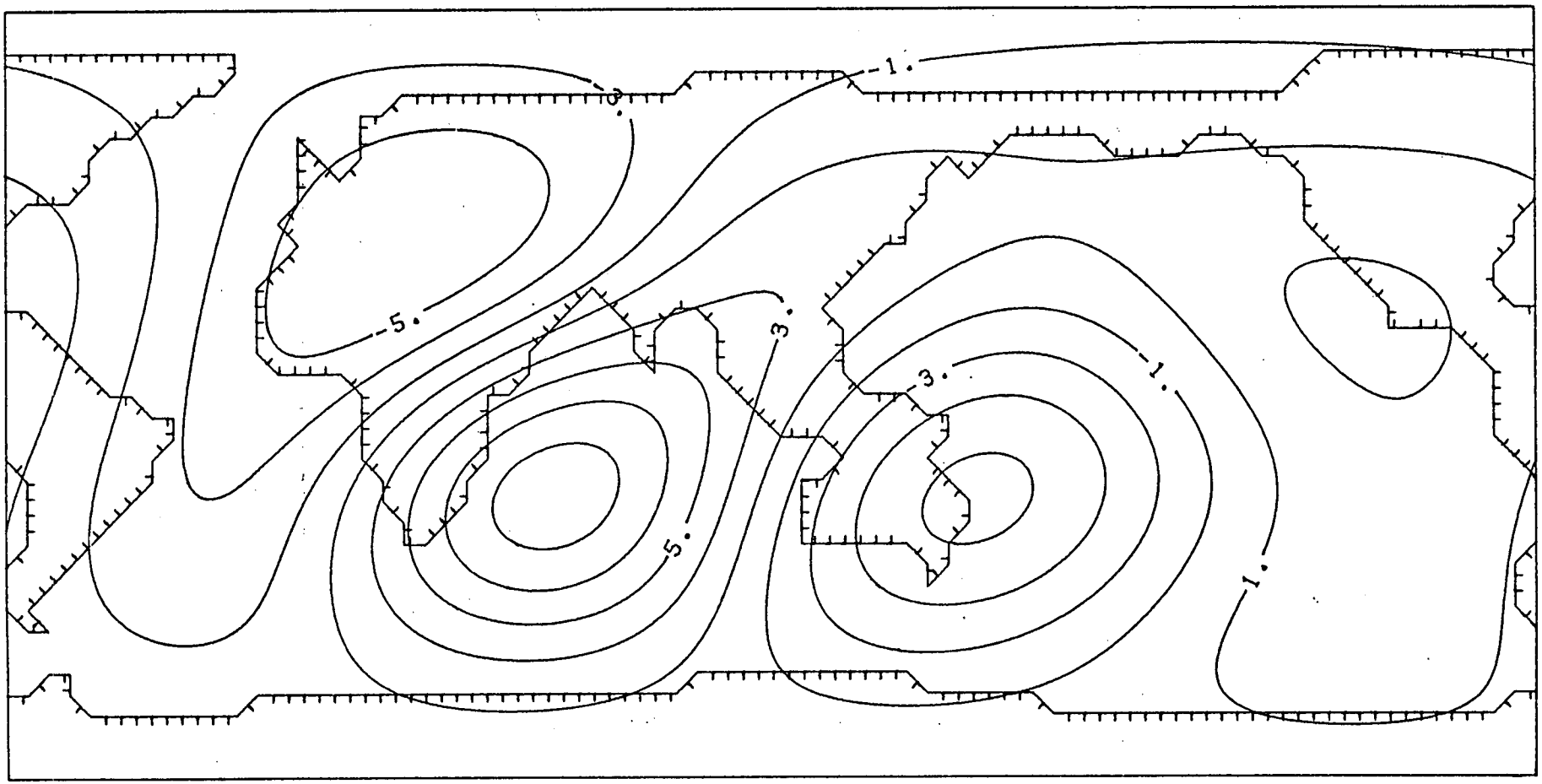

EQUIV (MALIN39) U.T.=8

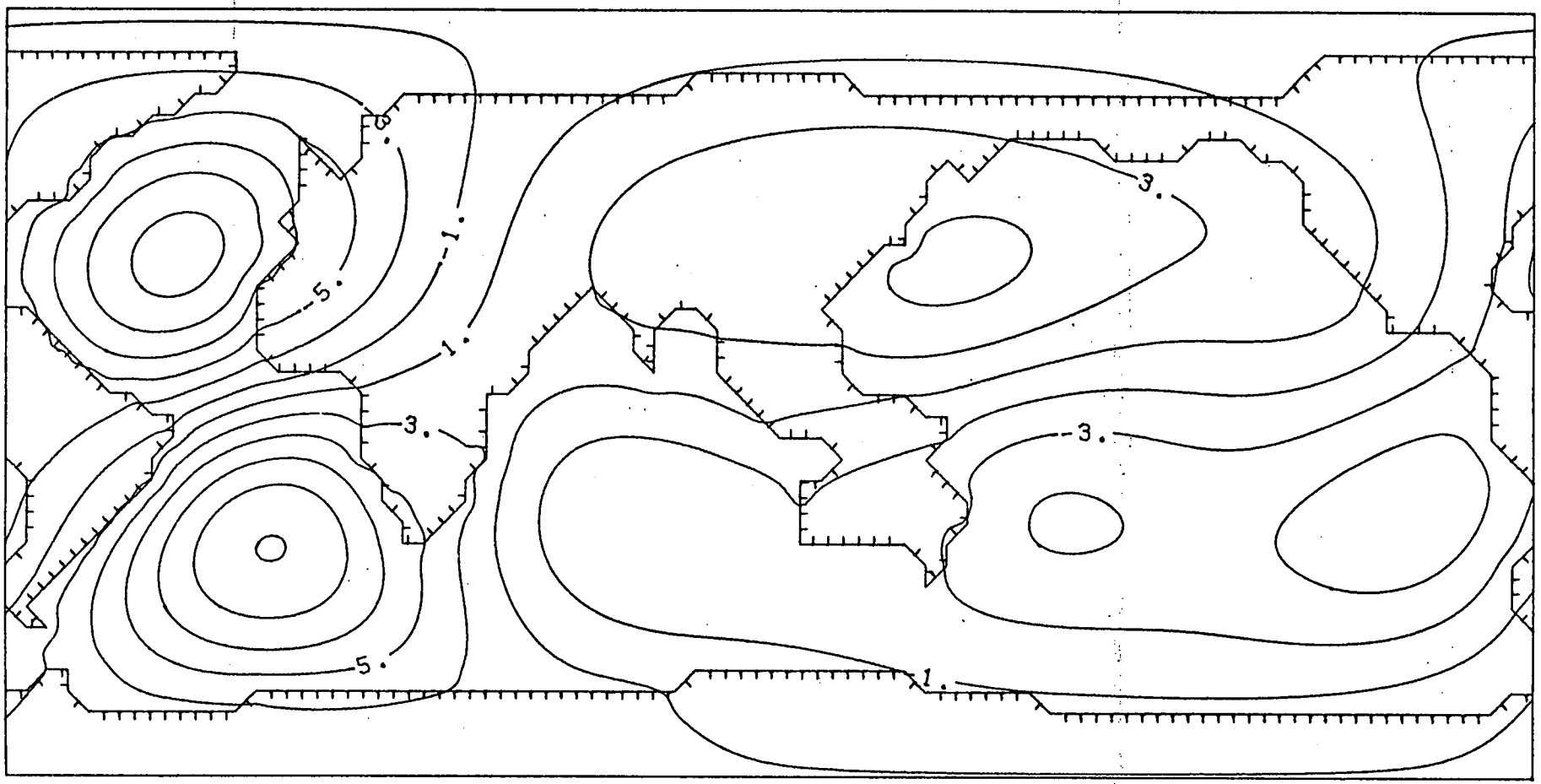

EQUIV (BANKS) U.T.=12

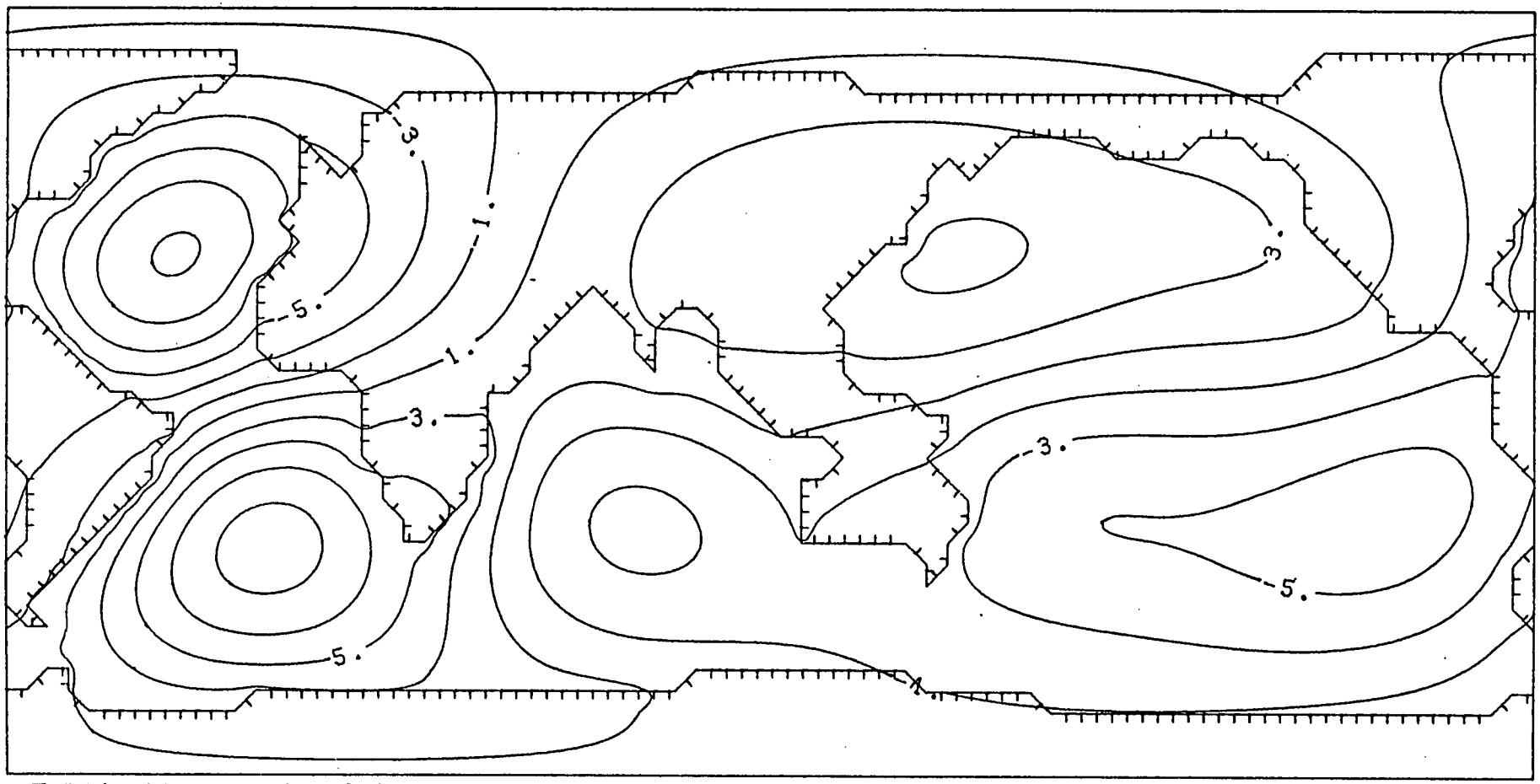

EQUIV (PERFECT) U.T.=12

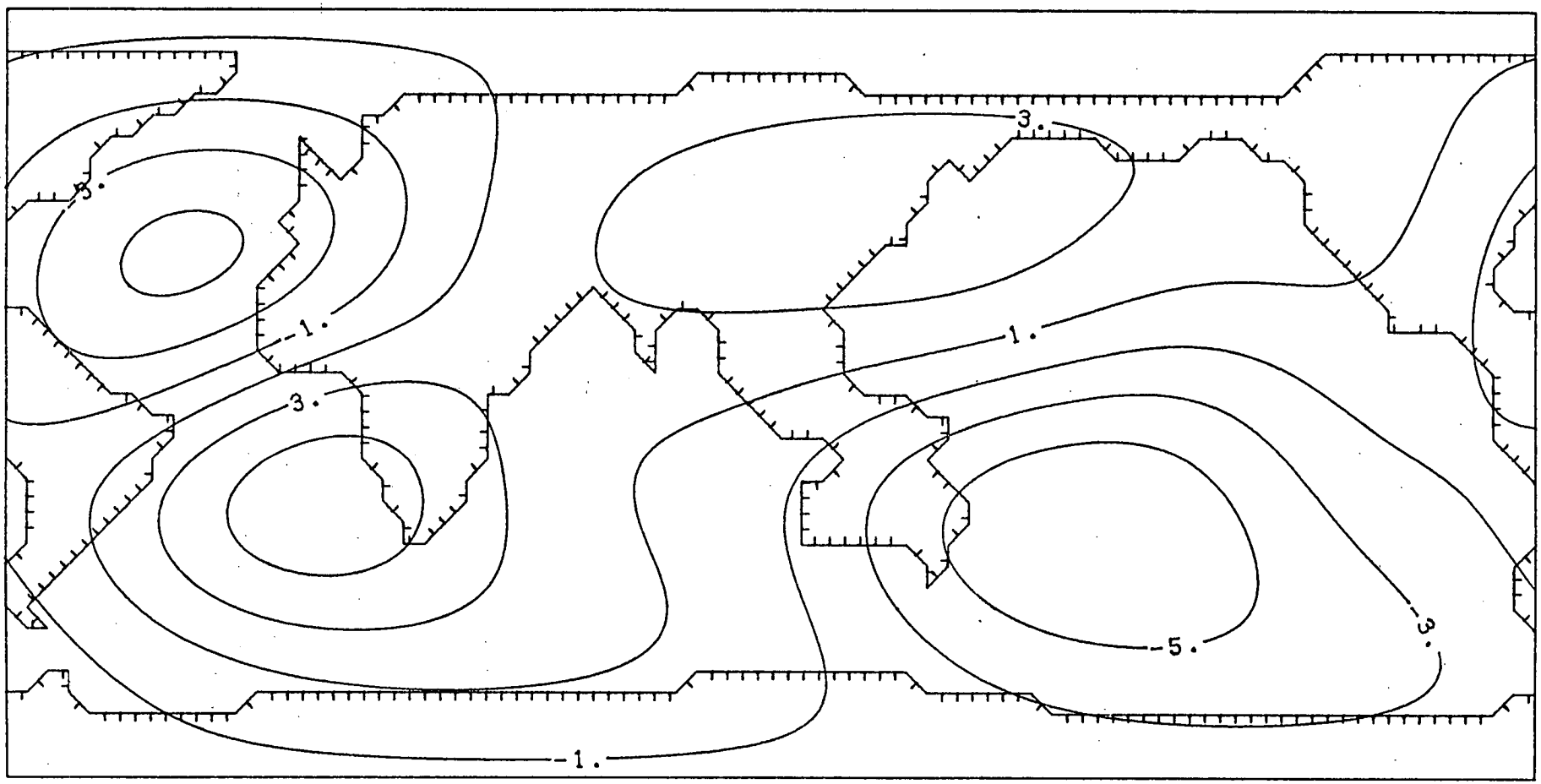

EQUIV (MALIN39) U.T.=12

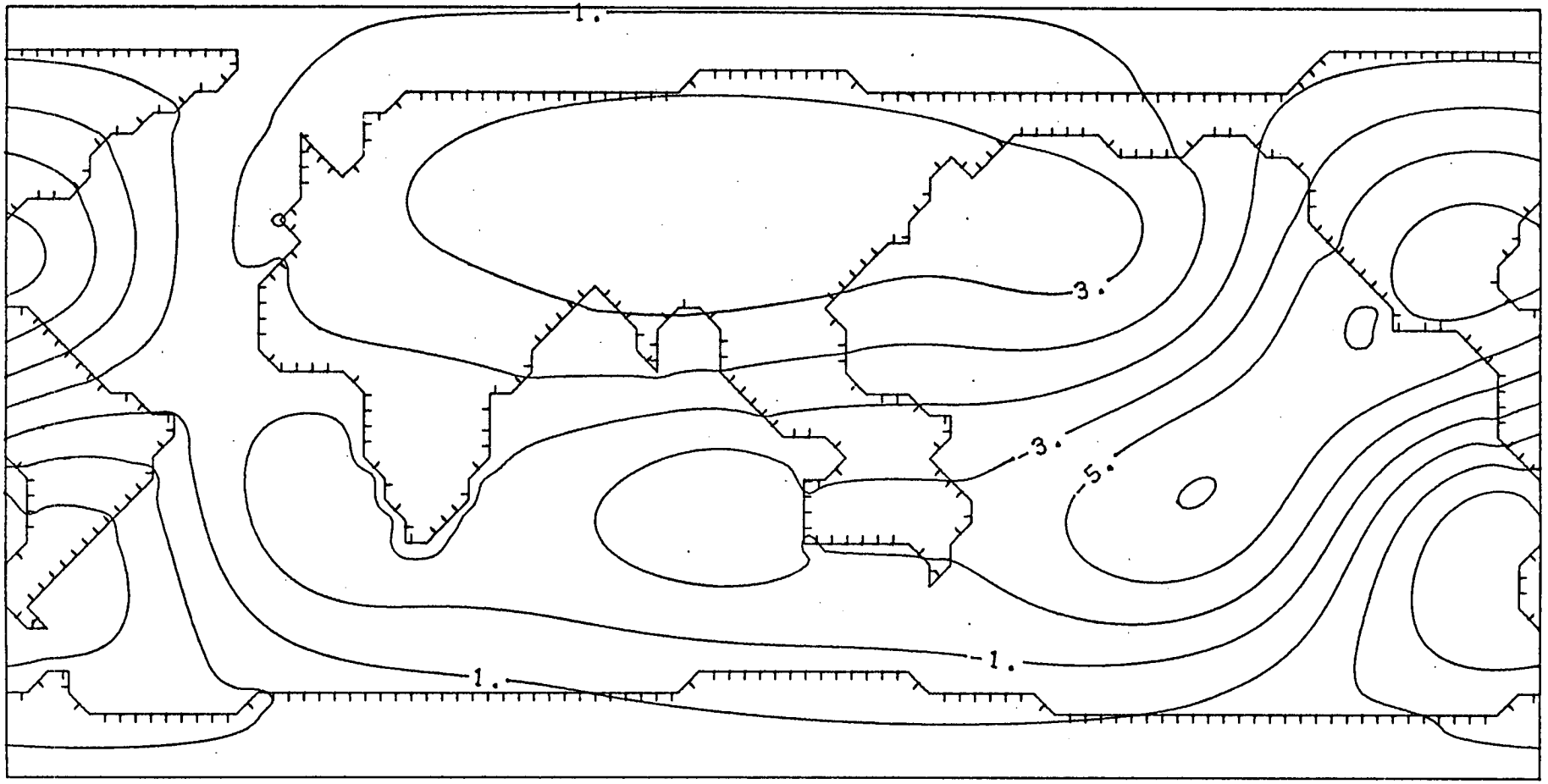

EQUIV (BANKS) U.T.=16

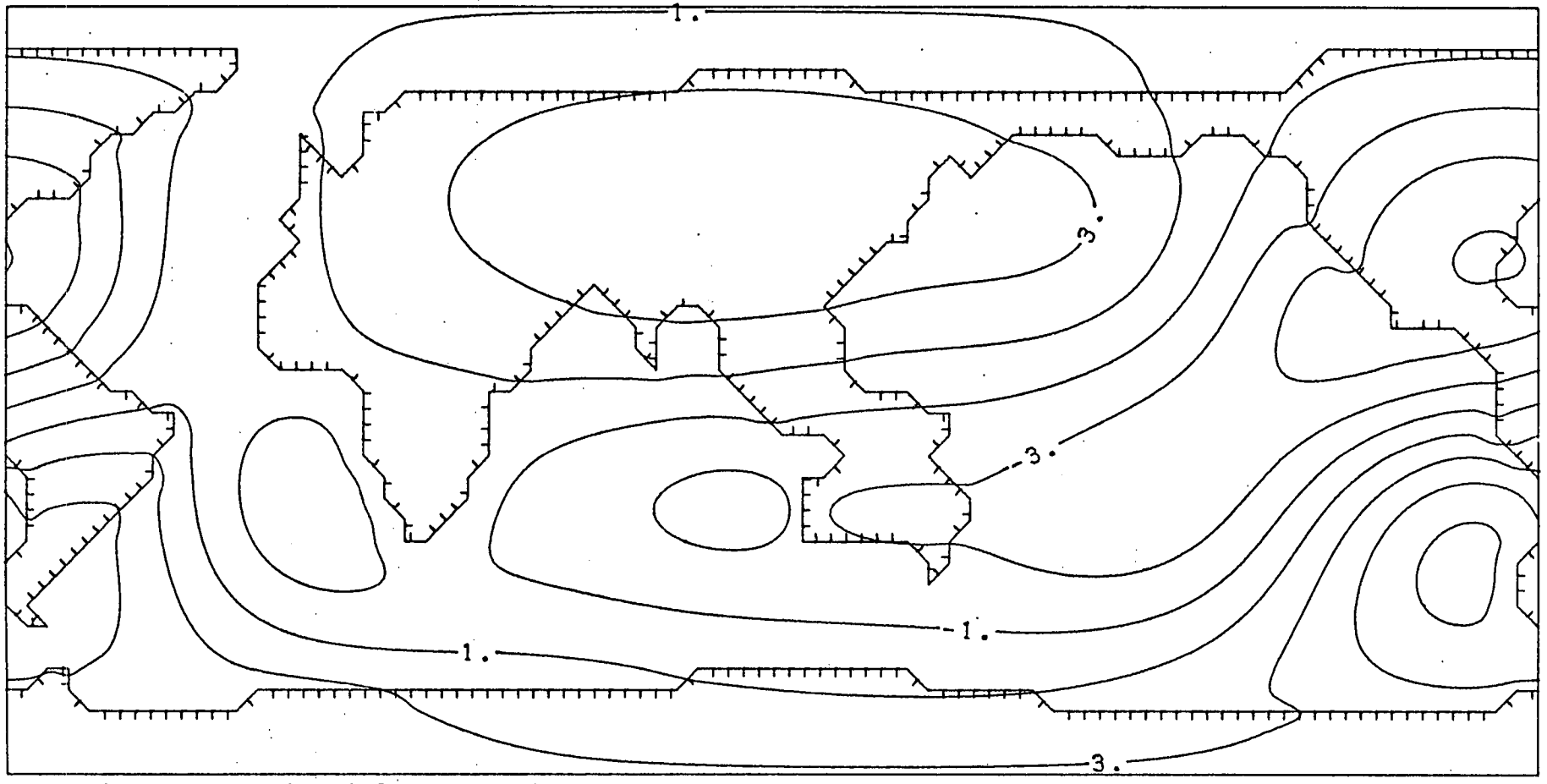

EQUIV (PERFECT) U.T.=16

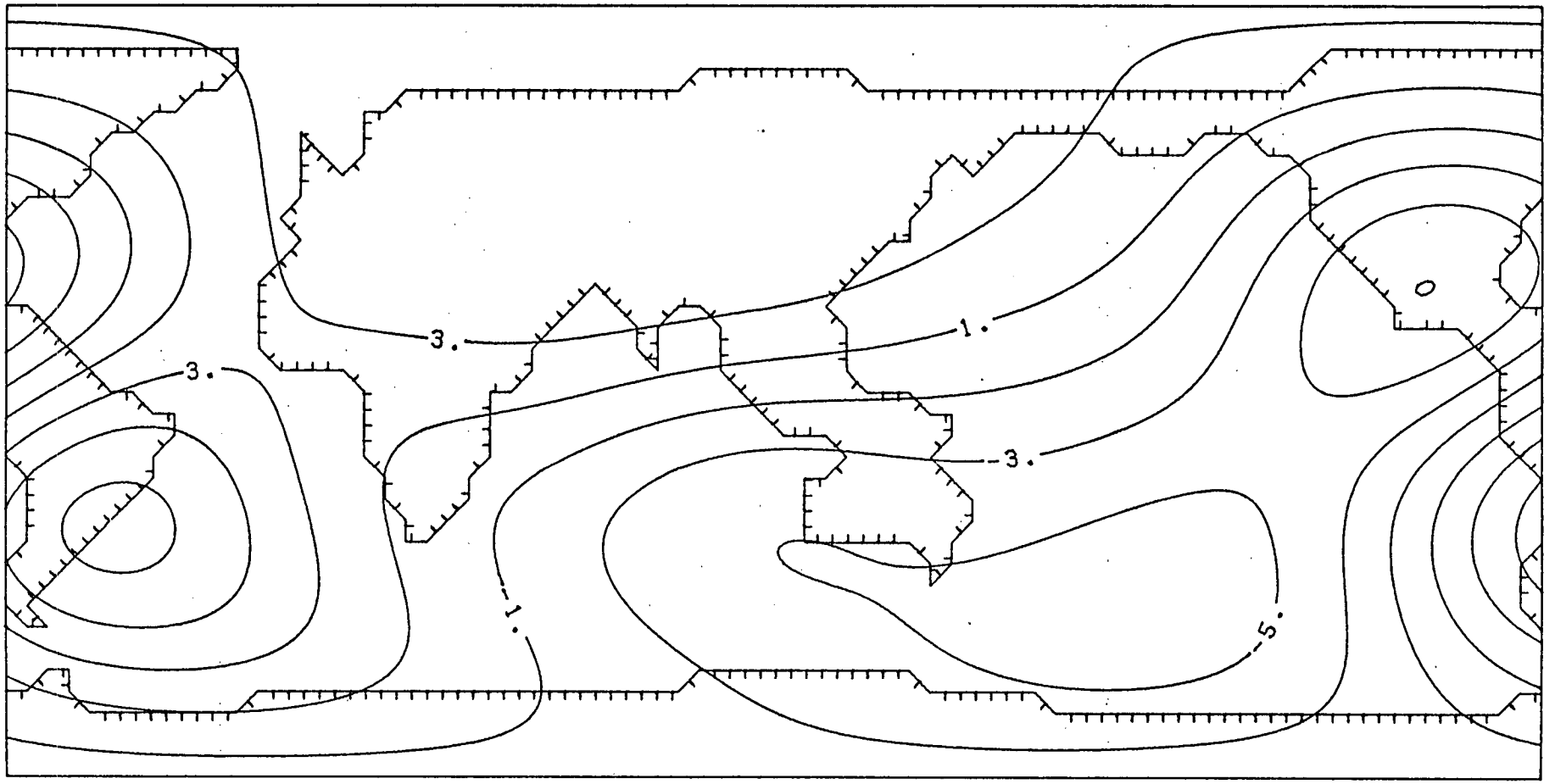

EQUIV (MALIN39) U.T.=16

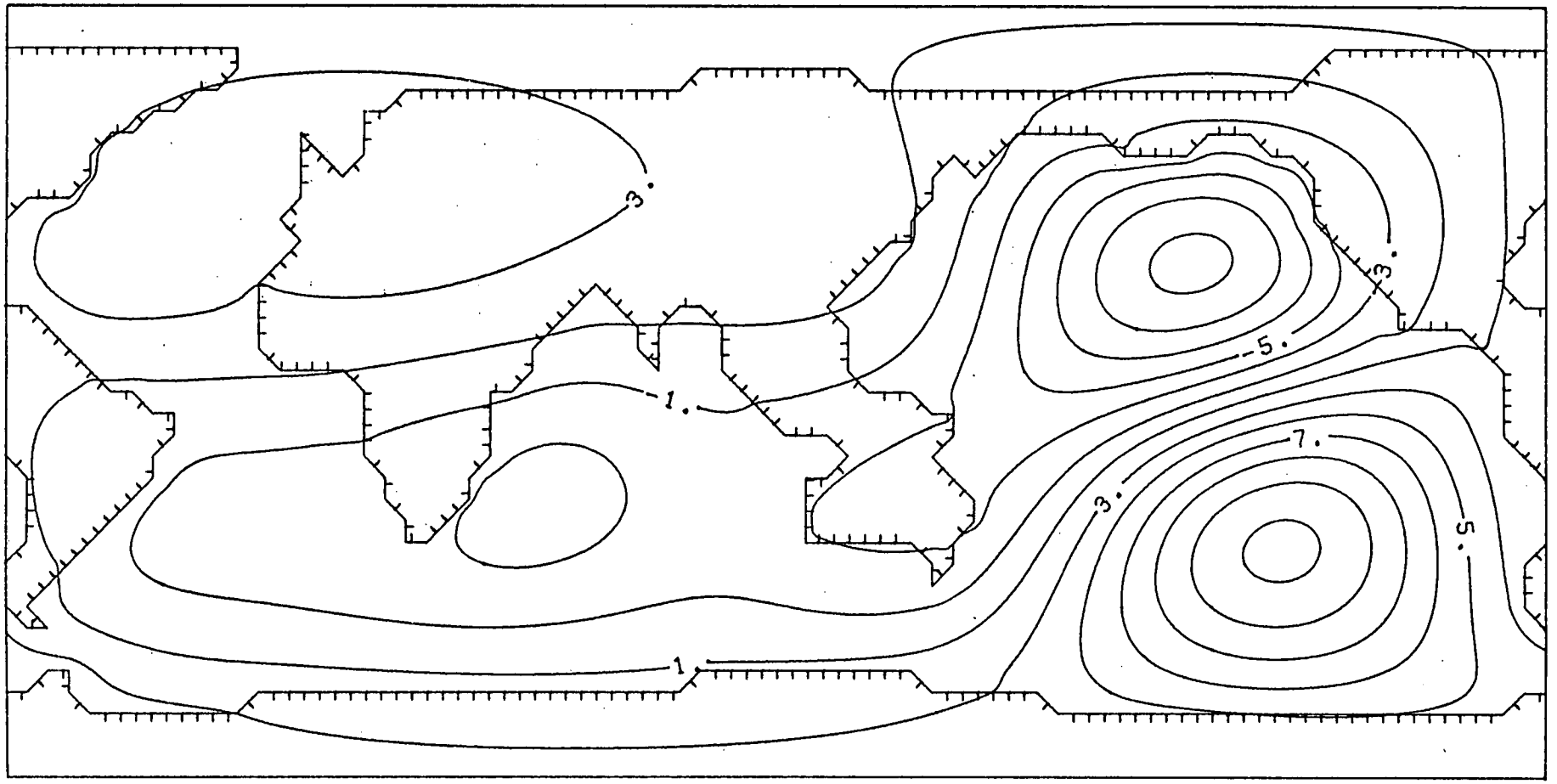

EQUIV (BANKS) U.T.=20

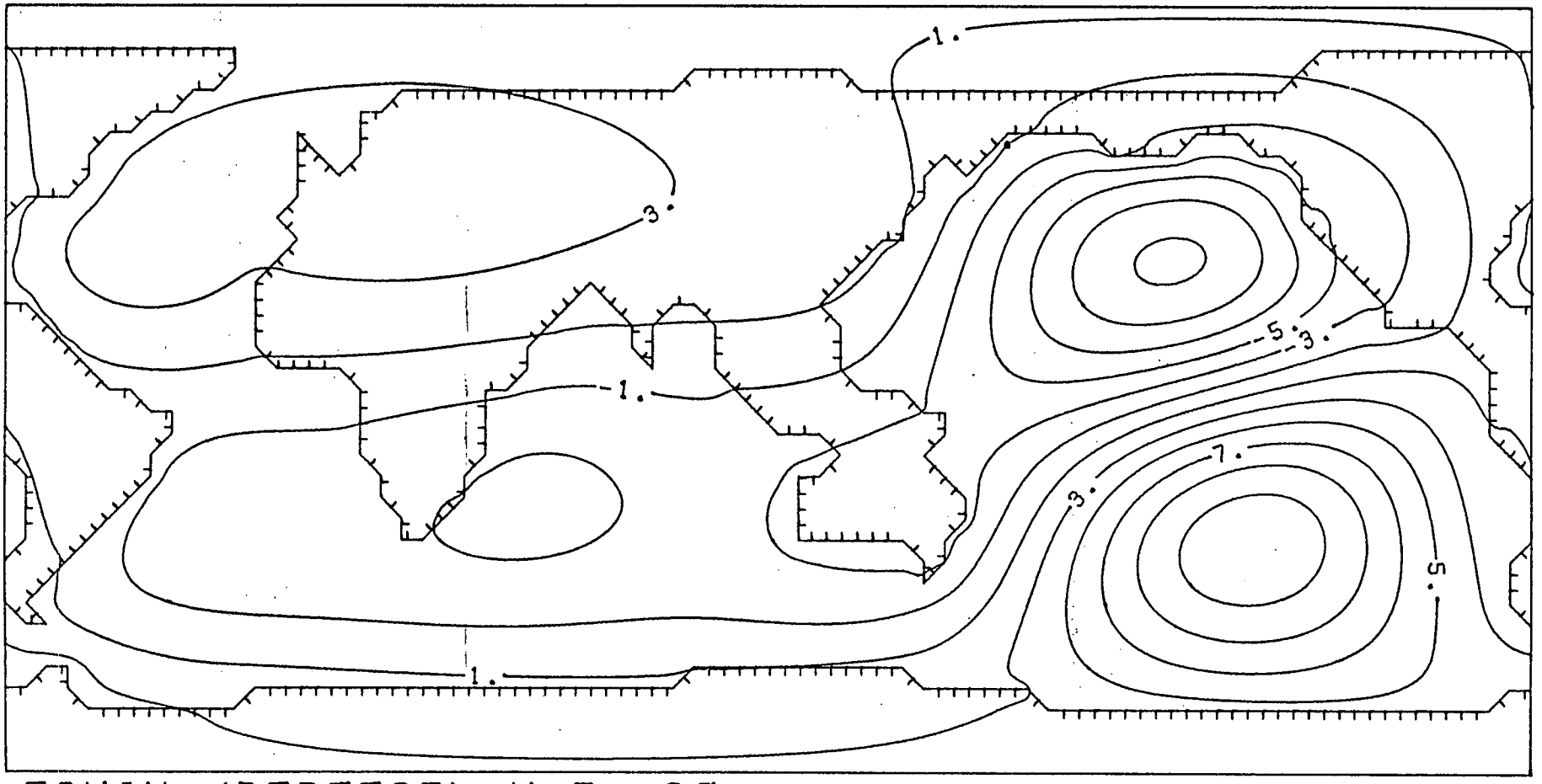

EQUIV (PERFECT) U.T.=20

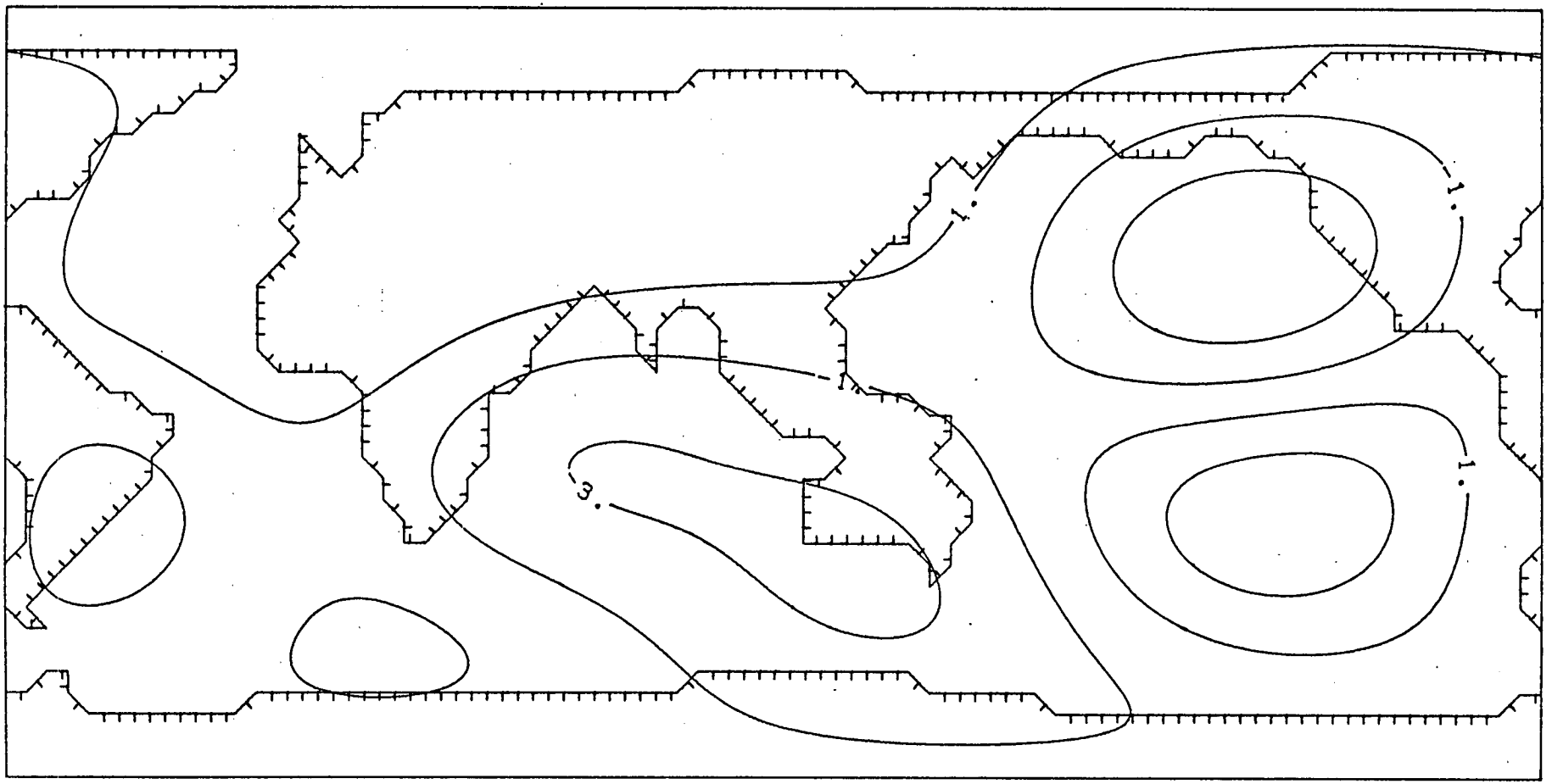

EQUIV (MALIN39) U.T.=20

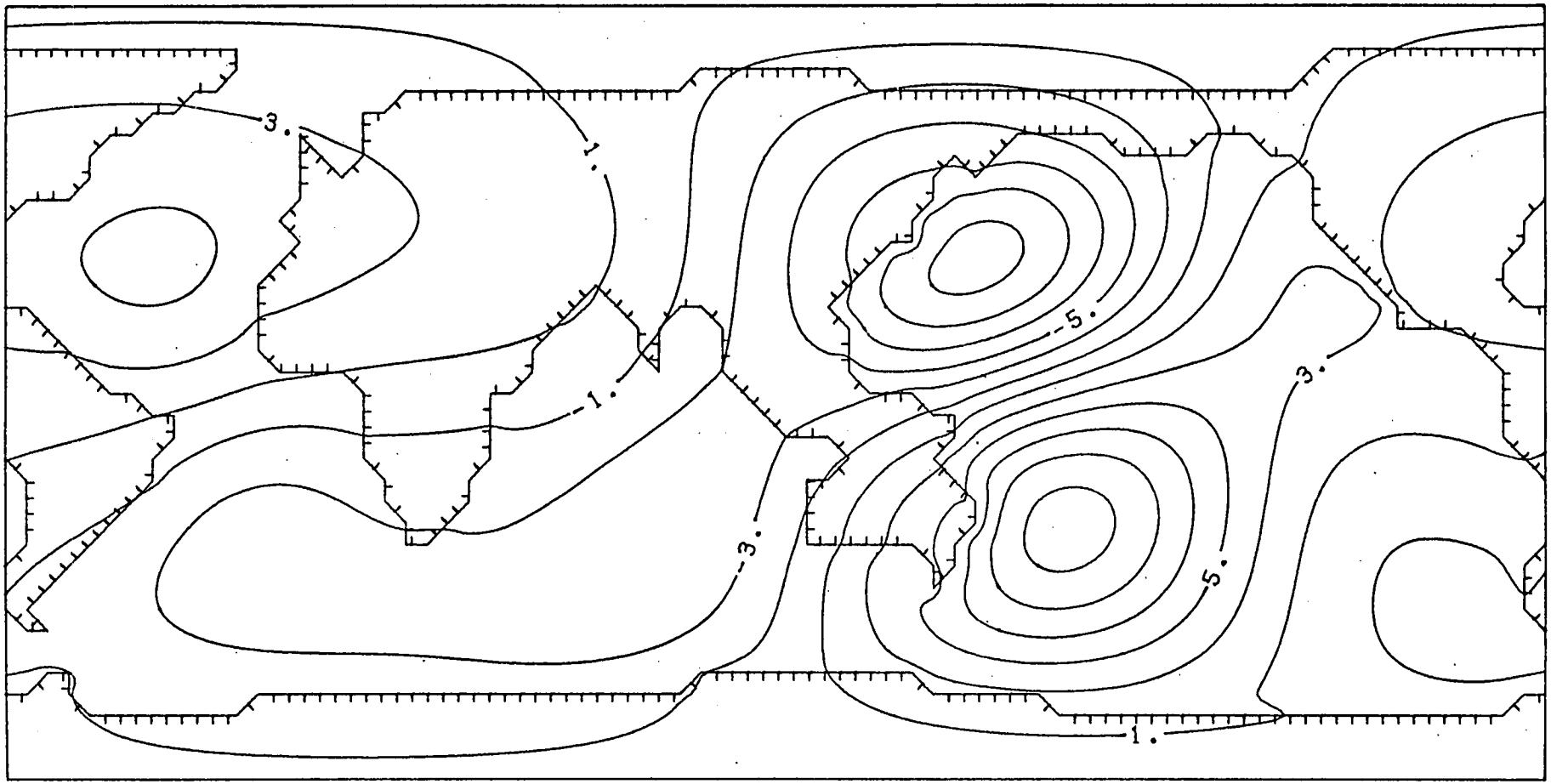

EQUIV (BANKS) U.T.=24

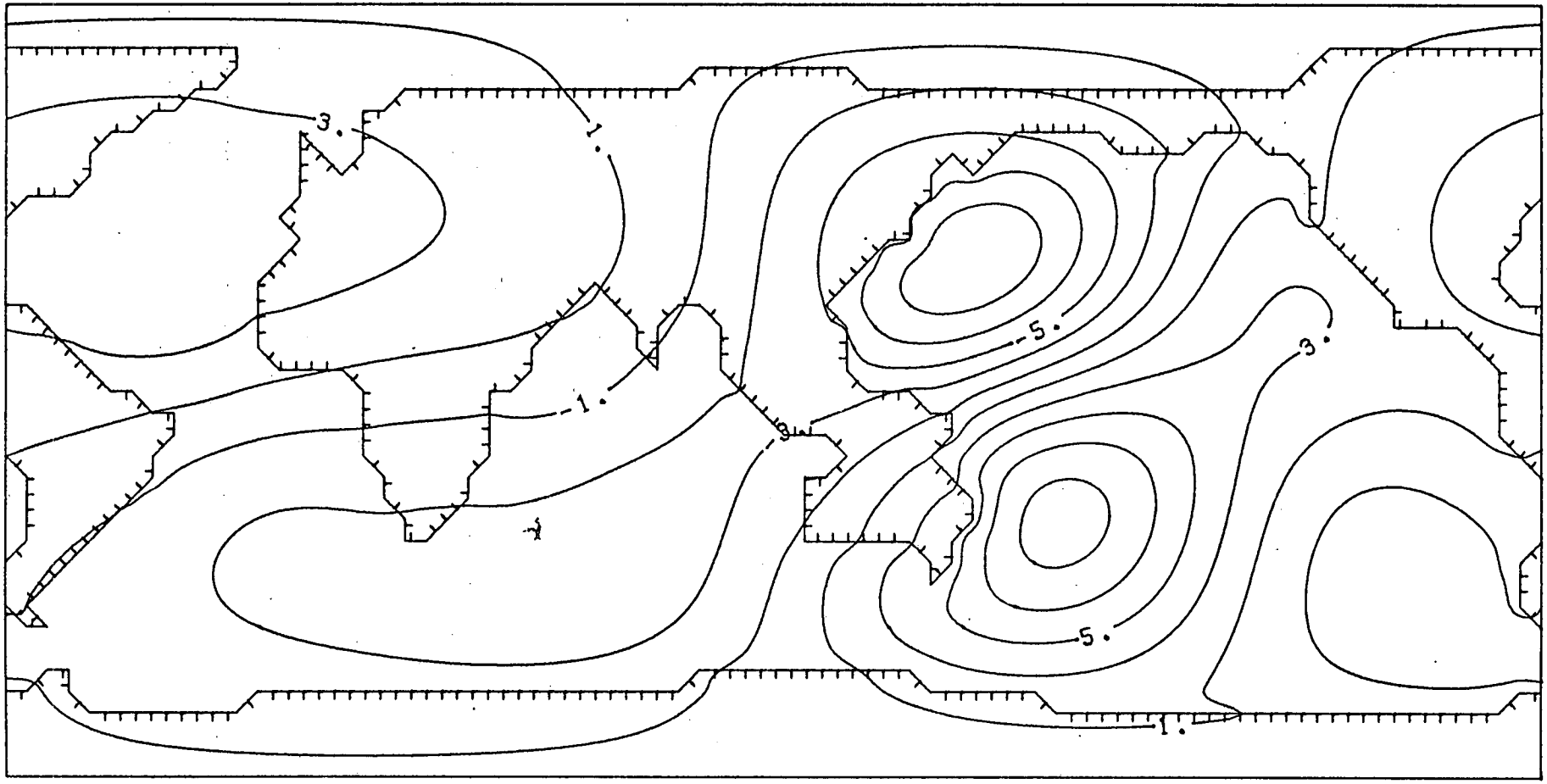

EQUIV (PERFECT) U.T.=24

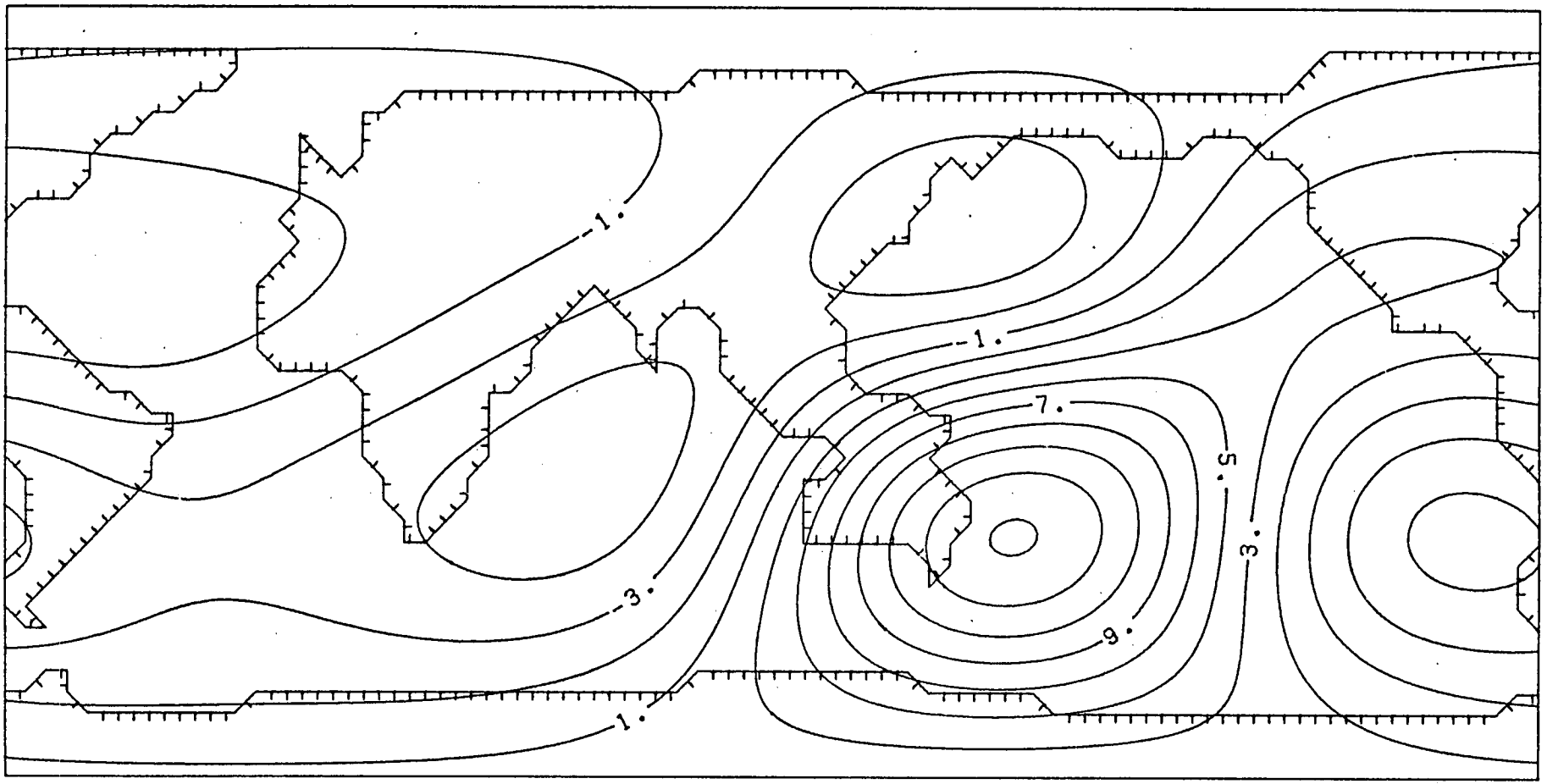

EQUIV (MALIN39) U.T.=24

0.9 earth radii at 8, 12, 20 and 24 hours U.T. This is in spite of the fact that some of the current streamline functions for individual harmonics, as shown in chapter 5, were smaller in strength when Banks' conductivity replaced the perfect conductor to simulate the mantle, which suggests that induction in the conductosphere is the dominant process as opposed to oceanic induction.

One criticism of comparing the observed and calculated equivalent current systems is that the one synthesised from Malin's 39 coefficients only contains terms up to fourth order, while the calculated systems must contain higher order harmonics, which are present because the complexity of the oceanic distribution introduces harmonics not present in the source field into the solution. However filtering the calculated equivalent current systems did not bring about any significant improvement in the comparison between modelling and observations.

Although the comparisons between the equivalent current systems seemed to be far from favourable, this analysis is rather subjective and it was decided to examine a more quantitative analysis.

6.4) Spherical Harmonic Analysis.

It was decided to do spherical harmonic analysis on the solutions so that it would be possible to calculate the ratio of internal to external parts of the magnetic potential. Since the equivalent current system is a way of representing the complete induced currents, its real and imaginary parts were subjected to spherical harmonic analysis at each period and the coefficients were converted from current streamline units to potential units by multiplying by a factor $n/(2n+1)$. The external part was taken

as the appropriate coefficient from the analysis of Malin and Gupta so that the ratio could be taken.

The spherical harmonic analysis was formulated as a least squares problem, which was not strictly necessary since the orthogonality of associated Legendre functions is practically obeyed even when the numerical surface integrations were performed on a 5°x5° grid. It was possible to make the analysis up to sixth order (a maximum of 49 coefficients, including a monopole) and the off diagonal terms of the normal equations matrix were always at least two orders of magnitude smaller than the diagonal terms. The least squares matrix approach was chosen for the analysis on the 5°x5° grid since it was hoped that the program could easily be converted for making the analysis using data only from the locations of geomagnetic observatories, when it would no longer be possible to use orthogonality on account of the irregular distribution.

The results of the spherical harmonic analysis for the three principal Sq harmonics are presented in Table (6.2), in terms of amplitude and phase, for modelling with both the perfect conductor and Banks' conductivity distribution together with the observed values from Banks (1972). The responses obtained with the conductosphere alone are also presented since they were known analytically and served as a check on the spherical harmonic analysis. There are two responses given for each harmonic in the cases of the models with the real oceanic distribution, because it is to be expected that a harmonic with a cosine longitudinal dependence would have a different response from the equivalent harmonic which varied as the sine of the longitude due to the fact that the oceans are not distributed

RATIOS OF INTERNAL TO EXTERNAL PARTS.

	Inner conductor only	Real Oceans added	Uniform 4 km. ocean	Uniform 1 km. ocean
Perfect conductor				
P_2^1 24 hr	.393, 0.	.431, 16.2	.511, 14.9	.406, 7.1
		.456, 6.5		
P_3^2 12 hr	.359, 0.	.529, 15.5	.649, 16.7	.418, 16.8
		.480, 20.5		
P_4^3 8 hr	.310, 0.	.559, 16.5	.723, 16.2	.445, 25.3
		.550, 17.4		
Banks' conductivity				
P_2^1 24 hr	.398, 7.8	.462, 14.8	.542, 15.1	.433, 13.9
		.449, 8.1		
P_3^2 12 hr	.422, 12.7	.559, 12.2	.665, 14.4	.506, 18.4
		.545, 15.1		
P_4^3 8 hr	.384, 16.4	.599, 13.9	.733, 14.4	.536, 23.6
		.598, 14.3		
Banks' observations				
P_2^1 24 hr	.376, 12.4			
P_3^2 12 hr	.442, 14.6			
P_4^3 8 hr	.433, 15.3			

Table 6.2

about the surface of the earth in a symmetric manner.

It can be seen that the addition of the oceanic sheet caused a substantial increase in the amplitude of the ratio of internal to external parts for both the perfectly and finitely conducting mantles, but the phases were smaller in the finitely conducting case, with only one exception, giving a better agreement with the observed phases. Since neither model was in good agreement with the amplitude observations, which were always on the high side, it was decided to examine the extent to which the response of the real oceanic distribution differed from that of a uniform shell representing an ocean 4km. deep. By examining the first three columns of Table (6.2) it can be seen that the amplitudes of the responses obtained by modelling with a real oceanic distribution fall roughly mid-way between those obtained with the conductosphere alone and with the uniform ocean plus the conductosphere. In order to achieve amplitudes which are comparable with the observations it was necessary to reduce the depth of the uniform ocean to the order of 1 km., in agreement with the work of Chapman and Whitehead (1922) and Jady (1974).

6.5) Possible Explanations for the Lack of Agreement Between Calculations and Observations.

Both of the methods employed in the previous section for comparing the results of modelling with observations showed that the amplitudes of the calculated responses were too high and it is essential to try to explain this state of affairs.

Since it has been shown that it is the field induced in the conductosphere that is the predominant fraction of the internal field, it is possible that the combination of Banks' model with the oceanic sheet is too highly conducting. Banks' model was

proposed as a radially symmetric model of the whole earth and it is probably unreasonable to expect to get a better comparison between calculations and observations simply by adding the equivalent of 4 km. of highly conducting ocean at the surface of the earth.

The surface conductivity in Banks' model was given as 0.01 Sm^{-1}, and although this is low by some geophysical standards, even lower conductivities have been proposed for some parts of the earth's crust (Jones and Hutton, 1979). However since roughly 70% of the earth is covered by the oceans, it is really the conductivity of the oceanic crust and upper mantle which is of interest here, but according to Cox (1978), suboceanic conductivities are not at all well established. The author has been unable to trace any global conductivity profile more recent than Banks' 1972 model and, although regional studies often indicate the existence of more highly resistive zones, it is dangerous to assume that these are representative of the earth as a whole. On the basis of the results pesented in the previous section, the author would recommend that the surface conductivities be reduced, perhaps by an order of magnitude, in any future attempts to model the oceanic induction problem.

The problem of near surface conductivities is even more important when the validity of having the oceans decoupled from the mantle is questioned. In order to be able to use Price's equation for induction in a thin sheet and the surface integral formulae, it is essential to inhibit any flow of electrical current between the oceans and the mantle. This implies that the induction is driven only by the vertical component of the magnetic field, which is a process called unimodal induction. Any

complete solution of the oceanic induction problem must allow for bimodal induction, when currents can flow between the oceans and the mantle and the horizontal fields aquire a new importance, however it would be necessary to adapt the work of Vasseur and Weidelt (1977) or Dawson and Weaver (1979) for use in spherical geometry before it would be possible to predict the effect of bimodal induction.

A possible defect of the model used is that the calculations were performed on a 5^{o} x5^{o} grid. Examination of the accuracy parameter over the entire grid demonstrated that a grid interval of 5^{o} could yield an accurate solution of the finite difference equations for tesseral and sectoral harmonic inducing fields, but the accuracy was poorer when the inducing field was a zonal harmonic. This was largely because a zonal harmonic inducing field tends to produce a large global circulation of current and a finite difference scheme with only one grid point between Tierra del Fuego and Antarctica is obviously too coarse to cope with a large circum-global flow. Global ciculation current is less pronouced when the inducing field is a tesseral or sectoral harmonic, as opposed to zonal, because the primary magnetic flux through the near-spherical cap of Antarctica is almost zero, and in accordance with Faraday's Law, there can only be a very small net circulation of current around this particular land mass.

An additional obvious defect of the model is that there are only two separate land masses: Antarctica and the rest of the world, which may force unrealistic constraints on the circulation of current. However the preliminary results of Beamish et al. (1979) demonstrated that, although separating Australia from

South-East Asia changed some of the flow patterns, the comparison between their calculations and observatory measurements was not improved by the modification.

One factor that deserves a special examination is the extent to which the distribution of geomagnetic observatories affects the separation of the field into its internal and external parts, as performed by Malin and Gupta. This method of analysis is now quite standard, the details of which can be found in Malin (1973).

It was decided that it would be instructive to compare the results of making a spherical harmonic analysis of the solutions, obtained for the effect of the oceans on Sq, using all of the points on the 5^{o} grid with the results from an analysis which used only the values at the positions of geomagnetic observatories. The spherical harmonic analysis presented at the beginning of this chapter was performed on the equivalent current system, at all grid points, to determine the internal coefficients, but the analysis of Malin and Gupta required the analysis of both the vertical and horizontal magnetic fields, which do not vary as smoothly as the equivalent current system does. Programs were developed for the analysis of the vertical and horizontal fields using the entire solution and using only data from the positions of geomagnetic observatories, which were found by a form of interpolation of the full solution on the 5^{o} grid. Since significant differences were found between the two different analyses of the vertical field, the complete field separation was not attempted because it was expected that any discrepancy between the analyses of the vertical field would be carried over into the field separation. It should be stressed that Malin

stated that the contribution of the vertical field analysis (Z analysis) to the internal and external coefficients was always greater than the contribution of the horizontal field analysis (X+Y analysis) (Malin, 1973, p.572).

Both analyses were made on the total vertical field predicted for Sq by using the model with the perfectly conducting mantle at periods of 24, 12 and 8 hours. The analysis using the complete grid involved the calculation of 49 coefficients (up to order 6), where the monopole term was included to ensure that it was small, while the analysis based on the observatory distribution used only the coefficients published by Malin and Gupta for each separate period.

Malin and Gupta used data from 108 geomagnetic observatories but in this work the author used only the geographic coordinates of the 100 observatories used, and published, by Malin in his earlier work on geomagnetic tides, Malin (1973), however it is unlikely that the exclusion of the extra observatories would have made any significant difference since most of them were in areas which had a high density of observatories, e.g. Japan, India and the western equatorial coast of South America. The locations of the 100 observatories are superimposed on the model of the oceans in Figure (6.3)

The values of the vertical field at the observatory sites were found by using a finite difference approximation of the two-dimensional Taylor series of the field about the grid point nearest each observatory. If the coordinates of the observatory were $(\theta+\varepsilon,\lambda+\delta)$, then: $Z(\theta+\varepsilon,\lambda+\delta) =$

$$Z(\theta,\lambda) + \varepsilon \frac{\partial Z}{\partial \theta} + \delta \frac{\partial Z}{\partial \lambda} + 1/2!\left(\varepsilon^2 \frac{\partial^2 Z}{\partial \theta^2} + 2\varepsilon\delta \frac{\partial^2 Z}{\partial \theta \partial \lambda} + \delta^2 \frac{\partial^2 Z}{\partial \lambda^2}\right) + \ldots\ldots \quad (6.6)$$

Figure 6.3

Distribution of Geomagnetic Observatories.

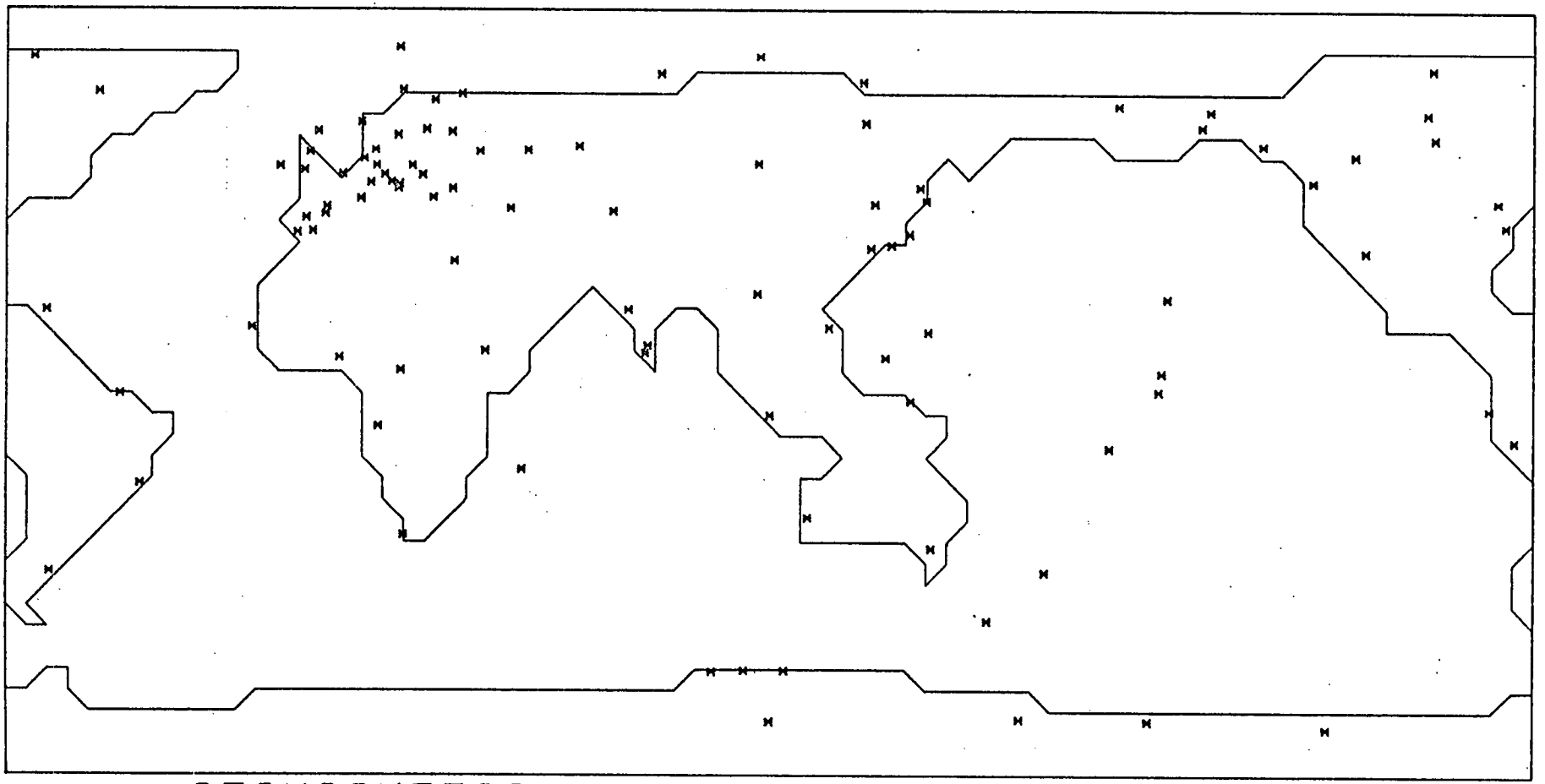

GEOMAGNETIC OBSERVATORIES

By truncating the Taylor series after the second order terms, it was possible to write the finite difference scheme in terms of the value at the grid point (θ,λ), closest to the observatory, and the values at the 8 next nearest grid points surrounding it. Trials with synthetic data showed that little improvement was brought about by using a third order Taylor series approximation, which involved the use of only 4 extra grid points, which brought the total required to 13.

The results of the two different analyses are presented in Tables (6.3a - 6.3c), where the real and imaginary parts from the analysis of the full 5 grid are shown first, followed by the real and imaginary parts of the equivalent coefficient derived from the analysis based on the geomagnetic observatories. In the later case, each coefficient is immediately followed by its respective standard deviation, as defined in equation (25) (Malin,1973):

$$\text{std. dev.} = (QW_n^m/(N-M))^{1/2} \quad (6.7)$$

where Q is the sum of the squares of the residuals from the least squares fit, W_n^m is the appropriate diagonal term of the inverse of the normal equtions matrix, N is the number of data points (100) and M is the number of coefficients being fitted. Although only the harmonics whose coefficients were determined by Malin and Gupta have been shown, it should be stated that eight and seven other coefficients had either a real or imaginary part greater than unity for periods of 24 and 12 hours respectively, in the sixth order analysis involving the entire grid.

It can be seen that some of the coefficients from the two analyses are in better agreement than others, while some of the coefficients from the observatory analysis have standard devia-

Spherical Harmonic Analysis of the Total Vertical Field

Period = 24 hours

Harmonic		5° Analysis		Observatory Analysis			
		Real	Imag	real	std. dev.	imag	std. dev.
P_1^0		0.01	0.26	0.41	0.31	-0.47	0.50
P_1^1	c	-0.22	-2.01	-0.11	0.32	-3.80	0.53
P_1^1	s	3.44	-0.40	5.49	0.37	-4.14	0.60
P_2^0		0.53	-5.57	-1.10	0.43	-6.23	0.70
P_2^1	c	-14.68	-2.48	-12.89	0.36	3.24	0.60
P_2^1	s	2.05	-12.41	-3.72	0.48	-9.13	0.79
P_2^2	c	0.14	0.21	-3.03	0.45	-1.91	0.74
P_2^2	s	-0.56	0.26	-0.67	0.46	1.64	0.76
P_3^0		-2.70	2.67	-2.29	0.57	3.92	0.94
P_3^1	c	-0.06	1.01	-0.03	0.40	-1.50	0.66
P_3^1	s	-0.62	0.34	1.69	0.52	-2.14	0.87
P_3^2	c	0.14	1.22	1.83	0.48	2.34	0.79
P_3^2	s	1.01	1.54	1.98	0.52	-1.01	0.86
P_4^1	c	5.46	1.57	3.38	0.54	0.45	0.90
P_4^1	s	-0.08	5.02	1.56	0.61	5.78	1.00

Table 6.3 a

Spherical Harmonic Analysis of the Total Vertical Field

Period = 12 hours

Harmonic		5° Analysis		Observatory Analysis			
		Real	Imag	real	std. dev.	imag	std. dev.
P_1^1	c	0.02	0.04	1.54	0.46	2.51	0.46
P_1^1	s	0.03	-0.11	-1.56	0.53	-1.36	0.53
P_2^1	c	0.35	-0.74	-3.55	0.52	-3.60	0.52
P_2^1	s	-0.09	-0.33	0.79	0.68	0.42	0.68
P_2^2	c	-2.10	2.23	1.12	0.65	5.21	0.65
P_2^2	s	-2.13	-1.34	-1.84	0.66	-0.25	0.66
P_3^1	c	-0.24	0.02	1.47	0.56	2.60	0.56
P_3^1	s	-0.08	-0.06	-0.94	0.73	-0.41	0.73
P_3^2	c	9.83	4.68	3.86	0.71	-3.96	0.71
P_3^2	s	-5.75	8.56	0.48	0.75	8.56	0.75
P_3^3	c	-0.20	-0.43	1.91	0.79	0.81	0.79
P_3^3	s	0.40	0.44	0.77	0.75	-0.11	0.75
P_4^2	c	-1.16	-1.24	0.59	0.66	3.44	0.66
P_4^2	s	1.36	-0.64	0.38	0.77	-0.50	0.77

Table 6.3 b

Spherical harmonic analysis of the total vertical field

Period = 8 hours

Harmonic		5° Analysis		Observatory Analysis			
		Real	Imag	real	std. dev.	imag	std. dev.
P_3^2	c	-0.24	0.42	1.54	0.47	0.03	0.32
P_3^2	s	-0.17	0.02	-0.53	0.48	1.86	0.33
P_3^3	c	3.11	-0.37	0.60	0.50	-0.04	0.34
P_3^3	s	0.59	2.28	1.60	0.50	-0.06	0.34
P_4^2	c	0.16	0.05	-0.33	0.44	0.12	0.30
P_4^2	s	-0.09	-0.02	1.90	0.49	-0.66	0.33
P_4^3	c	-1.64	-2.11	1.47	0.56	2.60	0.56
P_4^3	s	2.28	-1.50	1.07	0.39	-1.37	0.26
P_4^4	c	-0.15	0.22	1.21	0.58	-0.43	0.39
P_4^4	s	-0.52	-0.25	-2.01	0.54	-1.24	0.37

Table 6.3 c

tions which are comparable, or even greater than, the magnitude of the estimates, with the result that little physical significance should be placed on these values. It is more instructive to examine the principal harmonics for each period; P_2^1, P_3^2 and P_4^3 at periods of 24, 12 and 8 hours respectively, when the standard deviations are substantially smaller than the estimates. The real parts of the cosine component and the imaginary parts of the sine component of the P_2^1 harmonic were in reasonable agreement (to within 75% approximately) and although the other pairs agreed roughly in magnitude, they had opposite signs. In the case of the semi-diurnal harmonic, P_3^2, only the imaginary parts of the sine components agreed, while the estimates of the imaginary parts of the cosine component agreed in magnitude but not in sign. There was no agreement between its other coefficients. The real and imaginary parts of the P_4^3 harmonic with a sine longitudinal dependence were in agreement while those of the cosine component had opposite sign.

The coefficients obtained from the analysis using all the 2522 grid points can be taken as correct because the orthogonality of the associated Legendre functions is preserved even on a 5° grid, at least up to sixth order, and the values of the estimates did not depend on which harmonics were being used in the analysis. The situation is quite different when the observatory analysis is made, since it is necessary to reduce the number of coefficients to be calculated in order to find a stable estimate with a relatively small standard deviation. However the above comparisons show that use of the least squares procedure can still give estimates which are incorrect.

Assuming that the results of the modelling are a correct

representation of the effect of the oceans on Sq, then the above comparisons show that any spherical harmonic analysis based on observations at geomagnetic observatories would not yield the correct separation of the internal and external parts. This can be said, even although only the Z analysis has been performed, because the coefficients of the vertical field contribute more to the internal and external coefficients than the horizontal coefficients. On this basis alone, it is not surprising that the comparison between equivalent current systems derived from calculations and observations is poor.

It was later decided to examine how the ratios of internal to external parts, derived from the equivalent current system and the known external coefficients, depended on which type of analysis was used in their determination. The responses obtained from spherical harmonic analysis using all of the 5^{o} grid points has been shown and the observatory analysis was also attempted, using the same interpolation scheme to calculate the equivalent current system at the observatories as had been used to find the vertical fields. The same harmonics were kept in the observatory analysis of the equivalent current system as had been used for Z and the ratios of internal to external parts for the principal Sq harmonics are shown in Table (6.4), along with the respective ratios obtained from the analysis of the complete function, in terms of amplitude and phase.

The main difference between the two analyses is that the amplitudes obtained from the observatory analysis are always smaller than the corresponding amplitudes derived from the full analysis. This is observed in the two models considered, with either a perfectly or finitely conducting mantle, and although

RATIOS OF INTERNAL TO EXTERNAL PARTS.

	Full Analysis	Observatory Analysis
Perfect conductor		
P_2^1 24 hr	.431, 16.2	.416, 9.9
	.456, 6.5	.419, 0.6
P_3^2 12 hr	.529, 15.5	.372, 8.0
	.480, 20.5	.395 1.8
P_4^3 8 hr	.559, 16.5	.421, 10.8
	.550, 17.4	.346 8.2
Banks' conductivity		
P_2^1 24 hr	.462, 14.8	.438, 10.5
	.449, 8.1	.408, 6.6
P_3^2 12 hr	.559, 12.2	.441, 12.8
	.545, 15.1	.426, 10.5
P_4^3 8 hr	.599, 13.9	.536, 18.7
	.598, 14.3	.459, 20.1

Table 6.4

there are also large differences between the phases, the observatory analysis produces larger phases for the model with Banks' conductivity profile than for the model with the perfect conductor, which is generally the opposite of what is found from the analysis of the whole grid. The similarity in the amplitude and phase of the sine and cosine components of each harmonic, which is observable in the results from the full analysis, is no longer as close, which tends to suggest that any difference observed in the responses of these components is due to the distribution of observatories to a greater extent than it is to the surface conductivity distribution.

It should be stated that when synthetic data, containing only a few known spherical harmonics, were subjected to the observatory analysis, it was possible to obtain the correct coefficients, including zero where appropriate, provided all of the harmonics that were known to be present were included in the analysis. This, together with the above observations, bears out the work of Lowes (1978), who stated that the presence of higher order harmonics, not included in an analysis, results in errors in the estimates of the coefficients and that it is impossible to predict the magnitude of the errors by any 'internal goodness of fit'. This is analagous to the problem of leakage, or aliasing in the one-dimensional problem of time series analysis, where it is essential to filter out all frequencies higher than half the sampling frequency.

The large number and regular spacing of the grid points ensured that the analysis using all of the data was not subject to the problem of leakage and, as has already been stated, the values of the coefficients obtained did not depend on which other

harmonics were present in the analysis. It was possible to check this by the alternative means of surface integral filtering.

By constructing surface integral kernels of the form:

$$K_f(k,\theta) = 1/4\pi \sum_{n=1}^{k} (2n+1)\, P_n(\cos\theta) \qquad (6.8)$$

where k= 4,5 or 6, and calculating the basic integrals, it was possible to do low-pass filtering on any function defined on a 5^o grid by evaluting the surface integral of the product of the function with the filter kernel at each grid point. The value of the cut-off depended on the value chosen for k. The fact that this method gave the same result as the resynthesis of the function after spherical harmonic analysis, up to the appropriate order, had been done was further evidence that no leakage occurred.

The surface integral filter used much more c.p.u. time on the computer than spherical harmonic analysis, therefore it was not used once it was discovered that it was not necessary to do any filtering before calculating the coefficients, as is the practice in time series analysis. The analogy with some methods of time series analysis can be continued by way of the fact that the calculation of the type of surface integral in this work is the convolution of two functions over the surface of a sphere (e.g. the convolution of a current function with a mutual induction kernel) while spherical harmonic analysis is an operation in the spatial frequency domain.

REFERENCES.

Abramovici, F., & Chlamtac, M., (1978)

Fields of a Vertical Magnetic Dipole over a Vertically Inhomogeneous Earth.

Geophys., vol 43, No. 5, 954 - 966

Abramowitz, M., & Stegun, I.,A., (1965)

Handbook of Mathematical Functions. Pub. Dover.

Ashour, A.,A., (1950).

The Induction of Electric Currents in a Uniform Circular Disc. Quart. J. Mech. Appl. Math., 3, 119-128.

Ashour, A.,A., (1964).

On a Transformation of Coordinates by Inversion and its Application to Electromagnetic Induction in a Thin Perfectly Conducting Hemispherical Shell.

Proc. Lond. Math. Soc., 15, 557-576.

Ashour, A.,A., (1965).

The Coast-Line Effect on Rapid Geomagnetic Variations.

Geophys. J. R. astr. Soc., 10, 147-161.

Ashour, A.,A., (1971(a)).

The Magnetic Field of a Plane Current Sheet with Different Uniform Conductivities in Different Parts with Results for an Elliptical Area.

Geophys. J. R. astr. Soc., 22, 401-416.

Ashour, A.,A., (1971(b)).

Electromagnetic Induction in Thin Finite Sheets Having Conductivity Decreasing to Zero at the Edge, with Geophysical Applications -I.

Geophys. J. R. astr. Soc., 22, 417-433

Ashour, A.,A., (1971(c)).

Electromagnetic Induction in Thin Finite Sheets Having Conductivity Decreasing to Zero at the Edge, with Geophysical Applications - II.
Geophys. J. R. astr. Soc., 25, 447-467.

Bailey, R.,C., (1970)
Inversion of the Geomagnetic Induction Problem.
Proc. Roy. Soc. Lond., A, 315, 185 - 194

Bailey, R.,C., (1977).
Electromagnetic Induction over the Edge of a Perfectly Conducting Ocean.
Geophys. J. R. astr. Soc., 48, 385-392.

Banks, R.,J., (1969),
Geomagnetic Variations and the Electrical Conductivity of the Upper Mantle.
Geophys. J. R. astr. Soc., 17, 457 - 487

Banks, R.,J., (1972),
The Overall Conductivity Distribution of the Earth.
J. Geomag. Geoelectr., 24, 337 - 351.

Barber, N., and Longuet-Higgins, M.,S., (1948).
Water Movements and Earth Currents.
Nature, 161, 192-193.

Beal, H.,T., and Weaver, J.,T., (1970).
Calculations of Magnetic Variations Induced by Internal Ocean Waves.
J.G.R., 75, 6846-6852.

Beamish, D., Hewson-Browne, R.,C., Kendall, P.,C., Malin, S.,R.,C., and Quinney, D.,A., (1978(I)).
Induction in Arbitrarily Shaped Oceans IV: Sq for a Simple Case.

Submitted to Geophys. J. R. astr. Soc.

Beamish, D., Hewson-Browne, R.,C., Kendall, P.,C.,
Malin, S.,R.,C., and Quinney, D.,A., (1978(II)).
Induction in Arbitrarily Shaped Oceans V:
the Circulation of Sq-induced Currents around Land Masses.
Submitted to Geophys. J. R. astr. Soc.

Beamish, D., Hewson-Browne, R.,C., Kendall, P.,C.,
Malin, S.,R.,C., and Quinney, D.,A.,
Currents Induced by Sq in the Oceans.
Presented at European Geophysical Society meeting, Vienna
1979. Abstract in Trans. A. G. U. 60, no. 32, p 567

Berdichevskiy, M.,M., and Zhdanov, M.,S., (1974).
Separation of the Anomalies of the Variable Geomagnetic
Field from the Results of Spherical Analysis.
Geomag. and Aeron., 14, 425-430.

Bonnevier, B., Boström, R., & Rostoker, G., (1970)
Three-Dimensional Model Current System for Polar Magnetic
Substorms
J.G.R., vol 75, 107-122.

Brewitt-Taylor, C.,R., (1975).
A Model for the Coast Effect.
P.E.P.I., 10, 151-158.

Brewitt-Taylor, C.,R., (1976).
A Model for the Sea-floor Coast Effect in H-polarization
- Further Results. P.E.P.I., 13, 9-14

Bullard, E.,C., & Parker, R.,L., (1971)
Electromagnetic Induction in the Oceans.
The Sea, vol 4, Part 1, Chap. 18.

Chapman, S. (1919)

The Solar and Lunar Diurnal Variation of the Earth's Magnetism.

Phil. Trans. R. Soc. Lond. A, 218, 1-118.

Chan, R., and Dosso, H.,W., (1978).

The Effect of a Coastline Contour on Electromagnetic Induction for the Case of a Bay.

Murnau, 1978.

Chapman, S., & Whitehead, T.,T., (1922).

The Influence of Electrically Conducting Material within the Earth on Various Phenomena of Terrestrial Magnetism.

Trans. Camb. Phil. Soc., 22, 463 - 482.

Cherry, D.,W., and Stovold, A.,T., (1946).

Earth Currents in Short Submarine Cables.

Nature, 157, 766.

Cox, C., Kroll, N., Pistek, P., and Watson, K. (1978).

Electromagnetic Fluctuations Induced by Wind Waves on the Deep-Sea Floor.

J.G.R., 83, 431.

Cox, C.,S.,

Electromagnetic Induction in the Oceans and Inferences on the Constitution of the Earth.

Review presented at the 4th. I.A.G.A. Workshop on Electromagnetic Induction in the Earth and Moon, Bavaria 1978. To be published in J. Geomag. Geoelectr.

Dawson and Weaver, J.,T., (1979)

H-Polarization in Two Thin Half-Sheets.

J. Geomag. R. astr. Soc., 56, p. 419-438.

Doss, S.,S., and Ashour, A.,A., (1971).

Some Results on the Magnetic Field of Electric Currents

Induced in a Thin Hemispherical Shell of Finite Conductivity with Geomagnetic Applications

Geophys. J. R. astr. Soc., 22, 385-400.

Dosso, H.,W., (1973).

A Review of Analogue Model Studies of the Coast Effect.

P.E.P.I., 7, 294-302

Dosso, H.,W., Nienaber, W., and Hutton, V.,R.,S., (1978).

An Analogue Model Study of Electromagnetic Induction in the British Isles - Preliminary Results.

Murnau, 1978.

Ducruix, J., Courtillot, V., & Le Mouel, J.,L., (1977)

On the Induction Effects Associated with the Equatorial Electrojet.

J.G.R., vol 82, No 2,335-351.

Eckhardt, D., (1963).

Geomagnetic Induction in a Concentrically Stratified Earth.

J.G.R., vol 68, No. 23, 6273 - 6278.

Edwards, R.,N., Law, L.,K., and White, A. (1971)

Geomagnetic Variations in the British Isles and Their Relation to Electrical Currents in the Oceans and Shallow Seas. Phil. Trans. R. Soc. Lond., A 270, 289-323.

Fainberg, E.,B., (1978).

Electromagnetic Induction in a World Ocean.

Murnau, 1978. To appear in J. Geomag. Geoelectr.

Fischer, G., Schnegg, P.-A. and Usadel, K.,D.,(1978).

Electromagnetic Response of an Ocean-coast Model to E-polarization Induction.

Geophys. J. R. astr. Soc., 53, 599-616

Fraser, D.,C., (1965).

Magnetic Fields of Ocean Waves.

Nature, 206, 605-606.

Gradshteyn, I.,S., & Ryzhik, I.,M., (1965)

Table of Integrals, Series and Products.

Pub. Academic Press.

Green, V.,R., and Weaver,J.,T., (1978).

Two-dimensional induction in a Thin Sheet of Variable Integrated Condcutivity at the Surface of a Uniformly Conducting Earth.

Geophys. J. R. astr. Soc., 55, 721-736.

Hermance, (1968).

Can. J. Earth Sci., 5, 515-52.

Hewson-Browne R.,C., (1978).

Induction in Arbitrarily Shaped Oceans III: Oceans of Finite Conductivity. Geophys. J. R. astr. Soc., 55, 645-654.

Hewson-Browne, R.,C., and Kendall, P.,C., (1978(a)).

Some New Ideas on Induction in Infinitely Conducting Oceans of Arbitrary Shapes.

Geophys. J. R. astr. Soc., 53, 431-444.

Hewson-Browne, R.,C., and Kendall, P.,C., (1978(b)).

Induction in Arbitrary Shaped Oceans II: Edge Correction for the Case of Infinite Conductivity.

J. Geomag. Geoelectr., (in press).

Hobbs, B., A., (1971)

The Calculation of Geophysical Induction Effects Using Surface Integrals.

Geophys. J. r. astr. Soc. vol 25, 481-509.

Hobbs, B.,A., (1972).

A Comment on Certain Papers Involving Electromagnetic

Induction in Uniformly Conducting Hemispherical Shells.

Geophys. J. R. astr. Soc., 29, 109-115.

Hobbs, B., A., (1975)

Analytic Solutions to Global and Local Induction Problems of Electromagnetic Induction in the Earth.

P.E.P.I., vol 10, 250-261.

Hobbs, B.,A., & Dawes, G.,J.,K., (1979)

Calculation of the Effect of the Oceans on Geomagnetic Variations with an Application to the Sq Field during the I.G.Y.

J. Geophys. (in press)

Hobbs, B.,A., and Brignall, A.,M.,M., (1976).

A Method for Solving General Problems of Elecromagnetic Induction in the Oceans.

Geophys. J. R. astr. Soc., 45, 527-542.

Hobbs, B.,A., & Price, A.,T., (1970)

Surface Integral Formulae for Geomagnetic Studies.

Geophys. J. R. astr. Soc., vol 20, 49-63.

Hochstadt, H., (1971).

The Functions of Mathematical Physics.

Pub. Wiley-Interscience.

Honkura, Y., (1972).

Geomagnetic Variation Anomaly on Miyake-jima Island.

J. Geomag. Geoelectr., 23, 307-333.

Hutson, V.,C.,L., Kendall, P.,C., and Malin, S.,R.,C., (1972)

Computations of the Solution of Geomagnetic Induction Problems: A General Method, with Applications.

Geophys. J. R. astr. Soc., 28, 489-498.

Hutson, V.,C.,P., Kendall, P.,C., and Malin, S.,R.,C., (1973)

The Modelling of Oceans by Spherical Caps.
Geophys. J. R. astr. Soc., 33, 377-387.

Jady, R.,J., (1974).
The Conductivity of Spherically Symmetric Layered Earth Models Determined by Sq and Longer Period Magnetic Variations. Geophys, J. R. astr. Soc., 36, p. 399-410.

Jones, A.,G., and Hutton, R., (1979).
A Multi-station Magnetotelluric Study in Southern Scotland - II. Monte-Carlo Inversion of the Data and its Geophysical and Tectonic Implications.
Geophys. J. R. astr. Soc., 56, p. 351-368.

Kendall, P.,C., (1978)
Oceanic Induction and Shifting the Spectrum.
Geophys. J. R. astr. Soc., 52, 201-204.

Klein, and Larsen, J., (1978).
Magnetic Induction Fields (2-30 c.p.d.) on Hawaii Island and Their Implications Regarding the Electrical Conductivity in the Oceanic Mantle.
Geophys. J. R. astr. Soc., 53, 61-77.

Lahiri, B.,N., & Price, A.,T., (1939).
Electromagnetic Induction in Non-uniform Conductors, and the Determination of the Conductivity of the Earth from Terrestrial Magnetic Variations.
Phil. Trans. Roy. Soc., A, 237, 509 - 540.

Larsen, J.,C., (1971).
The Electromagnetic Field of Long and Intermediate Water Waves. J. Marine Reasearch, 29, 28-45.

Larsen, J.,C., (1968).
Eleectric and magnetic Fields Induced by Deep Sea Tides.

Geophys. J. R. astr. Soc., 16, 47-70.

Launay, (1970).

Ann. Geophys., 26, 805-810.

Lowes, F.,J., (1978).

Errors in Fourier and Spherical Harmonic Analysis.

Presented at U.K.G.A. II, Liverpool, April 1978.

Abstract in Geophys. J. R. astr. Soc., 53, 186.

Malin, S.,R.,C., (1973).

Worldwide Distribution of Geomagnetic Tides.

Phil. Trans. R. Soc. Lond., A 274, 551-594.

Malin, S.,R.,C., (1977).

Ocean Effects in Geomagnetic Tides.

Ann. Geophys., 33, 109-114

Malin, S.,R.,C., and Gupta, J.,C., (1977).

The Sq Current System during the International Geophysical Year. Geophys. J. R. astr. Soc, 49, p. 515-529.

Mareschal, M., & Kisabeth, J.,L., (1977).

Simulating the Earth's Induction Effects on Substorm Data Recorded at Mid-Latitude Stations: The Three Dimensional Problem.

J. Geomag. Geoelect., vol 29, 81-104.

Mason, R.,G., (1963).

Spatial Dependence of the Variation of the Geomagnetic Field on Oahu, Hawaii.

Trans. A. Geophys. Un., 44, 40.

National Physical Laboratory. (1965) Notes on Applied Science, No.16.

Modern Computing Methods. Pub. H.M.S.O.

Nicoll, M.,A., and Weaver,J.,T., (1977).

H-polarization Induction over an Ocean Edge Coupled to

the Mantle by a Conducting Crust.

Geophys. J. R. astr. Soc., 49, 427-442.

Parker, R.,L., (1968).

Elecromagnetic Induction in a Thin Strip.

Geophys. J. R. astr. Soc., 14, 487-495.

Parker, R.,L., (1971)

The Inverse Problem of Electrical Conductivity in the Mantle.

Geophys. J. R. astr. Soc., 22, 121 - 138.

Parkinson, W.,D., (1959)

Direction of Rapid Geomagnetic Fluctuations.

Geophys. J. R. astr. Soc., 2, 1.

Parkinson, W.,D., (1962)

The Influence of Continents and Oceans on Geomagnetic Variations.

Geophys. J. R. astr. Soc., 6, 441.

Parkinson, W.,D., (1964)

Conductivity Anomalies in Australia and the Coast Effect.

J. Geomag. Geoelectr., 15, 222-226.

Parkinson, W.,D., (1975).

The Computation of Electric Currents Induced in the Oceans.

J. Geomag. Geoelectr., 27, 33-46.

Price, A.,T., (1949).

The Induction of Electric Currents in Non-uniform Thin Sheets and Shells.

Quart. J. Mech. Appl. Math., 2, 283-310.

Price, A.,T., & Wilkins, G.,A., (1963).

New Methods for the Analysis of Geomagnetic Fields and their Application to the Sq field of 1932-33.

Phil. Trans. Roy. Soc., vol 256, A 31-98.

Quinney, D.,A., (1979).

A Note on Computing Coastal Edge Corrections for Induced Oceanic Electric Fields.

Geophys. J. R. astr. Soc., 56, 119-126.

Richards, M.,L., (1977)

Tidal Signals on Long Submarine Cables.

Ann. Geophys., 33, 177-178.

Rikitake, T., (1961).

The Effect of the Ocean on Rapid Geomagnetic Changes.

J. Geophys., 5, 1-15.

Rikitake, T., (1966)

Electromagnetism and the Earth's Interior. Pub. Elsevier.

Rikitake, T. and Yokoyama, I. (1955).

The Anomalous Behaviour of Geomagnetic Variations of Short Period in Japan and its Relation to Subterranean Structure.

Bull. Earthquake Res. Inst. Tokyo Univ., 33, 297-331.

Robinson, B., (1977).

Electromagnetic Induction in the Seas around the Orkney Islands.

Acta Geodaet., Geophys., et Montanist. Acad. Sci. Hung., 12, 191-194

Roden, R.,B., (1964).

The Effect of an Ocean on Geomagnetic Variations.

Geophys. J. R. astr. Soc., 8, 375-387.

Sanford, T.,B., (1971).

Motionally Induced Electric and Magnetic Fields in the Sea.

J.G.R., 76, 3476-3492.

Schmucker, U. (1964)

Anomalies of Geomagnetic Variations in the Southwestern United States.

J. Geomag. Geoelectr., 15, 193-221.

Schmucker, U. (1970)

Anomalies of Geomagnetic Variations in the Southwestern United States. Bulletin of the Scripps Institution of Oceanography, vol. 13.

Semerskiy, R.,B., Stavrov, K.,G., and Devrin, B.,N., (1978).

Possibility of Investigating the Magnetic Field of Ocean Waves by Towed Magnetometers.

Geomag. and Aeron., 18, 345-347

Sommerfeld, A.,(1949). Partial Differential Equations in Physics. Pub. Academic Press.

Spitta, P., (1977).

Electromagnetic Scale Model Experiments for the Coastline Effect of Geomagnetic Variations.

J. Geophys., 42, 507-520

Stark, P.,A., (1970)

Introduction to Numerical Methods. Pub. Macmillan.

Stratton, J.,A., (1941)

Electromagnetic Theory. Pub. McGraw-Hill.

Szidarovsky, F., & Yakowitz, S., (1978)

Principles and Procedures of Numerical Analysis.

Pub. Plenum Press.

Thomson, D.,J., & Weaver, J.,T., (1975)

The Complex Image Approximation for Induction in a Multilayer Earth.

J.G.R., vol 80, No 1, 123-129

Vasseur, and Weidelt, P., (1977).

Bimodal Electromagnetic Induction in Non-uniform Thin Sheets with an Application to the North Pyranean Induction Anomaly.

Geophys. J. R. astr. Soc., 51, p. 669-690.

Watson, G.,N., (1918).

Proc. Roy. Soc. Lond., vol 95.

Watson, G.,N., (1922).

Theory of Bessel Functions. Pub. Cambridge Univ. Press.

Weaver, J.,T., (1965). See below.

Weaver, J.,T., (1971)

Image Theory for an Arbitrary Quasi-static Field in the Presence of a Conducting Half Space.

Radio Sci., vol 6, no. 6, 647-653.

Weidelt, P., (1971).

The Electromagnetic Induction in Two Thin Half-sheets.

Zeitschr. für Geophys., 37, 649-665.

Westlake, J.,R., (1968)

A Handbook of Numerical Matrix Inversion and Solutions of Linear Equations.

Pub. J. Wiley & Sons.

White, A. and Polatajko, O.,W., (1978)

The Coast Effect in Geomagnetic Variations in South Australia.

J. Geomag. Geoelectr., 30, 109-120.

Young, D.,M., (1971)

Iterative Solution of Large Linear Systems.

Pub. Academic Press.

Zhigalov, L.,N., (1960).

Some Features of the Variation of the Geomagnetic Vertical Component in the Arctic Sea. Geomagnetic Disturbance (I.G.Y. Program) Acad. Sci. Press, Moscow.

Weaver, J.,T., (1965)

Magnetic Variations Associated with Ocean Waves and Swell.

J. Geophys. Res., 70, 1921 - 1929.